AEDC-TR-73-47

cy 2

AUG 1 1973
AUG 17 1973

MAY 29 1990

# WIND TUNNEL MODEL PARAMETRIC STUDY FOR USE IN THE PROPOSED 8 FT × 10 FT HIGH REYNOLDS NUMBER TRANSONIC WIND TUNNEL (HIRT) AT ARNOLD ENGINEERING DEVELOPMENT CENTER

W. K. Alexander, S. A. Griffin, R. L. Holt, et al.

General Dynamics Corporation

Convair Aerospace Division

March 1973

Approved for public release; distribution unlimited.

ARNOLD ENGINEERING DEVELOPMENT CENTER

AIR FORCE SYSTEMS COMMAND

ARNOLD AIR FORCE STATION, TENNESSEE

Property of U. S. Air Force
AEDC LIBRARY
F40600-74-C-0001

# NOTICES

When U. S. Government drawings specifications, or other data are used for any purpose other than a definitely related Government procurement operation, the Government thereby incurs no responsibility nor any obligation whatsoever, and the fact that the Government may have formulated, furnished, or in any way supplied the said drawings, specifications, or other data, is not to be regarded by implication or otherwise, or in any manner licensing the holder or any other person or corporation, or conveying any rights or permission to manufacture, use, or sell any patented invention that may in any way be related thereto.

Qualified users may obtain copies of this report from the Defense Documentation Center.

References to named commercial products in this report are not to be considered in any sense as an endorsement of the product by the United States Air Force or the Government.

# WIND TUNNEL MODEL PARAMETRIC STUDY FOR USE IN THE PROPOSED 8 FT X 10 FT HIGH REYNOLDS NUMBER TRANSONIC WIND TUNNEL (HIRT) AT ARNOLD ENGINEERING DEVELOPMENT CENTER

W. K. Alexander, S. A. Griffin, R. L. Holt, et al.
General Dynamics Corporation
Convair Aerospace Division

Approved for public release; distribution unlimited.

# FOREWORD

This report describes the work performed on Air Force contract F-40600-72-C-0015 by the Convair Aerospace Division of General Dynamics Corporation, San Diego operation, San Diego, California. The report is identified by contractor's number GDCA-DHJ72-001.

The work was administered by the Department of the Air Force, Headquarters, Arnold Engineering Development Center (TMP), Arnold Air Force Station, Tennessee. Mr. Ross G. Roepke, AEDC (DYX), is the Air Force technical representative.

This program was conducted in the research and engineering department of Convair and was managed by S. A. Griffin with W. K. Alexander as coordinating engineer. The work was accomplished between June and December 1972.

Principal contributors to the study include:

| | |
|---|---|
| Wind Tunnel Design | W. K. Alexander, S. B. Harkey |
| Dynamics | R. L. Holt |
| Materials Evaluation | R. T. Torgerson, R. W. Tryon |
| Aerodynamics | T. J. Fleck, G. J. Fatta |
| Structural Analysis | W. W. Johnstone, C. E. Edenfield |
| Test Operations | W. H. Lowe |
| Aerodynamic Consultant | H. Yoshihara |

The reproducibles used in the reproduction of this report were supplied by the author.

This technical report has been reviewed and is approved.

ROSS G. ROEPKE
Requirements Planning Division
Directorate of Technology

ROBERT O. DIETZ
Director of Technology

Col. Roland R.

Marshall K. Kingery
Facilities Div. Div
Deputy

## ABSTRACT

The need for a High Reynolds Number Transonic Wind Tunnel (HIRT) has been recognized throughout the industry for some years. The proposed HIRT facility at Arnold Engineering Development Center will provide a much needed tool for the study of phenomena sensitive to Reynolds number. The usefulness of the HIRT facility will be largely influenced by the ability of industry to design and build wind-tunnel models for an acceptable cost capable of operating within the severe environment of the tunnel. The object of this study is to determine the feasibility of designing and building models capable of withstanding the loads and environmental conditions of the facility. The aircraft configurations chosen for study cover a wide spectrum of flight conditions. A test plan is developed for each configuration which encompasses its complete flight envelope. Model loads and distortions are computed and presented to illustrate their magnitude under HIRT test conditions. Stress analyses of each aircraft configuration are presented for three different types of model. A summary of materials suitable for use in the HIRT facility is presented, and specific recommendations are made for model materials. Cost comparisons are made between models for testing in HIRT and similar models for testing in existing transonic wind tunnels. The study concludes that models capable of running in the HIRT facility can be built at a reasonable cost with present-day techniques and materials.

# TABLE OF CONTENTS


| Section | | Page |
|---|---|---|
| I | INTRODUCTION | 1 |
| II | PROGRAM ORGANIZATION | 4 |
| III | MODEL CONFIGURATION SELECTION | 5 |
| IV | MODEL SIZING | 6 |
| V | DESIGN PARAMETERS | 11 |
| | 5.1 MODEL TYPES | 11 |
| | 5.2 MATERIALS | 11 |
| | 5.3 LOADS | 11 |
| | 5.4 SURFACE FINISHES | 11 |
| | 5.5 SCALE EFFECTS | 12 |
| VI | BASIC DESIGN PHILOSOPHY | 13 |
| | 6.1 BALANCE AND SUPPORT SYSTEMS | 13 |
| | 6.2 BASIC FORCE MODELS | 14 |
| | 6.3 PRESSURE MODELS | 19 |
| | 6.4 BASELINE MATERIAL SELECTION | 27 |
| | 6.5 SURFACE FINISH | 27 |
| | 6.6 MISCELLANEOUS OBSERVATIONS | 27 |
| VII | TEST PLAN | 29 |
| | 7.1 TUNNEL USE | 29 |
| | 7.2 OPERATING ENVELOPES | 29 |
| | 7.3 TEST PLAN DEVELOPMENT | 36 |
| | 7.4 DATA STORAGE | 36 |
| VIII | AEROELASTIC ANALYSIS | 38 |
| | 8.1 METHODS | 38 |
| | 8.2 TUNNEL OPERATING CONDITIONS INFLUENCE ON MODEL LOADS | 39 |
| | 8.3 MODEL LOADS | 46 |
| | 8.4 MODEL WING DEFORMATION | 63 |
| | 8.5 MODEL SCALE EFFECTS ON WING DEFORMATION | 70 |
| | 8.6 REYNOLDS NUMBER EFFECT ON WING DEFORMATION | 71 |

TABLE OF CONTENTS, Contd


| Section | | Page |
|---|---|---|
| IX | STRUCTURAL ANALYSIS | 72 |
| | 9.1 ATT MODEL | 72 |
| | 9.2 F-111 AIRCRAFT | 96 |
| | 9.3 DELTA CANARD FIGHTER | 108 |
| | 9.4 SPACE SHUTTLE BOOSTER | 116 |
| X | MATERIALS ANALYSIS | 120 |
| | 10.1 CURRENT MODEL MATERIALS | 120 |
| | 10.2 HIRT MODEL REQUIREMENTS | 120 |
| | 10.3 MATERIALS SEARCH | 121 |
| | 10.4 GENERAL DISCUSSION OF MATERIAL CLASSES | 121 |
| | 10.5 PROMISING MATERIAL CANDIDATES | 123 |
| | 10.6 ALLOY SELECTION | 125 |
| | 10.7 PROCUREMENT SPECIFICATIONS | 127 |
| | 10.8 DESIGN ALLOWABLES | 127 |
| | 10.9 SURFACE FINISH | 129 |
| | 10.10 PROTECTIVE COATINGS | 130 |
| XI | MODEL COSTS | 131 |
| XII | CONCLUSIONS | 133 |
| XIII | RECOMMENDATIONS | 135 |
| | 13.1 RECOMMENDATIONS FOR FURTHER ANALYSES | 135 |
| | 13.2 ADDITIONAL STUDY AREAS | 135 |
| XIV | REFERENCES | 137 |
| Appendix | | |
| I | TYPICAL COMPUTER RUN PROGRAM 4278 | 139 |
| II | SAFETY FACTOR BASED ON FRACTURE MECHANICS | 159 |

# LIST OF FIGURES


| Figure | | Page |
|---|---|---|
| 1 | Program Operations Chart | 4 |
| 2 | Basic Geometry — ATT | 7 |
| 3 | Basic Geometry — F-111 | 8 |
| 4 | Basic Geometry — Space Shuttle Booster | 9 |
| 5 | Basic Geometry — Delta Canard | 10 |
| 6 | Balance Diameter vs Normal Force Capability | 13 |
| 7 | ATT Basic Force Model | 15 |
| 8 | F-111 Basic Force Model | 16 |
| 9 | Delta Canard Fighter Basic Force Model | 17 |
| 10 | Space Shuttle Booster Basic Force Model | 18 |
| 11 | ATT Pressure Wing, Method I | 21 |
| 12 | ATT Pressure Wing, Method II | 22 |
| 13 | F-111 Pressure-Instrumented Wing | 23 |
| 14 | Delta Canard Fighter Pressure Wing | 24 |
| 15 | Space Shuttle Booster Pressure Wing | 25 |
| 16 | Reynolds Number Ranges of Aircraft Chosen for Study | 29 |
| 17 | ATT Operating Envelope | 30 |
| 18 | Delta Canard Operating Envelope | 31 |
| 19 | Space Shuttle Booster Operating Envelope | 32 |
| 20 | F-111 (50 deg) Operating Envelope | 33 |
| 21 | F-111 (26 deg) Operating Envelope | 34 |
| 22 | F-111 (72-1/2 deg) Operating Envelope | 35 |
| 23 | Aeroelastic Program Geometry | 41 |
| 24 | Reynolds Number vs Dynamic Pressure at 300°K | 43 |
| 25 | Reynolds Number vs Dynamic Pressure at 240°K | 44 |
| 26 | ATT – Effects of 300°K vs 240°K Tunnel Operation | 45 |
| 27 | ATT — Model Loads — Condition 5 | 47 |
| 28 | ATT — Model Loads — Condition 6 | 48 |
| 29 | ATT — Model Loads — Condition 7 | 49 |
| 30 | ATT — Model Loads — Condition 1 | 50 |
| 31 | ATT — Model Loads — Condition 3 | 51 |
| 32 | ATT — Model Loads, 1/16 Scale — Conditions 37 and 41 | 52 |
| 33 | ATT — Model Loads, 1/16 Scale — Conditions 38 and 42 | 53 |
| 34 | ATT — Model Loads, 1/12 Scale — Conditions 39 and 43 | 54 |
| 35 | ATT — Model Loads, 1/12 Scale — Conditions 40 and 44 | 55 |
| 36 | F-111 (50 Deg) — Model Loads — Condition 14 | 56 |
| 37 | F-111 (50 Deg) — Model Loads — Condition 17 | 57 |
| 38 | F-111 (26 Deg) — Model Loads — Condition 20 | 58 |
| 39 | F-111 (72-1/2 Deg) — Model Loads — Condition 22 | 59 |

LIST OF FIGURES, Contd


| Figure | | Page |
|---|---|---|
| 40 | Delta Canard — Model Loads — Condition 24 | 60 |
| 41 | Delta Canard — Model Loads — Condition 27 | 61 |
| 42 | Space Shuttle Booster — Model Loads — Condition 29 (T = 300°K) | 62 |
| 43 | ATT — Elastic Wing Twists | 64 |
| 44 | ATT — Model Wing and Airplane Wing Twist Due to Matching Operating Envelope | 65 |
| 45 | ATT — Wing Deflections — 1/24 Scale Model and Full-Scale Airplane | 66 |
| 46 | ATT — Effect on Deflection Due to Removing Aft 35% Chord | 66 |
| 47 | F-111 (50 Deg) — Elastic Wing Twist | 67 |
| 48 | F-111 (50 Deg) — Wing Deflections | 67 |
| 49 | F-111 — Elastic Wing Twist vs Wing Sweep | 68 |
| 50 | F-111 — Wing Deflections vs Wing Sweep | 68 |
| 51 | Delta Canard — Elastic Wing Twist | 69 |
| 52 | Delta Canard — Wing Deflection | 69 |
| 53 | Space Shuttle Booster — Elastic Wing Twist | 70 |
| 54 | Space Shuttle Booster — Wing Deflection | 70 |
| 55 | ATT — Elastic Wing Twist vs Tunnel Temperature and Model Scale | 71 |
| 56 | ATT — Effect of Reynolds Number on Wing Twist | 71 |
| 57 | ATT Wing — Location of Sections Used For Structural Analysis | 74 |
| 58 | ATT — Comparison of Wing Types vs Stress (Condition 7) | 75 |
| 59 | ATT — Wing Stress at Wing Section 4 Resulting from Matching Flight Conditions for M=1.0 at 30,000 ft from 1.0 g to 2.5 g's | 76 |
| 60 | ATT — Comparison of Wing Stresses vs Tunnel Temperature and Model Scale | 78 |
| 61 | ATT Wing — Minimum Inertias | 79 |
| 62 | F-111 — Wing Stresses vs Wing Sweeps (Solid Wing) | 97 |
| 63 | F-111 — Wing Types vs Stress at 50-Degree Sweep | 97 |
| 64 | F-111 — Horizontal Tail Bracket Stress vs Incidence | 97 |
| 65 | Delta Canard — Wing Section Properties | 110 |
| 66 | Strength and Room Temperature Fracture Toughness Relationships | 126 |
| 67 | Strength and Low Temperature Fracture Toughness Relationships | 126 |

# LIST OF TABLES


| Table | | Page |
|---|---|---|
| 1 | Admissible Roughness Estimates (Surface Finish) | 28 |
| 2 | Test Plan | 37 |
| 3 | Model Loads, Empennage, and Total Lift | 63 |
| 4 | Model Loads Directory | 64 |
| 5 | Stress Analysis — Minimum Safety Factor Summary | 73 |
| 6 | ATT Wing Section Properties and Bending Analysis — 100% Chord Solid Wing | 80 |
| 7 | ATT Wing Section Properties and Bending Analysis — 65% Chord Solid Wing | 81 |
| 8 | ATT Wing Section Properties and Bending Analysis — 100% Chord Pressure Model (Method I) | 82 |
| 9 | ATT Wing Section Properties and Bending Analysis — 65% Chord Pressure Model (Method II) | 83 |
| 10 | Comparative Properties of General Classes of Materials (Ambient Temperature) | 122 |
| 11 | Material Specification for Recommended Alloys | 127 |
| 12 | Design Mechanical and Physical Properties of Materials Recommended for HIRT Test Models | 128 |
| 13 | Model Fabrication Cost Comparisons | 131 |

# ABBREVIATIONS AND SYMBOLS

| Symbol | Nomenclature | Units |
|---|---|---|
| A | Area | $in.^2$ |
| B.L. | Buttock line station | in. |
| C | Chord or dimension | in. |
| C | Specific heat | BTU/lb F |
| $C_L$ | Coefficient of lift | in. |
| C.P. | Center of pressure | |
| $c_L$ | Distance to lower fibers | in. |
| $c_U$ | Distance to upper fibers | in. |
| D | Diameter | in. |
| E | Modulus of elasticity | $lb/in.^2$ |
| E.A. | Elastic axis | |
| $E_c$ | Modulus of elasticity in compression | $lb/in.^2$ |
| e/D | Edge distance/diameter | |
| e | Elongation | % |
| F | Fahrenheit | degrees |
| $F_A$ | Axial force | lb |
| $F_b$ | Allowable bending stress | $lb/in.^2$ |
| $F_{bru}$ | Ultimate bearing stress | $lb/in.^2$ |
| $F_{bry}$ | Bearing yield stress | $lb/in.^2$ |
| $F_{cy}$ | Compressive yield stress | $lb/in.^2$ |
| $F_n$ | Ultimate tension allowable | $lb/in.^2$ |
| $F_{su}$ | Ultimate shear allowable | $lb/in.^2$ |
| $F_{tu}$ | Ultimate tension allowable | $lb/in.^2$ |
| $F_{ty}$ | Tensile yield stress | $lb/in.^2$ |
| F.S. | Fuselage station | in. |
| $f_b$ | Calculated bending | $lb/in.^2$ |
| $f_{br}$ | Calculated bearing stress | $lb/in.^2$ |

| Symbol | Nomenclature | Units |
|---|---|---|
| $f_c$ | Calculated compressive stress | lb/in.$^2$ |
| $f_n$ | Calculated principal stress | lb/in.$^2$ |
| $f_s$ | Calculated shear stress | lb/in.$^2$ |
| $f_{st}$ | Calculated shear stress (torsion) | lb/in.$^2$ |
| $f_t$ | Calculated tension stress | lb/in.$^2$ |
| G | Modulus of rigidity | lb/in.$^2$ |
| I | Moment of inertia | in.$^4$ |
| J | Polar moment of inertia | in.$^4$ |
| K | Thermal conductivity | BTU/hr ft$^2$°F |
| $K_{1c}$ | Plane strain fracture toughness | ksi in. |
| L | Load | lb |
| l | Length | in. |
| M | Moment | in-lb |
| MAC | Mean aerodynamic chord | ft |
| Method I | ATT Model gun-drilled pressure wing (Figure 11) | |
| Method II | ATT Model removeable T.E. pressure wing (Figure 12) | |
| n | Designates a number | |
| P | Load | lb |
| $P_S$ | Shear load | lb |
| $P_{SA}$ | Allowable shear load | lb |
| $P_T$ | Tensile load | lb |
| $P_{TA}$ | Allowable tensile load | lb |
| Q | Static moment of a cross-section | in-lb |
| $q_\infty$ | Freestream dynamic pressure | lb/ft$^2$ |
| $R_e$ | Reynolds number | |
| S | Translational deflection | in. |
| S.F. | Safety factor | |

| Symbol | Nomenclature | Units |
|---|---|---|
| S.S. | Span station | in. |
| T | Torsion | in.-lb |
| T.E. | Trailing edge | |
| T.S. | Tail panel station | in. |
| t | Thickness | in. |
| u | Median length | in. |
| V | Shear load | lb |
| W.S. | Wing station | in. |
| $x_{cp}$ | Axial center of pressure location | in. |
| $y_L$ | Distance to lower fibers | in. |
| $y_T$ | Distance to upper fibers | in. |
| $z_{cp}$ | Polar section modulus | $in.^3$ |
| $\alpha$ | Coefficient of thermal expansion | |
| $\Delta$ | Incremental or differential | |
| $\Lambda$ L.E. | Leading edge sweep angle | deg. |
| $\mu$-in. | Microinch | $in. \times 10^{-6}$ |
| $\chi$ | Rotational deflection | deg. |
| $\omega$ | Density | $lb/in.^3$ |
| °K | Degrees Kelvin | deg. |
| $\parallel$ | Parallel | |
| $\perp$ | Perpendicular | |
| $+$ | Vectorial addition symbol | |

# SECTION I

# INTRODUCTION

The international concern over the inability of existing wind-tunnel facilities to approach or match full-scale Reynolds numbers has led to the development of a variety of plans to construct high Reynolds number transonic wind tunnels. One proposed facility is HIRT, a large Ludwieg tube tunnel (8 ft × 10 ft test section), to be located at Arnold Engineering Development Center, Arnold Air Force Station, Tennessee (References 1 and 2). HIRT will operate over a range of Reynolds numbers from those available in present-day wind tunnels up to full-scale values for future flight vehicles.

Reynolds number performance in a wind tunnel is achieved through a balance of tunnel size, dynamic pressure, and temperature. Tunnel size is the prime parameter when relating to facility cost. The financial gains resulting in tunnel size reduction must be weighed against the restraints on testing capability due to model limitations. As the test section size is reduced (with a corresponding reduction in allowable model scale), the dynamic pressure must increase to maintain the desired Reynolds number performance. Model, balance, and support system stresses and deflections increase, while allowable surface finishes and model tolerances decrease. Model design, fabrication techniques, materials selection, balance system requirements, and, of course, model costs must be considered along with tunnel fabrication and operating costs when selecting an optimum tunnel size.

The objective of this study is to identify and analyze various problem areas associated with the design and fabrication of four configurations of wind tunnel models for use in the HIRT facility. The variety of aircraft studied included:

a. A variable wing sweep supersonic airplane (F-111).

b. A high-performance delta-wing fighter (Delta Canard).

c. An advanced technology transport (ATT).

d. A space shuttle booster.

Section III and Section IV respectively cover the selection of the specific aircraft to be studied and the sizing of models for use in the 8 ft × 10 ft HIRT test section. Basic model geometry drawings are presented.

The design parameters are discussed in Section V:

a. Types of models.

b. Model materials.

c. Model loads.

d. Surface finishes.

e. Model scale effects.

The basic design philosophy applied to this study is discussed in Section VI. Model conceptual drawings for each of the four model configurations are presented. Balance requirements and various support system stings are shown. Pressure-instrumented wings with approximately 400 pressure orifices are shown for each configuration. The ATT model is used to present two pressure wing design concepts. Baseline material selections were made for the basic model construction and model support system. Model surface finish requirements due to aerodynamics are discussed and admissible roughness computed for each of the models.

It is anticipated that the proposed HIRT facility will be heavily used and, unlike present-day transonic tunnels, that test plans will be very sensitive to the high Reynolds number capability. The high demand for occupancy will require a more limited test plan, with emphasis placed on testing critical areas of the operating envelope to confirm configuration performance.

A computer program was developed to compute design loads for each model and the corresponding deformations due to twisting and bending. In Section VIII each design point in the test plan was analyzed, and data were plotted to show wing loadings and deformations including:

a. Shear load.

b. Bending moment and pitching torque.

c. Wing loading.

d. Vertical deflection.

e. Elastic wing twist.

Basic structural analyses are performed on each of the models presented. Basic wing stresses, wing-to-fuselage attachments, empennage stresses, and the degradation of allowable loading due to the installation of pressure instrumentation in the model wings are analyzed and presented in Section IX.

The ATT model is used to analyze the effects on model stresses and model deformation resulting from increasing the model scale. The HIRT scale (1/24) was increased by factors of 1.5 (1/16 scale) and 2.0 (1/12 scale). Scale effects are covered in Sections VIII and IX.

Materials suitable for use in the fabrication of wind-tunnel models for the HIRT facility are presented in Section X. Alloy selections, procurement specifications, design

allowables, surface-finish procedures, and protective coatings for models are also presented.

In Section XI, model cost estimates are given, and comparisons are made between HIRT model costs and model costs for existing wind tunnels. Cost increments are given for various model surface finishes and model scales.

Due to the large scope of the subject of the design of wind-tunnel models for the HIRT tunnel, this study had to be very selective in the choice of subjects to be explored. Several interesting problem areas were recognized but were not analyzed in detail in this report. Section XIII contains recommendations for subjects for future detailed analyses.

# SECTION II

## PROGRAM ORGANIZATION

Convair Aerospace Division established a program team within its research and engineering department to conduct the parametric study of high Reynolds number wind-tunnel models. The team organized to conduct this study was led by Mr. S. A. Griffin, who reports to Mr. W. T. MacCarthy, manager of wind tunnels. The entire organization is under the senior management of the division vice president of research and engineering, Mr. R. H. Widmer.

The program operations chart, Figure 1, illustrates the flow of information from the various technical groups, through design, to the final report.

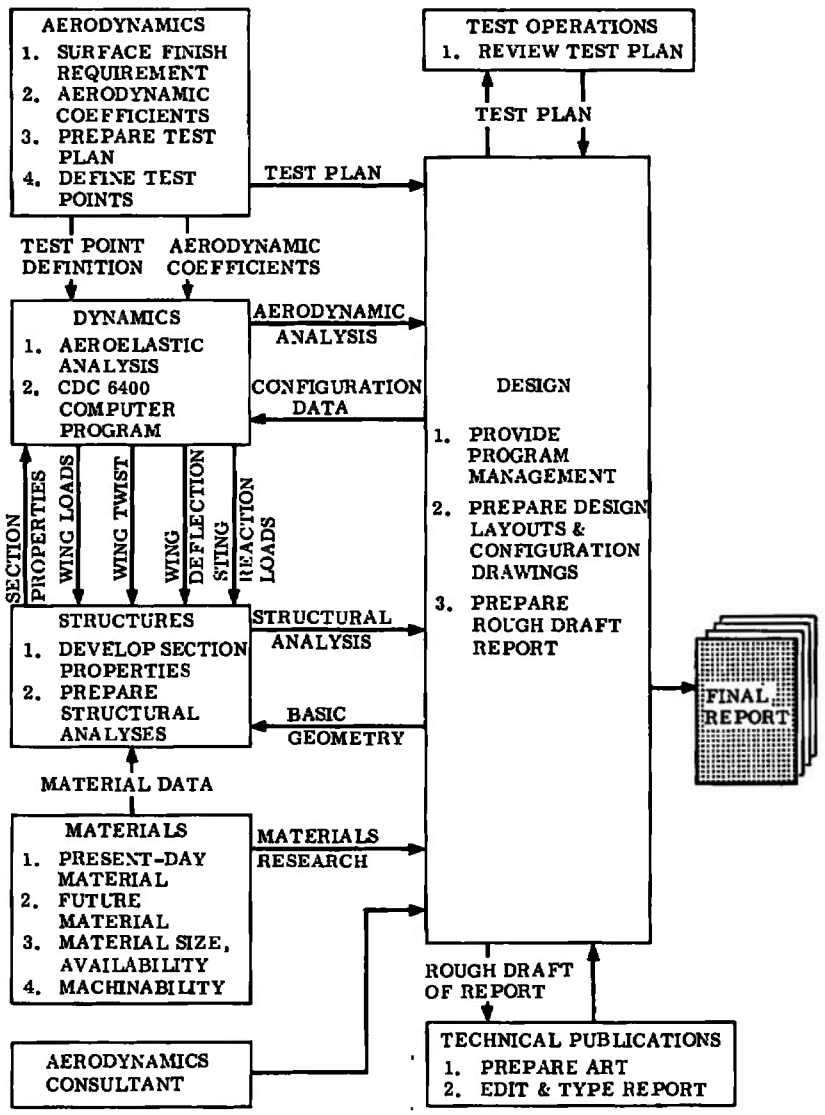


Figure 1. Program Operations Chart

# SECTION III

## MODEL CONFIGURATION SELECTION

Four types of aircraft have been selected to be analyzed during this study. These models are typical of the type of aircraft that would be likely candidates for testing in the HIRT facility. The wind tunnel model configurations selected are:

a. Advanced Technology Transport (ATT) – a highly loaded, large, swept-wing transport aircraft.

b. Convair Aérospace F-111 – a swing-wing supersonic aircraft.

c. Convair Aerospace space shuttle booster – a large delta-wing space vehicle capable of launching an orbiter space vehicle and returning to earth for a landing.

d. Convair Aerospace delta canard fighter (delta canard) – a highly maneuverable fighter aircraft consisting of delta planform wings and canards.

# SECTION IV

# MODEL SIZING

Model sizing was accomplished using criteria based on model size requirements recommended by the General Dynamics high speed wind tunnel and AGARD data (Reference 3). Sizing criteria:

a. Wing span ≤60% of the tunnel width.

b. Frontal area of the model at zero angle of attack ≤ 1% of the test section cross sectional area.

c. Wing area ≤ 5% of the test section cross sectional area.

d. Model length ≤ test section height.

HIRT test section dimensions:

a. Height = 8 feet

b. Width = 10 feet

c. Cross sectional area = 80 feet$^2$

Resulting model scales, wing spans, and body lengths:

| Model | Scale | Wing span (in.) | Fuselage length (in.) |
|---|---|---|---|
| ATT | 1/24 | 67.55 | 91.67 |
| F-111 (26 deg sweep) | 1/12 | 60.0 | 71.20 |
| (50 deg sweep) | 1/12 | 48.22 | 71.20 |
| (72 1/2 deg sweep) | 1/12 | 32.0 | 71.20 |
| Delta Canard | 1/9.6 | 35.61 | 56.00 |
| Space Shuttle Booster | 1/46.5 | 37.40 | 59.80 |

Basic model geometries are shown in Figures 2 through 5.

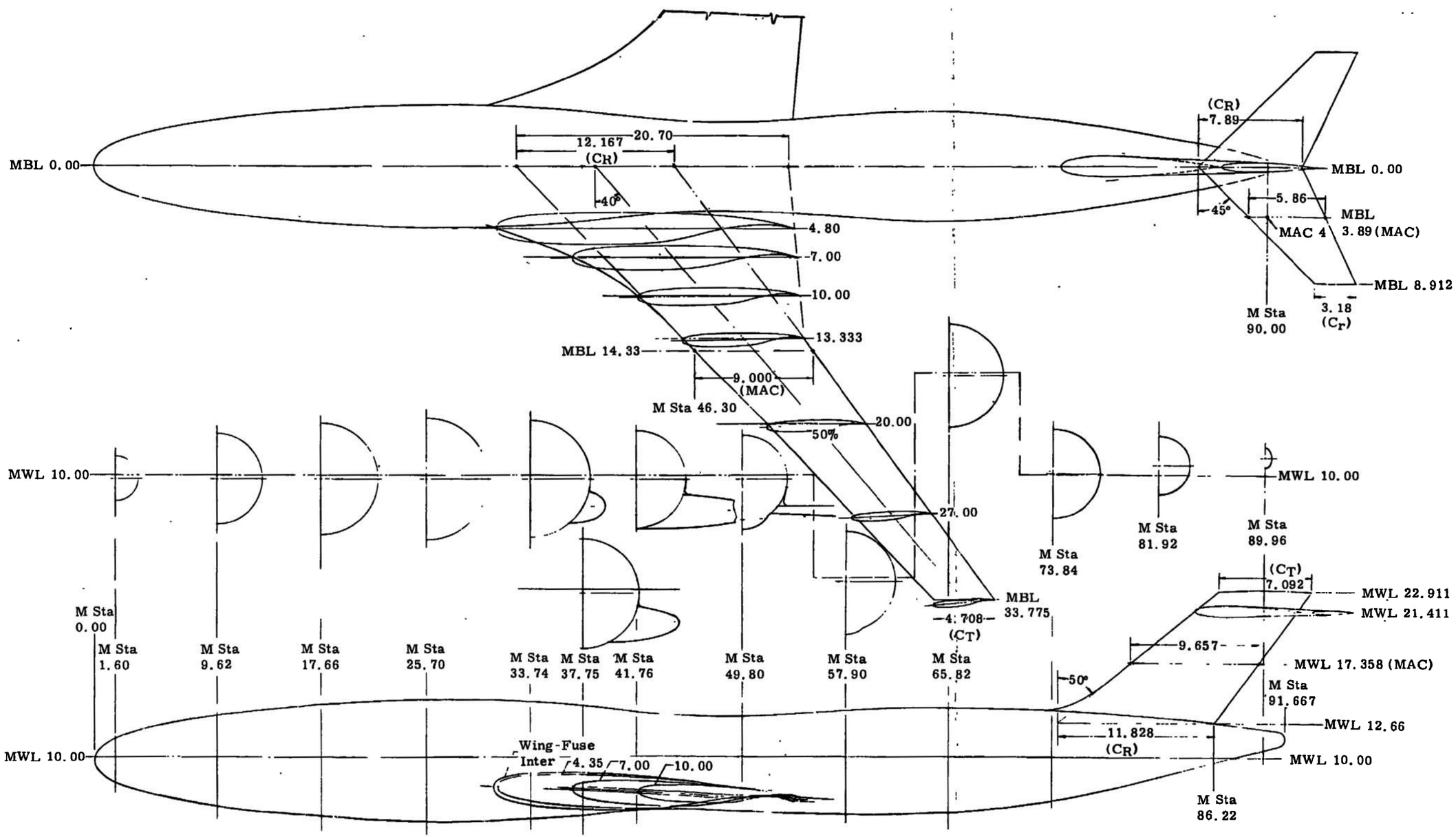


1/2 MODEL SCALE
Ref. FN 7197120

Figure 2. Basic Geometry – ATT

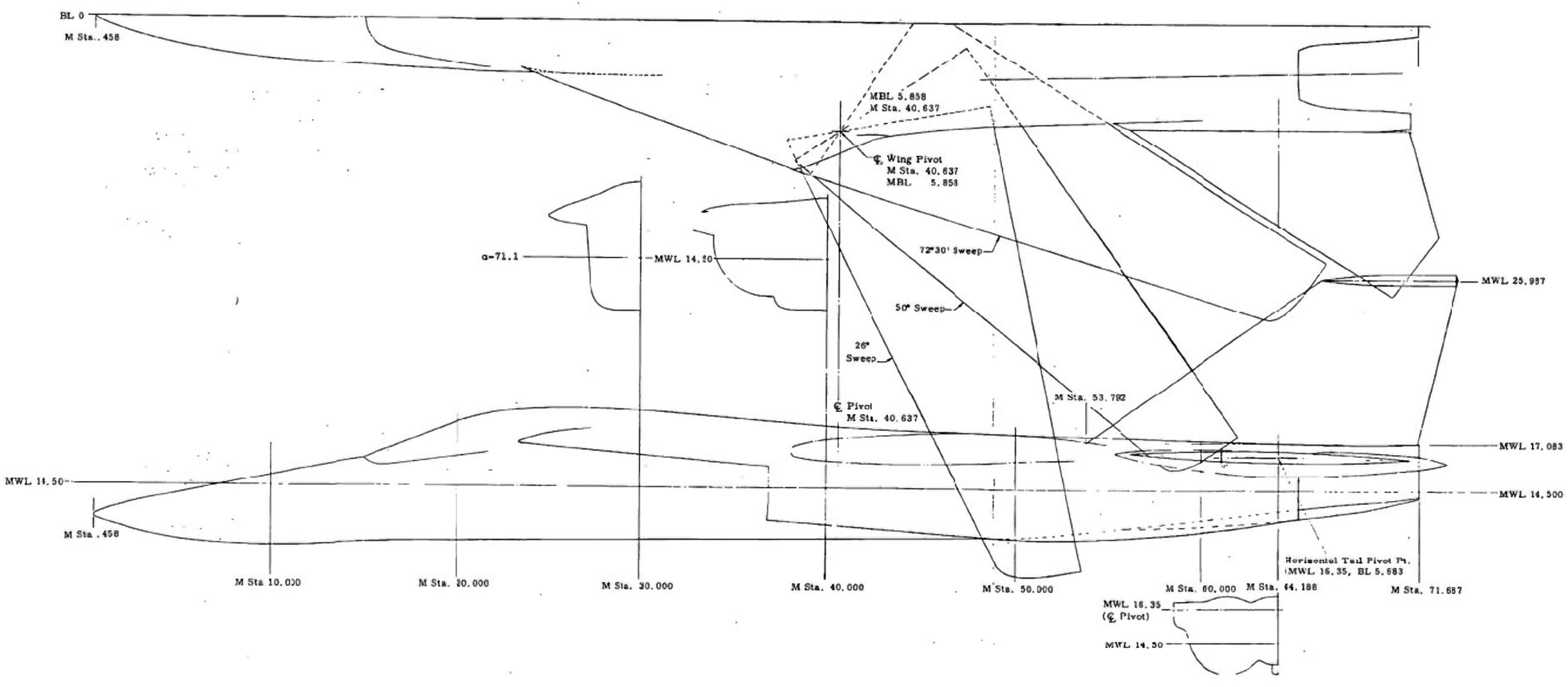


Figure 3. Basic Geometry – F-111

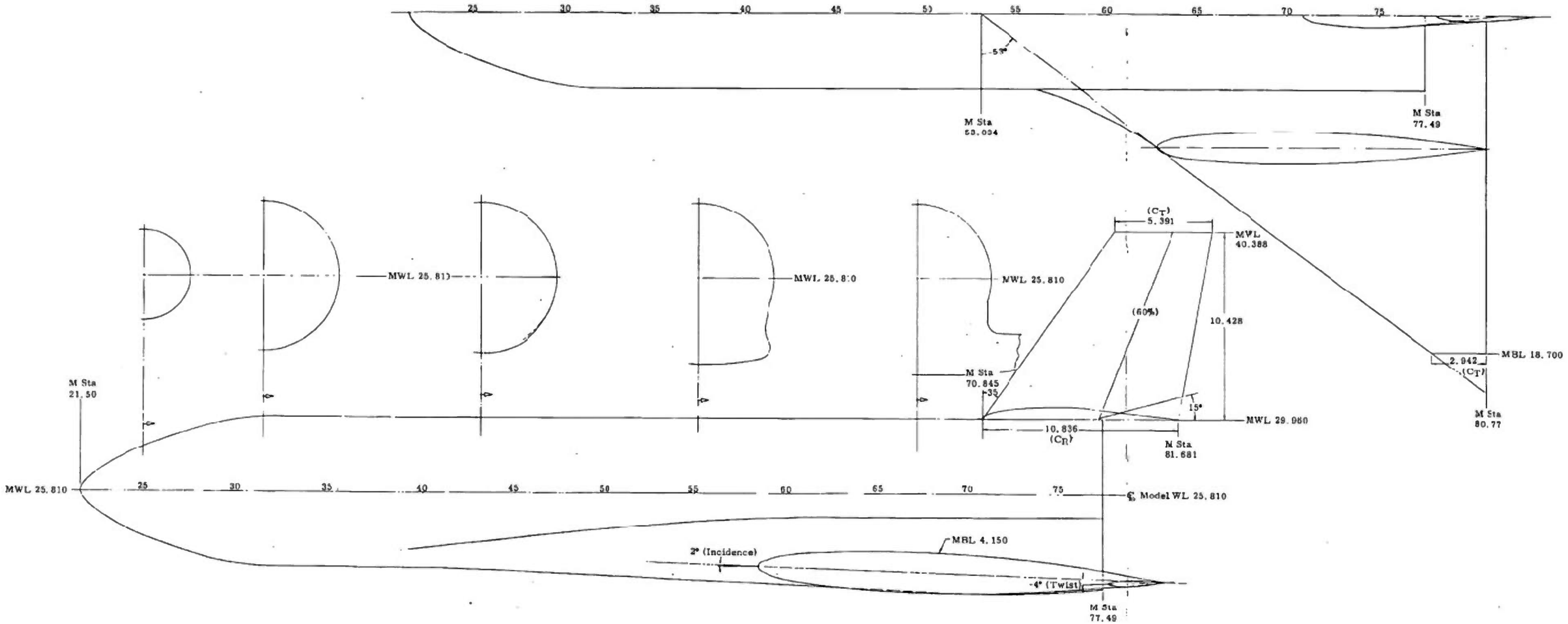


Figure 4. Basic Geometry – Space Shuttle Booster

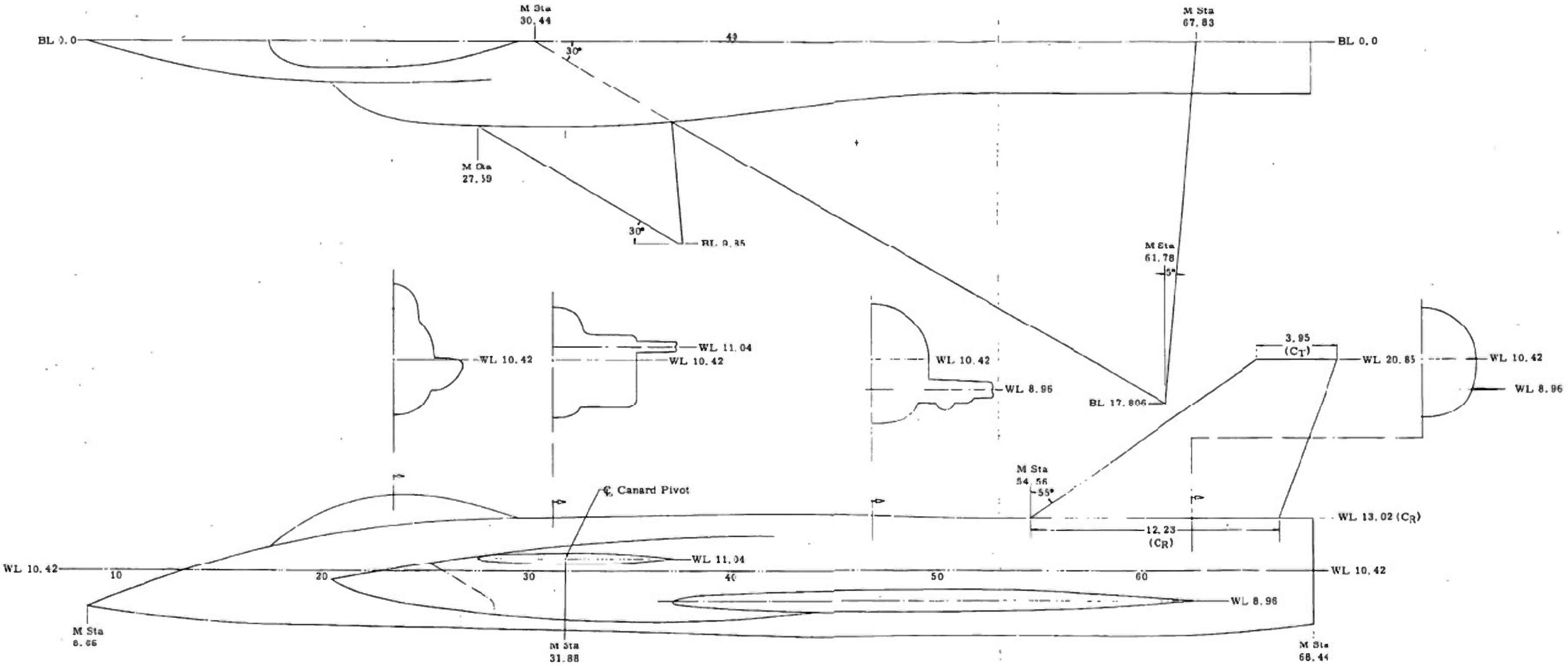


Figure 5. Basic Geometry – Delta Canard

# SECTION V

# DESIGN PARAMETERS

The study of the design and fabrication of wind tunnel models for use in the HIRT facility is multi-faceted with an infinite number of challenging problems. This report limits the areas of study to a number of parameters considered basic to the argument as to the usability of HIRT due to model/tunnel operating limitations.

## 5.1 MODEL TYPES

Each aircraft configuration is analyzed by considering at least three basic types of models per configuration:

a. Basic force model with a solid (no variable geometry capability) wing.

b. Solid wing model with provisions to vary flap or control surfaces.

c. Instrumented model with 100 to 400 pressure orifices in the wings.

## 5.2 MATERIALS

The same state-of-the-art material is used as a baseline material for the structural, aeroelastic, and cost analysis of each model type.

## 5.3 LOADS

All model loads are computed based on the actual or predicted aircraft operating envelopes for each configuration (Reference Figures 17 through 22). The points selected for analyses are discussed in the test plan (Section VII).

## 5.4 SURFACE FINISHES

Model surface finishes are analyzed with regard to the impact of special finishes on model costs. Three conditions were considered:

a. Complete model finished to a surface finish of 32 to 16 microinches.

b. First 30% of the airfoil and fuselage finished to 8 microinches with the remainder of the model finished to 16 microinches.

c. A 4 microinch finish for the first 30% of the airfoil and fuselage with the remainder of the model finished to 16 microinches.

The impact of model surface finishes on model cost is shown in Section XI, Table 13.

## 5.5 SCALE EFFECTS

The ATT model configuration was checked to determine the structural and aeroelastic effects of two larger model scales on the solid-wing model. Alternate model scales are:

a. 1.5 basic model size (1/16 scale).

b. 2.0 basic model size (1/12 scale).

The impact of model scale on model cost is shown in Section XI, Table 13.

# SECTION VI

# BASIC DESIGN PHILOSOPHY

Since detail design of any model for the HIRT facility will most certainly be greatly influenced by aircraft geometry and/or testing mission, this study does not dwell on some of the details that are most influenced by geometry. No attempt is made to perform detailed designs of these models. Model geometry drawings (Figures 2 through 5), basic force model assembly drawings (Figures 7 through 10), and typical pressure wing drawings (Figures 11 through 15) for each configuration illustrate possible model details and assemblies.

## 6.1 BALANCE AND SUPPORT SYSTEMS

The effects of the interference of the model support system on the flow over the model wing and fuselage are very real and difficult to analyze. Various techniques have been developed to account for these effects. Acceptable techniques depend on company and/or facility preferences or policies. No attempt has been made to explore this problem.

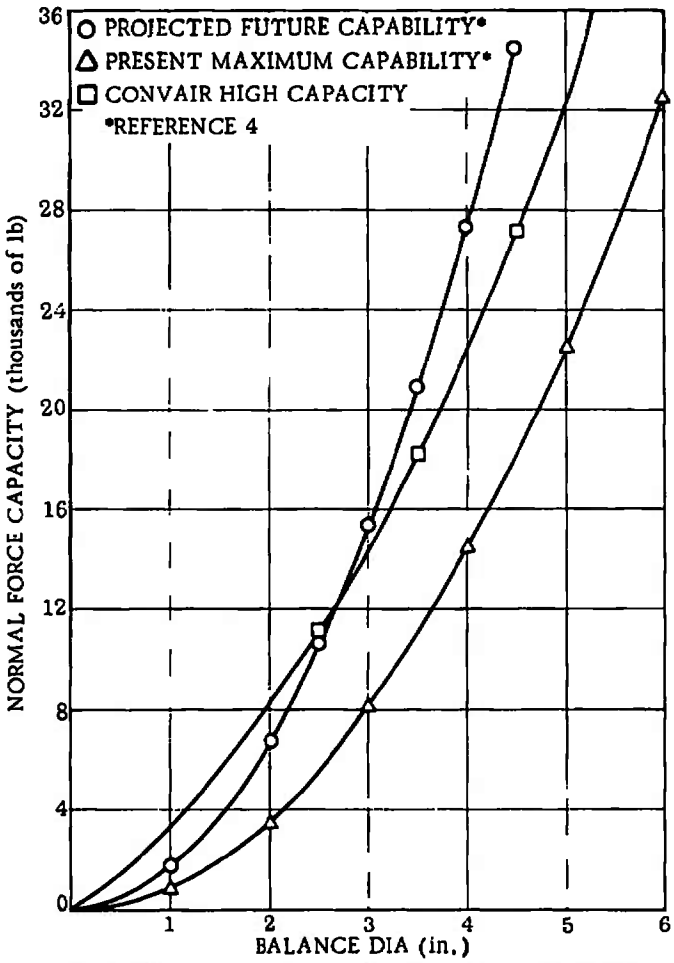


Figure 6. Balance Diameter vs Normal Force Capability

All models are supported by a sting/balance arrangement. Balances are sized to be consistent with the anticipated high capacity balances, with a balance load carrying capability (NF/diameter$^2$) of 1,700 psi. This load range appears to be consistent with current General Dynamics Convair Aerospace work and other studies (see Figure 6). No consideration is given to the problems of sting-to-balance attachment (it is recognized that a one-piece sting/balance combination might be required in some cases). It has been assumed that a conventional balance-to-model attachment (i.e., pins, etc.) will be required. Sting sizes are based on high-strength, maraging type steels. No attempt has been made to optimize sting shapes. All stings are assumed to have a circular cross section.

The aft portions of the fuselages on the F-111, ATT, and delta canard models have been revised to accept the model sting. The resulting shapes are noted in Figures 7, 8 and 9.

## 6.2 BASIC FORCE MODELS

### 6.2.1 Advanced Transonic Transport Model

Figure 7 presents a basic force model design for the ATT. A solid steel wing, split at the fuselage ℄ is used. Based on a maximum model load of 24,000 lb (Table 3), a 3.7-inch-diameter balance (Figure 6) is shown. Two sting sizes are shown to illustrate the relative size of stings required for a cruise versus a maximum maneuver loading condition. The horizontal tail is shown as a one-piece design mounted on a conventional vertical tail arrangement. Flow-through nacelles are mounted to the aft fuselage.

### 6.2.2 F-111 Aircraft

Figure 8 presents a basic force model design for the F-111. Individual wings are shown for each of the three wing sweeps considered, (26, 50, and 72-1/2 degrees). A maximum model load of 30,370 lb (Table 3) requires a 4.125-inch-diameter balance (Figure 6) for this configuration. A 65% chord alternate wing construction method is shown. This wing was analyzed to simulate a wing that was modified to allow flaps, ailerons, etc., to be carried by a portion of the total airfoil. Horizontal tails are attached with brackets to accommodate changes in tail incidence.

### 6.2.3 Delta Canard Fighter

Figure 9 is a basic force model of the delta canard fighter. A solid steel wing and an alternate wing with elevons are shown. The total model load, 22,000 lb at ambient tunnel conditions and 14,700 lb at 240°K (Table 3), are noted by the presentation of two balance and sting diameters. This design features a movable canard through the use of incidence blocks and cover plate fairings.

### 6.2.4 Space Shuttle Booster

Figure 10 is a basic force model of the space shuttle booster. The wing is shown as a one-piece wing using a keyway or tongue-and-groove attachment to the fuselage. A total model load, at ambient tunnel conditions, of 34,950 lb (Table 3) indicates that a 4.5-inch-diameter balance (Figure 6) is required. This model is the most straightforward design of all the configurations chosen.

ALTERNATE WING CONSTRUCTION
Typical Section for Wing with Removable Section for Control Surface Deflections

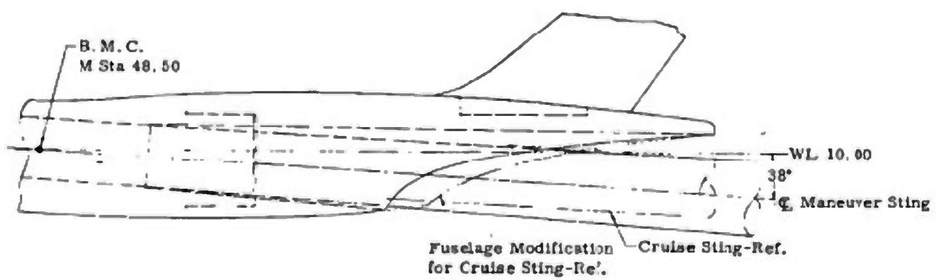


ALTERNATE FUSELAGE CONFIGURATION FOR MANEUVER STING

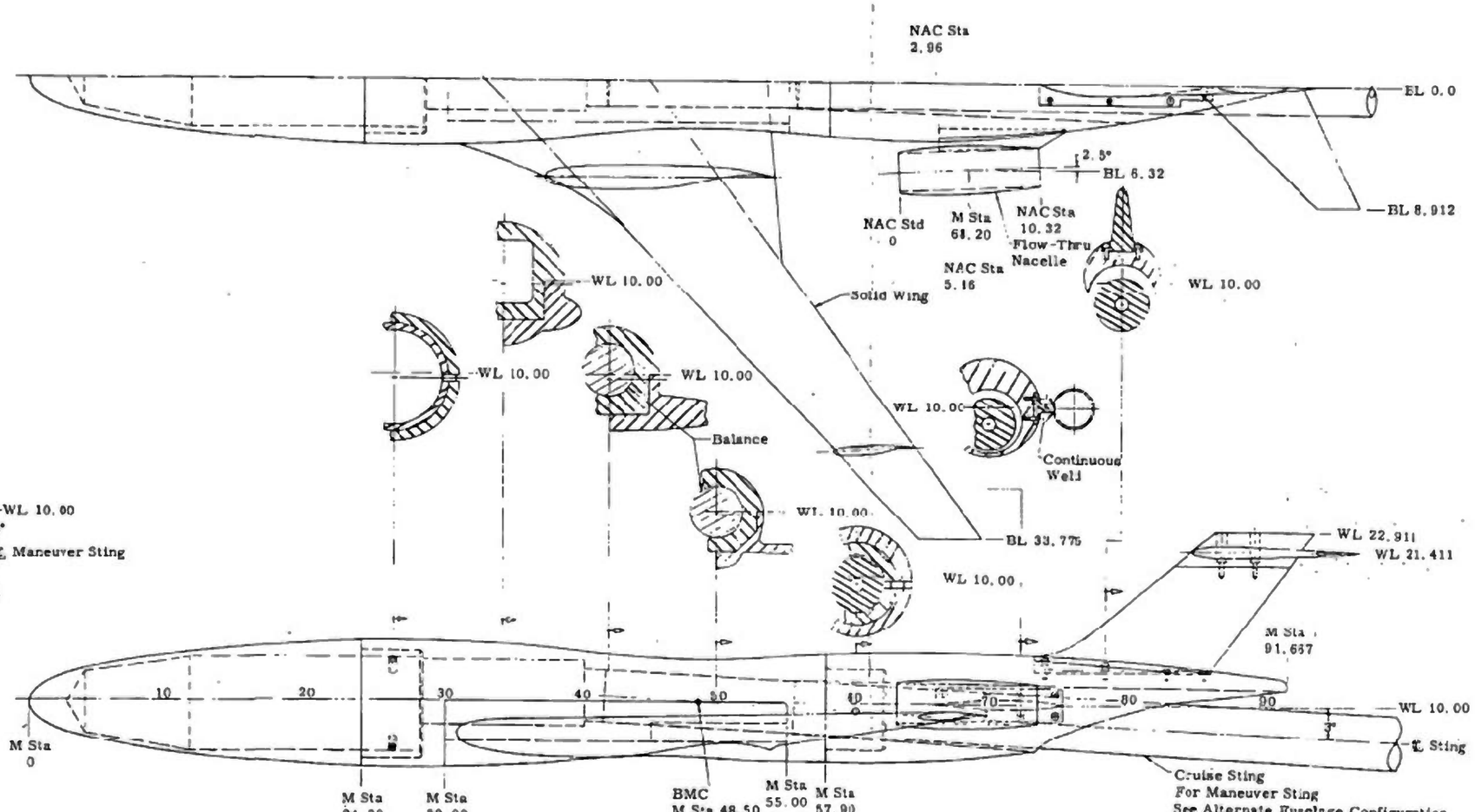


1/2 MODEL SCALE

Figure 7. ATT Basic Force Model

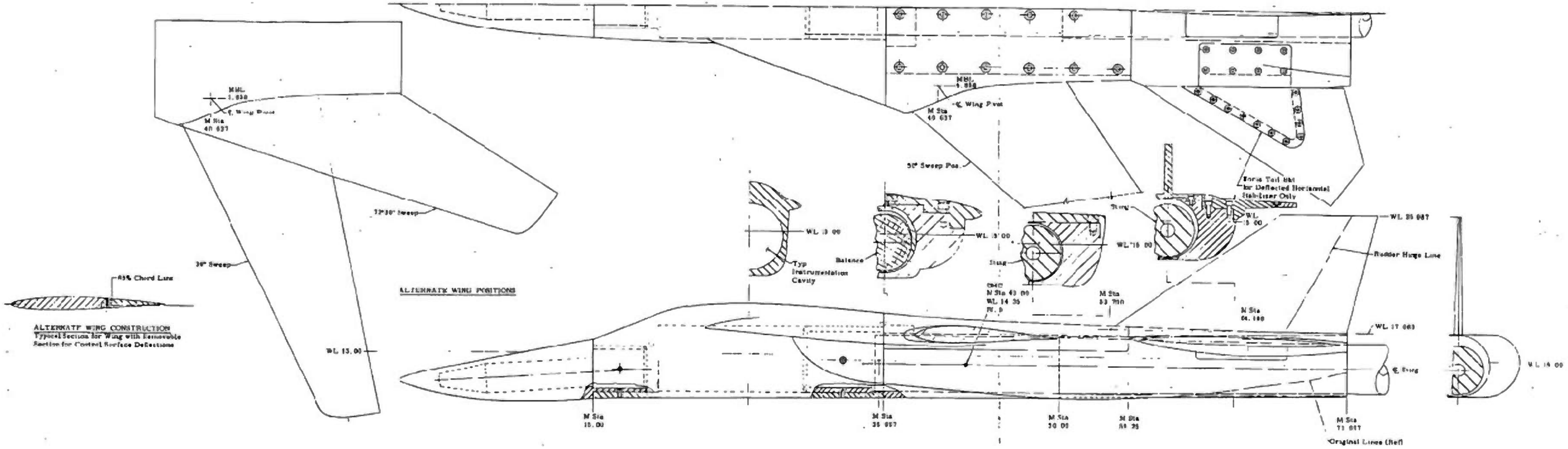


Figure 8. F-111 Basic Force Model

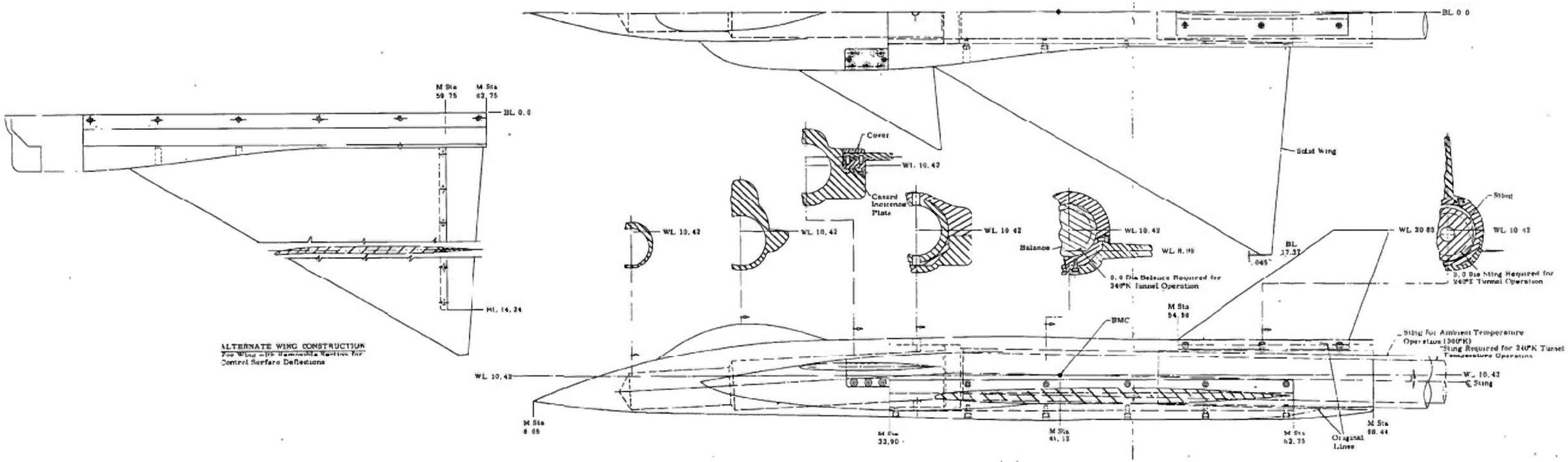


Figure 9. Delta Canard Fighter Basic Force Model

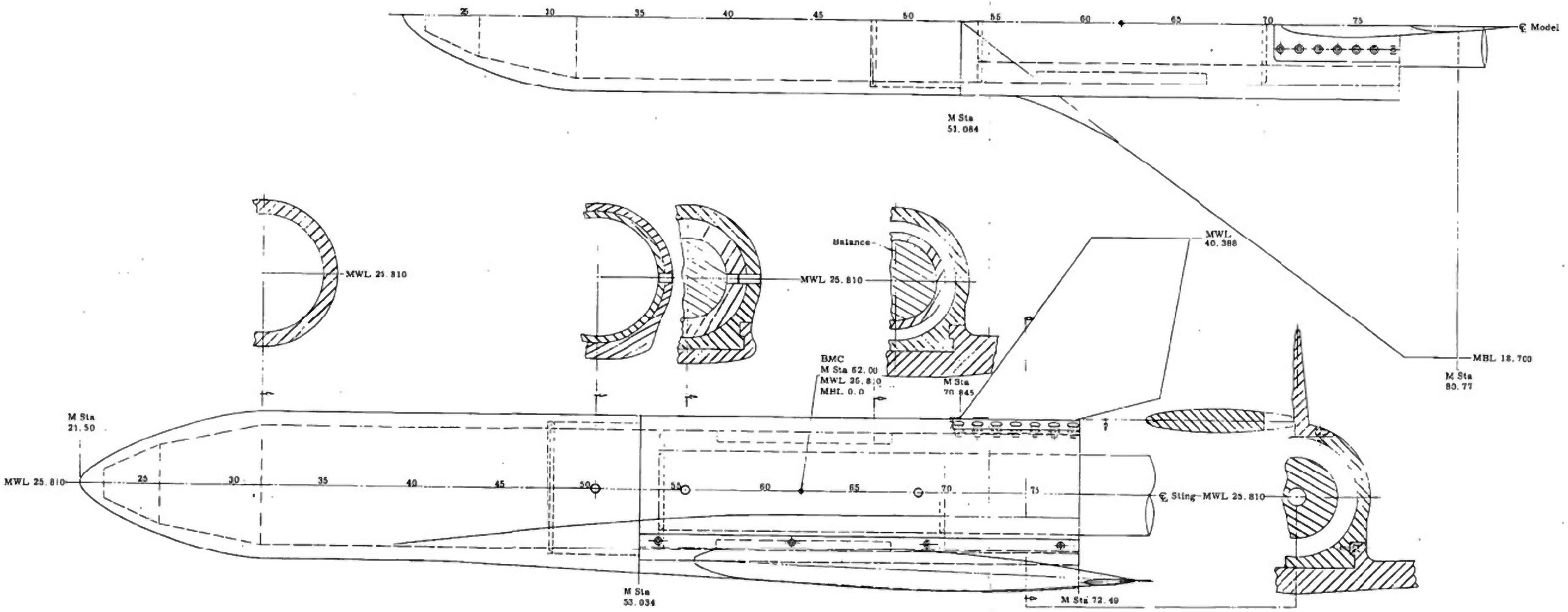


Figure 10. Space Shuttle Booster Basic Force Model

## 6.3 PRESSURE MODELS

Pressure models for use in the HIRT facility do not present any unique design problems. Conventional state-of-the-art methods of designing and fabricating pressure models are adequate. A requirement for superfine surface finishes appears to be a moot point when compared to the effect of several rows of pressure orifices.

The size of models used in the HIRT facility should provide adequate room for storage of transducer packages in nose/fuselage cavities. Errors in pressure measurements due to the tubing and transducer volume lag can be made small (0.5 percent) by selecting proper tube length-to-diameter ratio (Ref. 5). Pressure tubing with 0.049-inch outside diameter (0.025 I.D.) was selected for this study. Larger tubing is not compatible with HIRT scale-model airfoil sections.

Two methods of designing pressure wings for the ATT model are shown in Figures 11 and 12.

a. Method I, Figure 11, features gun-drilled spanwise tube routing holes with locally machined tube routing slots on the outside surface for each pressure orifice. The tube routing slots are filled with a material such as soft solder and finished to wing contour.

b. Method II, Figure 12, features a removable trailing-edge portion, which facilitates pressure-tube routing. Slots (located near the neutral axis) are eloxed at each row of pressure orifices to allow room for pressure tube installation and routing.

Method II is preferred from both a structural and a manufacturing standpoint. Pressure-tube installation and routing are easier to accomplish, and this method is not nearly as configuration-limited as the gun-drilled hole method. Method II was used for the design of pressure-instrumented wings for the F-111, delta canard, and space shuttle booster. Figure 13 is a pressure installation on the 50-deg sweep F-111 wing. Figures 14 and 15 show the pressure-tube installation for the two delta-wing models (delta canard fighter and space shuttle booster).

Results of the structural analysis of each method are presented in Section IX. It should be noted that all upper surface pressure orifices have been located on the left-hand wing panel and all lower surface pressure orifices on the right-hand panel. This procedure was followed to minimize the decline in allowable wing loading due to the installation of pressure tubes. The small size of wing airfoil sections for HIRT scale models is not compatible with the removal of material from the upper and lower surfaces at the same span station: approximately four hundred orifices (two hundred per side) are considered in this study.

Installation of fuselage orifices is basically straightforward.

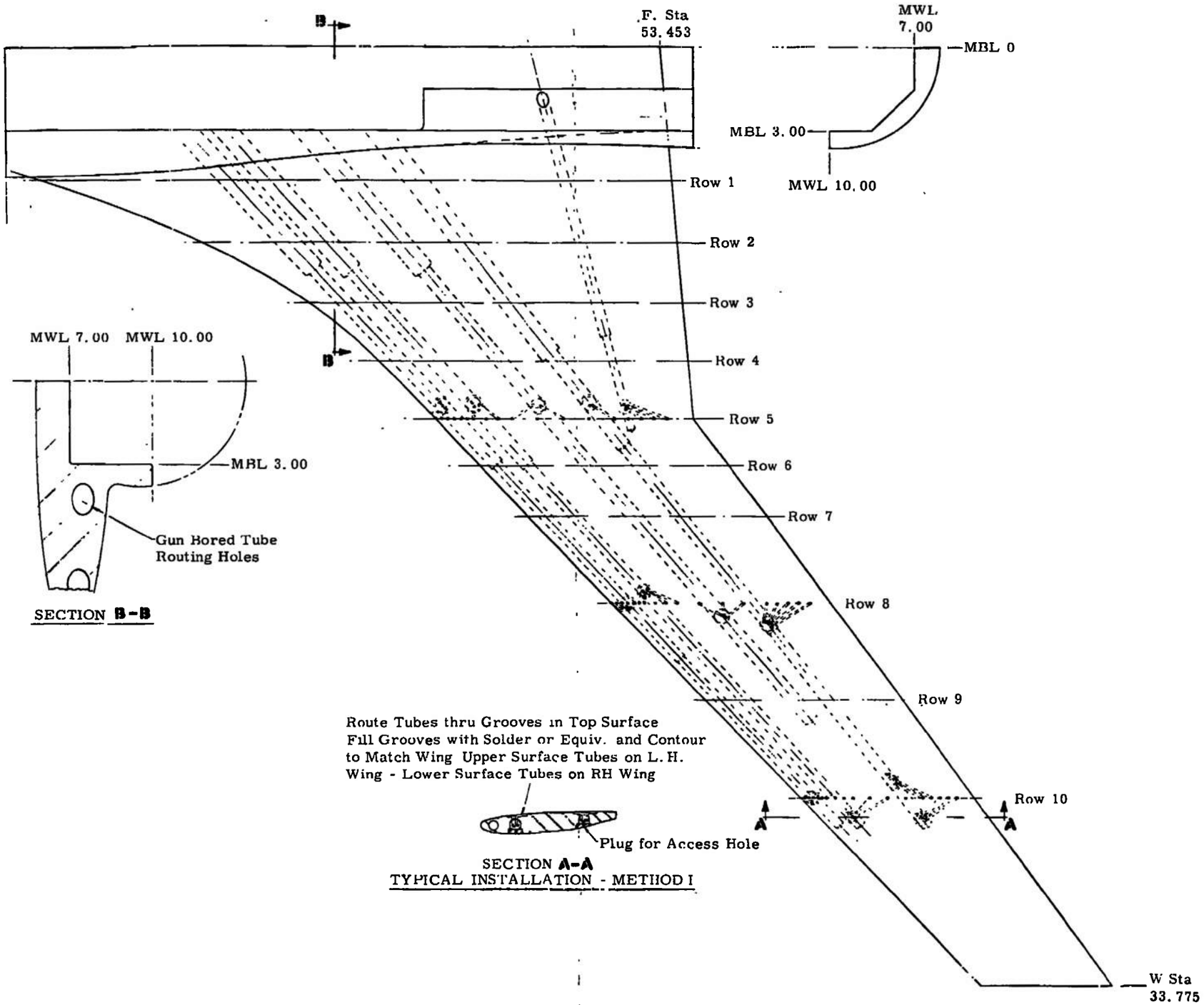


Figure 11. ATT Pressure Wing, Method I

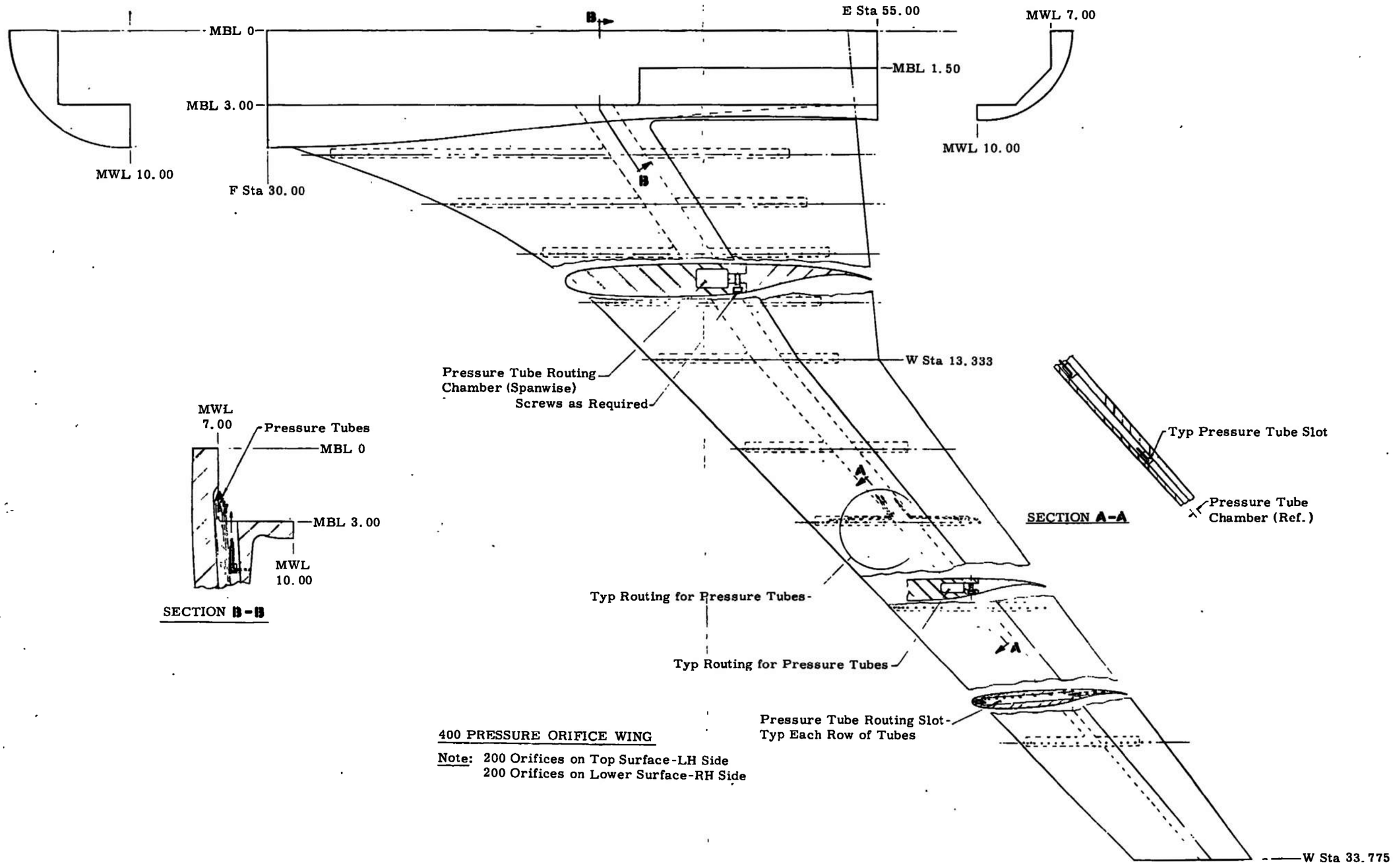


400 PRESSURE ORIFICE WING

Note: 200 Orifices on Top Surface-LH Side
200 Orifices on Lower Surface-RH Side

Figure 12. ATT Pressure Wing, Method II

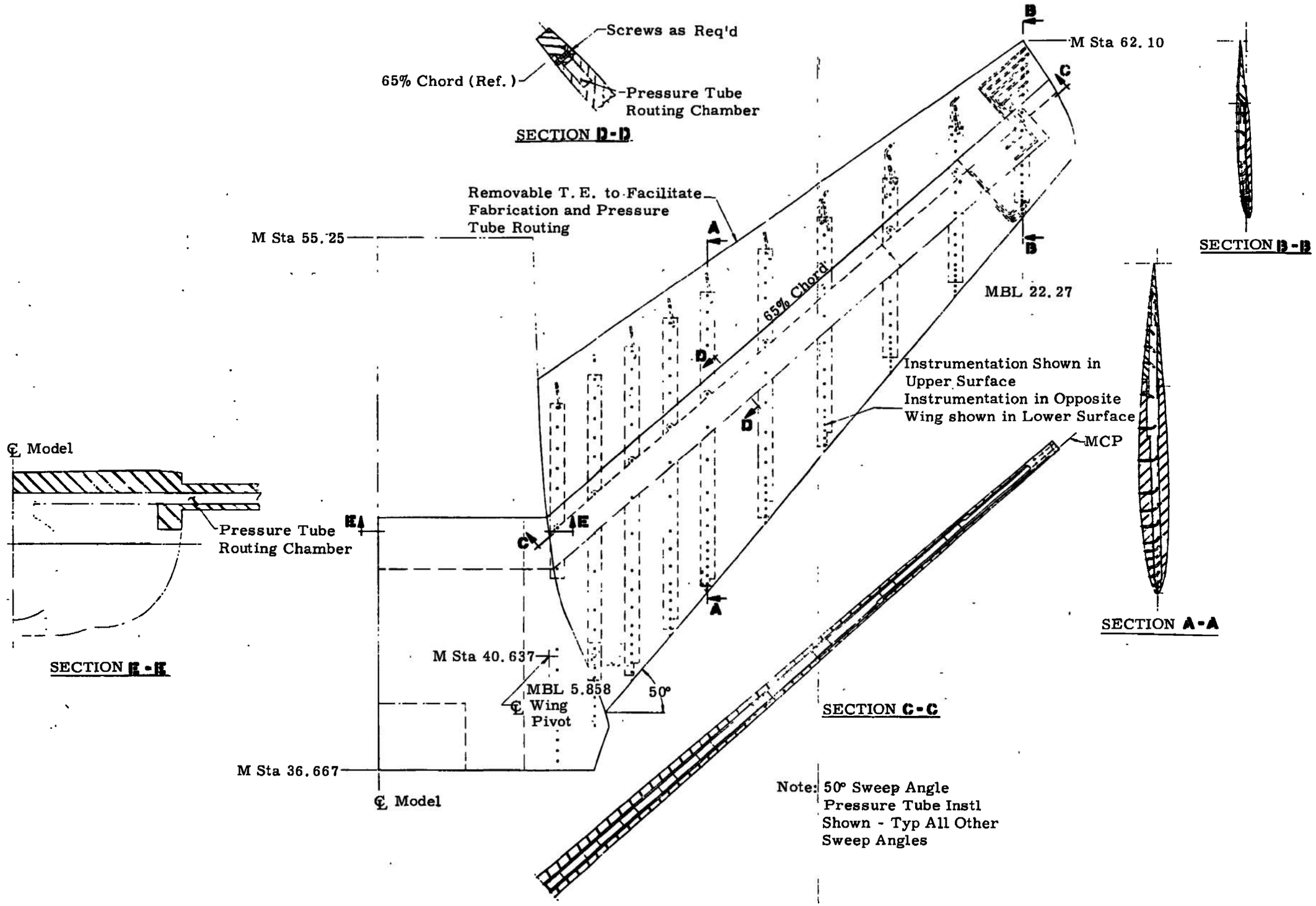


Figure 13. F-111 Pressure-Instrumented Wing

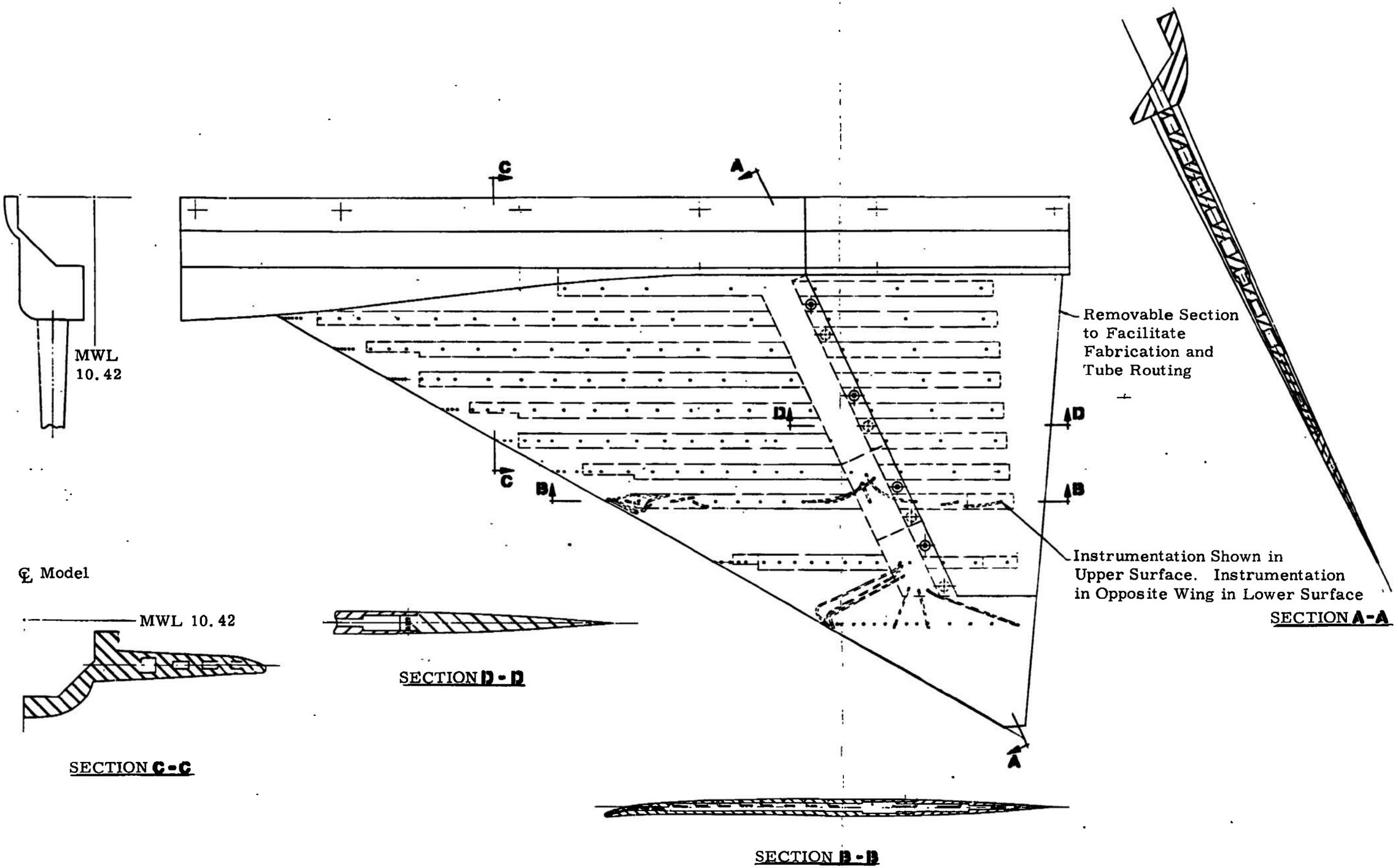


Figure 14. Delta Canard Fighter Pressure Wing

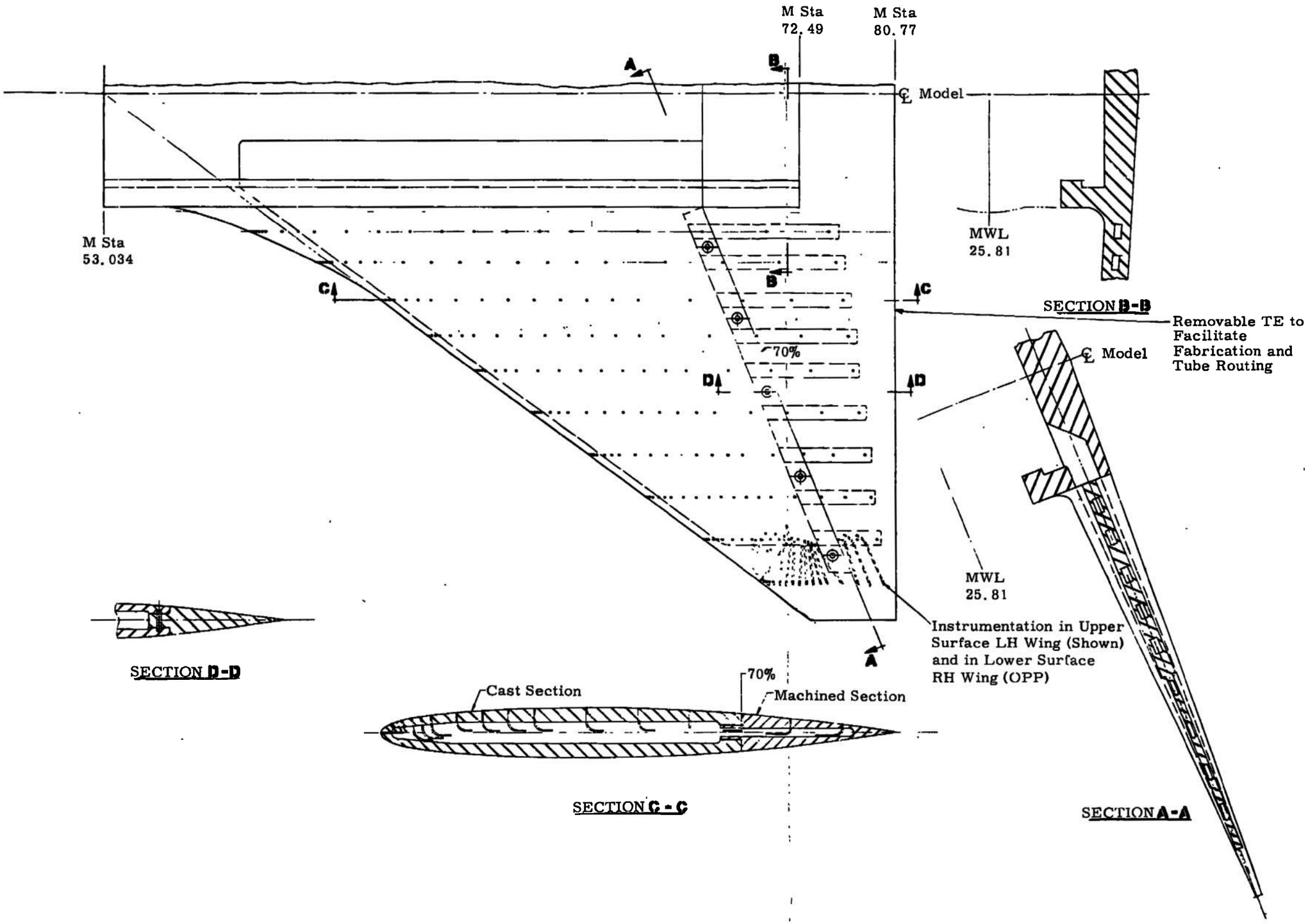


Figure 15. Space Shuttle Booster Pressure Wing

## 6.4 BASELINE MATERIAL SELECTION

Model cost and structural analyses were performed using one basic material for all model fabrication and another basic material for the stings. The present state-of-the-art materials selected for each task are:

a. Model details – PH 13-8 Mo steel; HT – H1000.

b. Stings – PH 13-8 Mo steel or 18Ni-300 grade (or -350 grade) maraging steel.

An analysis of candidate materials for use in the HIRT facility is presented in Section X.

## 6.5 SURFACE FINISH

The HIRT facility will produce very thin model boundary layers. As a consequence, surface roughness should be scaled down accordingly so that it does not contribute appreciably to drag or the momentum thickness of the boundary layer. The latter would influence the configuration characteristics associated with the shock boundary layer interaction.

For study purposes, Schlichting's admissible roughness criterion was used (Reference 6). Table 1 shows the admissible wing roughness for the study configurations. These values of roughness would pertain to a flat plate at zero incidence and should be a reasonable indication of leading edge requirements. Since the laminar sublayer will become larger with increasing distance from the leading edge, the admissible roughness will be increased.

The impact of the required surface finish qualities on the models is shown in Section XI, Table 9.

## 6.6 MISCELLANEOUS OBSERVATIONS

Special emphasis should be placed on some basic design rules when designing a model for a high Reynolds number test.

a. Careful attention should be given to the design of wing/fuselage attachment joints. Streamwise parting lines (located in the least critical flow area possible) should be used. It should be noted that the deflection between two parts in a joint under load is much more critical due to the added emphasis on surface finishes.

b. Basic split lines and attachments will greatly influence the ultimate surface finish achieved on the model. Tradeoff studies will be needed to obtain the maximum versatility/structural integrity/surface finish required for each test situation.

c. Each model must be analyzed to determine whether it is best to seal the internal model cavities or to provide passages for venting air from within the model to the tunnel during the start of a run. For example, calculations based on test condition 8, Table 2, (ATT model at M = 0.5, sea level, T = 300°K, storage pressure = 500 psia, Re/ft = 85.33 × $10^6$) indicate that approximately 0.06 second would be required to equalize the pressure of the volume of air (approximately 1,100 in.$^3$) of the nose cavity forward of the model balance through a 1.0-in.$^2$ venting duct.

Table 1. Admissible Roughness Estimates (Surface Finish)

| Condition | Advanced transonic transport | | | F-111 | Delta Canard | Space shuttle Booster |
|---|---|---|---|---|---|---|
| | Basic model 1/24 scale | 1.5 × size 1/16 scale | 2.0 × size 1/12 scale | 1/12 scale | 1/9.6 scale | 1/46.5 scale |
| MAC (ft) | 0.750 | 1.125 | 1.500 | 0.753 | 1.800 | 1.558 |
| $R_{e_{MAC}} \times 10^6$ | | | | | | |
| Cruise | 57.33 | 38.30 | 28.75 | 60.45 | 16.50 | 107.23 |
| Maneuver | 85.33 | 41.75 | 31.35 | 59.30 | 35.44 | 89.04 |
| Maneuver | 62.72 | | | 45.05 | 28.90 | 43.44 |
| $K_{admissible}$ (in.) | | | | | | |
| Cruise | 0.000020 | 0.000031 | 0.000042 | 0.000019 | 0.000072 | 0.000011 |
| Maneuver | 0.000014 | 0.000023 | 0.000038 | 0.000020 | 0.000034 | 0.000013 |
| Maneuver | 0.000019 | | | 0.000026 | 0.000042 | 0.000028 |

$$K_{ADM} = MAC \frac{100}{R_{e_{MAC}}} \text{ (Reference 6)}$$

$$\left.\begin{array}{l} 16\sqrt{} = 16 \text{ microinches } (0.000016) \\ 8\sqrt{} = 8 \text{ microinches } (0.000008) \\ 4\sqrt{} = 4 \text{ microinches } (0.000004) \end{array}\right\} \text{ (Reference 24)}$$

# SECTION VII

# TEST PLAN

## 7.1 TUNNEL USE

It is anticipated that a great demand for test time in the HIRT facility will result in a situation where testing will necessarily be restricted to tests that are very Reynolds-number dependent (as is the case with the Canadian N. A. E. high Reynolds number 15 in. x 60 in. two-dimensional facility). Hence, use of the HIRT facility will be somewhat unlike that of current transonic wind tunnels in that test plans will probably be much more operating envelope oriented or will concentrate on one particular test problem. It is current practice to test a configuration without particular regard to its flight envelope so that data is obtained beyond the limits that the flight article can achieve. Such practice cannot be justified for HIRT testing because of the impact of high model loads and model deformation. HIRT testing will best be carried out by testing in critical areas of the operation envelope to obtain the configuration performance (typically design point cruise and maneuvering parameters.)

## 7.2 OPERATING ENVELOPES

For the purpose of this study, the points of interest in an operation envelope are the maximum loading conditions, for if the model can be designed to take the full-scale $R_e$ at these conditions, it is feasible to test at full-scale $R_e$ throughout the envelope. Reynolds number ranges for the aircraft covered in this test plan are illustrated in Figure 16.

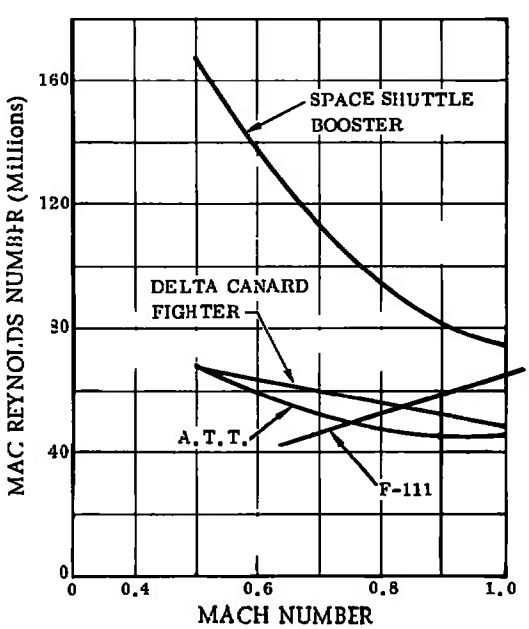


Figure 16. Reynolds Number Ranges of Aircraft Chosen for Study

Flight article operational envelopes for the four study configurations are shown in Figures 17 through 22. Two plots are presented for each configuration. The (a) plot shows $Re_{MAC}\ C_L$ as a function of Mach number and altitude up to the structural limit load factor. The critical high loading corners are readily apparent. The (b) plots show the HIRT tunnel dynamic pressures for the equivalent envelope.

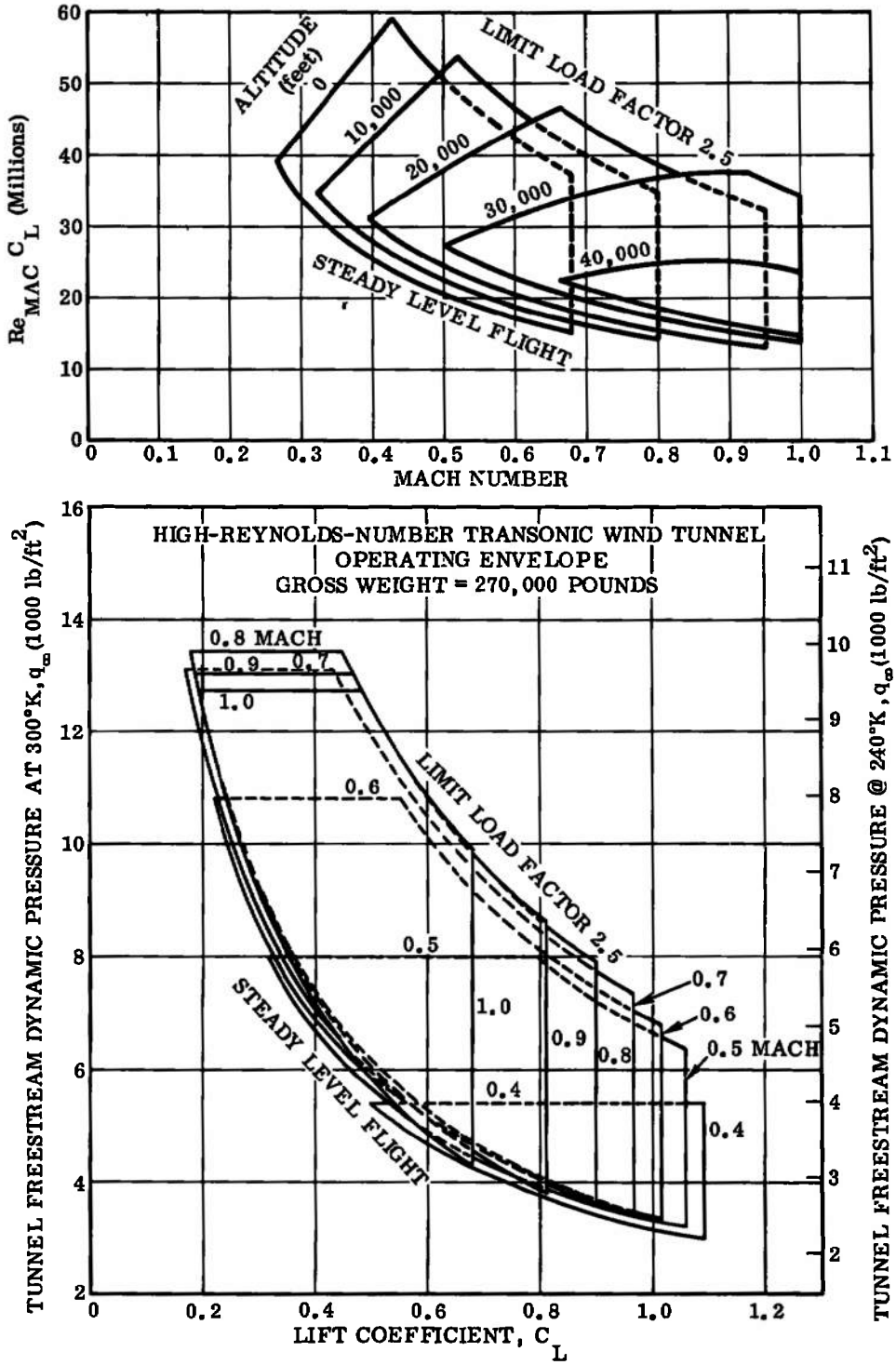


Figure 17. ATT Operating Envelope

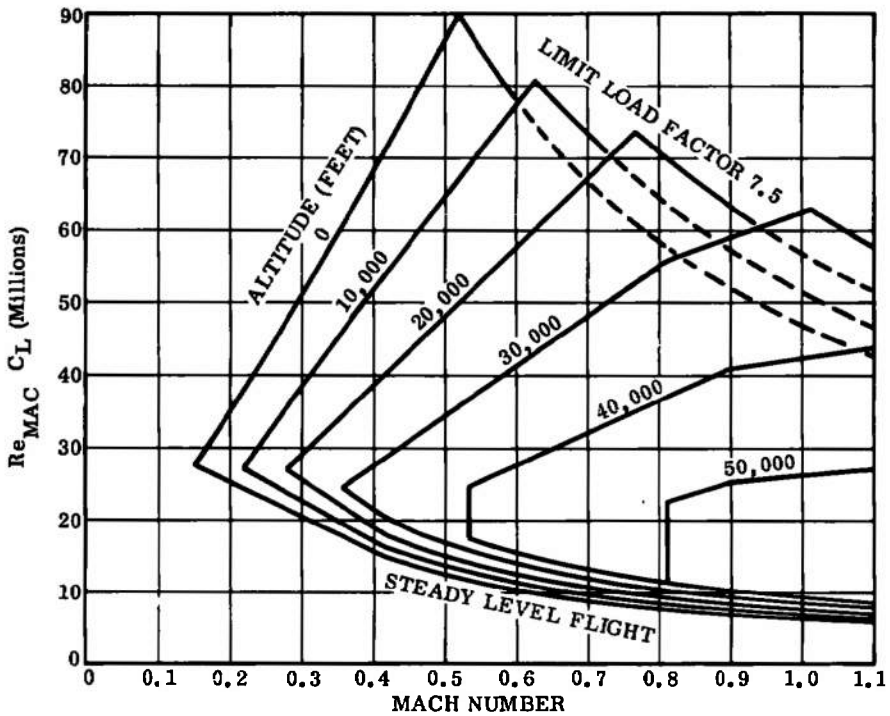


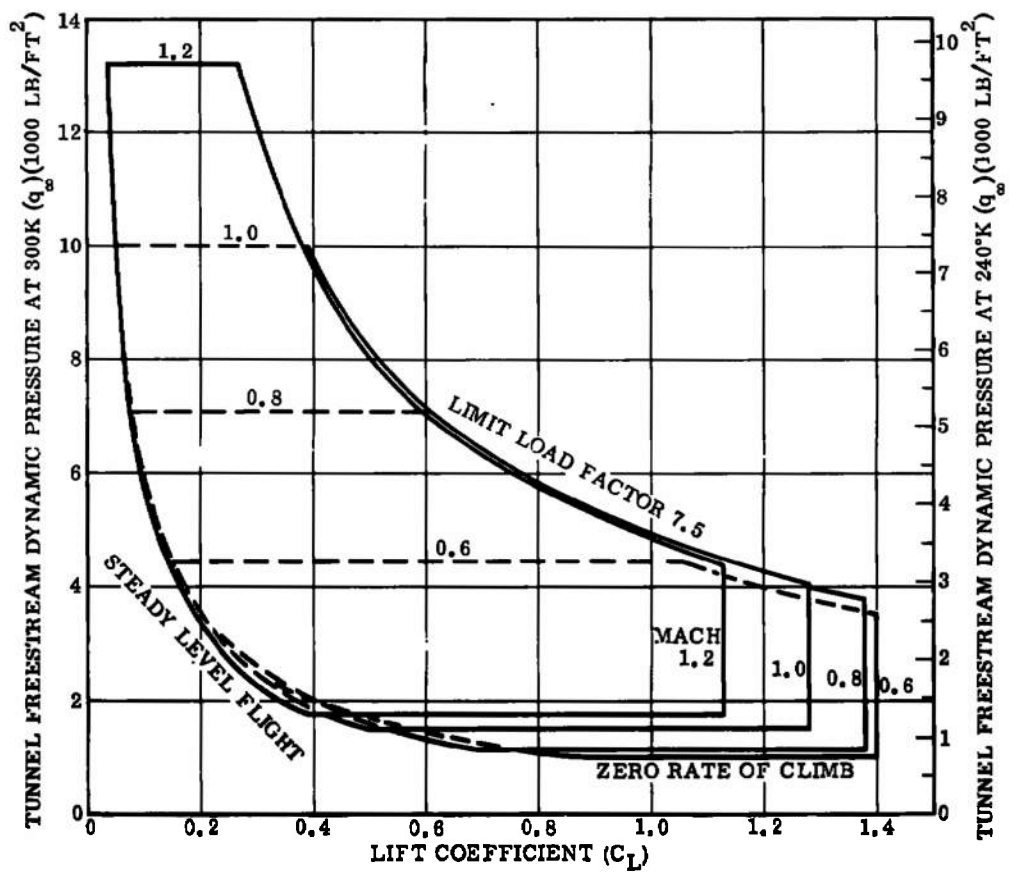


Figure 18. Delta Canard Operating Envelope

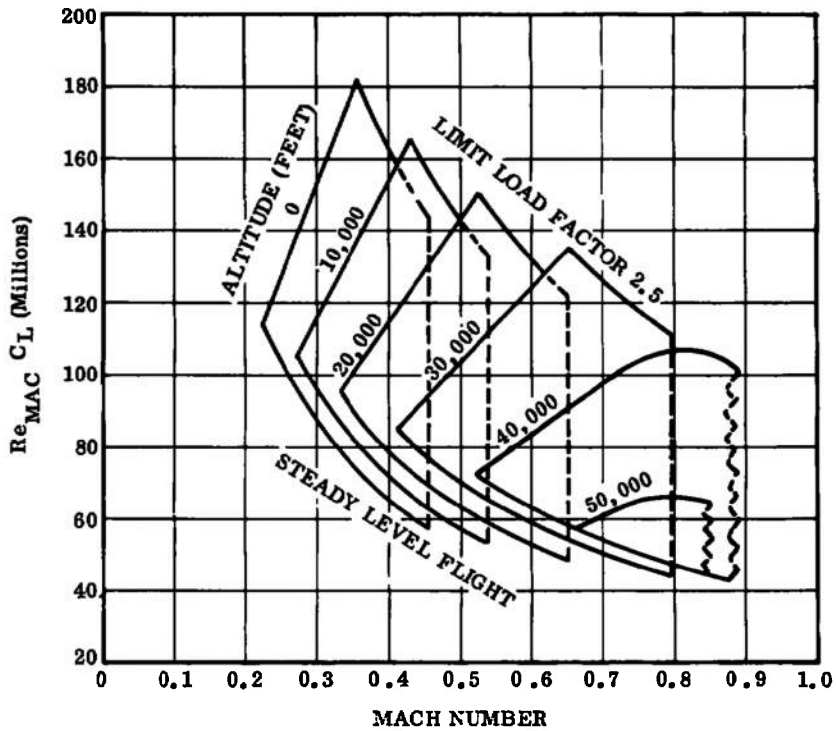


HIGH REYNOLDS NUMBER TRANSONIC WIND TUNNEL OPERATING ENVELOPE

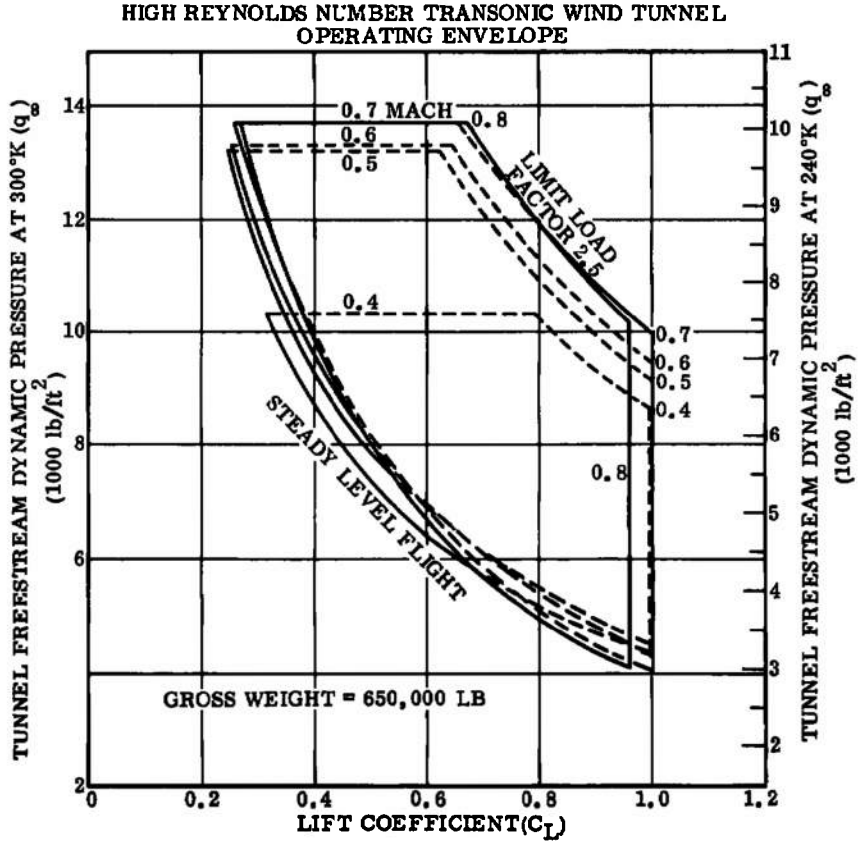


Figure 19. Space Shuttle Booster Operating Envelope

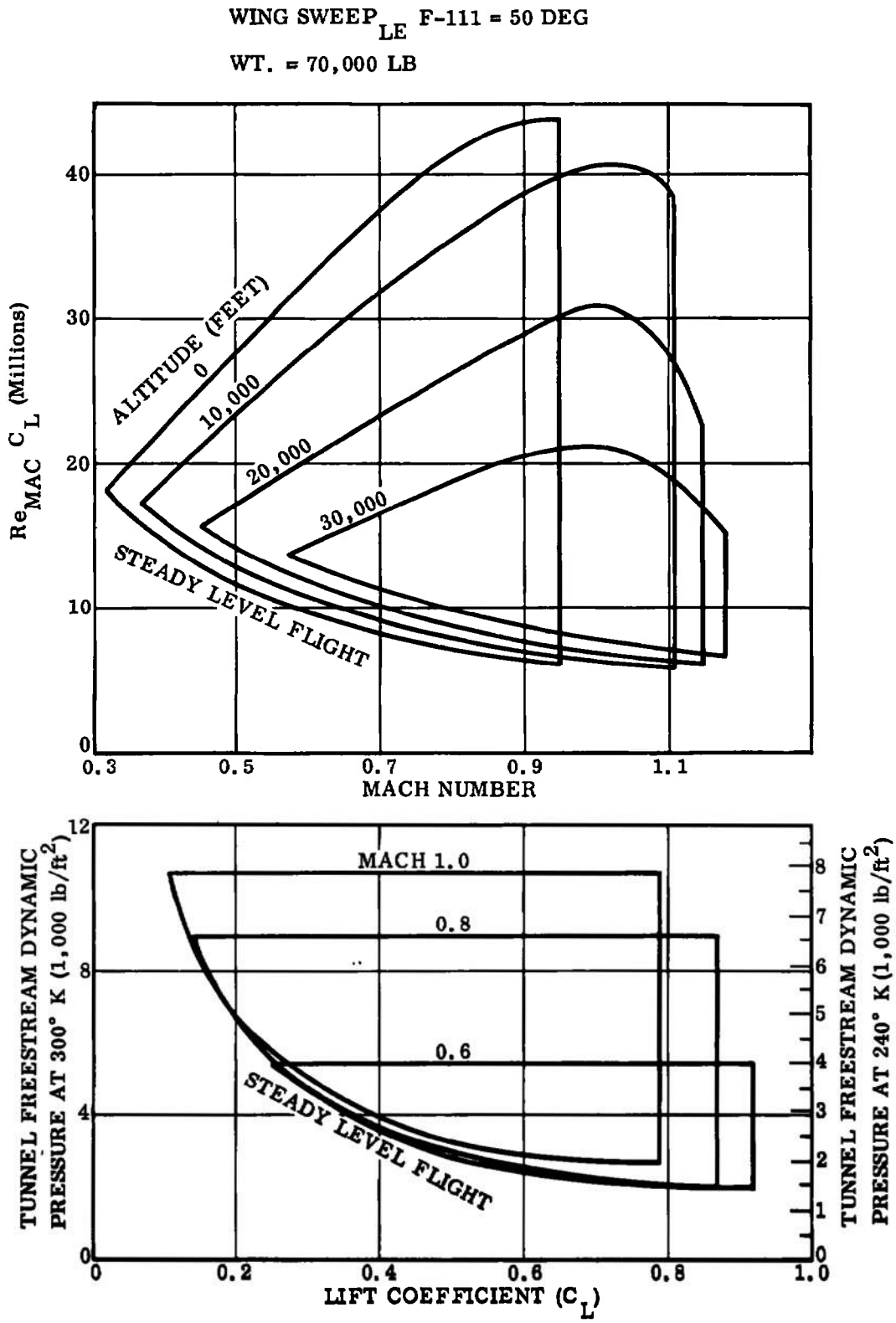


Figure 20. F-111 (50 deg) Operating Envelope

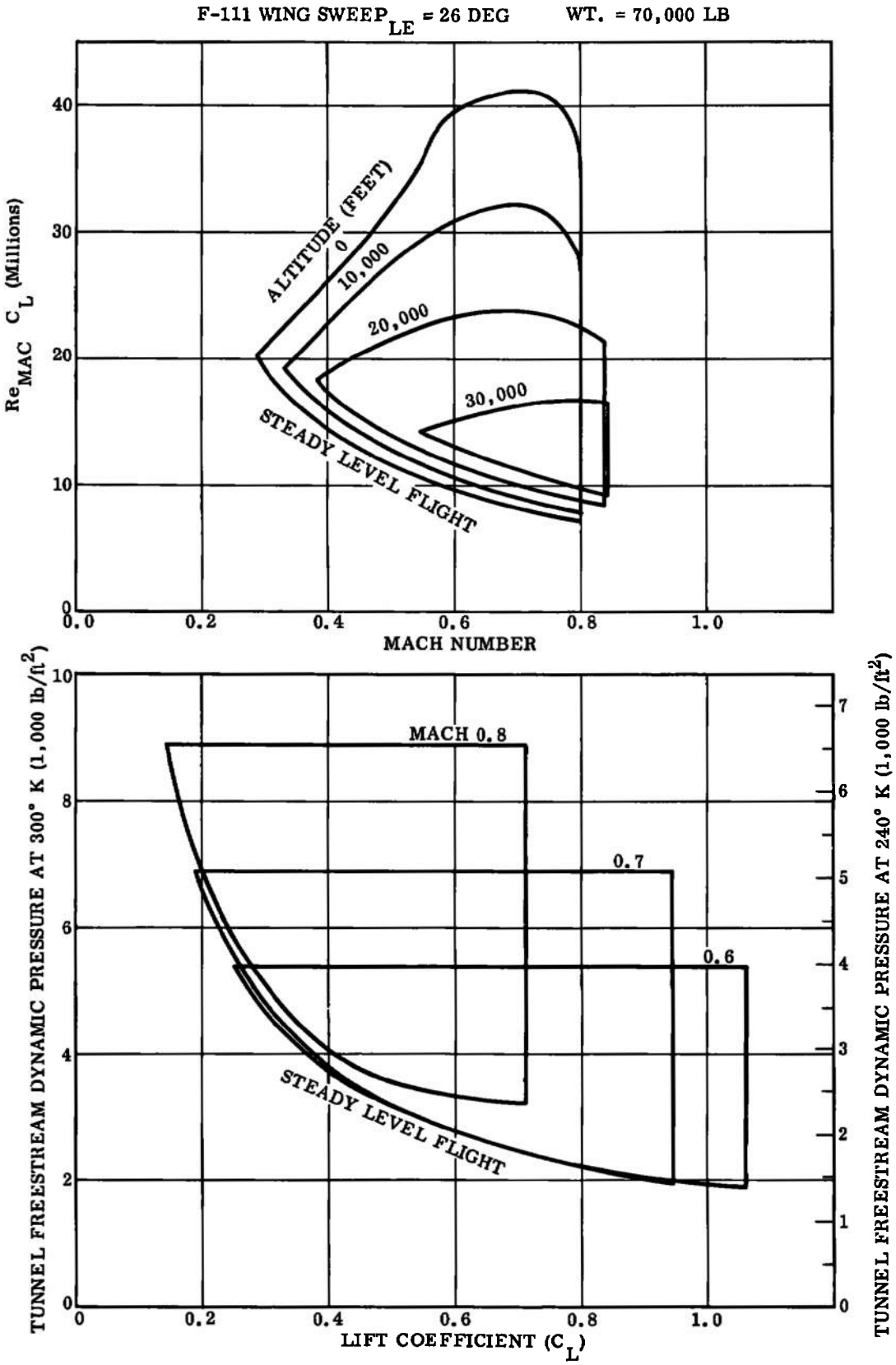


Figure 21. F-111 (26 deg) Operating Envelope

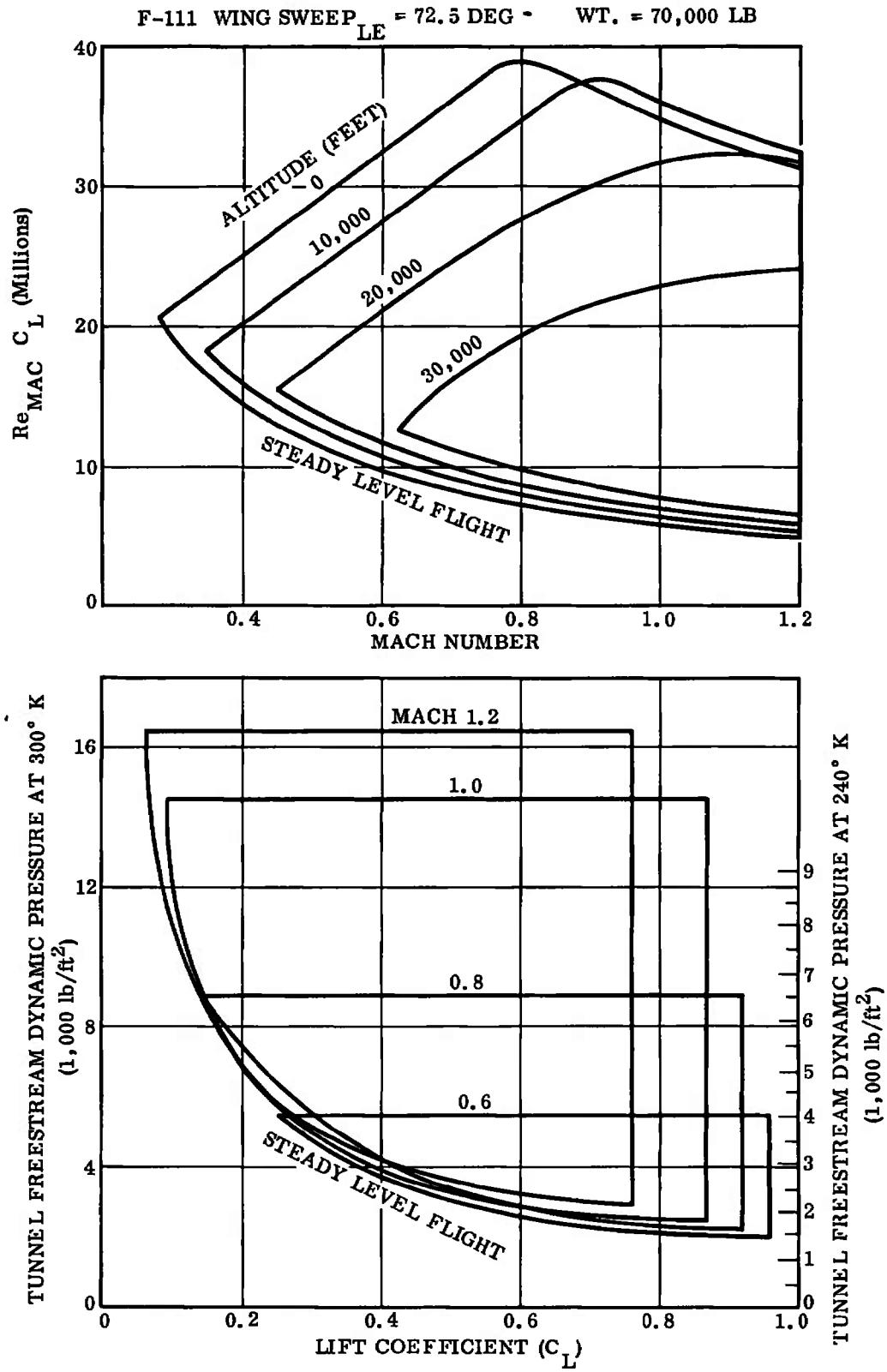


Figure 22. F-111 (72-1/2 deg) Operating Envelope

The conditions selected for detailed study are:

a. The maximum loaded condition the airplane could experience within its operating envelope.

b. A typical cruise condition.

c. Item a. (maximum loaded condition) with a reduced angle of attack or Reynolds number.

Note that Item c. is used if required for an acceptable stress level for a given model.

## 7.3 TEST PLAN DEVELOPMENT

Table 2, Test Plan, presents a summary of all the model test conditions selected for analysis in this study. Each of the test conditions was analyzed to determine:

a. Wing shear loads.

b. Wing pitching torques.

c. Wing bending moments.

d. Wing loading.

e. Wing distortions (vertical deflection and wing twist).

f. Wing section properties (EI, GJ).

g. Total model vertical force.

h. Model angle of attack.

i. Horizontal tail loads.

The results of each test condition were analyzed and the most pertinent information used to compute model stresses and distortions as presented in Sections VIII and IX.

## 7.4 DATA STORAGE

Complete computer printouts from program P4278 for each of the test conditions are on file at General Dynamics Convair Aerospace. A typical computer run (test condition 7 – 1/24 scale ATT at Mach 1.0, 2.5g maneuver, 30,000 feet, $R_e$/ft = $69.5 \times 10^6$, tunnel temperature = 240°K) is presented in Appendix I of this report.

# Table 2. Test Plan

| Model | Condition no. | Load factor (g) | Mach no. | Altitude ($10^3$ ft) | Tunnel temperature (degrees Kelvin) | Tunnel dynamic pressure (psi) | Tunnel storage pressure (psi) | Tunnel Model Re/ft (millions) | Model angle of attack (degrees) | Wing structural cross section (%) | Computer code | Run description |
|---|---|---|---|---|---|---|---|---|---|---|---|---|
| ATT (1/24 scale) | 1 | 2.5 | 0.5 | S. L. | 240 | 40.84 | 360 | 85.33 | 9.79 | 100 | A24-9 | Maneuver |
| | 2 | 2.5 | 0.5 | S. L. | 240 | 40.84 | 380 | 85.33 | 9.79 | 65 | A24-13 | Maneuver |
| | 3 | 1.0 | 1.0 | 35 | 240 | 43.75 | 190 | 57.53 | 3.55 | 100 | A24-1 | Cruise |
| | 4 | 1.0 | 1.0 | 35 | 240 | 43.75 | 190 | 57.63 | 3.55 | 65 | A24-11 | Cruise |
| | 5 | 1.0 | 1.0 | 30 | 240 | 52.76 | 225 | 69.5 | 3.23 | 100 | A24-3 | Cruise |
| | 6 | 1.75 | 1.0 | 30 | 240 | 52.76 | 225 | 69.5 | 5.59 | 100 | A24-5 | Intermediate |
| | 7 | 2.5 | 1.0 | 30 | 240 | 52.78 | 225 | 69.5 | 7.95 | 100 | A24-7 | Maneuver |
| | 8 | 2.5 | 0.5 | S. L. | 300 | 55.55 | 500 | 85.33 | 9.79 | 100 | A23-5 | Maneuver |
| | 9 | 1.0 | 1.0 | 35 | 300 | 57.64 | 250 | 57.53 | 3.55 | 100 | A23-1 | Cruise |
| | 10 | 1.0 | 1.0 | 30 | 300 | 69.60 | 300 | 69.5 | 3.23 | 100 | A23-2 | Cruise |
| | 11 | 1.75 | 1.0 | 30 | 300 | 69.60 | 300 | 69.5 | 5.59 | 100 | A23-3 | Intermediate |
| | 12 | 2.5 | 1.0 | 30 | 300 | 69.60 | 300 | 69.5 | 7.95 | 100 | A23-4 | Maneuver |
| F-111 (1/12 scale) | | | | | | | | | | | | |
| 50° | 13 | 6.0 | 0.9 | S. L. | 300 | 73.60 | 340 | 76.56 | 22.47 | 100 | F11-3 | Maneuver |
| 50° | 14 | 6.0 | 0.9 | S. L. | 240 | 54.12 | 255 | 76.55 | 22.47 | 100 | F13-4A | Maneuver |
| 50° | 15 | 6.0 | 0.9 | S. L. | 240 | 54.12 | 255 | 76.55 | 22.47 | 65 | F13-5A | Maneuver |
| 50° | 16 | 1.0 | 1.0 | 40 | 300 | 23.26 | 100 | 22.96 | 12.64 | 100 | F11-9 | Cruise |
| 50° | 17 | 1.0 | 1.0 | 40 | 240 | 17.10 | 60 | 22.96 | 12.64 | 100 | F13-10A | Cruise |
| 50° | 18 | 1.0 | 1.0 | 40 | 240 | 17.10 | 60 | 22.98 | 12.64 | 65 | F13-11A | Cruise |
| 26° | 19 | 5.2 | 0.75 | S. L. | 300 | 54.17 | 310 | 63.90 | 13.13 | 100 | F11-1 | Maneuver |
| 26° | 20 | 5.2 | 0.75 | S. L. | 240 | 39.83 | 235 | 63.90 | 13.13 | 100 | F13-2A | Maneuver |
| 72 1/2° | 21 | 6.0 | 1.0 | S. L. | 300 | 64.72 | 370 | 85.1 | 25.16 | 100 | F11-7 | Maneuver |
| 72 1/2° | 22 | 6.0 | 1.0 | S. L. | 240 | 62.29 | 270 | 85.1 | 25.16 | 100 | F13-8A | Maneuver |
| Delta canard fighter (1/9.6 scale) | 23 | 7.5 | 0.52 | S. L. | 300 | 22.92 | 240 | 35.44 | 31.03 | 100 | C01-1 | Maneuver |
| | 24 | 7.5 | 0.52 | S. L. | 240 | 16.85 | 210 | 35.44 | 31.03 | 100 | C02-2A | Maneuver |
| | 25 | 7.5 | 0.52 | S. L. | 240 | 16.65 | 210 | 35.44 | 31.03 | 65 | C02-3A | Maneuver |
| | 26 | 1.0 | 0.90 | 40 | 300 | 15.97 | 65 | 16.52 | 6.62 | 100 | C01-5 | Cruise |
| | 27 | 1.0 | 0.90 | 40 | 240 | 11.74 | 30 | 16.52 | 6.62 | 100 | C02-6A | Cruise |
| | 28 | 1.0 | 0.90 | 40 | 240 | 11.74 | 30 | 16.52 | 6.62 | 65 | C02-7A | Cruise |
| Space shuttle booster (1/46.5 scale) | 29 | 2.5 | 0.6 | 30 | 300 | 95.14 | 490 | 106.097 | 16.74 | 100 | S08-12 | Maneuver |
| | 30 | 2.5 | 0.6 | 30 | 240 | 70.83 | 360 | 106.097 | 16.74 | 100 | S09-14 | Maneuver |
| | 31 | 2.5 | 0.8 | 30 | 240 | 70.83 | 360 | 106.097 | 16.74 | 70 | S09-16 | Maneuver |
| | 32 | 2.5 | 0.3 | S. L. | 300 | 46.61 | — | 99.04 | 38.21 | 100 | S07-10A | Landing |
| | 33 | 2.5 | 0.3 | S. L. | 240 | 35.74 | — | 99.04 | 36.21 | 100 | S07-5A | Landing |
| | 34 | 2.5 | 0.3 | S. L. | 240 | 35.74 | — | 99.04 | 36.21 | 70 | S07-6A | Landing |
| | 36 | 2.5 | 0.3 | S. L. | 300 | 46.61 | — | 99.04 | 38.21 | 70 | S07-11A | Landing |
| | 36 | 2.5 | 0.6 | 30 | 300 | 95.14 | 490 | 106.097 | 16.74 | 70 | S09-15 | Maneuver |
| ATT 1/16 scale | 37 | 1.0 | 1.0 | 30 | 240 | 35.4 | 225 | 69.5 | 3.23 | 100 | A27-21 | Cruise |
| 1/16 scale | 38 | 2.5 | 1.0 | 30 | 240 | 35.4 | 225 | 69.5 | 7.95 | 100 | A27-22 | Maneuver |
| 1/12 scale | 39 | 1.0 | 1.0 | 30 | 240 | 26.5 | 225 | 69.5 | 3.23 | 100 | A27-25 | Cruise |
| 1/12 scale | 40 | 2.5 | 1.0 | 30 | 240 | 26.5 | 225 | 69.5 | 7.95 | 100 | A27-26 | Maneuver |
| 1/16 scale | 41 | 1.0 | 1.0 | 30 | 300 | 47.2 | 300 | 69.5 | 3.23 | 100 | A27-19 | Cruise |
| 1/16 scale | 42 | 2.5 | 1.0 | 30 | 300 | 47.2 | 300 | 69.5 | 7.95 | 100 | A26-20 | Maneuver |
| 1/12 scale | 43 | 1.0 | 1.0 | 30 | 300 | 35.4 | 300 | 69.5 | 3.23 | 100 | A27-23 | Cruise |
| 1/12 scale | 44 | 2.5 | 1.0 | 30 | 300 | 35.4 | 300 | 69.5 | 7.95 | 100 | A27-24 | Maneuver |
| 1/24 scale | 7a | 2.5 | 1.0 | 30 | 240 | 22.7 | 225 | 69.5 | 7.95 | 100 | A29-7a | Maneuver |
| 1/24 scale | 7b | 2.5 | 1.0 | 30 | 240 | 30.3 | 225 | 69.5 | 7.95 | 100 | A29-7b | Maneuver |
| 1/24 scale | 7c | 2.5 | 1.0 | 30 | 240 | 37.9 | 225 | 69.5 | 7.95 | 100 | A29-7c | Maneuver |
| Full scale | 5x | 1.0 | 1.0 | 30 | — | — | — | — | 3.23 | — | 3 ATT | Cruise |
| Full scale | 6x | 1.75 | 1.0 | 30 | — | — | — | — | 5.59 | — | 5 ATT | Intermediate |
| Full scale | 7x | 2.5 | 1.0 | 30 | — | — | — | — | 7.95 | — | 7 ATT | Maneuver |

# SECTION VIII

# AEROELASTIC ANALYSIS

## 8.1 METHODS

Considerable aeroelastic deformation of models in the HIRT facility are a certainty. A means of accounting for the model elasticity is necessary before the test data can be rationally applied to the full-scale design problem. Simultaneous solution of equations that contain both the aerodynamic influence function and the structural influence function are necessary for this task. A method and digital program, P4278, (Reference 7) in FORTRAN IV language for computing steady-state spanwise load distribution on an elastic airplane wing for specified airplane weights and load factors was used to accomplish this analysis. The method is based on a modification of the Weissinger L-Method, from theory originally developed for subsonic flow. It is valid for supersonic flight, providing that the flow over the wing is subsonic (this is a possible case for swept wings that operate in the low supersonic Mach number range in which the shock cone lines are ahead of the leading edge and no other shocks are generated on the wing.) Program 4278 capabilities include the effects of external stores, fuselage, and tail boom on spanwise loading.

The Weissinger L-Method of digital program 4278 is an outgrowth of NACA TN 3030 (Reference 8). Surveys and texts on the methods of calculating aerodynamic loads on aircraft structures invariably reference TN 3030. TN 3030 was used in the design of the CV880 and CV990 jet transports, and more recently Boeing employed this method in the design analysis of the 747 transport. Approximately one-half of the technical papers being written today on the subject of interaction between fuselage and wing make use of the principle of image vortices as described by Gray, Schenk, and Lennertz. The Air Force Flight Dynamics Laboratory has revived interest in this method (References 9 and 10). More recently Blackwell at NASA Langley extended the method to include sidewash and backwash (Reference 11) in addition to the usual downwash.

Convair Aerospace continues to use the Weissinger L-Method in proposal work for subsonic aircraft and transonic wings that have enough leading edge sweep so that the Mach cone lies ahead of the wing.

The digital program performs symmetric and asymmetric balances and then distributes the shears, moments, and torques over the vehicle for each condition. Angles of attack along the wing span are calculated for checking stall characteristics and for recommendation of the wing twist to counter this problem.

Program 4278 was used to provide design loads for each model and the corresponding deformations due to twisting and bending. Program 4278 is a strip theory program and solves the aeroelastic distribution of a load in a single run on the digital computer.

Model geometries used for the aeroelastic analyses are presented in computer format in Figure 23.

In order to determine the distributed loads and aeroelastic deflections, the rigid aerodynamic characteristics of the study configurations were determined. This was accomplished by using wind-tunnel data, when it was available, and DATCOM (Reference 12).

Each design test point as shown in Table 2 was analyzed and the following data were plotted using the conventional SC4020 plotting output:

a. Shear load (air + inertia).

* b. Bending moment and pitching torque (air + inertia)

c. Wing loading ($C_L cq$) (air only)

d. Wing vertical deflection (y)

e. Elastic wing twist ($\theta$)

Note that all plots are presented versus wing semispan.

A typical computer printout is included in the appendix of this report.

## 8.2 TUNNEL OPERATING CONDITIONS INFLUENCE ON MODEL LOADS

### 8.2.1 Cooled Storage Air

Tunnel operating conditions were obtained from a set of estimated flow property curves for the proposed HIRT facility (Reference 13). These curves were supplied by the government for use in this study. Dynamic pressure ($q_\infty$) versus Reynolds number per foot ($R_e$/ft) for two storage temperatures, ambient (300°K) and cooled (-30°F, 240°K) are presented in Figures 24 and 25. Since Reynolds number is very sensitive to free-stream temperature, a significant lowering of dynamic pressure can be obtained by using cooled storage air. Figure 26 illustrates the effects of cooled air versus ambient air on the elastic twist, deflection of the wing, maximum wing stress, and the maximum lift force on the ATT model.

Note that model loads are based on using 240°K storage air unless noted otherwise.

### 8.2.2 Model Problems Due to Temperature

Running models in a 240°K (-30°F) environment does not present any large physical problems. Model material selection must be accomplished with the temperature in mind. The material selected for use as a baseline material for this study (PH 13-8 Mo steel) has few restrictions at these temperatures (Reference Section X).

* Bending moments & torque taken about wing elastic axis (see Figure 23 for E.A. location).

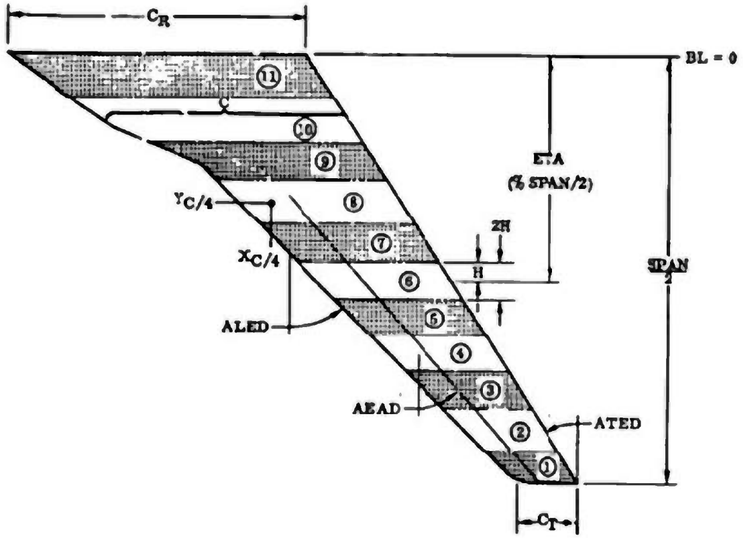


**LEGEND**

ETA = DISTANCE FROM BL = 0 TO CENTER OF STRIP (% SEMISPAN)
C = CHORD LENGTH AT A GIVEN ETA
2H = WIDTH OF STRIP
$X_{C/4}$ = FUSELAGE STATION LOCATION OF QUARTER CHORD OF AIRFOIL AT ETA
$Y_{C/4}$ = BUTTOCK LINE LOCATION OF QUARTER CHORD OF AIRFOIL AT ETA
$Z_{C/4}$ = WATER LINE LOCATION OF QUARTER CHORD OF AIRFOIL AT ETA
EA = ELASTIC AXIS (% CHORD)
ALED = SLOPE OF WING LEADING EDGE (deg)
AEAD = SLOPE OF ELASTIC AXIS (deg)
ATED = SLOPE OF WING TRAILING EDGE (deg)

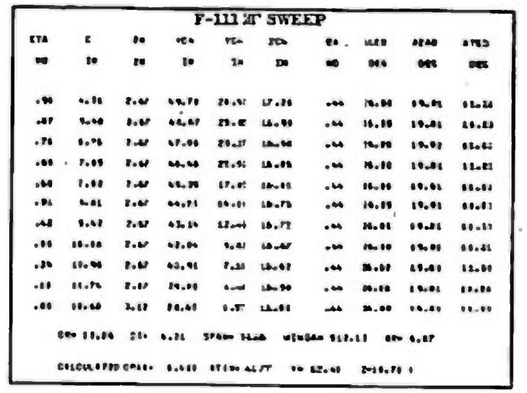


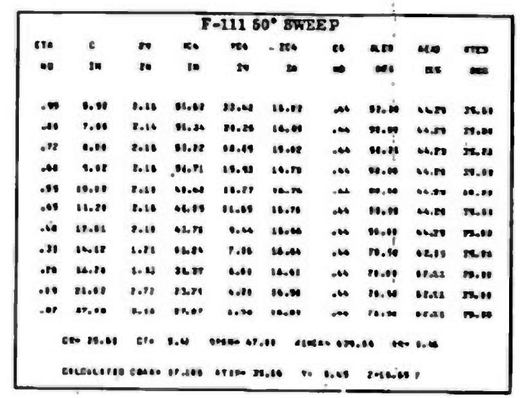


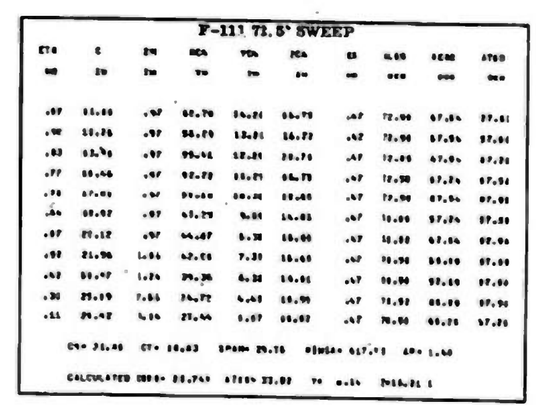


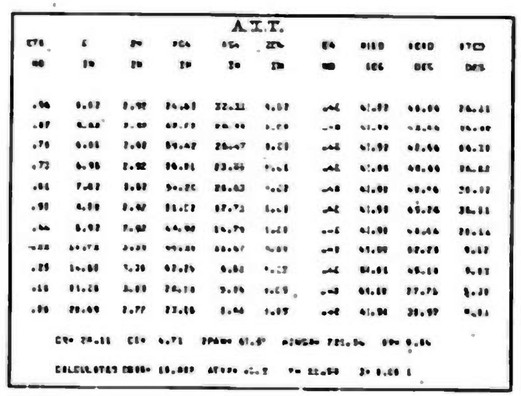


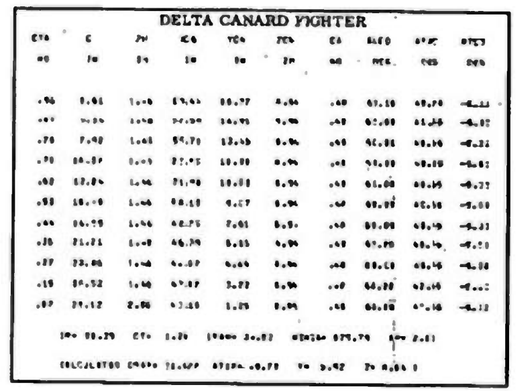


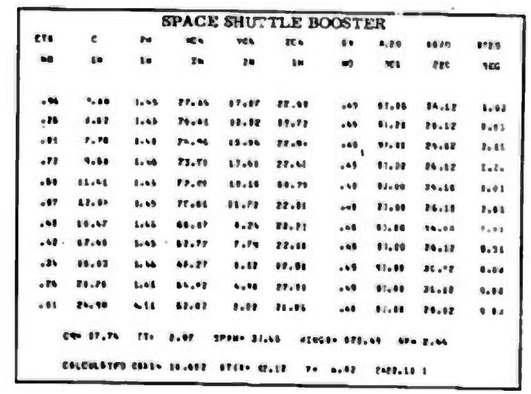


Figure 23. Aeroelastic Program Geometry

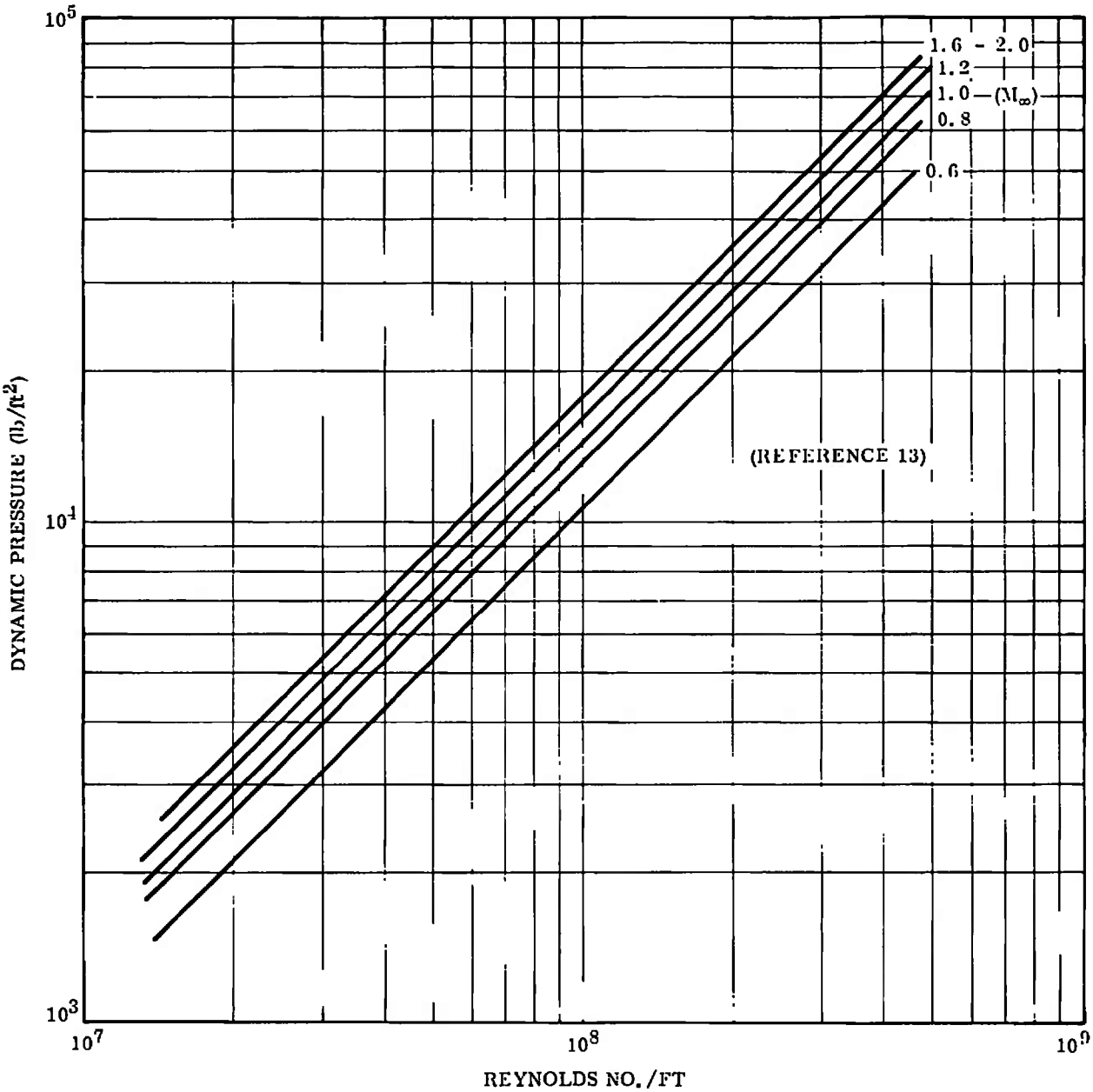


Figure 24. Reynolds Number vs Dynamic Pressure at 300°K

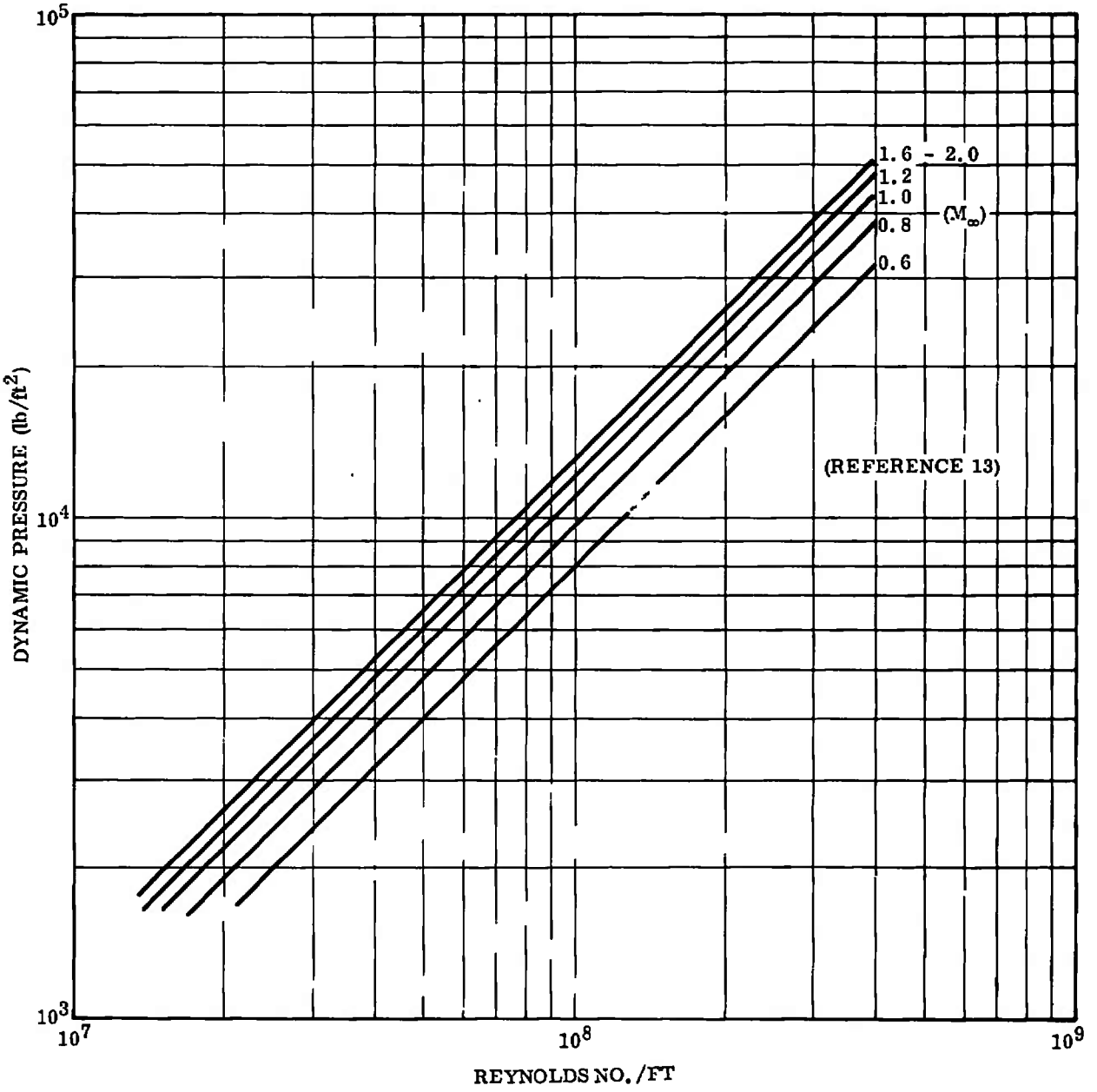


Figure 25. Reynolds Number vs Dynamic Pressure at 240°K

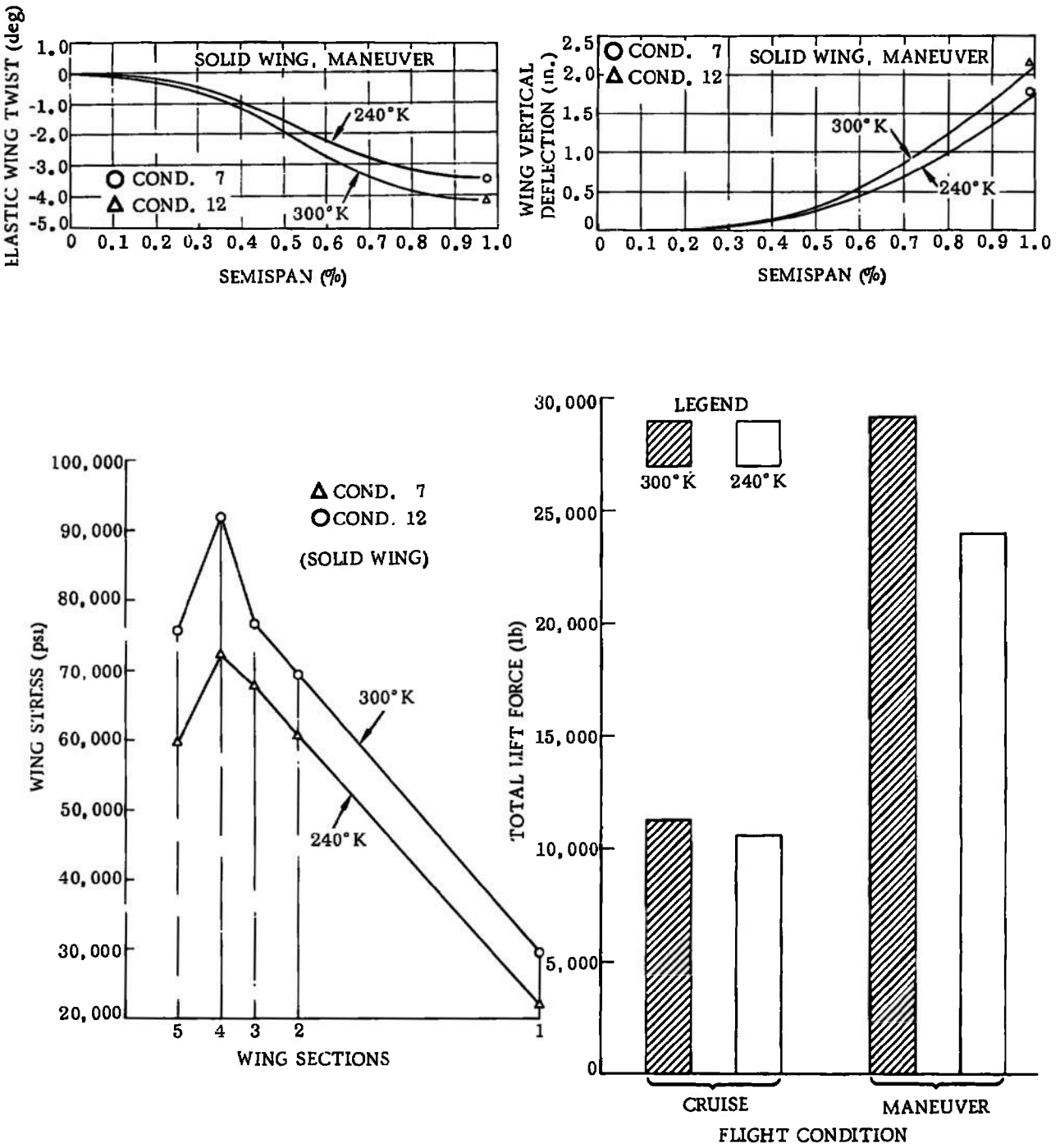


**Figure 26. ATT — Effects of 300°K vs 240°K Tunnel Operation**

Model balances and onboard instrumentation, such as pressure transducers, will have to be temperature compensated and/or thermally protected to minimize temperature effects.

Model change procedures must be developed to handle -30°F models.

## 8.3 MODEL LOADS

Model loads were computed using Program 4278 supplemented by hand calculations as required. Loads are based on actual or estimated operating envelopes for each of the aircraft configurations. These operating envelopes were presented in Figures 17 through 22. Wing shear, bending moment, pitching torque, and $C_L cq$ (wing loading) were computed for each model configuration and condition shown in the test plan (Table 2). These data were used for all structural analysis work.

All model loads are based on steady-state conditions only.

### 8.3.1 ATT Model – Wing Loads

Loads for the Advanced Technology Transport configuration were computed for several test points. Low-speed, low-altitude maneuvering; high-speed, high-altitude maneuvering, and various high speed cruise conditions. Test plan (Table 2) conditions 5, 6 and 7, (Figures 27 through 29) were selected as most representative of cruise, mid-maneuver (1.75g) and maximum maneuver (2.5g) conditions. Loads for conditions 1 and 3 are presented in Figures 30 and 31.

The ATT configuration was selected to explore the results of increasing the model scale by 150% and 200%. The loads resulting from these model scales are shown in Figures 32 through 35.

### 8.3.2 F-111 Model – Wing Loads

The 50-degree wing sweep version of the F-111 is the highest loaded configuration. Loads for a 40,000-foot cruise and a sea-level, 6-g maneuver condition are shown in Figures 36 and 37. Maximum maneuvering loads for the 26-degree sweep and 72-1/2-degree sweep configurations are presented in Figures 38 and 39.

### 8.3.3 Delta Canard Fighter – Wing Loads

The loads for this delta-wing fighter are shown in Figures 40 and 41. A 40,000-foot cruise condition and a sea-level, 7.5-g maneuvering condition are represented.

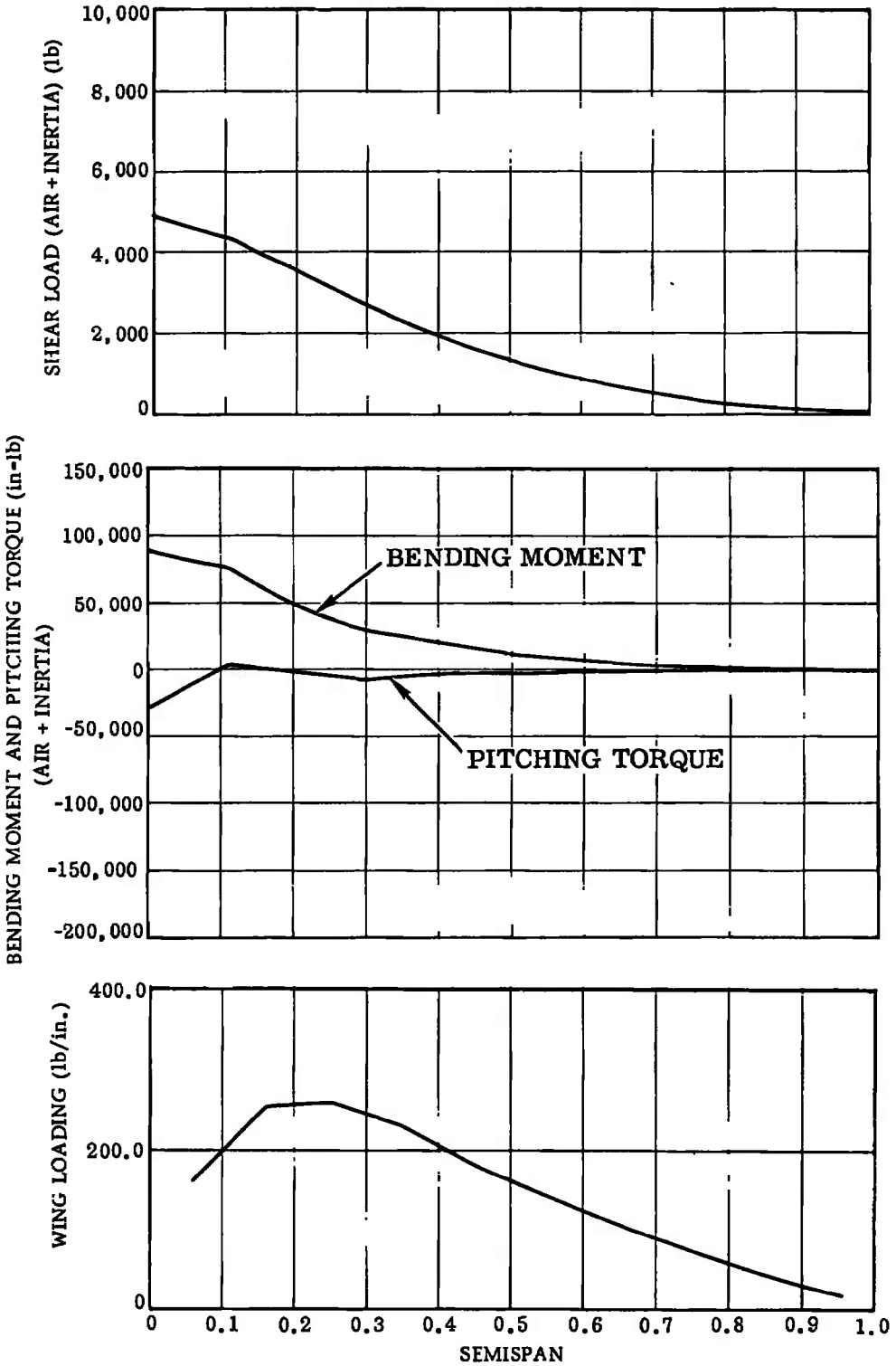


Figure 27. ATT — Model Loads – Condition 5

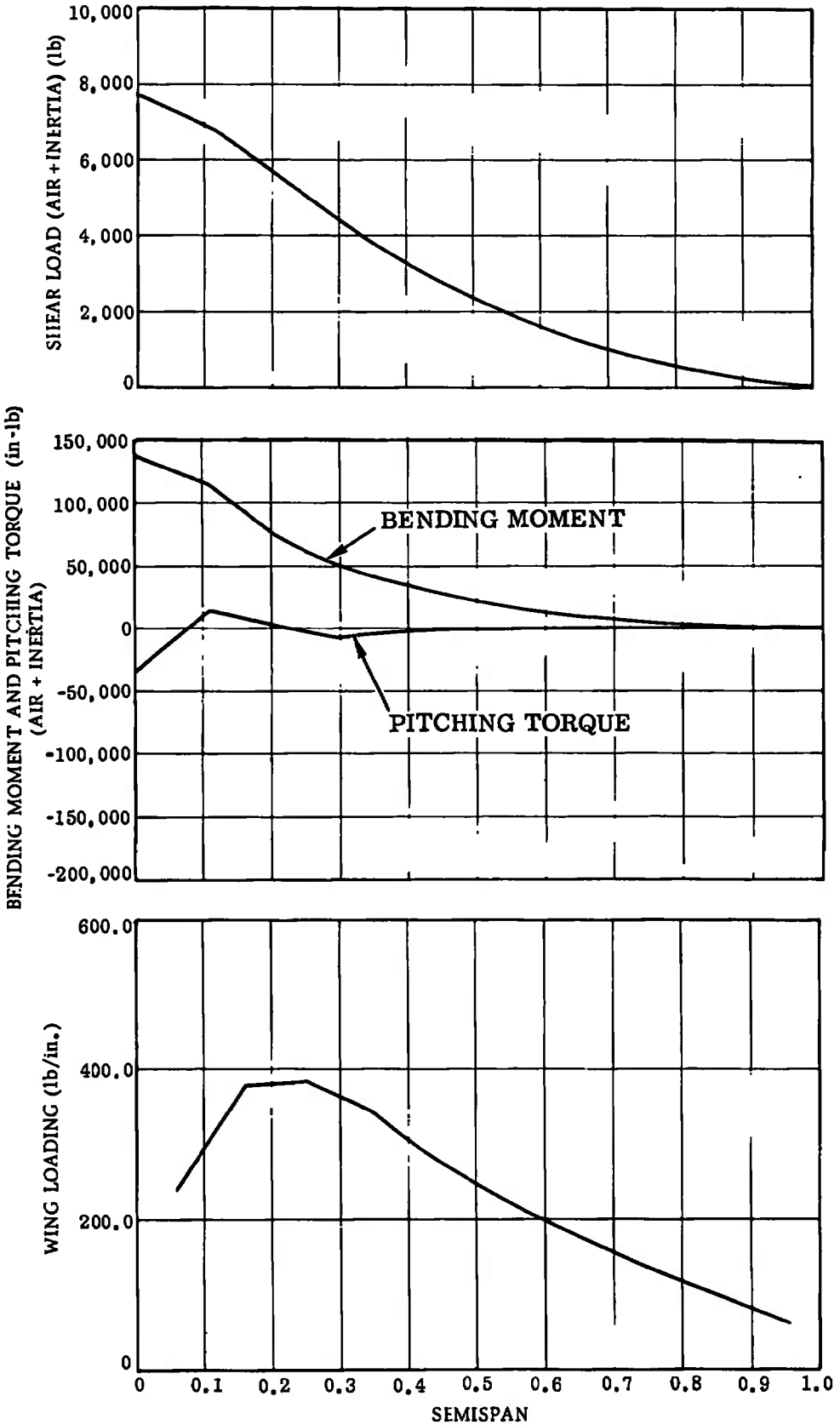


Figure 28. ATT – Model Loads – Condition 6

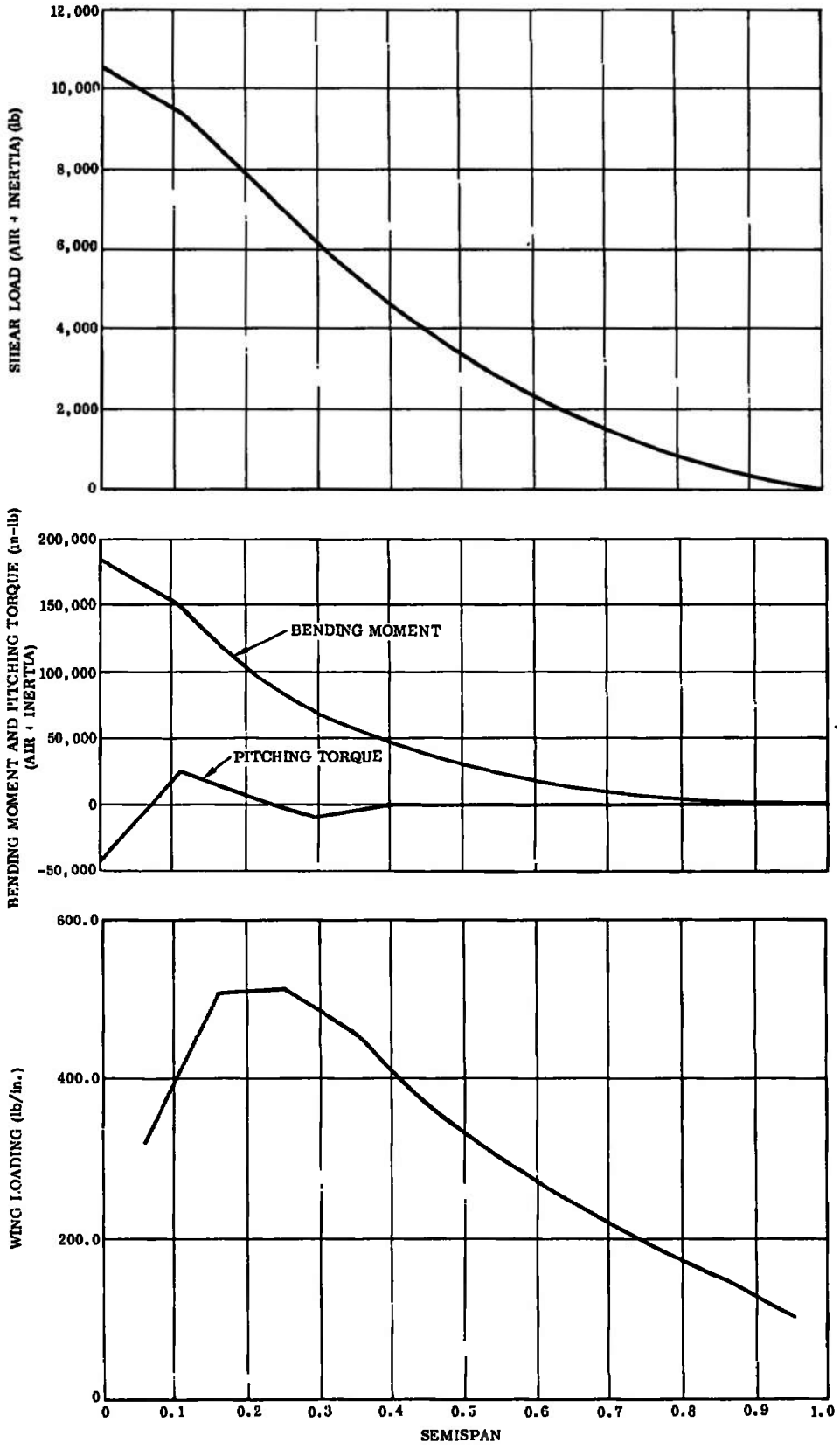


Figure 29. ATT — Model Loads — Condition 7

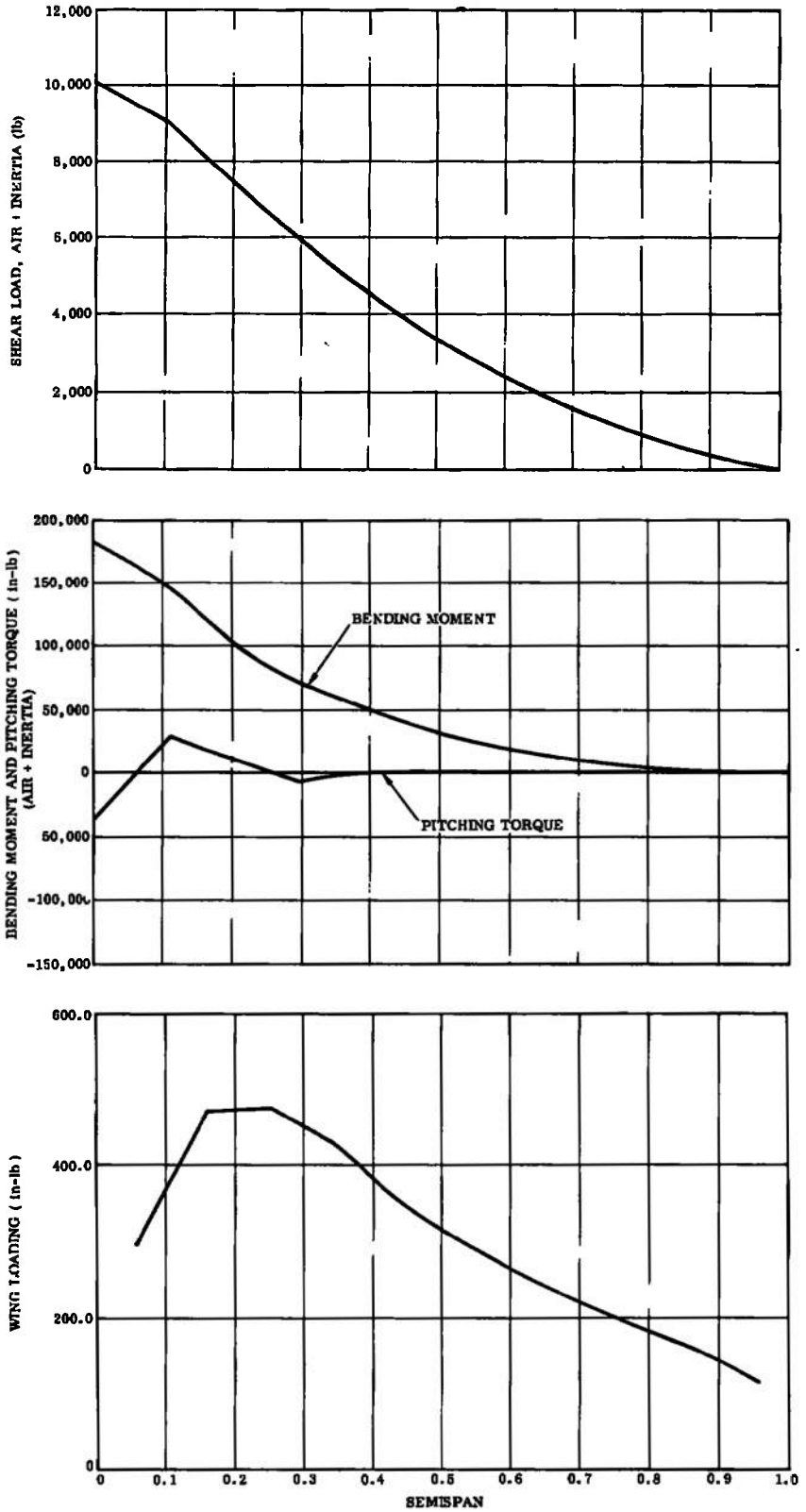


Figure 30. ATT — Model Loads — Condition 1

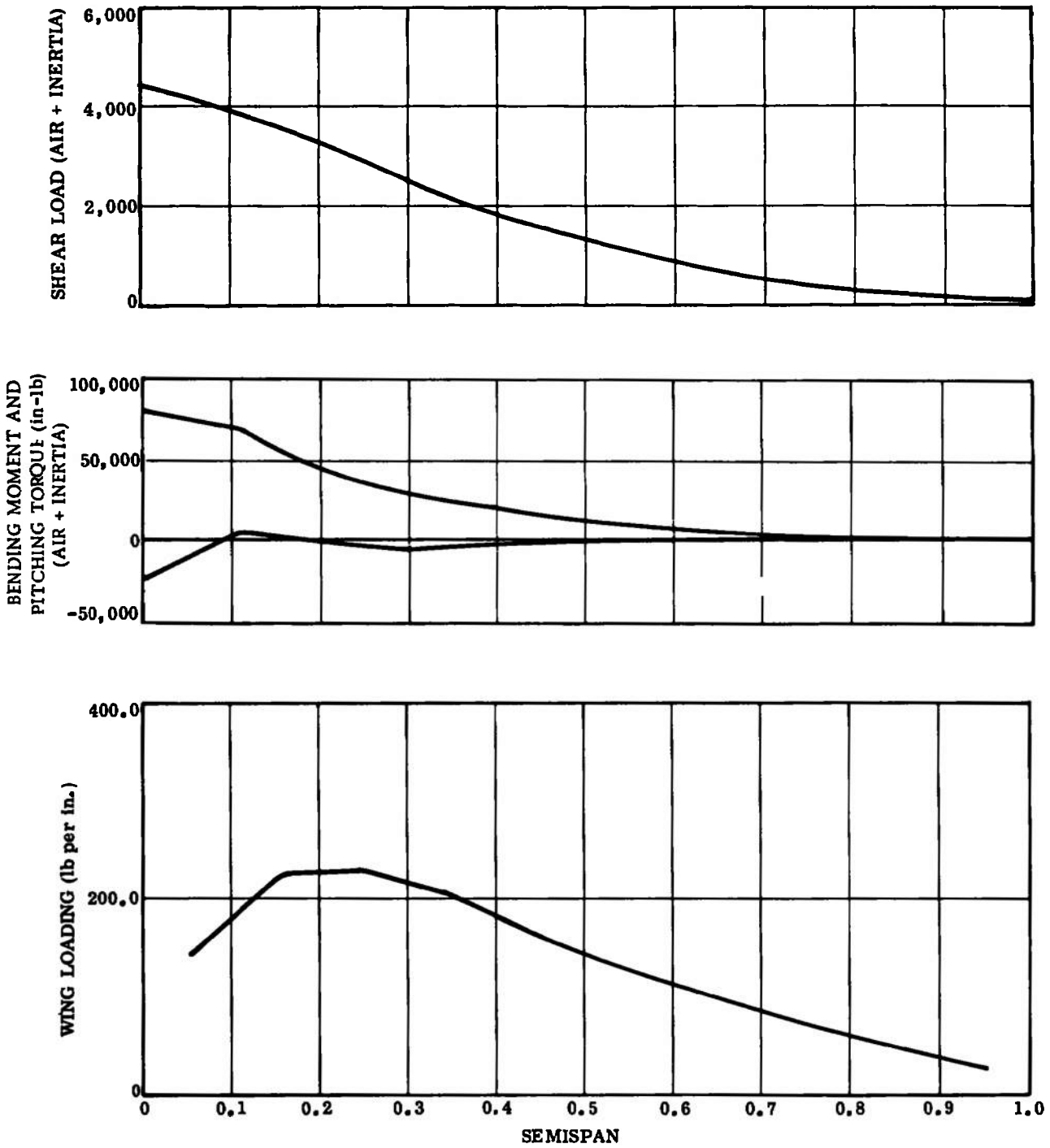


Figure 31. ATT – Model Loads – Condition 3

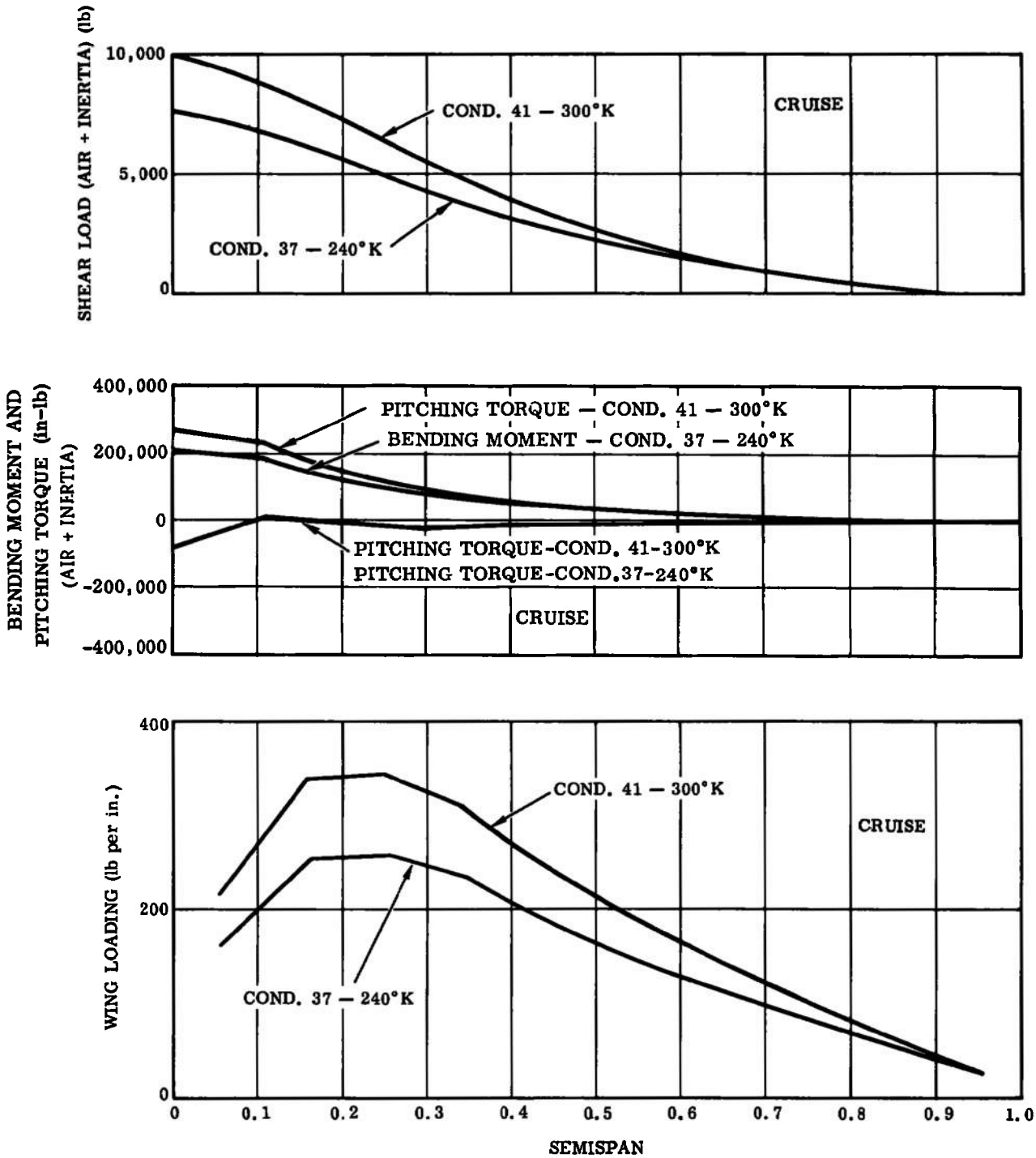


Figure 32. ATT — Model Loads, 1/16 Scale — Conditions 37 and 41

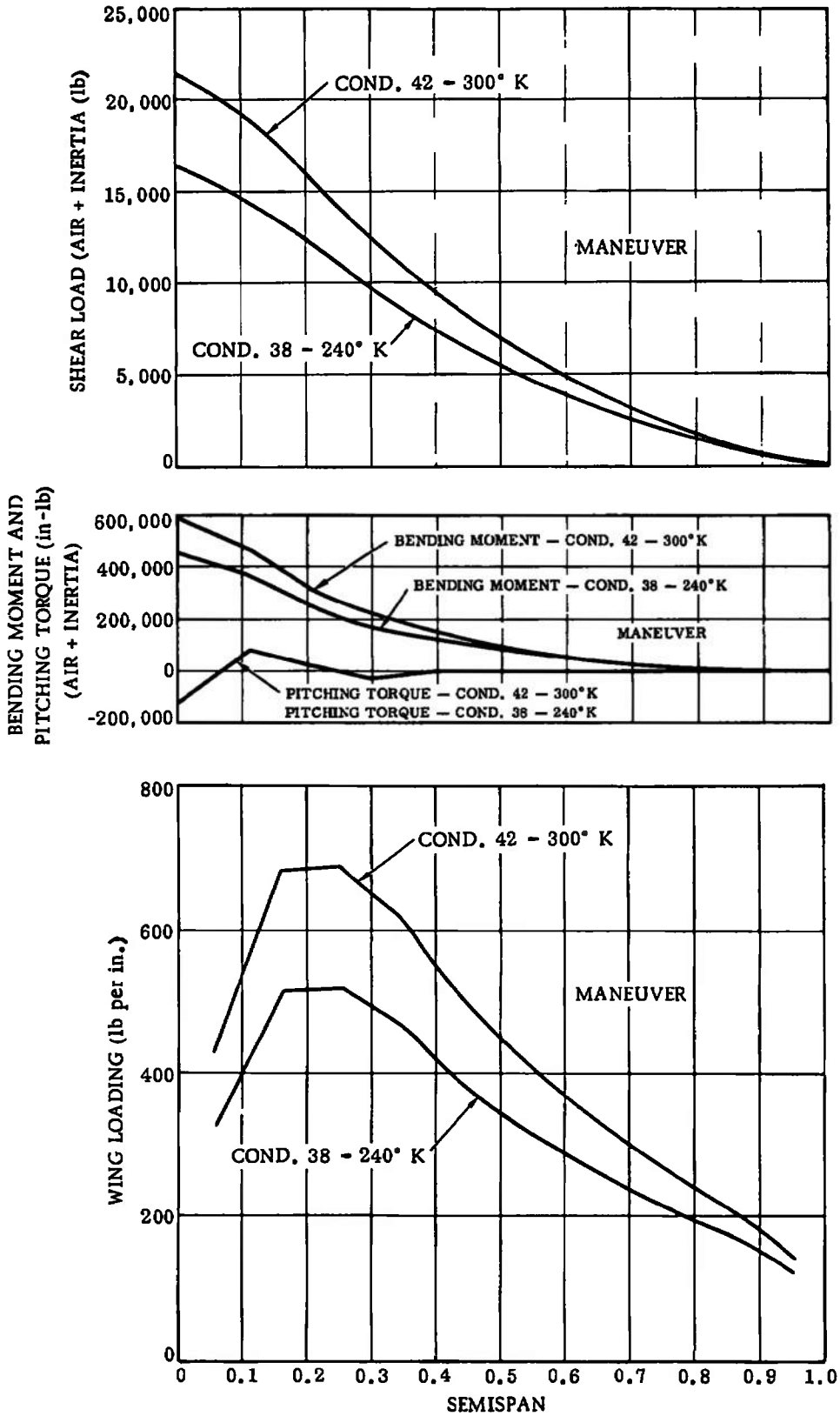


Figure 33. ATT – Model Loads, 1/16 Scale – Conditions 38 and 42

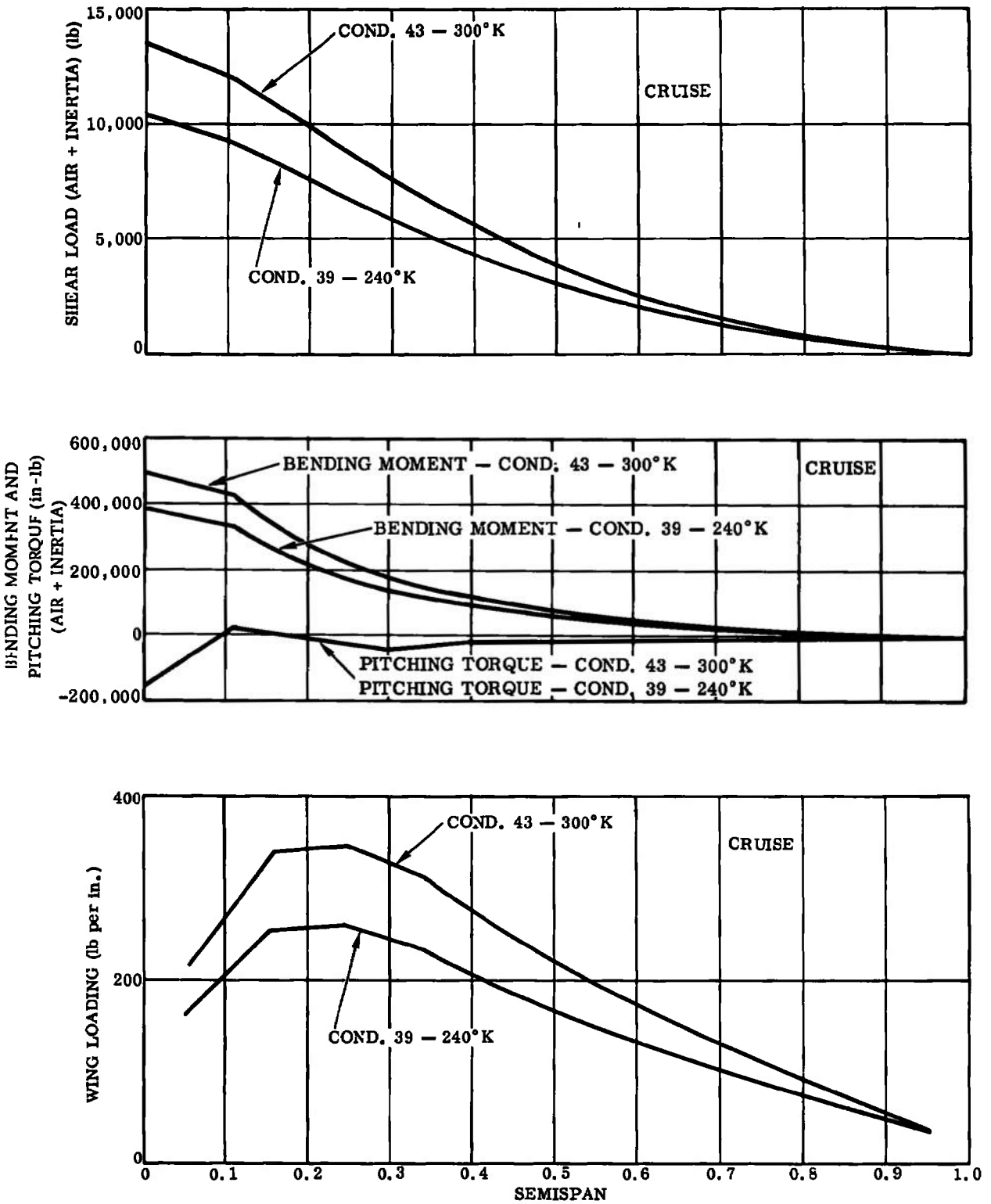


Figure 34. ATT – Model Loads, 1/12 Scale — Conditions 39 and 43

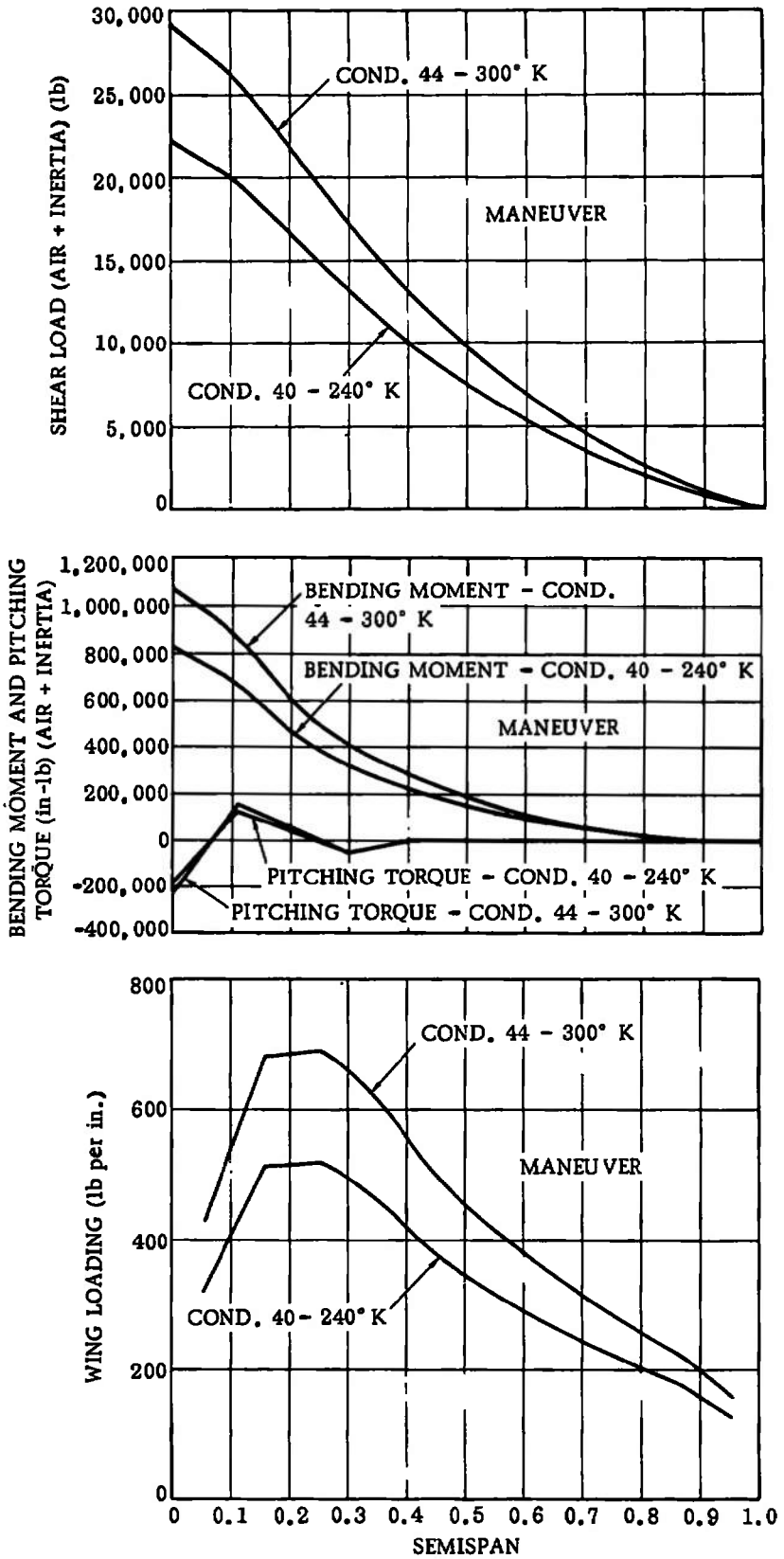


Figure 35. ATT – Model Loads, 1/12 Scale – Conditions 40 and 44

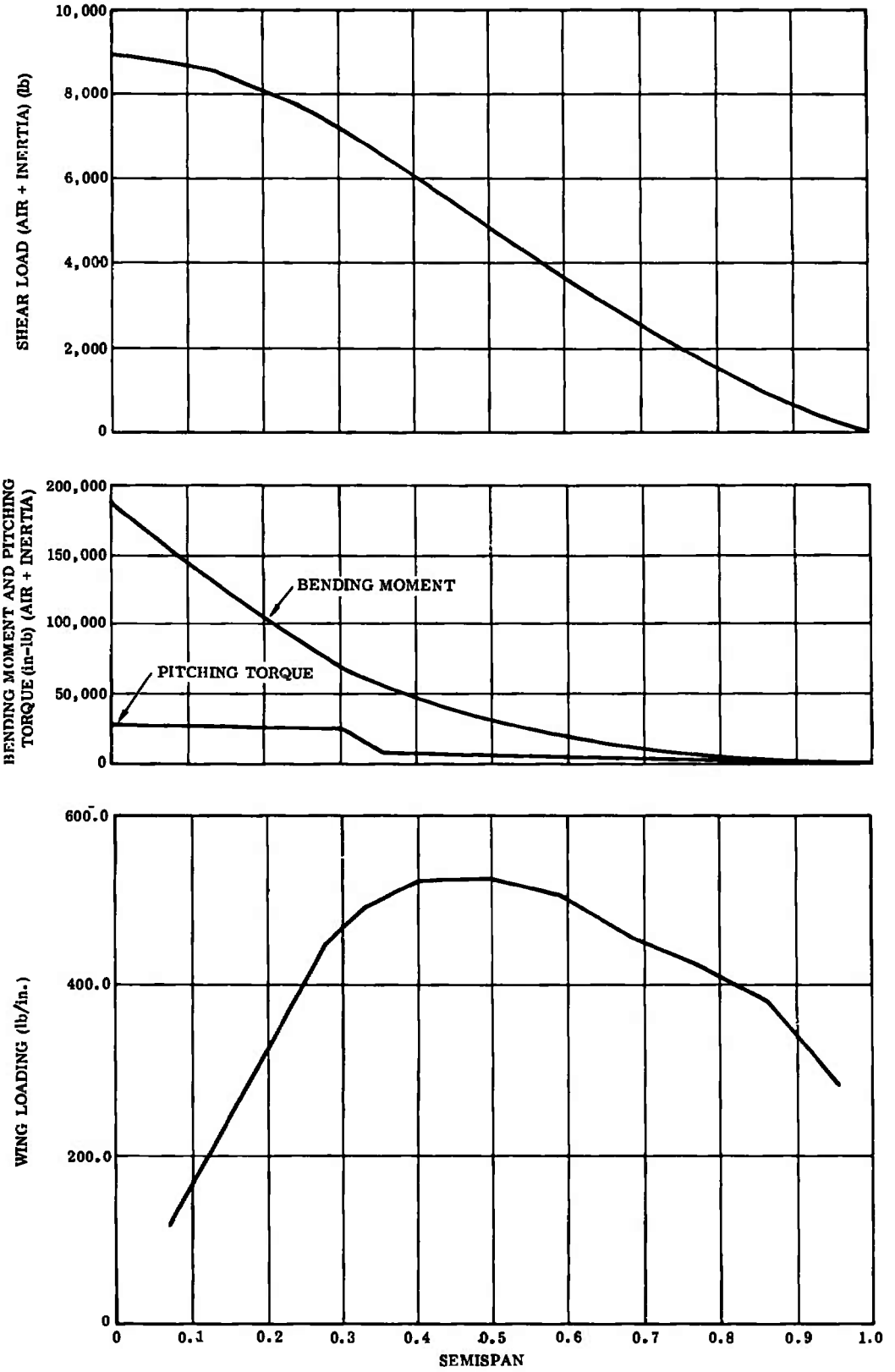


Figure 36. F-111 (50 Deg) – Model Loads – Condition 14

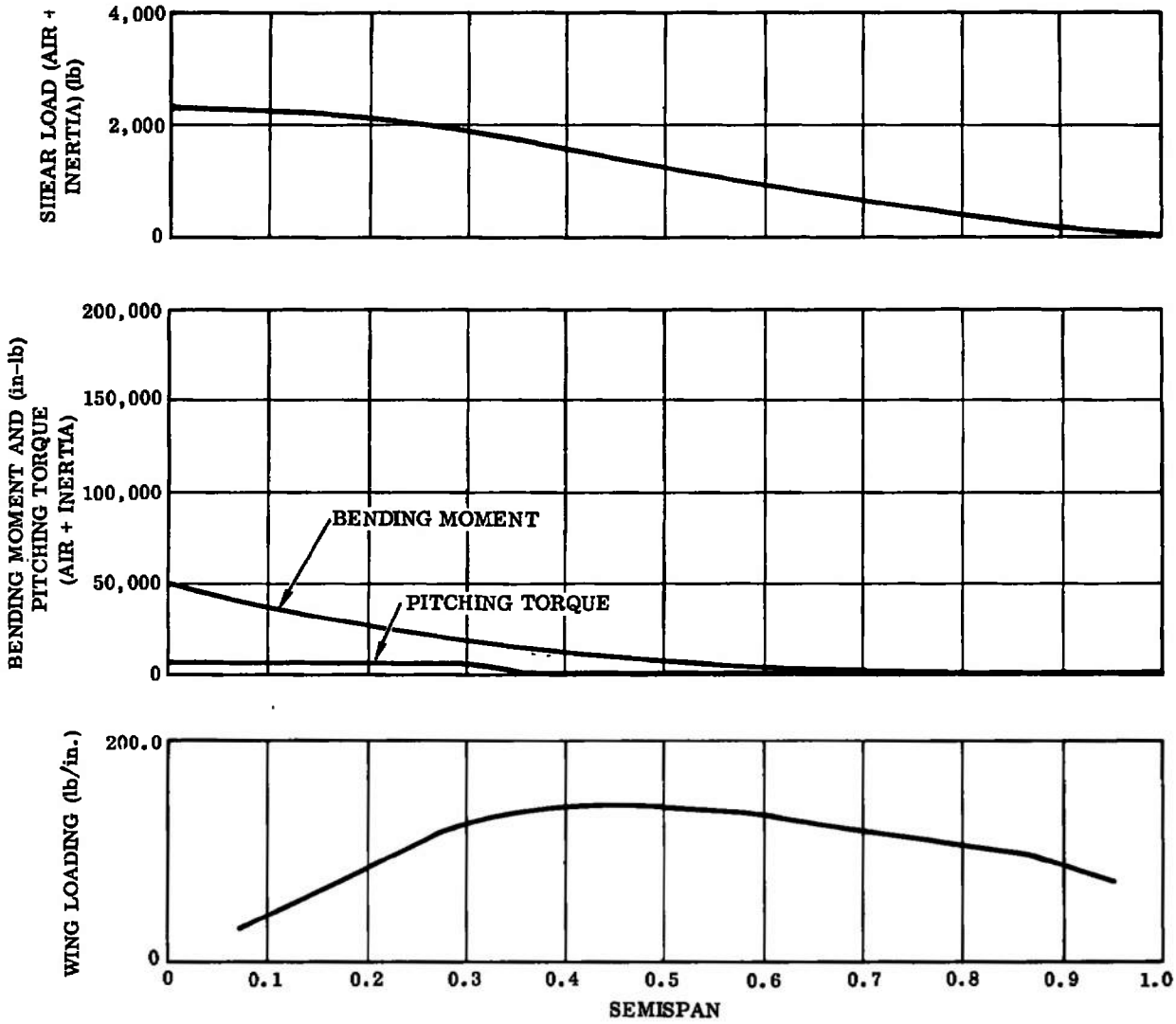


Figure 37. F-111 (50 Deg) – Model Loads – Condition 17

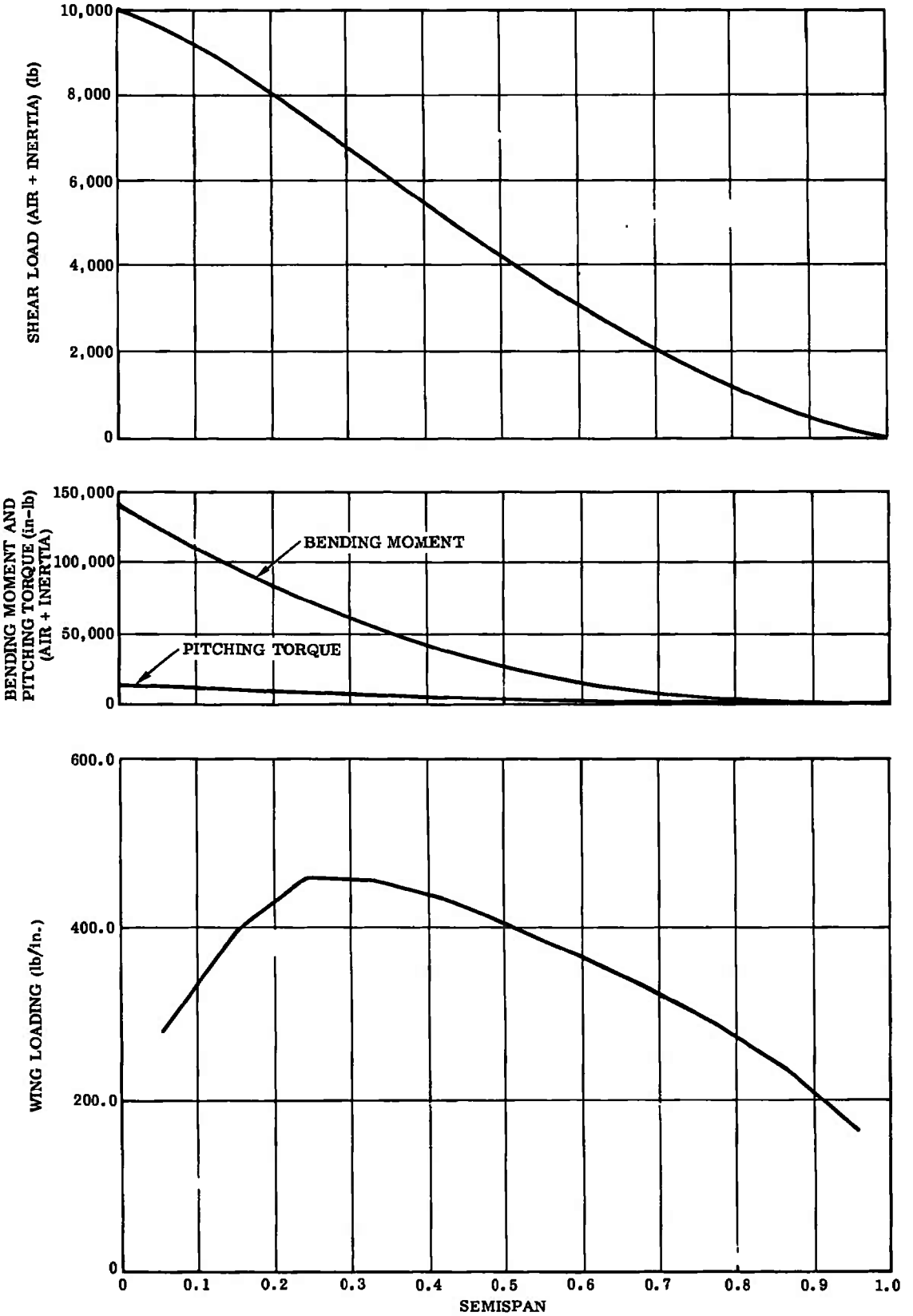


Figure 38. F-111 (26 Deg) – Model Loads – Condition 20

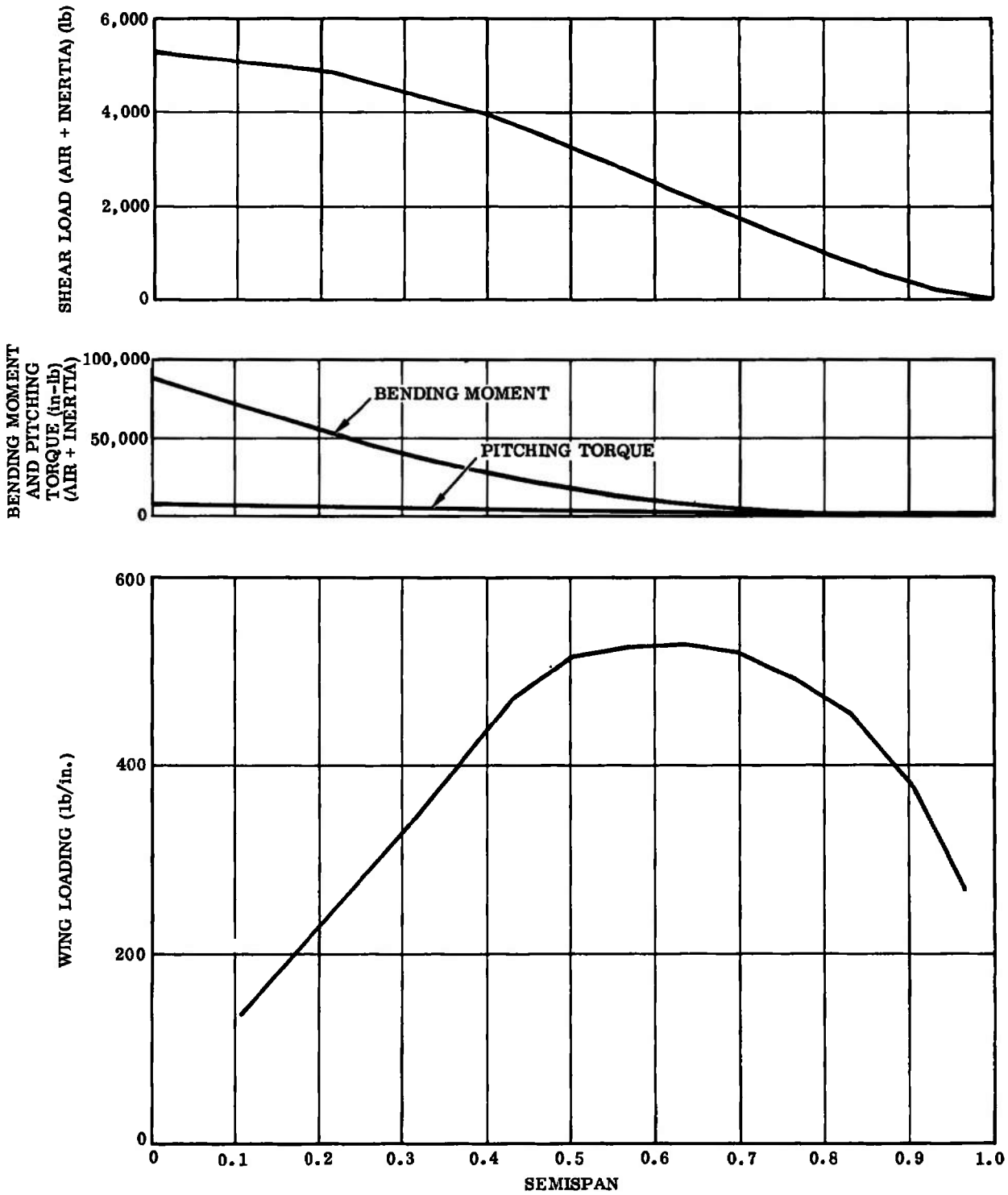


Figure 39. F-111 (72-1/2 Deg) – Model Loads – Condition 22

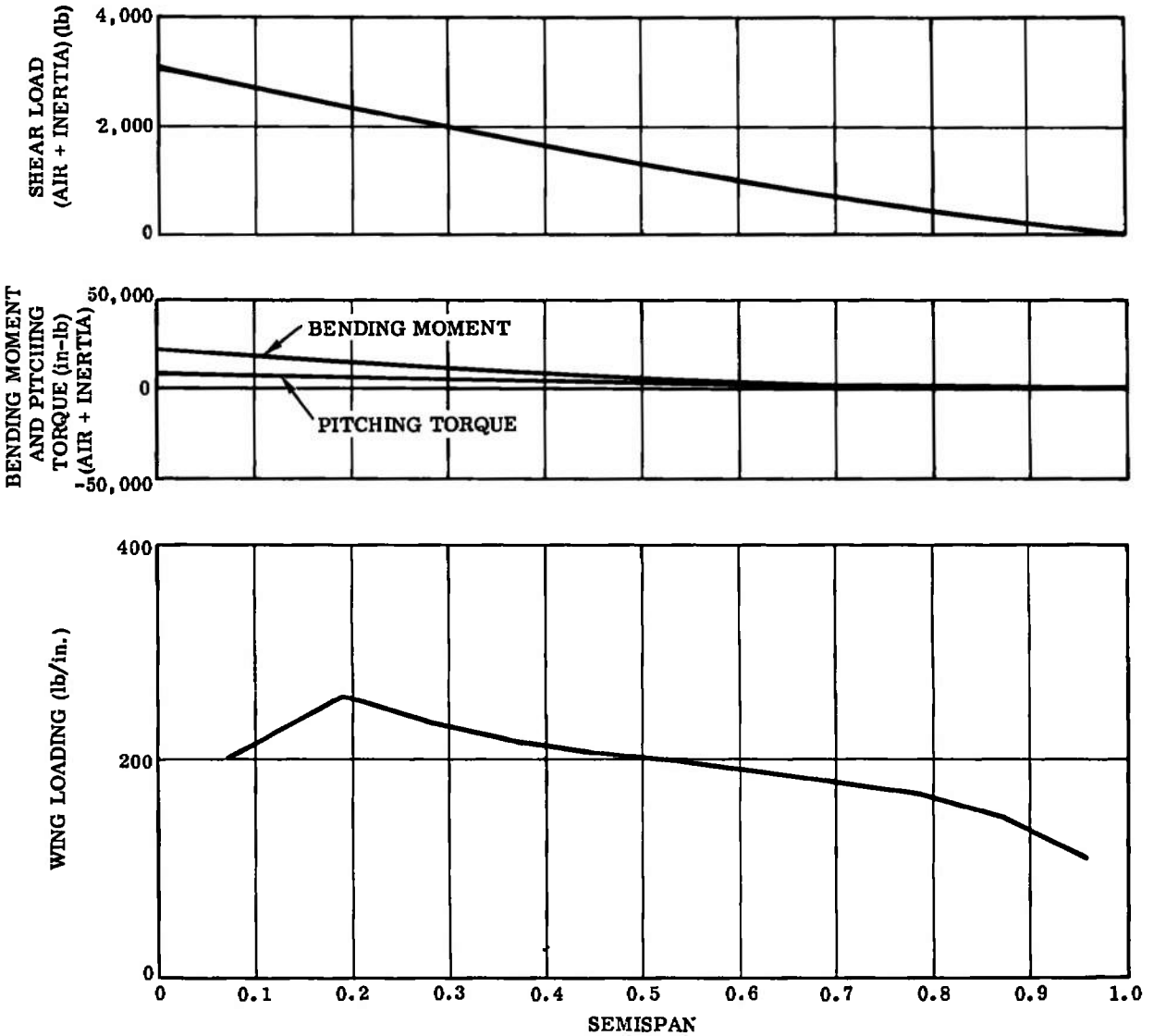


Figure 40. Delta Canard – Model Loads – Condition 24

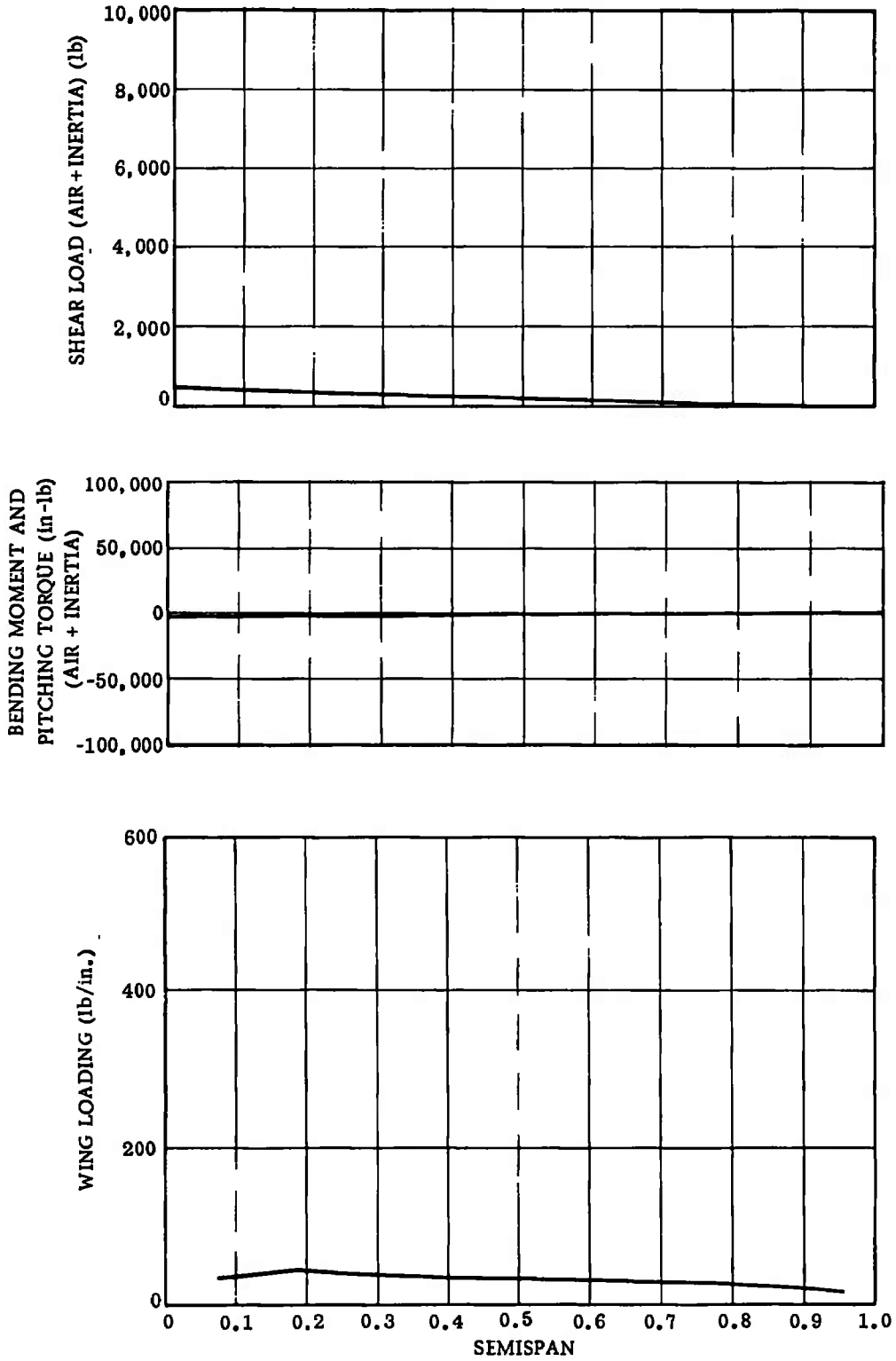


Figure 41. Delta Canard – Model Loads – Condition 27

### 8.3.4 Space Shuttle Booster – Wing Loads

The space shuttle booster model loads are representative of a 2.5-g, 30,000-foot maneuver condition. These loads are presented in Figure 42.

Note that these loads are for ambient tunnel temperature operation (300°K).

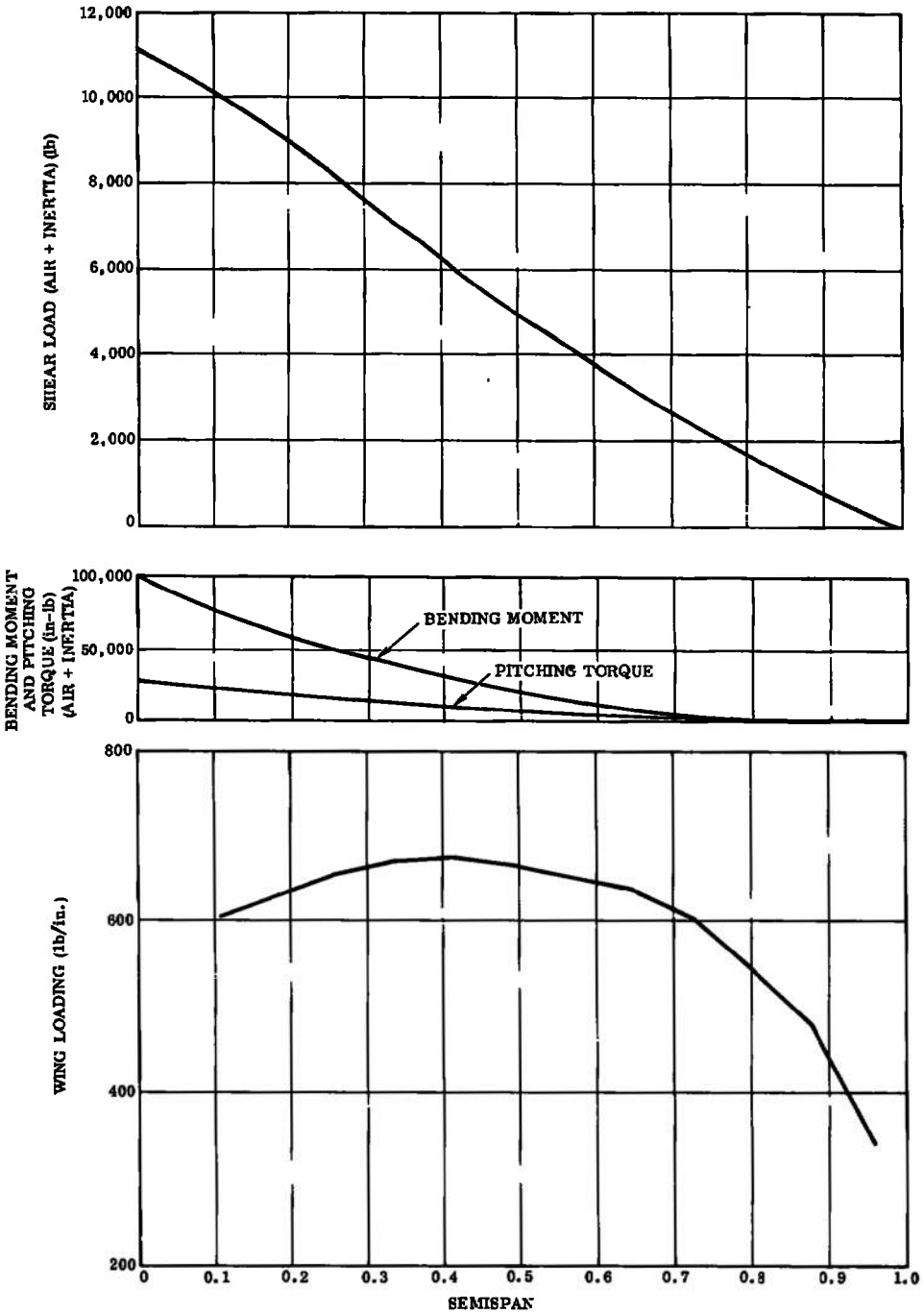


Figure 42. Space Shuttle Booster — Model Loads — Condition 29 (T = 300°K)

### 8.3.5 Empennage and Balance Loads

The total vertical force acting on each of the models was computed using Program 4278. The maximum vertical force value for each of the model configurations was used as a representative load for balance cavity and sting sizing. Balance and stings are shown only to represent feasibility.

Vertical tail and horizontal loads were computed by hand and represent general values for each configuration.

Empennage and total vertical force values for each of the models are shown in Table 3.

Table 3. Model Loads, Empennage, and Total Lift

| Configuration | Vertical tail load (lb) | Horizontal tail (per side) (lb) | Temperature (°K) | Maximum total lift (balance load) and location (lb) |
|---|---|---|---|---|
| ATT | 3,070 | 950 | 240 | 24,100 at F. STA. 44.790 |
| F-111 | 2,500 | 4,500 | 240 | 30,370 at F. STA. 43.105 |
| Delta canard | 2,450 | --- | 300 | 22,000 at F. STA. 46.136 |
| | 1,800 | | 240 | 14,700 |
| Space shuttle booster | 8,320 | --- | 300 | 34,950 at F. STA. 66.820 |
| | 6,200 | | 240 | 30,761 |
| ATT (1.5 size) | --- | 1,435 | 240 | 37,370 |
| | --- | 1,910 | 300 | 48,900 |
| ATT (2.0 size) | --- | 1,910 | 240 | 50,473 |
| | --- | 2,550 | 300 | 66,400 |

### 8.3.6 Model Loads Directory

Table 4 may be used as an index to the location of the various model loads.

## 8.4 MODEL WING DEFORMATION

### 8.4.1 1/24 Scale ATT Model

Some representative aeroelastic wing twists for the ATT model wing are shown in Figure 43. Aeroelastic twists are shown for a 100% chord solid steel wing and for a solid steel wing with the aft 35% chord removed to illustrate the effect of simulating deflected surfaces, etc. Solid steel wings (100% chord) twist from a maximum of 1.5 degrees at a Mach 1.0 cruise, 30,000 feet, to a maximum of 3.4 degrees at a 2.5 g

Table 4. Model Loads Directory

| Configuration | Test condition no. (see Table 2) | Figure no. Bending moment Pitching torque Shear Wing loading | Table no. Vertical tail Horizontal tail Total lift |
|---|---|---|---|
| ATT | 1 | 30 | 3 |
| | 3 | 31 | |
| | 5 | 27 | |
| | 6 | 28 | |
| | 7 | 29 | |
| F-111 | | | |
| 50 deg | 14 | 36 | |
| 50 deg | 17 | 37 | |
| 26 deg | 20 | 38 | |
| 72-1/2 deg | 22 | 39 | |
| Delta canard fighter | 24 | 40 | |
| | 27 | 41 | |
| Space shuttle booster | 29 | 42 | |
| ATT | | | |
| 1.5 size | 37 & 41 | 32 | |
| | 38 & 42 | 33 | |
| 2.0 size | 39 & 43 | 34 | |
| | 40 & 44 | 35 | 3 |

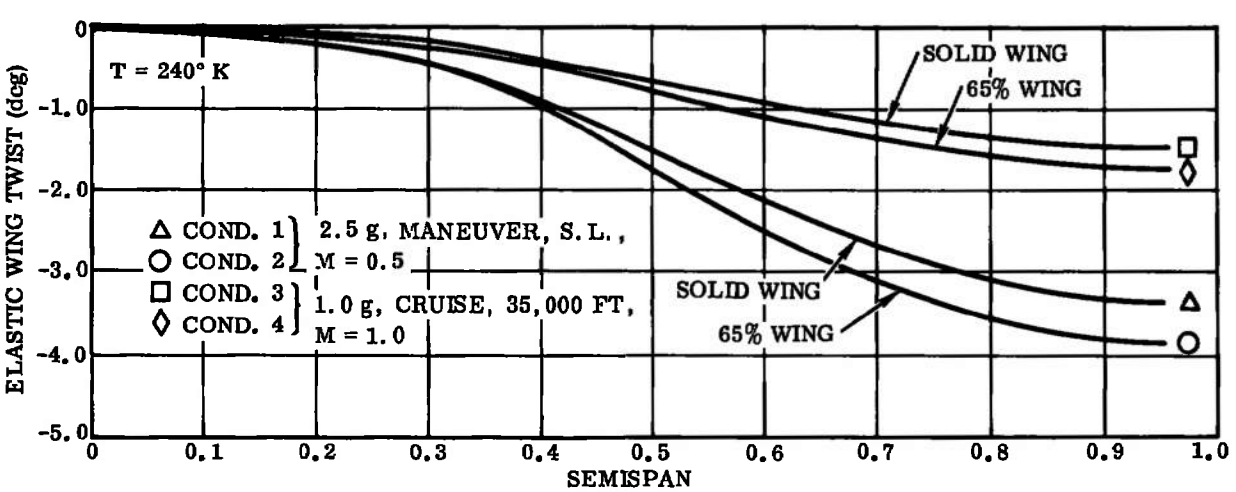


Figure 43. ATT – Elastic Wing Twists

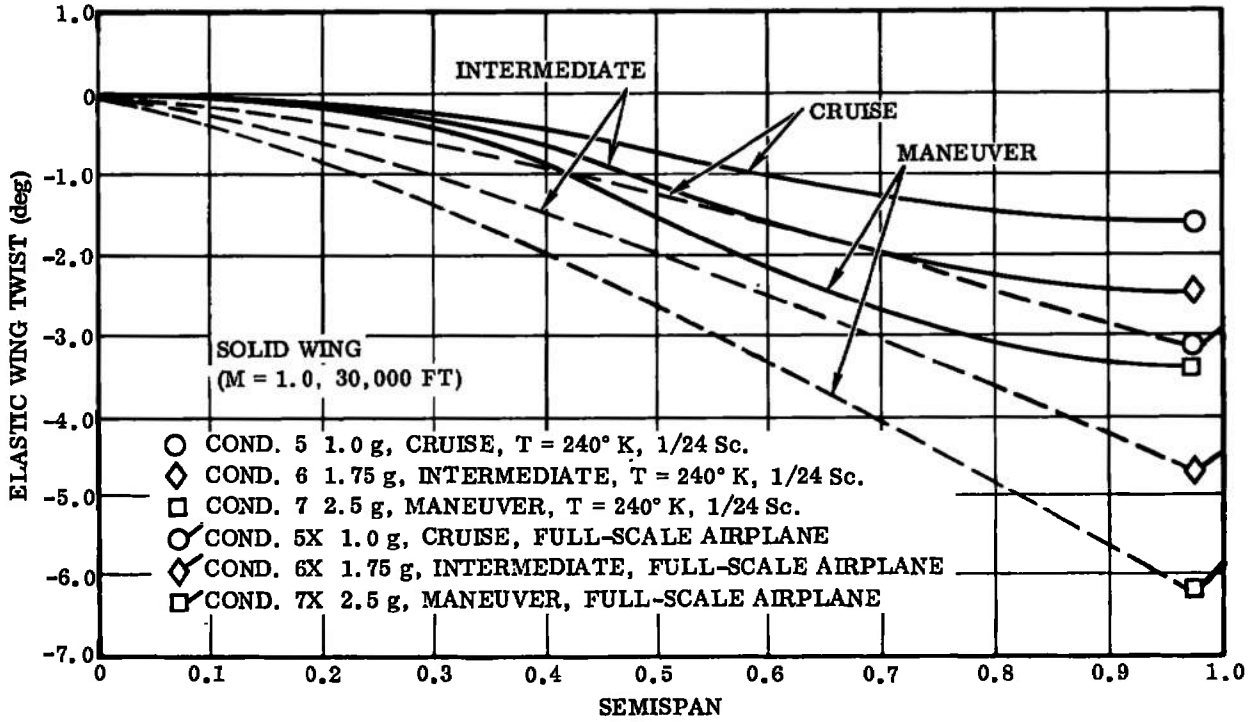


Figure 44. ATT – Model Wing and Airplane Wing Twist Due to Matching Operating Envelope

maneuver at 30,000 feet (reference Figure 44). Figure 44 is a plot of the change in elastic twist of a solid wing model due to varying the angle of attack to match the airplane operating envelope for Mach 1.0, 30,000 feet - cruise ($\alpha$ = 3.23 degrees), intermediate ($\alpha$ = 5.59 degrees), and 2.5 g maneuver ($\alpha$ = 7.95 degrees) conditions.

Wing deflections vary from 0.7 to 1.75 inches for solid wings and from 0.75 to 2.0 inches for 65% chord wings (cruise to 2.5 g maneuver conditions). The wing deflections for the solid-wing model are shown in Figure 45. The effect of removing the aft 35% of the wing is illustrated in Figure 46.

### 8.4.2 Full-Scale ATT Airplane

The predicted aeroelastic twist and deflection for the full-scale ATT airplane are included in Figures 44 and 45. The aeroelastic solutions for the airplane are based on representative airplane structure for this type of wing. The twist for the airplane is -6.2 degrees at a 2.5 g maneuver and -3.1 degrees at a 1 g cruise condition (compared to -3.4 degrees and -1.5 degrees for a solid-wing model). The airplane wing vertical deflection varies from 103.6 inches (4.3 inches at 1/24 scale) to 42.2 inches (1.8 inches at 1/24 scale) compared to 1.75 inches and 0.7 inch for a solid-wing model.

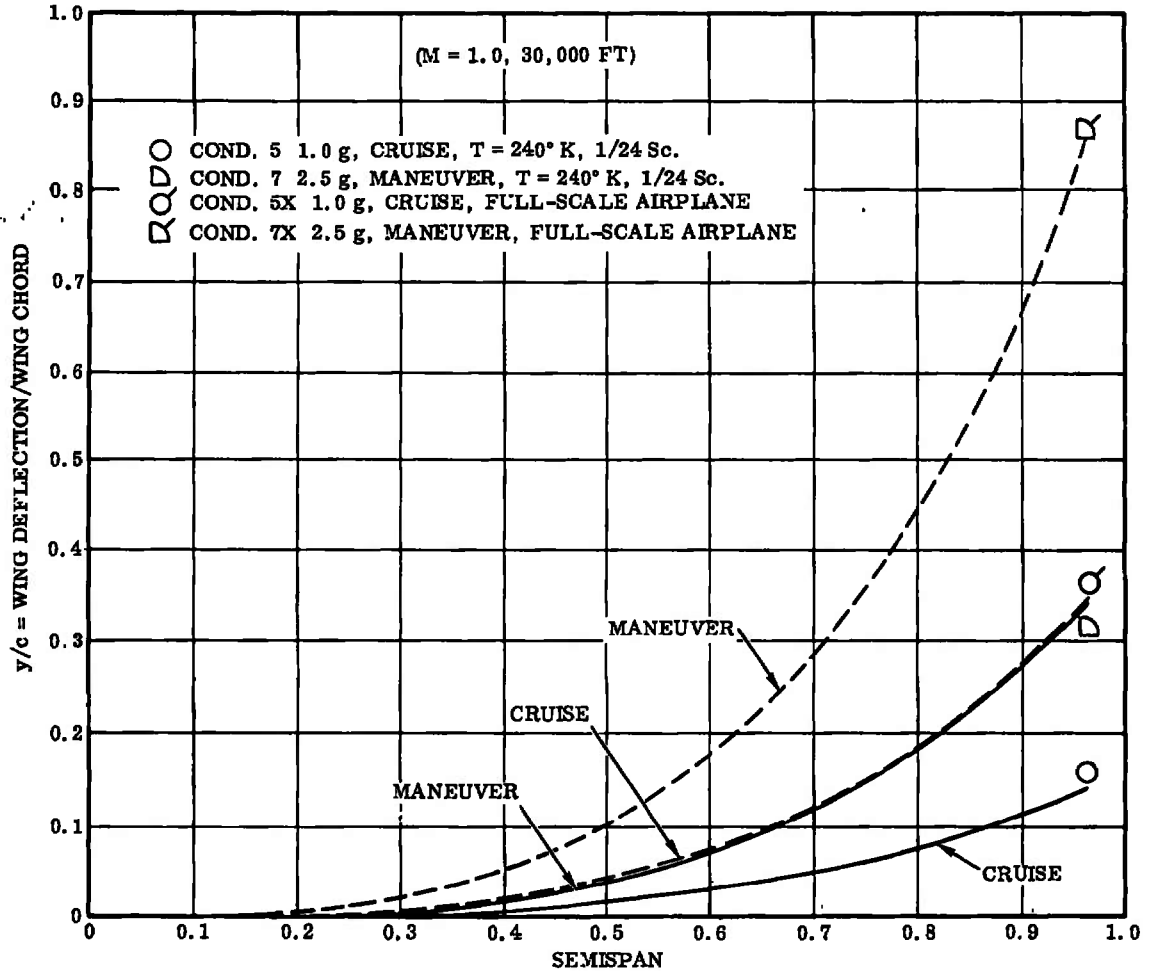


Figure 45. ATT – Wing Deflections – 1/24 Scale Model and Full-Scale Airplane

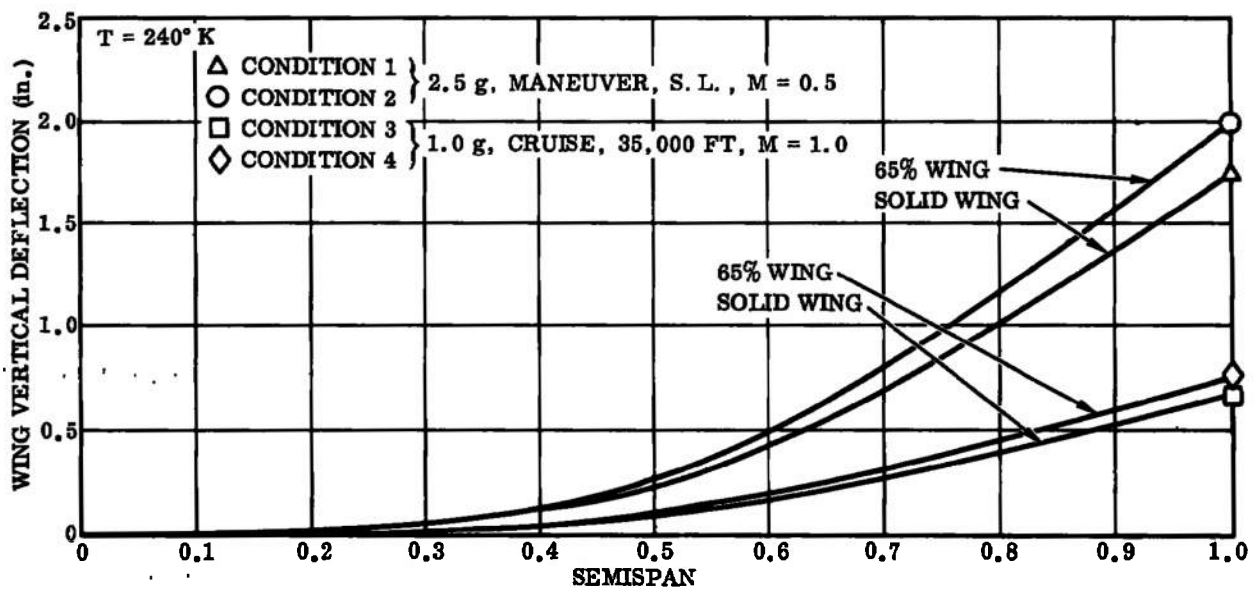


Figure 46. ATT — Effect on Deflection Due to Removing Aft 35% Chord

### 8.4.3 1/12 Scale F-111 Model

The 50-degree sweep version of the F-111 is the highest loaded configuration. The aeroelastic wing twists for the 50-degree wing sweep version of the F-111 model are presented in Figure 47. Maximum wing twists vary from -1.29 degrees (solid) and -1.4 degrees (65% C) at cruise to -4.83 degrees (solid) and -5.42 degrees (65% C) at 6.0 g maneuver.

Maximum wing deflections vary from 0.42 inch to 2.37 inches. The wing deflections for the F-111 configurations are shown in Figure 48.

The effects of wing sweep and airplane envelope restrictions on the F-111 solid-wing elastic twists and deflections are illustrated in Figures 49 and 50.

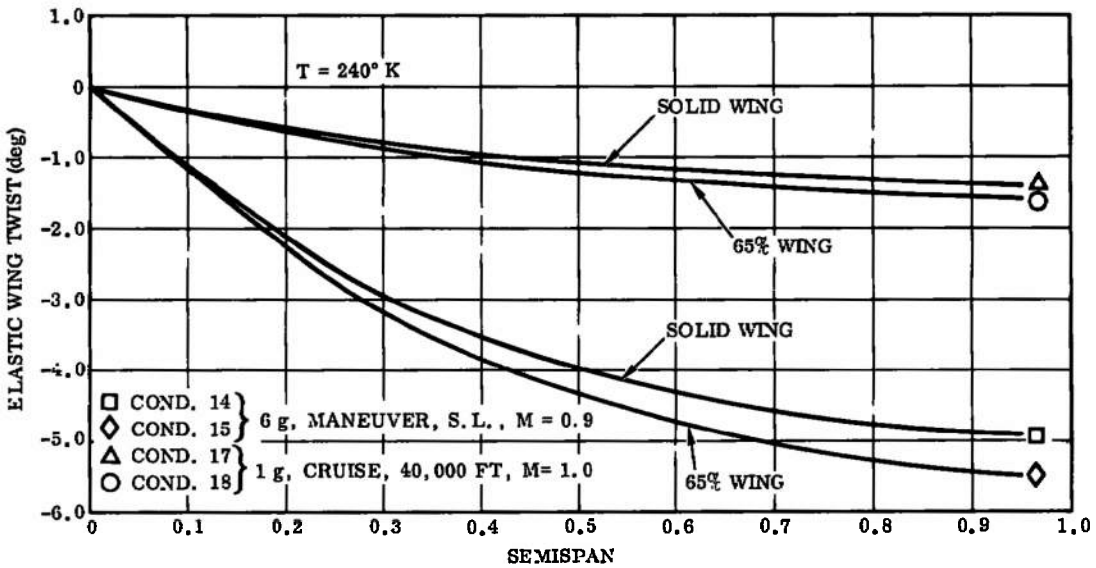


Figure 47. F-111 (50 Deg) – Elastic Wing Twist

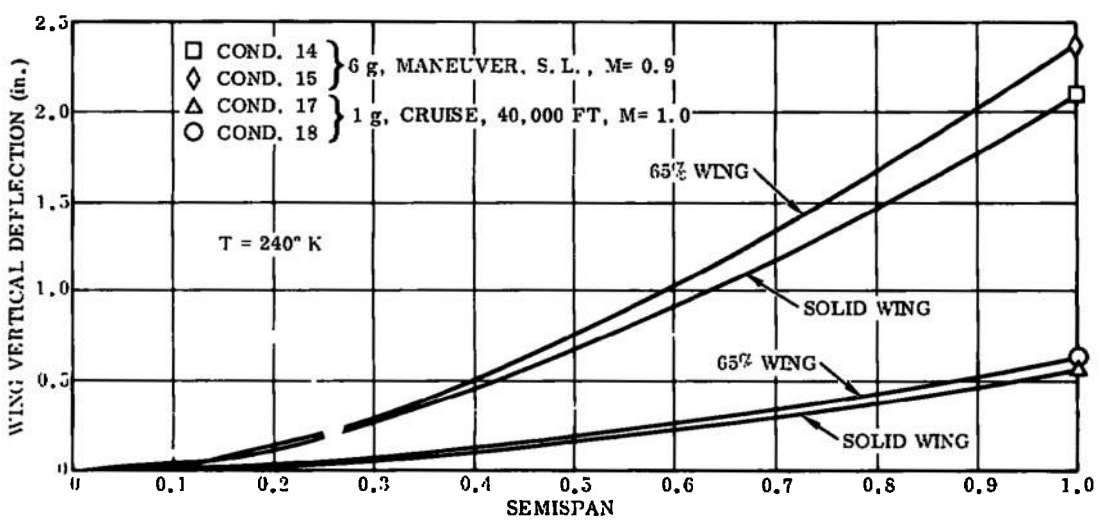


Figure 48. F-111 (50 Deg) – Wing Deflections

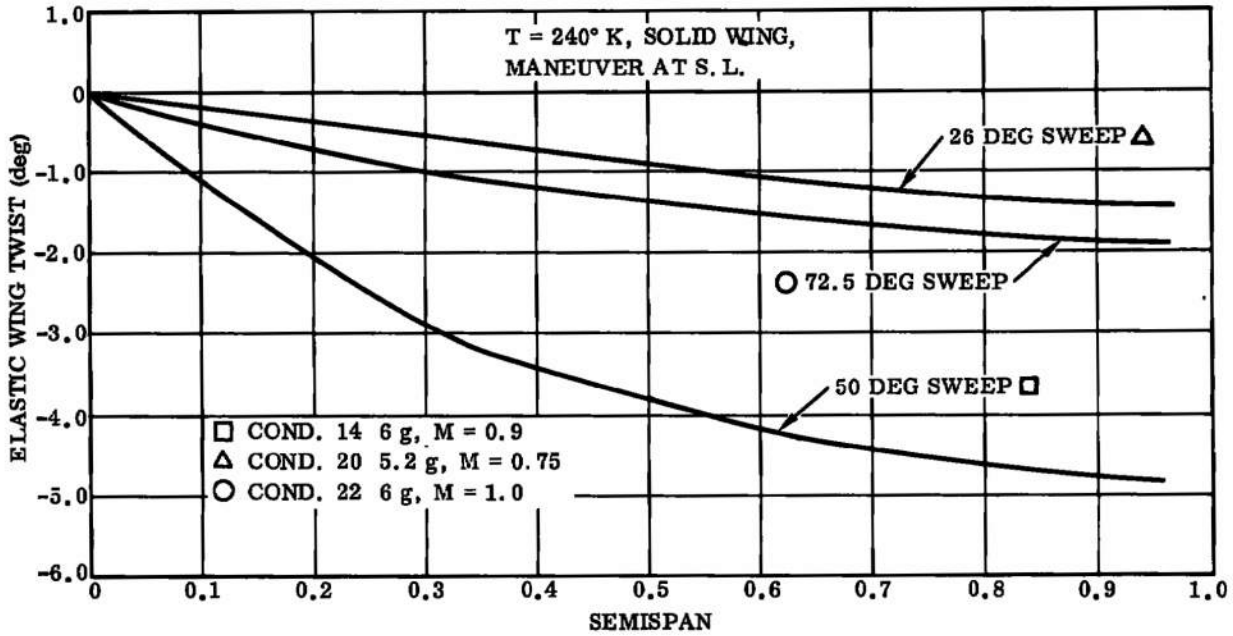


Figure 49. F-111 - Elastic Wing Twist vs Wing Sweep

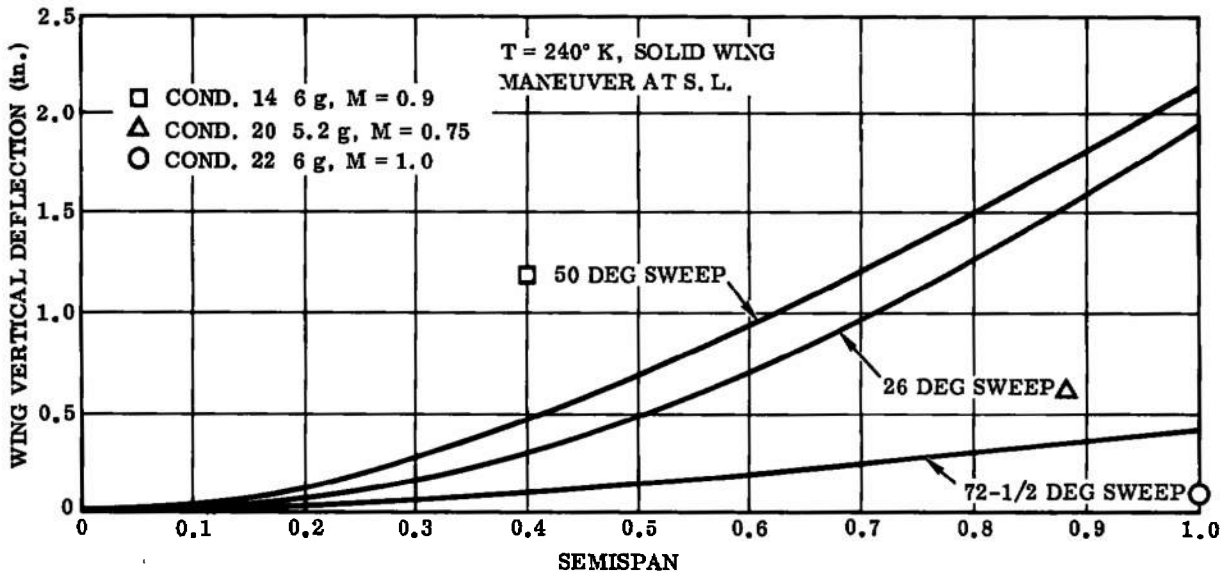


Figure 50. F-111 – Wing Deflections vs Wing Sweep

### 8.4.4 Delta Canard Fighter

The maximum aeroelastic twists on the delta canard fighter model solid wing vary from 0.4 degree at cruise to 1.73 degrees in a 7.5 g maneuver at 240°K tunnel conditions and up to 2.35 degrees for an ambient temperature condition. Removal of the aft 35% of the wing structure for control surfaces, etc., results in a twist of 4.92 degrees at 240°K. (Note: excessive wing twist outboard of 0.65 semispan due to removing a constant percent chord from a delta wing. In practice, this would be avoided.) Wing-tip deflections vary from zero to 0.4 inch for solid wings and zero to 0.7 inch for the 70% version. Model wing twists and deflections for the delta canard are shown in Figures 51 and 52.

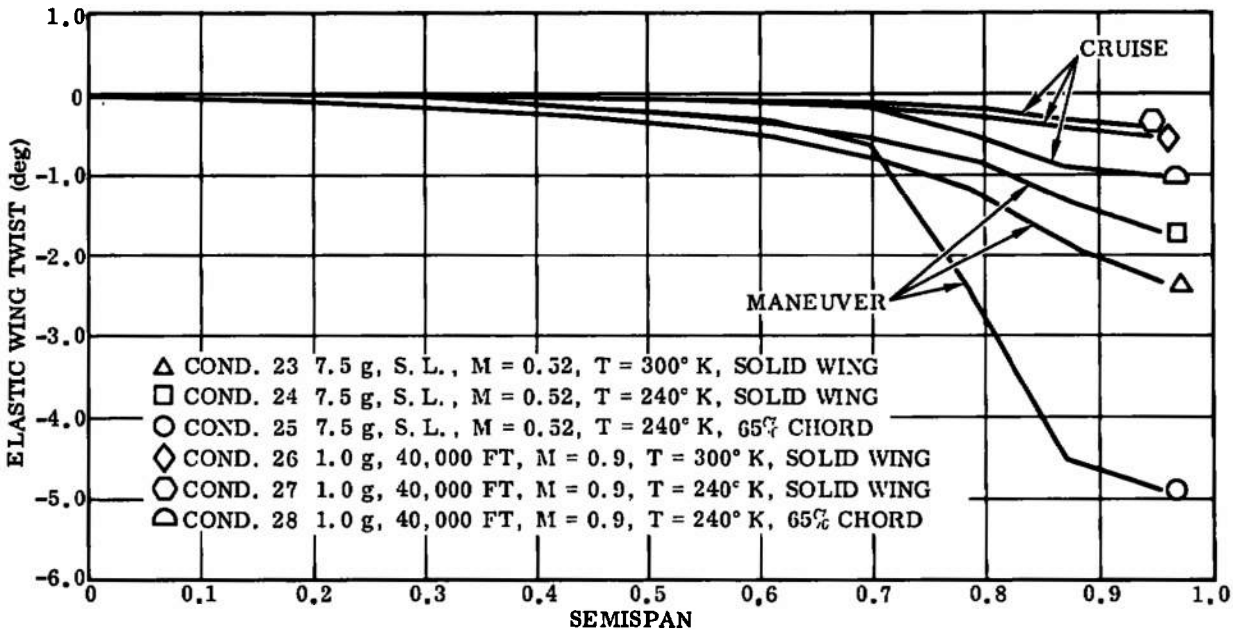


Figure 51. Delta Canard — Elastic Wing Twist

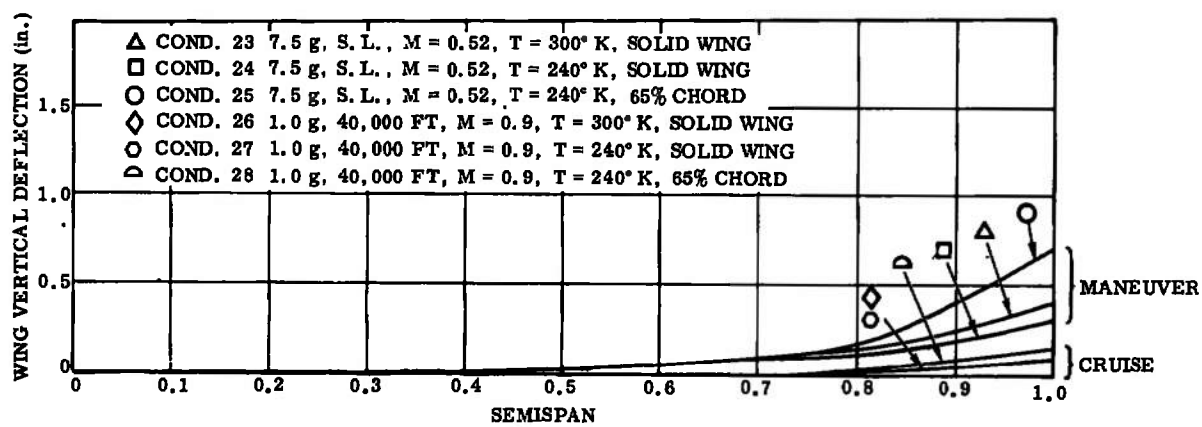


Figure 52. Delta Canard — Wing Deflection

### 8.4.5 Space Shuttle Booster

The space shuttle booster wing has a relatively low wing loading when compared to high aspect ratio vehicles. The deformation of this wing under the maximum loading conditions at 300°K results in only 0.25 degree twist and 0.8 inch deflection at the wing tip. Model wing twist is illustrated in Figure 53 and model wing deflection in Figure 54.

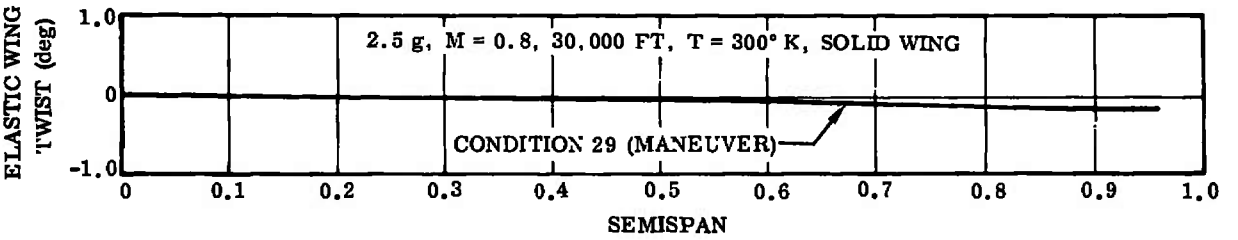


Figure 53. Space Shuttle Booster – Elastic Wing Twist

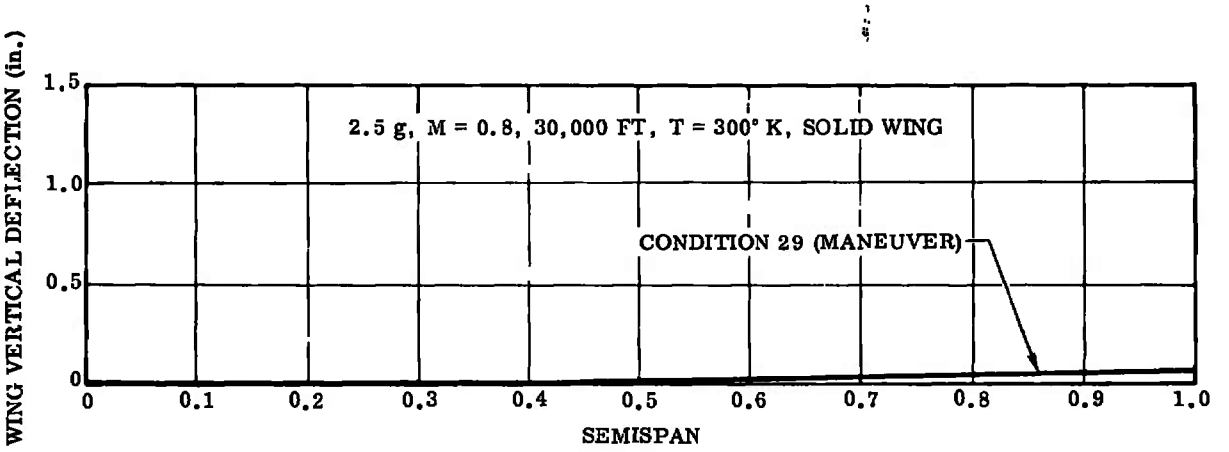


Figure 54. Space Shuttle Booster – Wing Deflection

## 8.5 MODEL SCALE EFFECTS ON WING DEFORMATION

The ATT model was selected to illustrate the effects on various model parameters due to a change in model scale of 1.5 and 2.0. Model test conditions 37 through 44 (Table 2), were computed for this study. Conditions 37, 38 and 39, 40 are equivalent to conditions 5 and 7. Conditions 41, 42 and 43, 44 are equivalent to conditions 10 and 12. Tunnel operating pressure and temperature were varied to provide the same $R_{e_{MAC}}$ for each of the three model sizes.

The effects of scale and temperature on wing twist are illustrated in Figure 55. The maximum wing twist at ambient temperature (300°K) and basic model scale (1/24) at the 2.5-g maneuvering condition is 4.1 degrees. The twist is reduced from 4.1 degrees to 3.1 degrees and to 2.5 degrees by changing the model scale from 1/24 to 1/16 and to 1/12. Note that the 4.1-degree twist can be reduced to 3.25 degrees by operating the tunnel at -30° F (240°K).

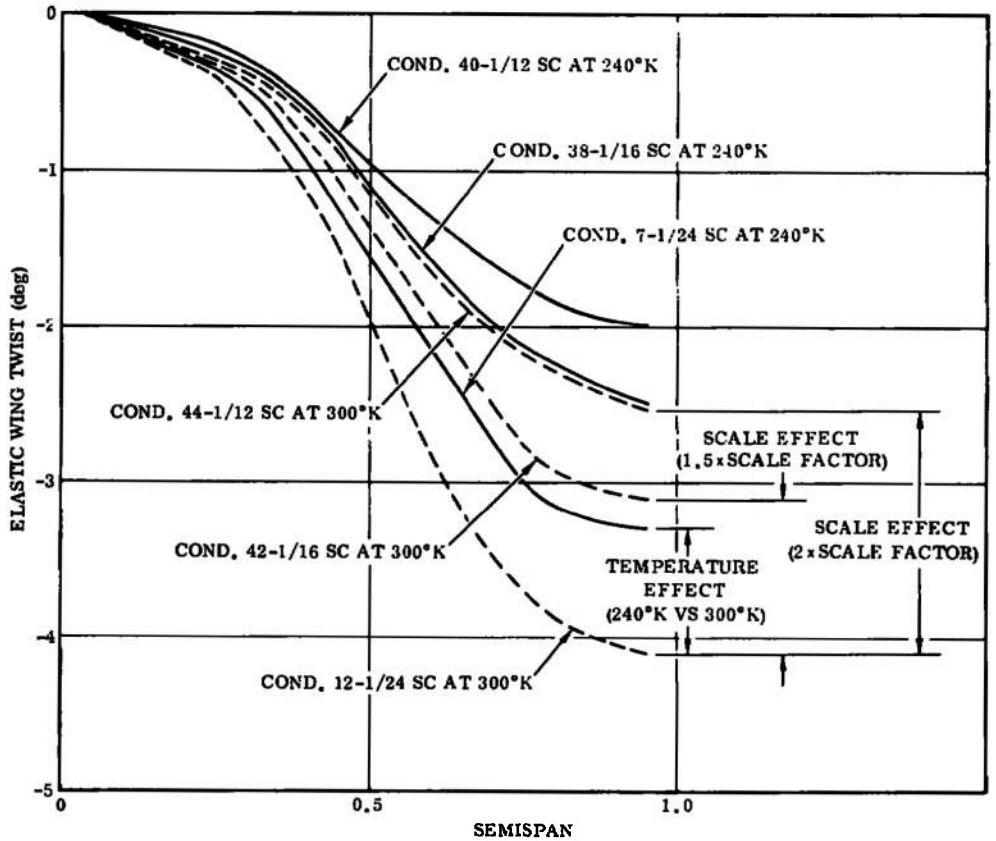


Figure 55. ATT – Elastic Wing Twist vs Tunnel Temperature and Model Scale

## 8.6 REYNOLDS NUMBER EFFECT ON WING DEFORMATION

The effect on wing twist due to running at a reduced Reynolds number (i.e., dynamic pressure) is shown in Figure 56. Test conditions 7a, 7b, and 7c (Table 2) are the same as condition 7 except that they represent a variety of Reynolds numbers, all of which are less than full scale. The maximum wing twist for the 1/24-scale ATT model at -30°F (240°K) tunnel operating temperature is -3.4 degrees at $R_e/ft = 70 \times 10^6$ (a model $R_{e_{MAC}}$ equivalent to the full-scale airplane $R_{e_{MAC}}$). Wing twist is reduced to 2.6 degrees, 2.1 degrees, and 1.8 degrees by reducing the Reynolds numbers to $49.5 \times 10^6$, $39.5 \times 10^6$, and $29.5 \times 10^6$ respectively. Note that decreasing the Reynolds number by 50% reduces the wing twist to the same value as computed for the 1/12 scale model (Figure 55).

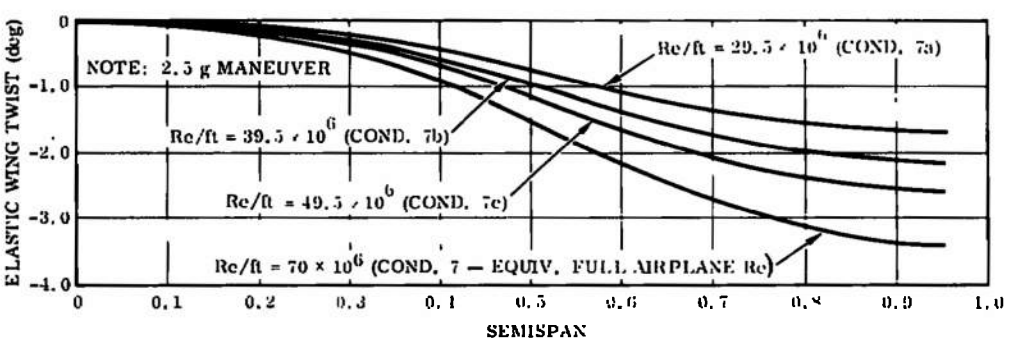


Figure 56. ATT — Effect of Reynolds Number on Wing Twist

# SECTION IX

# STRUCTURAL ANALYSIS

The basic structural analyses performed on each of the model configurations are:

a. Basic wing stresses.

b. Wing/fuselage attachment.

c. Empennage stresses.

d. Empennage attachment.

e. The degradation of maximum allowable loading due to:

   1. Incorporation of pressure orifices in the wing.

   2. Removal of an aft portion of the wing to allow for control-surface attachments.

f. Model sting stress and deflection. Note: since no balance stiffness data is available, an estimated angle of rotation was used for sting/balance deflection analysis.

Each model is analyzed to determine working stress levels. PH13-8 Mo steel, heat treated to an H1000 condition, is used as a baseline material for each configuration. (The mechanical properties of 13-8 PH steel are found in Table 12.)

Structural analyses are based on 240°K operation unless noted otherwise. Table 5 presents a summary of model achieved safety factor.

## 9.1 ATT MODEL

The critical section for the ATT model wing is located at the intersection of wing station 14.87 and the elastic axis and is labeled Section 4. (Figure 57.) The maximum wing bending stress varies from 72,200 psi for a solid wing to 94,000 psi for the pressure wing configuration. Stresses for the various wing configurations at the maximum maneuver test condition (Condition 7) are shown in Figure 58.

The change in stress level of the critical wing section (Section 4) due to varying the model angle of attack and $Re\,C_L$ to match the aircraft operating envelope is illustrated in Figure 59. The values of $Re\,C_L$ (13.73, 24.07 and 34.40 millions) represent 1.0 g, 1.75 g, and 2.5 g conditions at M = 1.0, 30,000 feet (conditions 5, 6 and 7 in Table 2).

A wing-to-fuselage attachment analysis shows that there are no particular problems in that area.

Table 5. Stress Analysis – Minimum Safety Factor Summary

| Model | Location | Mode | S. F. |
|---|---|---|---|
| Delta-Canard 1/9.6 scale | | | |
| Screws, wing to fuselage | Juncture, wing to fuselage | Shear | 2.26 |
| Screws, tail to fuselage | Juncture, tail to fuselage | Tension | 2.12 |
| Tail | Base section | Bending | 2.32 |
| Screws, canard to fuselage | Juncture, canard to fuselage | Tension | 3.61 |
| Sting support | Station 68.44 | Bending | 2.88 |
| F-111 – 1/12 scale | | | |
| Solid wing | Section A (ref. page 114) | Bending + torsion | 2.86 |
| 65% solid wing | Section A (ref. page 114) | Bending + torsion | 2.48 |
| 100% pressure wing | Section A (ref. page 114) | Bending + torsion | 2.11 |
| 65% pressure wing | Section A (ref. page 114) | Bending + torsion | 1.92 |
| Horizontal tail | Section AA (10 deg incidence) | Bending + torsion | 1.29 |
| Sting (constant dia) | Station 71.667 | Bending | 2.43 |
| Sting (tapered) | Station 71.667 | Bending | 2.43 |
| Space Shuttle | | | |
| Solid wing | B. L. 4.15 | Bending + torsion | 32.27 |
| Pressure wing | B. L. 4.15 | Bending + torsion | 25.16 |
| Tail | Base section | Bending + torsion | 5.63 |
| Screws, tail to fuselage | Juncture, tail to fuselage | Tension | 3.91 |
| Sting support | Station 77.49 | Bending | 4.94 |
| ATT 1/24 scale | | | |
| Solid wing | Station 14.87 | Bending | 2.78 |
| 65% solid wing | Station 14.87 | Bending | 2.61 |
| 100% pressure wing | Station 14.87 | Bending | 2.14 |
| 65% pressure wing | Station 14.87 | Bending | 2.69 |
| Screws, T.E. joint | Station 13.33 | Shear | 1.93 |
| Dowels, wing-fuselage | Juncture, wing to fuselage | Shear | 2.15 |
| Screws, horizontal tail | Horizontal to vertical tail | Tension | 2.80 |
| Screws, vertical tail | Vertical tail to fuselage | Tension | 3.12 |
| Maneuver sting | Station 91.667 | Bending | 3.81 |
| Cruise sting | Station 91.667 | Bending | 3.26 |
| ATT 1/16 scale | | | |
| Solid wing | Station 22.305 | Bending | 2.91 |
| ATT 1/12 scale | | | |
| Solid wing | Station 29.74 | Bending | 3.63 |

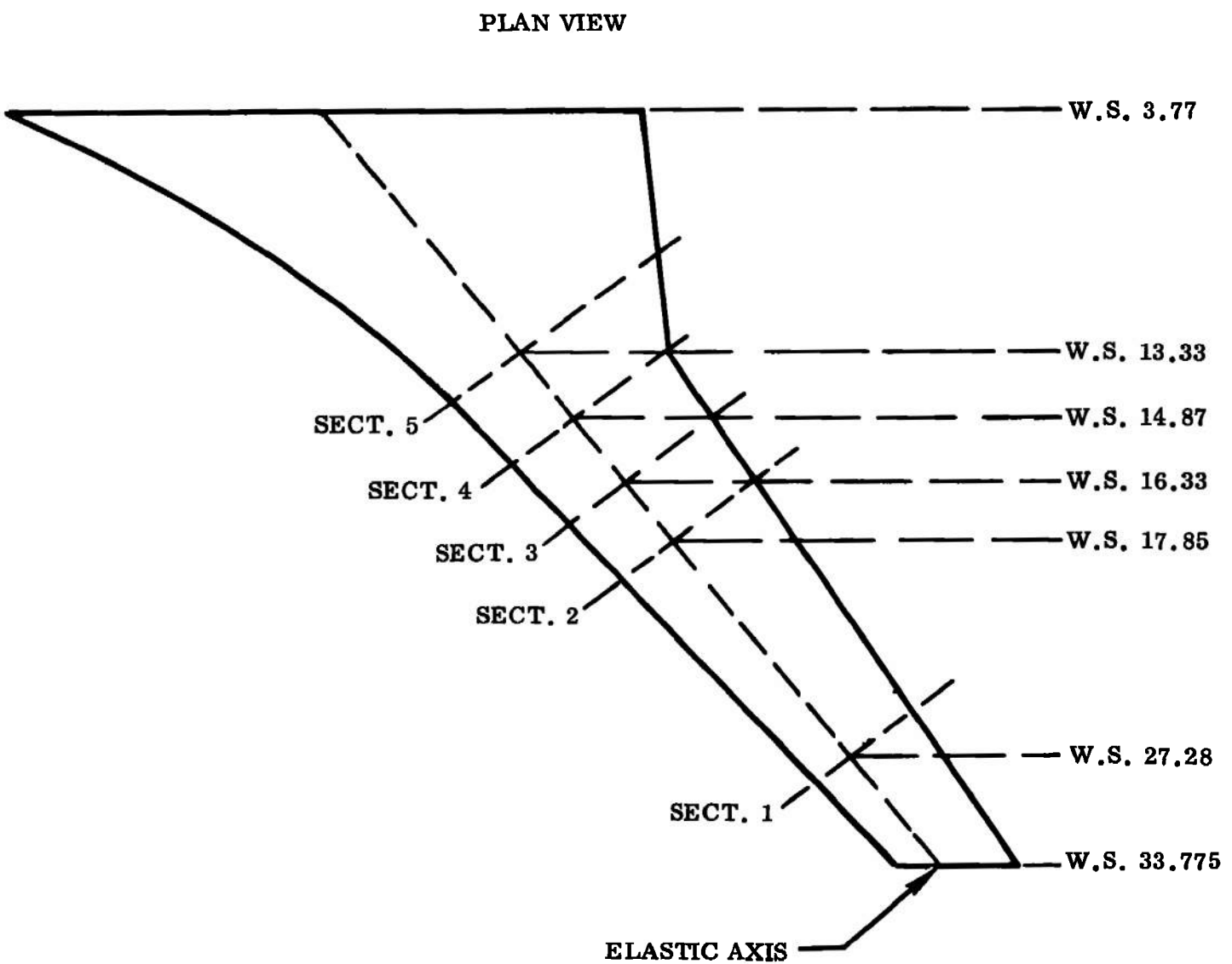


Figure 57. ATT Wing — Location of Sections Used For Structural Analysis

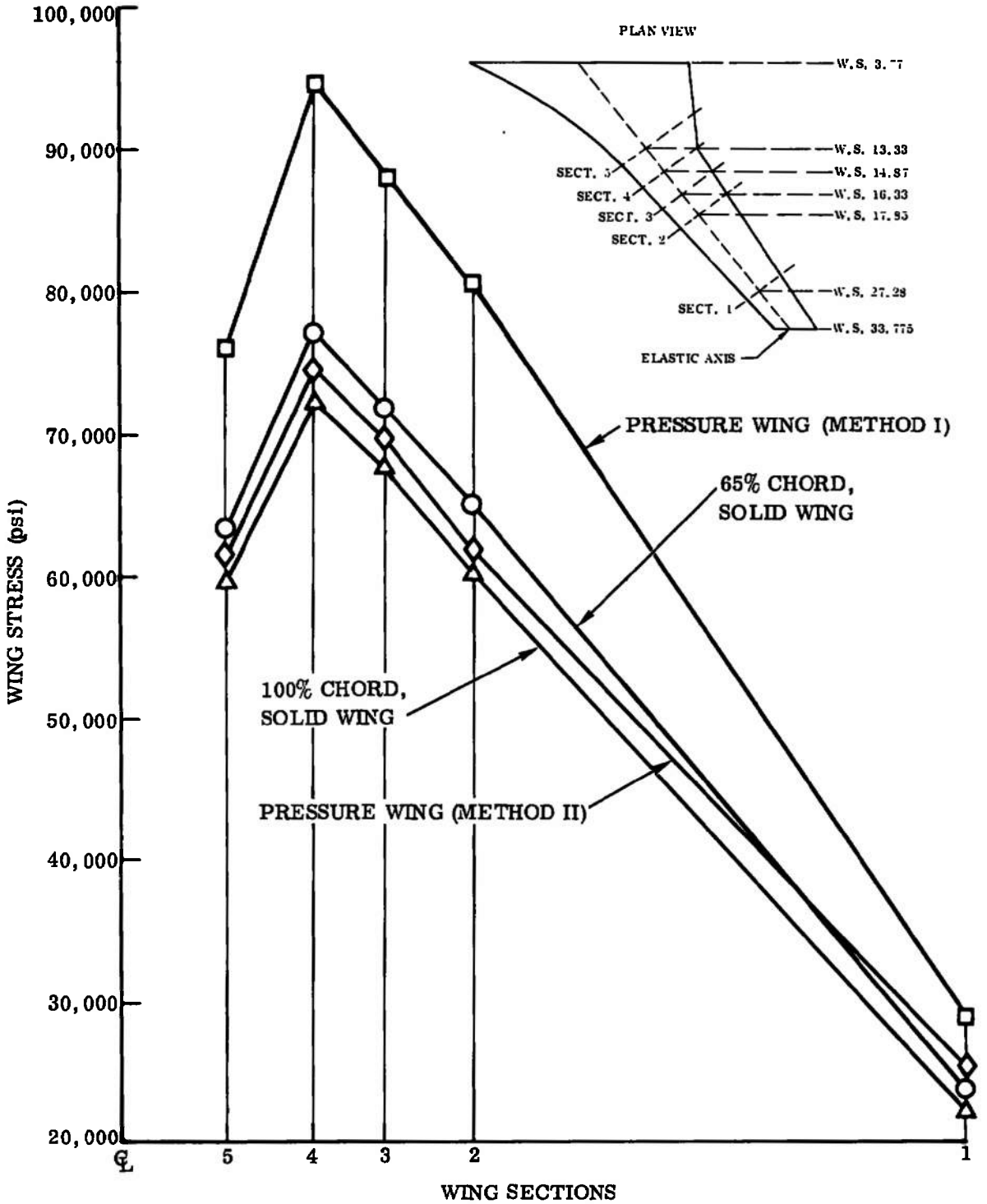


Figure 58. ATT – Comparison of Wing Types vs Stress (Condition 7)

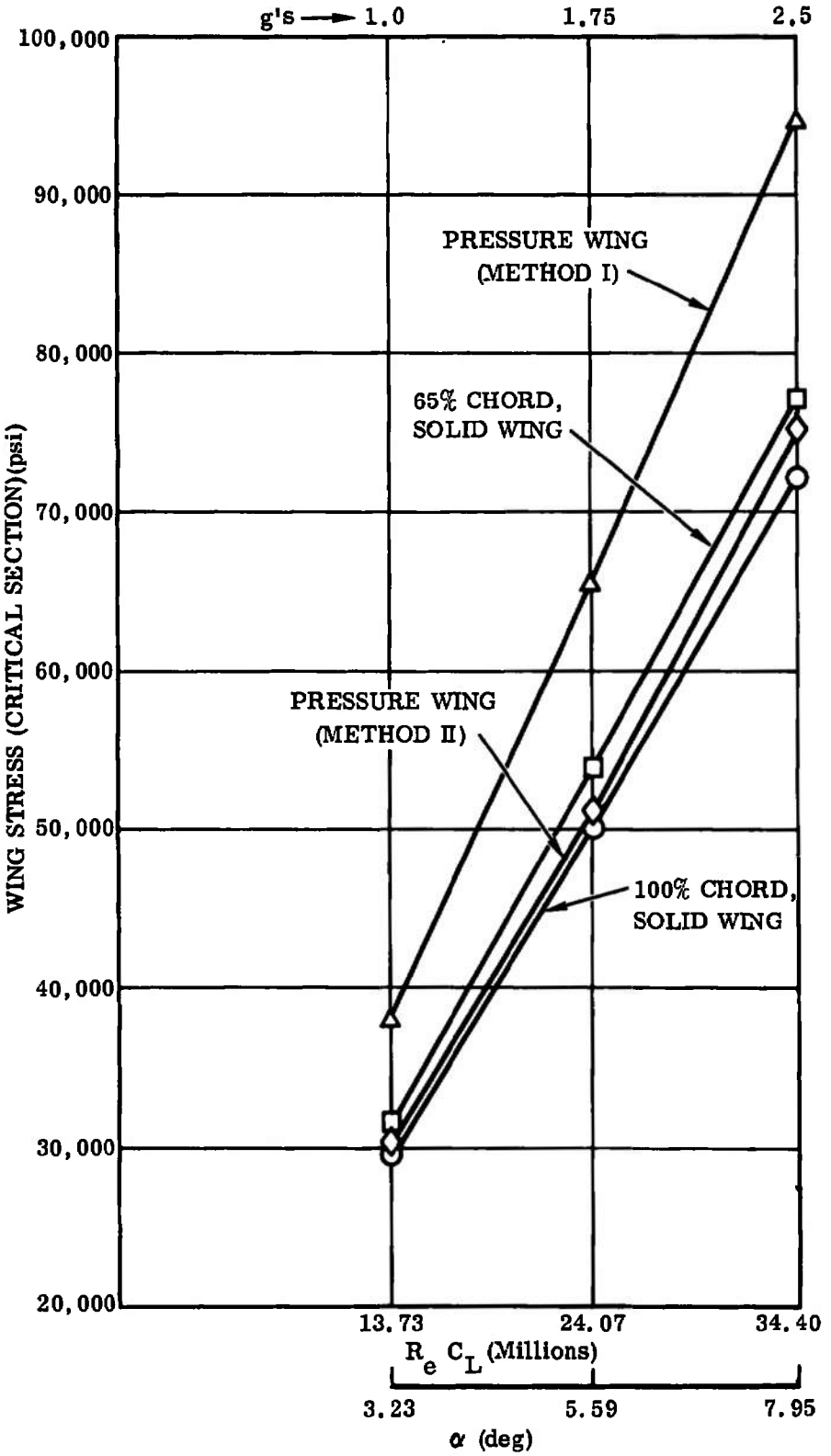


Figure 59. ATT — Wing Stress at Wing Section 4 Resulting from Matching Flight Conditions for M = 1.0 at 30,000 ft from 1.0 g to 2.5 g's.

Horizontal tail stresses are small if the horizontal tail is fabricated in one piece. The vertical tail stresses are also quite standard.

The attachment of fuselage-mounted, flow-through type engine nacelles is no structural problem. Engine simulators should not be too difficult to install physically but may be very difficult or even impossible to operate in the high dynamic pressure environments of the HIRT tunnel.

A representative sting and balance combination indicates that combinations of sting diameter and model cavities can be found to handle the model loads.

### 9.1.1 ATT Model Scale Effects on Stress

The basic ATT configuration is 1/24 scale. When model loads were revised to simulate the same test conditions ($R_{e_{MAC}}$ of the model equal to $R_{e_{MAC}}$ of the airplane) for 1/16 scale and 1/12 scale models, the stress levels were reduced. Maximum wing stress for a solid-wing configuration decreased from 72,200 psi for 1/24 scale to 69,000 psi for 1/16 scale and 55,295 psi for 1/12 scale. Figure 60 illustrates the effects of model scale and tunnel operating temperature on the ATT model wing stresses.

### 9.1.2 Detailed Stress Analysis — 1/24 - Scale Model

The analysis is performed on four different ATT wing configurations:

a. 100% chord solid wing.

b. 65% chord solid wing.

c. 100% chord pressure wing (Method I).

d. 65% chord pressure wing (Method II).

Bending stresses have been calculated for three conditions: Conditions 5, 6, and 7 (reference Table 2). (The resulting range of stresses experienced are plotted versus Reynolds numbers in Figure 59.)

The following analyses use section properties contained in Figure 61.

#### Solid Wing Configuration (Reference Figure 7)

The wing is machined from PH 13-8 Mo stainless steel and heat treated to condition H1000. Wing Sections 1 through 5 (Figure 57) are used for each of the wing analyses. Section properties and the results of the 100% chord solid wing analysis are presented in Table 6.

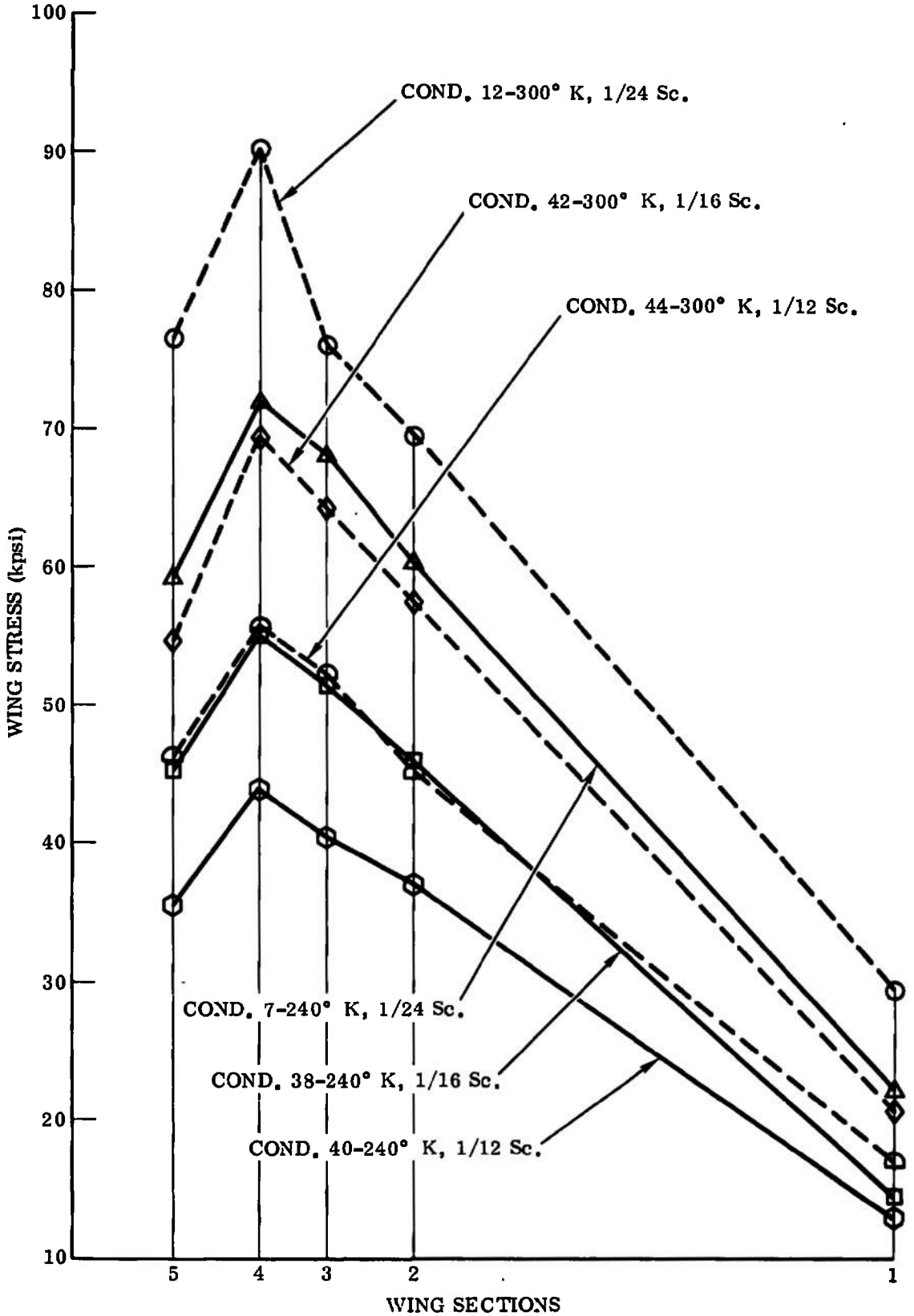


Figure 60. ATT – Comparison of Wing Stresses vs Tunnel Temperature and Model Scale

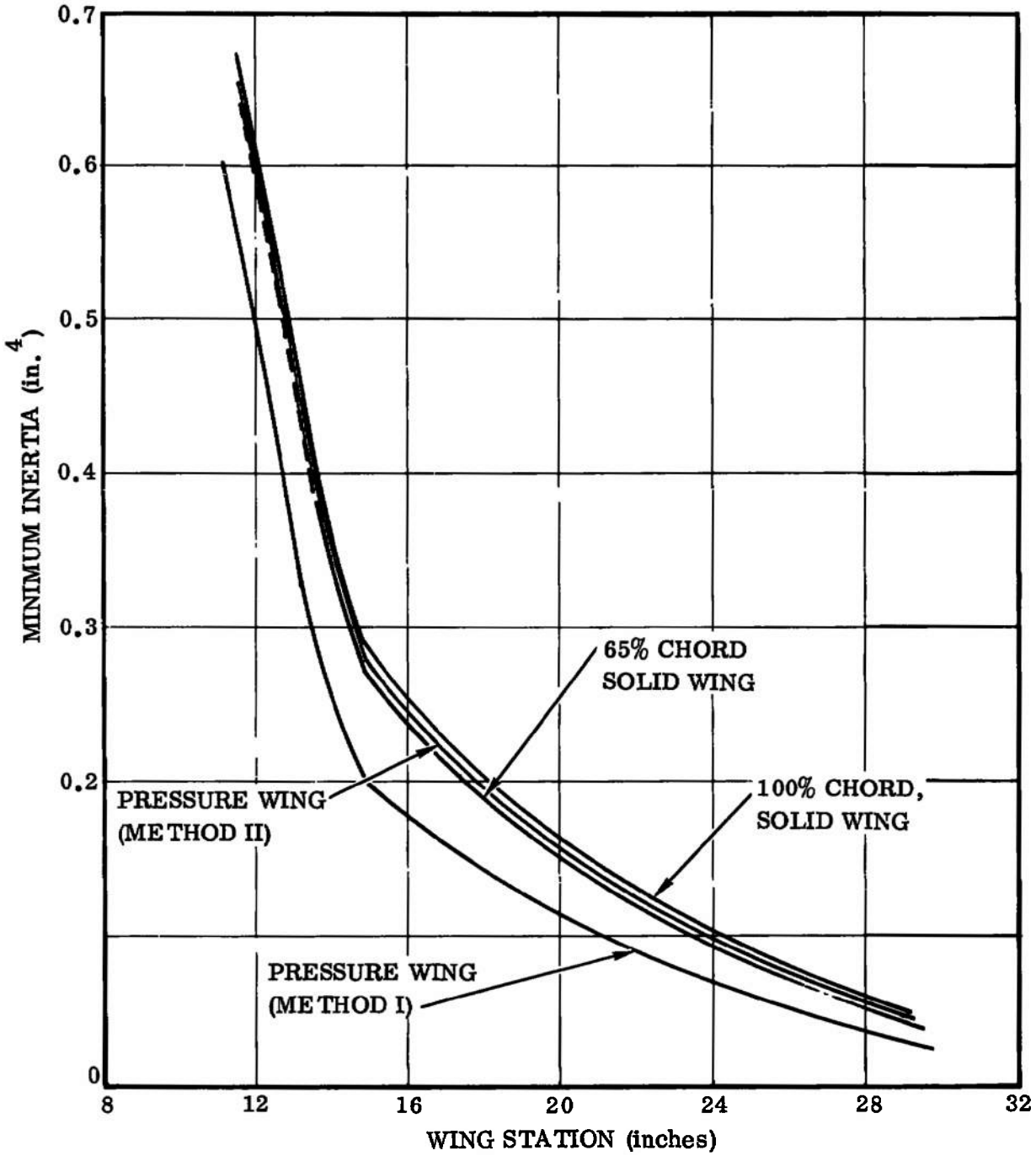


Figure 61. ATT Wing — Minimum Inertias

Table 6. ATT Wing Section Properties and Bending Analysis — 100% Chord Solid Wing

TYPICAL CROSS SECTION

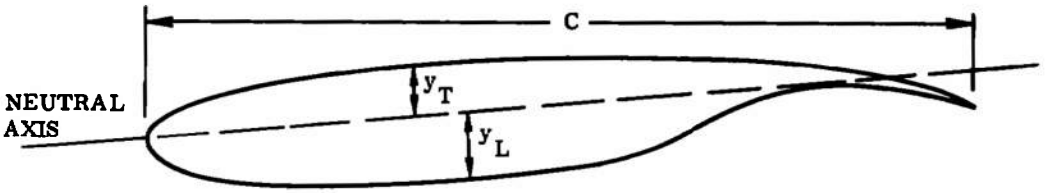


SECTION PROPERTIES

| Section (Ref. Fig. 57) | Wing station (in.) | C (in.) | $y_T$ (in.) | $y_L$ (in.) | $I_{min}$ (in.$^4$) |
|---|---|---|---|---|---|
| 1 | 27.28 | 4.78 | 0.32 | 0.37 | 0.0637 |
| 2 | 17.85 | 6.42 | 0.44 | 0.48 | 0.2074 |
| 3 | 16.33 | 6.69 | 0.46 | 0.50 | 0.2446 |
| 4 | 14.87 | 8.20 | 0.48 | 0.52 | 0.2880 |
| 5 | 13.33 | 9.78 | 0.51 | 0.55 | 0.4470 |

BENDING ANALYSIS (240°K)

| Condition | Section | Wing station (in.) | $M_{E.A.}$ (in-lb) | $f_b$ (psi) | $F_b$ (psi) | S. F. |
|---|---|---|---|---|---|---|
| 5 | 1 | 27.28 | 2,310 | 13,418 | 201,000 | 14.98 |
| | 2 | 17.85 | 10,000 | 23,144 | 201,000 | 8.68 |
| | 3 | 16.33 | 13,100 | 26,778 | 201,000 | 7.51 |
| | 4 | 14.87 | 16,200 | 29,250 | 201,000 | 6.87 |
| | 5 | 13.33 | 20,000 | 24,608 | 201,000 | 8.17 |
| 6 | 1 | 27.28 | 3,080 | 17,890 | 201,000 | 11.24 |
| | 2 | 17.85 | 18,500 | 42,816 | 201,000 | 4.69 |
| | 3 | 16.33 | 21,600 | 44,154 | 201,000 | 4.55 |
| | 4 | 14.87 | 27,700 | 50,014 | 201,000 | 4.02 |
| | 5 | 13.33 | 34,600 | 42,573 | 201,000 | 4.72 |
| 7 | 1 | 27.28 | 3,850 | 22,362 | 201,000 | 8.99 |
| | 2 | 17.85 | 26,200 | 60,636 | 201,000 | 3.31 |
| | 3 | 16.33 | 33,100 | 67,661 | 201,000 | 2.97 |
| | 4 | 14.87 | 40,000 | 72,222 | 201,000 | 2.78 |
| | 5 | 13.33 | 48,300 | 59,429 | 201,000 | 3.38 |
| | | | 300°K | | | |
| 12 | 1 | 27.28 | 5,000 | 29,000 | 201,000 | 6.94 |
| | 2 | 17.85 | 30,000 | 69,400 | 201,000 | 2.90 |
| | 3 | 16.33 | 38,000 | 76,500 | 201,000 | 2.63 |
| | 4 | 14.87 | 50,000 | 90,200 | 201,000 | 2.23 |
| | 5 | 13.33 | 62,000 | 76,300 | 201,000 | 2.64 |

65% Chord Solid Wing (Ref. Figure 7)

The aft 35% of the wing is removable. The material for both portions is PH 13-8 Mo H1000 stainless steel. The bending sections considered have the same locations as the solid wing sections. Section properties and the results of the bending analysis of the 65% chord solid wing configuration are presented in Table 7.

Table 7. ATT Wing Section Properties and Bending Analysis — 65% Chord Solid Wing

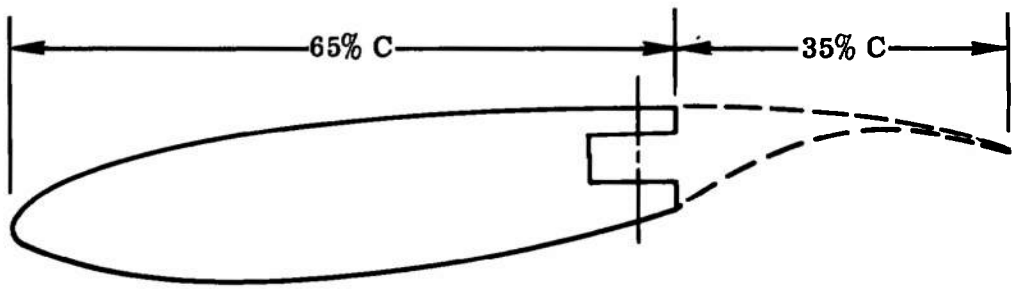


SECTION PROPERTIES (T.E. CONSIDERED INEFFECTIVE)

| Section (Ref. Fig. 57) | Wing station (in.) | C (in.) | $y_T$ (in.) | $y_L$ (in.) | $I_{min}$ (in.$^4$) |
|---|---|---|---|---|---|
| 1 | 27.28 | 4.78 | 0.32 | 0.37 | 0.0599 |
| 2 | 17.85 | 6.42 | 0.45 | 0.47 | 0.1893 |
| 3 | 16.33 | 6.69 | 0.46 | 0.50 | 0.2294 |
| 4 | 14.87 | 8.20 | 0.48 | 0.52 | 0.2698 |
| 5 | 13.33 | 9.78 | 0.51 | 0.55 | 0.4183 |

PRIMARY BENDING ANALYSIS (240°K)

| Condition | Section | Wing station (in.) | $M_{E.A.}$ (in-lb) | $f_b$ (psi) | $F_b$ (psi) | S. F. |
|---|---|---|---|---|---|---|
| 5 | 1 | 27.28 | 2,310 | 14,269 | 201,000 | 13.74 |
| | 2 | 17.85 | 10,000 | 24,828 | 201,000 | 8.10 |
| | 3 | 16.33 | 13,100 | 28,553 | 201,000 | 7.04 |
| | 4 | 14.87 | 16,200 | 31,223 | 201,000 | 6.44 |
| | 5 | 13.33 | 20,000 | 26,297 | 201,000 | 7.64 |
| 6 | 1 | 27.28 | 3,080 | 19,025 | 201,000 | 10.57 |
| | 2 | 17.85 | 18,500 | 45,932 | 201,000 | 4.38 |
| | 3 | 16.33 | 21,600 | 47,079 | 201,000 | 4.27 |
| | 4 | 14.87 | 27,700 | 53,388 | 201,000 | 3.76 |
| | 5 | 13.33 | 34,600 | 45,498 | 201,000 | 4.42 |
| 7 | 1 | 27.28 | 3,850 | 23,781 | 201,000 | 8.45 |
| | 2 | 17.85 | 26,200 | 65,051 | 201,000 | 3.09 |
| | 3 | 16.33 | 33,100 | 72,145 | 201,000 | 2.79 |
| | 4 | 14.87 | 40,000 | 77,094 | 201,000 | 2.61 |
| | 5 | 13.33 | 48,300 | 63,507 | 201,000 | 3.19 |

100% Chord Pressure Model (Method I) (Ref. Figure 11)

The wing is machined from PH 13-8 Mo H1000 stainless steel. The bending sections under consideration have the same locations as those used for the other ATT wing configurations. The results of the stress analysis and the section properties for the Method I pressure model are presented in Table 8.

Table 8. ATT Wing Section Properties and Bending Analysis — 100% Chord Pressure Model (Method I)

EFFECTIVE CROSS SECTION AT PRESSURE PICKUP LOCATION

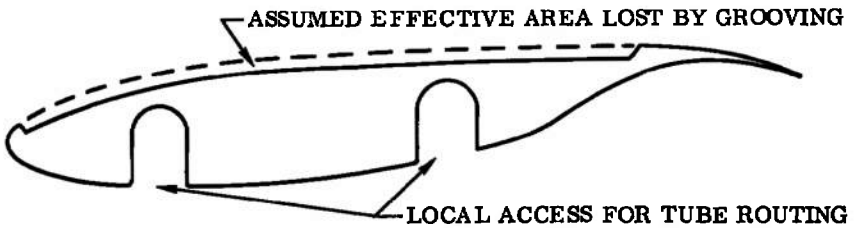


SECTION PROPERTIES

| Section (Ref. Fig. 57) | Wing station (in.) | C (in.) | $y_T$ (in.) | $y_L$ (in.) | $I_{min}$ (in.$^4$) |
|---|---|---|---|---|---|
| 1 | 27.28 | 4.78 | 0.29 | 0.33 | 0.0441 |
| 2 | 17.85 | 6.42 | 0.40 | 0.44 | 0.143 |
| 3 | 16.33 | 6.69 | 0.42 | 0.45 | 0.169 |
| 4 | 14.87 | 8.20 | 0.43 | 0.47 | 0.200 |
| 5 | 13.33 | 9.78 | 0.46 | 0.49 | 0.310 |

BENDING ANALYSIS (240°K)

| Condition | Section | Wing station (in.) | $M_{E.A.}$ (in-lb) | $f_b$ (psi) | $F_b$ (psi) | S. F. |
|---|---|---|---|---|---|---|
| 5 | 1 | 27.28 | 2,310 | 17,286 | 201,000 | 11.63 |
| | 2 | 17.85 | 10,000 | 30,769 | 201,000 | 6.53 |
| | 3 | 16.33 | 13,100 | 34,881 | 201,000 | 5.76 |
| | 4 | 14.87 | 16,200 | 38,070 | 201,000 | 5.28 |
| | 5 | 13.33 | 20,000 | 31,613 | 201,000 | 6.36 |
| 6 | 1 | 27.28 | 3,080 | 23,048 | 201,000 | 8.72 |
| | 2 | 17.85 | 18,500 | 56,923 | 201,000 | 3.53 |
| | 3 | 16.33 | 21,600 | 57,515 | 201,000 | 3.49 |
| | 4 | 14.87 | 27,700 | 65,095 | 201,000 | 3.09 |
| | 5 | 13.33 | 34,600 | 54,690 | 201,000 | 3.68 |
| 7 | 1 | 27.28 | 3,850 | 28,810 | 201,000 | 6.98 |
| | 2 | 17.85 | 26,200 | 80,615 | 201,000 | 2.49 |
| | 3 | 16.33 | 33,100 | 88,136 | 201,000 | 2.28 |
| | 4 | 14.87 | 40,000 | 94,000 | 201,000 | 2.14 |
| | 5 | 13.33 | 48,300 | 76,345 | 201,000 | 2.63 |

65% Chord Pressure Model (Method II) (Ref. Figure 12)

The aft 35% of the wing is removable. The material for both portions is PH 13-8 Mo H1000 stainless steel. The bending sections under consideration have the same locations as those used for the solid wing sections. The stress analysis and section properties for this configuration are presented in Table 9.

Table 9. ATT Wing Section Properties and Bending Analysis — 65% Chord Pressure Model (Method II)

TYPICAL CROSS SECTION

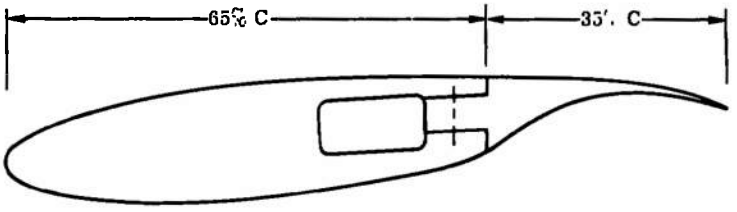


SECTION PROPERTIES (T.E. CONSIDERED EFFECTIVE)

| Section (Ref. Fig. 57) | Wing section (in.) | C (in.) | $y_T$ (in.) | $y_L$ (in.) | $I_{min}$ (in.$^4$) |
|---|---|---|---|---|---|
| 1 | 27.28 | 4.78 | 0.32 | 0.37 | 0.0563 |
| 2 | 17.85 | 6.42 | 0.45 | 0.47 | 0.2000 |
| 3 | 16.33 | 6.69 | 0.46 | 0.50 | 0.2371 |
| 4 | 14.87 | 8.20 | 0.48 | 0.52 | 0.2780 |
| 5 | 13.33 | 9.78 | 0.51 | 0.55 | 0.4350 |

BENDING ANALYSIS (240°K)

| Condition | Section | Wing station (in.) | $M_{E.A.}$ (in-lb) | $f_{bmax}$ (psi) | $F_b$ (psi) | S. F. |
|---|---|---|---|---|---|---|
| 5 | 1 | 27.28 | 2,310 | 15,181 | 201,000 | 13.24 |
| | 2 | 17.85 | 10,000 | 23,500 | 201,000 | 8.55 |
| | 3 | 16.33 | 13,100 | 27,625 | 201,000 | 7.28 |
| | 4 | 14.87 | 16,200 | 30,302 | 201,000 | 6.63 |
| | 5 | 13.33 | 20,000 | 25,287 | 201,000 | 7.95 |
| 6 | 1 | 27.28 | 3,080 | 20,242 | 201,000 | 9.93 |
| | 2 | 17.85 | 18,500 | 43,475 | 201,000 | 4.62 |
| | 3 | 16.33 | 21,600 | 45,550 | 201,000 | 4.41 |
| | 4 | 14.87 | 27,700 | 51,813 | 201,000 | 3.93 |
| | 5 | 13.33 | 34,600 | 43,747 | 201,000 | 4.59 |
| 7 | 1 | 27.28 | 3,850 | 25,302 | 201,000 | 7.94 |
| | 2 | 17.85 | 26,200 | 61,570 | 201,000 | 3.26 |
| | 3 | 16.33 | 33,100 | 69,802 | 201,000 | 2.88 |
| | 4 | 14.87 | 40,000 | 74,820 | 201,000 | 2.69 |
| | 5 | 13.33 | 48,300 | 61,069 | 201,000 | 3.29 |

## Trapezoidal Distribution for C.P. at 40.5%

From the torsional load plots, Figure 29, the c.p. coincides with the E.A. at 40.5% C.

For Section 3,

| | | % of Section Stiffness |
|---|---|---|
| $I_{42\%}$ | = 0.159 in.$^4$ | 67 |
| $I_{48.5\%}$ | = 0.181 in.$^4$ | 76 |
| $I_{65\%}$ | = 0.221 in.$^4$ | 93 |
| $I_{100\%}$ | = 0.237 in.$^4$ | 100 |

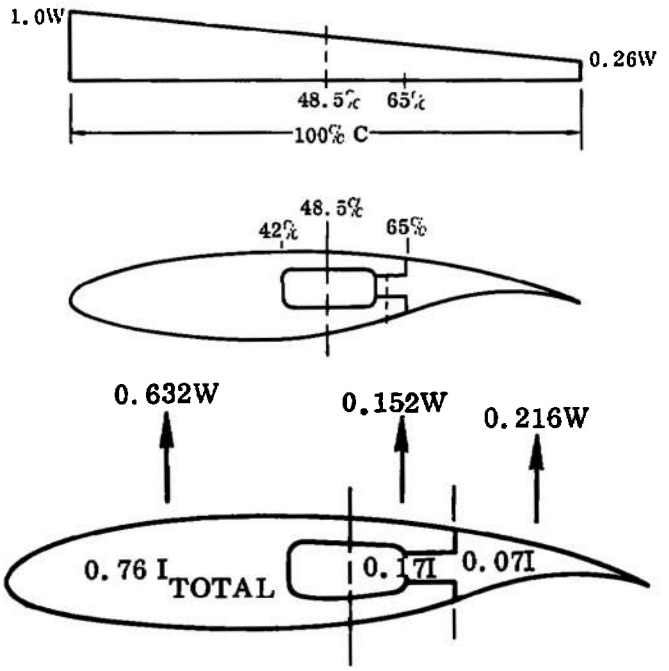


For the preceding chordwise distribution (running chordwise load, W) the distribution over three segments is shown at right.

From shear plot, Figure 29, W = 300 lb/in. at Section 3.

Since the 35% trailing edge portion of the wing deflects in unison with the 65% portion, it tends to carry loads in direct proportion between its stiffness and the stiffness offered by the 65% portion. Therefore loads in excess of this amount must be transferred to the forward section.

Using this approach, the following analysis of the trailing edge attachments and relieved out area is made:

Amount of load carried by T. E. (aft 35% chord) = 0.07 W,

∴ Load Trans. Fwd = 0.146 W

Amount of load carried by 48.5% → 65% = 0.17 W,

∴ Load Trans. Fwd = 0.138 W

From the above, 0.146 W must be transmitted across the trailing edge attachment. Also from the above, 0.133 W must be transmitted across the relieved-out area.

## Trailing Edge Joint Analysis for Typical Section

M at line of attach = 43.8 × 141

= 61.6 in-lb

Screw shear = 61.6 ÷ 0.44

= 140 lb

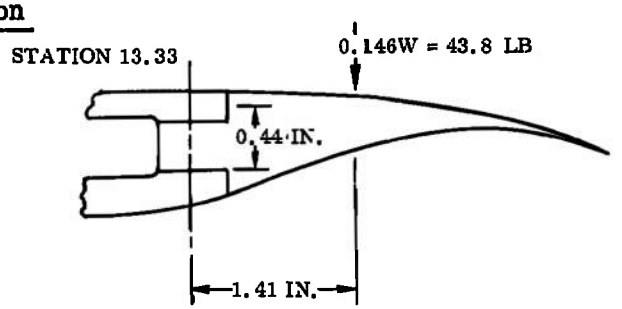

Additional $\frac{VQ}{I}$ shear:

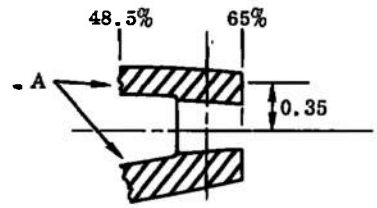


48.5% C → 65% C Inertia = 0.040 in.$^4$
(Ref. page 122)

$$V_{section} = 0.17\ (V_{total}) = 0.17 \times 3800$$

$$= 645 \text{ lb}$$

$$A = 0.82 \text{ in.} \times \overline{0.19} = 0.156 \text{ in.}^2$$

$$\text{Shear at screw shear face} = \frac{VQ}{I} = \frac{645\ (0.156 \times 0.35)}{0.040} = 880 \text{ lb/in.}$$

$$\text{Resultant screw shear} = 140 \nearrow 880 = 892 \text{ lb/in.}$$

$$\text{No. 10 screws at 1.0-in. spacing, } S_{allow} = \frac{95}{160}\ (2,892) = 1,718 \text{ lb}$$

$$\text{S.F.} = \frac{1,718}{892} = \underline{\underline{1.93}}$$

Secondary plate bending effects due to shear transferred forward in a chordwise direction across the relieved-out area.

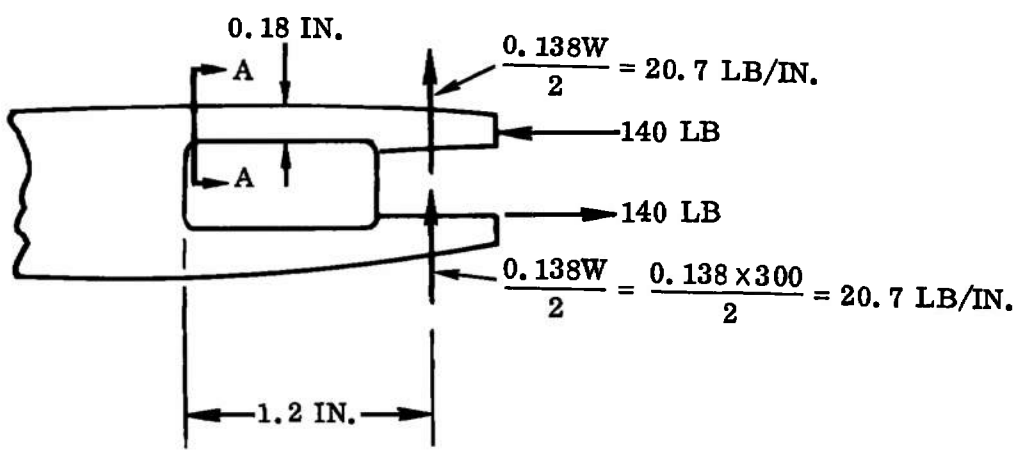


Section A-A, plate bending, 1 inch width (full fixity for shear transfer)

$$f_b = \frac{(20.7 \times 1.2)6}{1 \times 0.18^2} = \pm 4,600 \text{ psi}$$

$$f_{AX} = \frac{140}{0.18} = -775 \text{ psi}$$

$$\Sigma f_c = -5,375 \text{ psi } \underline{\underline{\text{(not critical).}}}$$

Wing Attachment to Fuselage (Ref. Figure 7)

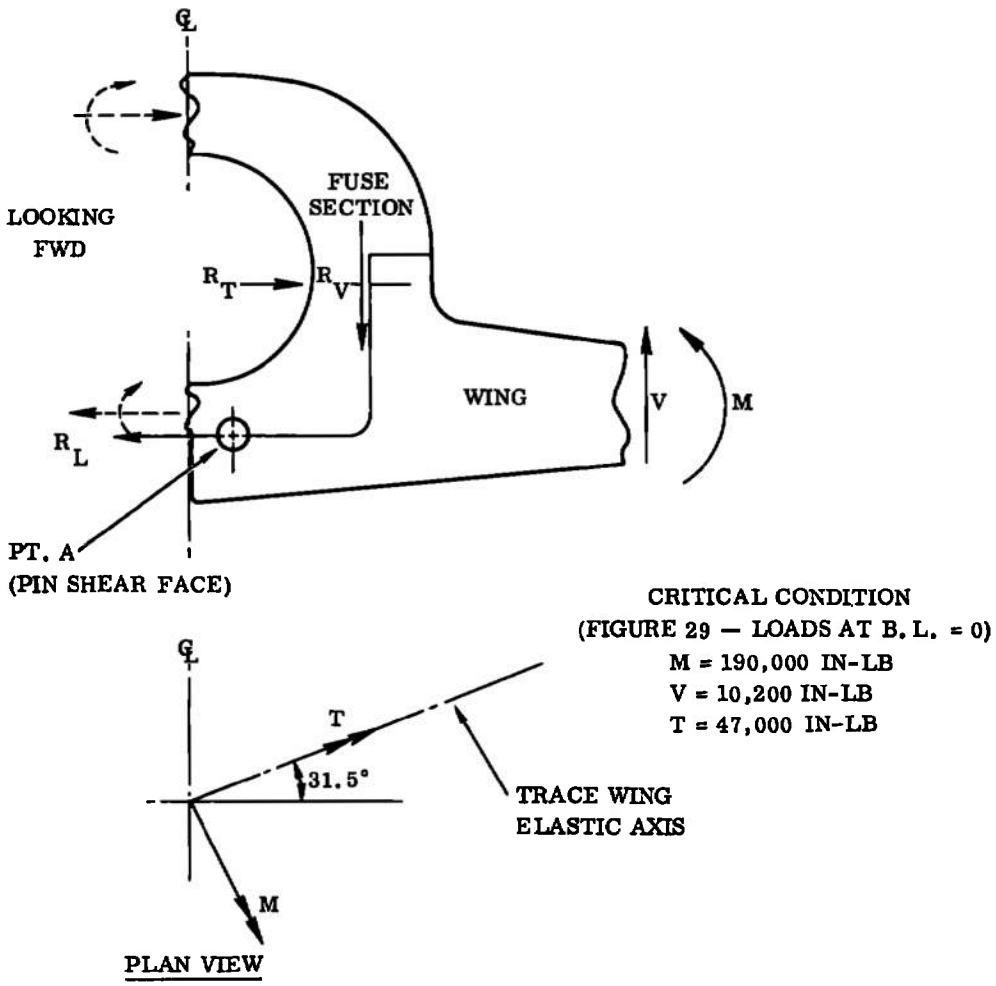


Loads Parallel and Perpendicular to Fuselage ℄ (at Fuselage ℄)

$$M' = 190,000 \cos 31.5° - 37,740 \sin 31.5° = 142,300 \text{ in-lb}$$

$$T' = 190,000 \sin 31.5° + 37,740 \cos 31.5° = -131,500 \text{ in-lb}$$

$$M \text{ at } A = 142,300 - 10,200 \times 2.25 \text{ in.} = 132,100 \text{ in-lb}$$

Row along A has 6-1/2 in. dia. dowels effective for the 65% solid wing version (which is the most critical since the trailing edge is not attached for this version).

$$\text{Couple load due to } M = \frac{132,100}{2.5} = 52,900 \text{ lb}$$

$$\text{Couple load due to } T = \frac{131,500}{2.5} = 52,500 \text{ lb}$$

$$\text{Shear/dowel} = \frac{52,900}{6} + \frac{52,500}{6} = 12,450 \text{ lb}$$

$$\text{Dowel S. F. (lower row)} = \frac{28,700^*}{12,450} = \underline{\underline{2.30}}$$

Upper Row of Dowels

V = 10,200 lb, assuming dowels take vertical shear.

$$\text{Shear/dowel (4 dowels effective)} = \frac{10,200}{4} + \frac{52,500}{4} = 13,350 \text{ lb}$$

$$\text{Dowel S. F. (upper row)} = \frac{28,700^*}{13,350} = \underline{\underline{2.15}}$$

Horizontal Tail (13-8 Mo H1000 Steel)

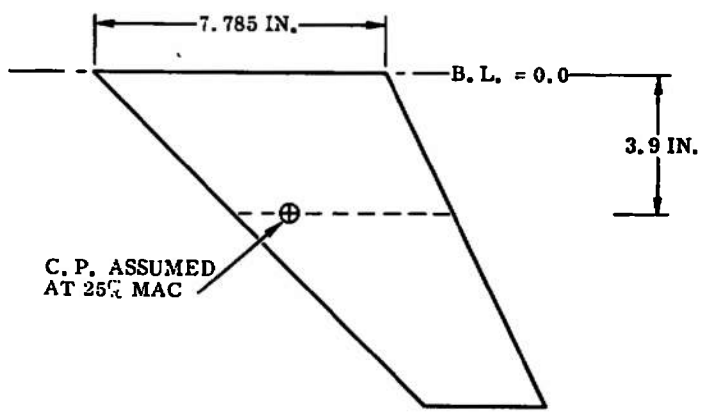


Critical condition is No. 7; total load = 1901.5 lb (Table 3).

Bending Section Check at Root

$$I_X = I_{min} = 0.1427 \text{ in.}^4$$

$$y_{max} = 0.383 \text{ in.}$$

(From a numerical integration of root cross section)

$$M = \frac{1,901.5}{2} \times 3.9 = 3,710 \text{ in-lb}$$

$$f_b = \frac{3,710 \times 0.387}{0.1427} = 10,320 \text{ psi } \underline{\underline{\text{(not critical)}}}$$

Attachment to Vertical

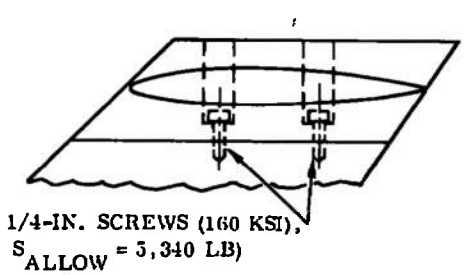


Assume the entire vertical load is taken by the forward screw.

$$\text{S. F.} = \frac{5,340}{1,901.5} = \underline{\underline{2.80}}$$

*Allowable shear load for 1/2-in. dia. dowel.

Vertical Tail (13-8 Mo H1000 Steel)

Critical vertical tail load is 3,070 lb (Table 3)

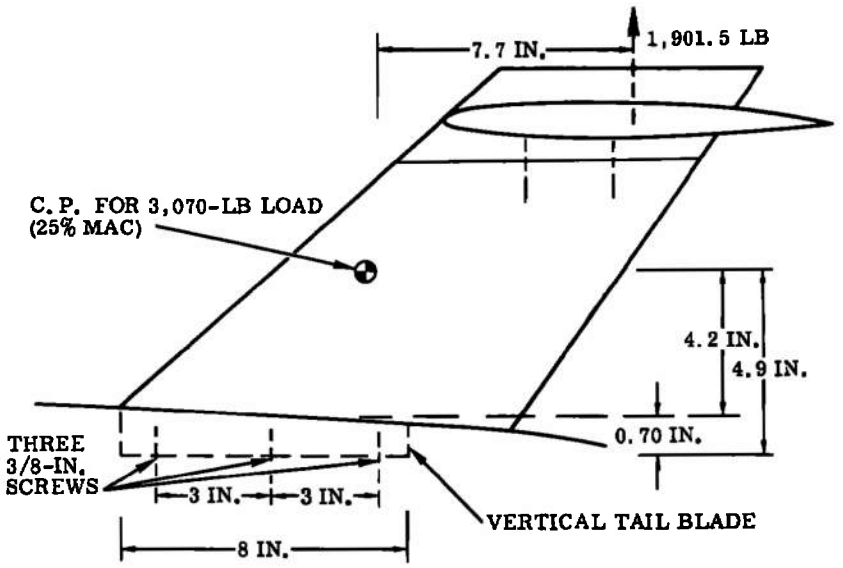


Bending Check of Blade Section at Juncture with Fuselage

Blade width = 1.0 in.

$$\text{Blade bending, } f_b = \frac{(4.2 \times 3{,}070)\,6}{8 \times 1.0^2} = 9{,}650 \text{ psi}$$

$$\text{Blade torsion, } f_s = \frac{3T}{at^2} = \frac{3\,(3 \times 3{,}070)}{8 \times 1.0^2} = 3{,}450 \text{ psi}$$

Blade and tail stresses not critical

Bearing stress distribution between blade and fuselage in reacting side shear, moment, and torque:

$$\text{Bearing stress, } f_{br} = \frac{6\,(4.55 \times 3{,}070)}{8 \times 0.70^2} + \frac{6\,(3 \times 3{,}070)}{0.70 \times 8^2} + \frac{3{,}070}{8 \times 0.70}$$

$$= 28{,}070 \text{ psi (not critical)}$$

Vertical Tail Attachment

Tension due to horizontal tail load:

$$M = 1{,}901.5 \times 10.7 = 20{,}350 \text{ in-lb}$$

Couple arm = 3 in. + (2/3)4 = 5.67 in.

$$P_T = \frac{20,350}{5.67} + \frac{1,901.5}{3} = 4,224 \text{ lb}$$

3/8-in. screw allowable = 13,180 lb tension

$$S.F. = \frac{13,180}{4,224} = \underline{\underline{3.12}}$$

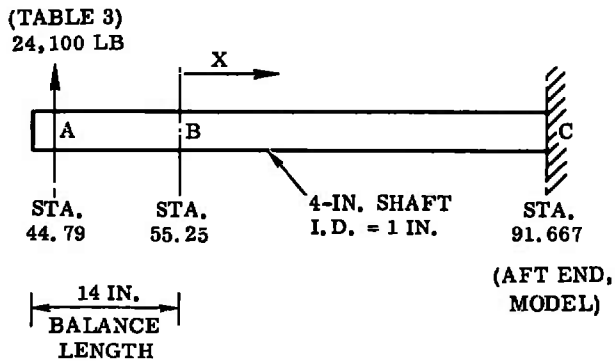


Relative Deflection of Sting Support with Respect to Aft End of Model

$\alpha$ = rotation of B with respect to C $= \int \frac{Mds}{EI}$

$$\alpha = \int_0^{36.417} \frac{24,100(10.46 + x)\,dx}{EI}$$

$$= 252,086\,x + \frac{24,100\,x^2}{2}\Big]_0^{36.417}$$

$$\alpha = \frac{25,160,900}{EI}$$

Where

$$I = \frac{\pi}{4}(R^4 - r^4) = \frac{\pi}{4}(2^4 - 0.5^4)$$

$$= 15.9375 \text{ in.}^4$$

$E = 27.0 \times 10^6$ psi; maraging steel 300 (MIL-S-46850A, Type 3, grade 300)

$$\therefore \alpha = \frac{25,160,900}{(15.9375 \times 27 \times 10^6)} = 0.05847 \text{ radians}$$

Relative deflection, $\delta_R$, due to rotation at B = $36.417\alpha$

$$\delta_R = 36.417 \times 0.05847 = 2.129 \text{ in.}$$

Translation of point B, $\delta_V$, with respect to C:

$$\delta_V = \int_0^{36.417} \frac{Mmds}{EI}$$

$$= \int_0^{36.417} \frac{24,100\,(10.46+x)\,x\,dx}{EI}$$

$$= \left.\frac{252,086\,x^2}{2} + \frac{24,100\,x^3}{3}\right]_0^{36.417} \frac{1}{EI}$$

$$= \frac{555,137,020}{27 \times 10^6 \times 15.9375} = 1.290 \text{ in.}$$

Balance rotation, $\delta_R$: assume = 0.75°, (0.013089 radian)

$$\delta_R' = (0.013089)\ 36.417 = 0.473 \text{ in.}$$

Relative deflection at C between sting and fuselage:

$$\delta_{NET} = 2.129 + 0.473 - 1.290 = \underline{\underline{1.312 \text{ in.}}}$$

Bending Check at Point C (Station 91.667)

$$f_b = \frac{24,100\ (46.877)\,2}{15.9375} = 141,770 \text{ psi}$$

$$F_{tu} = 300,000 \text{ psi}$$

$$S.F. = \frac{300,000}{141,000} = \underline{\underline{2.116}}$$

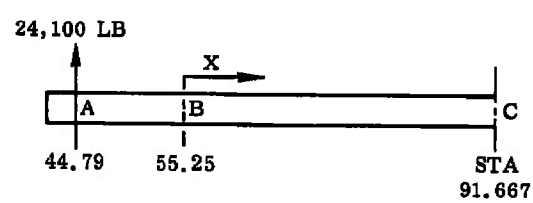


Maneuver Sting Configuration

The sting material is maraging steel 300, MIL-S-46850A, Type 3, grade 300.

The relative deflection at point C between sting and fuselage is a function of the balance rotation, $\alpha_A$; the rotation and vertical displacement of point B with respect to C.

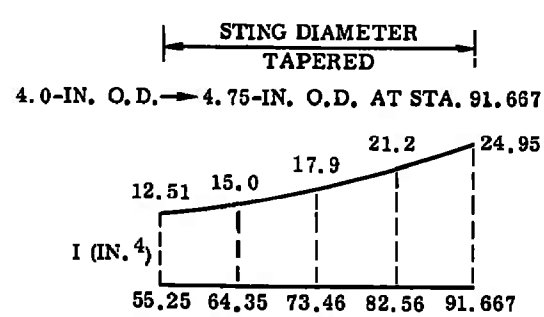

$\alpha_A$, balance rotation, assume = 0.75° = (0.01309 radian)

$$\alpha_B, \text{ rotation of point B} = \int \frac{Mds}{EI} = \int_0^{36.417} \frac{24,100\,(10.46+x)\,dx}{E\,(I)}$$

$\alpha_B$, from numerical integration = 0.04947 radian

$$\delta_B, \text{ displacement of B} = \int \frac{Mxds}{EI} = \int_0^{36.417} \frac{24,100\,(10.46+x)\,xdx}{E(I)}$$

$\delta_B$, from numerical integration = 1.0048 in.

The relative deflection at C between sting and fuselage is:

$$\delta_{net} = \alpha_A\,(36.417) + \alpha_B\,(36.417) - \delta_B$$

$$= 0.01309\,(36.417) + 0.04947\,(36.417) - 1.0048$$

$$= 0.4734 + 1.7989 - 1.0048 = \underline{\underline{1.2675 \text{ in.}}}$$

Bending Check at Point C (Station 91.667)

$$f_b = \frac{24,100\,(46.877)\,2.375}{24.95^*} = 107,540 \text{ psi}$$

$F_{tu}$ = 300,000 psi

$F_b$ = 409,500 psi (Ref. page 122)

$$S.F. = \frac{409,500}{107,540} = \underline{\underline{3.808}}$$

Cruise Sting Configuration (13-8 Mo H1000)

The critical condition is condition 10 (300°K) - Table 2.

The relative deflection at point C between sting and fuselage is a function of the balance rotation, $\alpha_A$; the rotation and vertical displacement of point B with respect to C.

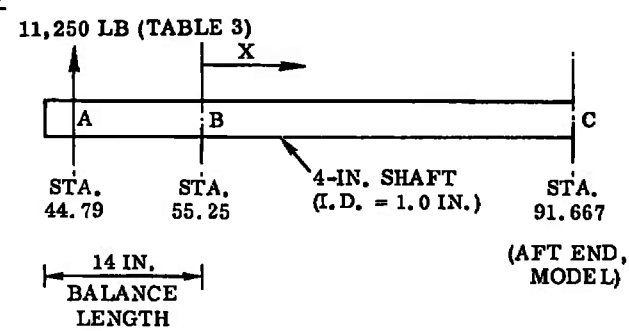


$^*I = \frac{\pi}{4}(R^4 - r^4) = \frac{\pi}{4}(2.375^4 - 0.5^4) = 24.95 \text{ in.}^4$

$\alpha_A$, balance rotation, assume = 0.75 deg = 0.01309 radian

$$\alpha_B, \text{ rotation of point B} = \int_0^{36.417} \frac{M\,ds}{EI} = \int_0^{36.417} \frac{11{,}250\,(10.46+x)\,dx}{EI}$$

$$\alpha_B = \frac{11{,}744{,}777}{EI}$$

Where:

$$I = \frac{\pi}{4}\,(R^4 - r^4)$$

$$= \frac{\pi}{4}(2.0^4 - 0.5^4)$$

$$= 12.517 \text{ in.}^4$$

$$E = 28.3 \times 10^6 \text{ psi}$$

$$\therefore \alpha_B = 0.03315 \text{ radian}$$

The translation of point B, $\delta_B$, with respect to C is:

$$\delta_B = \int_0^{36.417} \frac{M m\,ds}{EI} = \int_0^{36.417} \frac{11{,}250\,(10.46+x)\,x\,dx}{EI}$$

$$= \frac{259{,}137{,}960}{28.3 \times 10^6 \times 12.517} = 0.7315 \text{ in.}$$

The relative deflection at C between sting and fuselage is

$$\delta_{net} = \alpha_A\,(36.417) + \alpha_B\,(36.417) - \delta_B$$

$$= 0.01309\,(36.417) + 0.03315\,(36.417) - 0.7315$$

$$= \underline{\underline{0.9524 \text{ in.}}}$$

<u>Bending Check at Point C (Station 91.667)</u>

$$f_b = \frac{11{,}250\,(46.877)\,2.00}{12.517} = 84{,}264 \text{ psi}$$

$$F_{tu} = 201{,}000 \text{ psi}$$

$$F_b \simeq 1.365^* \,(201{,}000) = 274{,}365 \text{ psi}$$

---

* Form factor ≃ 1.365, Ref. page 123.

$$S.F. = \frac{274,365}{84,264} = \underline{\underline{3.256}}$$

## Nacelle

The critical part of the nacelle is the weldment between the nacelle and its support.

WELD SECTION

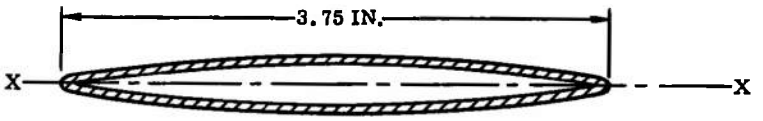


## Section Properties

$A = 0.445 \text{ in.}^2$

$y = 0.18 \text{ in.}$

$I_x = 0.0046 \text{ in.}^4$

$A_{enclosed} = 0.69 \text{ in.}^2$

## Load

Assume:

Lift = 100 lb

Drag = 30 lb

$M_x = 100 \times 0.9 = 90$ in-lb

$M_y = 30 \times 0.9 = 27$ in-lb

$T = 100 \times 2.1 = 210$ in-lb

## Analysis

$$f_b = \frac{M_x y}{I} = \frac{90 \times 0.18}{0.0046} = 3,522 \text{ psi}$$

$$f_{s(direct)} \approx \frac{1.5 \times \text{drag}}{A} = \frac{1.5 \times 30}{0.445} = 101 \text{ psi}$$

$$q_T = \frac{T}{2A} = \frac{210}{(2 \times 0.69)} = 152.174 \text{ lb/in}$$

$$f_{s(torsion)} = \frac{q_T}{t} = \frac{152.174}{0.06} = 2,536 \text{ psi}$$

$$f_{s(total)} = 2,536 + 101 = 2,637 \text{ psi}$$

$$f_{s_{max}} = \sqrt{(f_s)^2 + (f_b/2)^2} = \sqrt{(2,637)^2 + (1,761)^2} = 3,171 \text{ psi}$$

$$f_{n_{max}} = f_{s_{max}} + \frac{f_b}{2} = 3,171 + 1,761 = 4,932 \text{ psi}$$

S. F. = large

Attachment Screws

A check shows the screws to be noncritical.

### 9.1.3 Detailed Stress Analysis — 1/16-Scale Model

Solid Wing

Bending stresses have been calculated (see page 112) for conditions 37, 38, 41, and 42 (Table 2) the resulting range of stresses experienced are plotted versus 1/24-scale stresses in Figure 60.

The following analysis uses section properties shown below.

TYPICAL CROSS SECTION

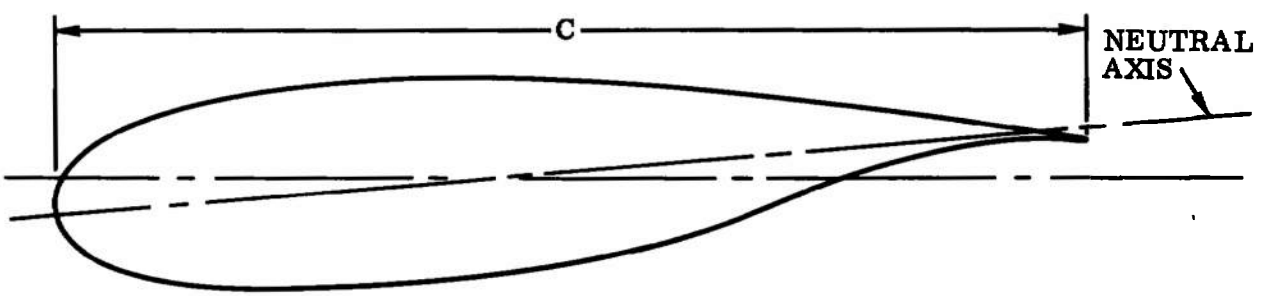


SECTION PROPERTIES (1/16 Scale ATT Wing)

| Section (Ref. Fig. 57) | Wing station (in.) | C (in.) | $y_T$ (in.) | $y_L$ (in.) | $I_{min}$ (in.$^4$) |
|---|---|---|---|---|---|
| 1 | 40.920 | 7.170 | 0.480 | 0.555 | 0.3225 |
| 2 | 26.775 | 9.630 | 0.660 | 0.720 | 1.0500 |
| 3 | 24.495 | 10.035 | 0.690 | 0.750 | 1.2383 |
| 4 | 22.305 | 12.300 | 0.720 | 0.780 | 1.4580 |
| 5 | 19.995 | 14.670 | 0.765 | 0.825 | 2.2629 |

BENDING ANALYSIS (1/16 Scale ATT Wing)

| Condition | Section (Ref. Fig. 57) | Wing station (in.) | $M_{E.A.}$ (in-lb) | $f_b$ (psi) | $F_b$ (psi) | S. F. |
|---|---|---|---|---|---|---|
| 37 | 1 | 40.920 | 4,000 | 6,884 | 201,000 | 29.198 |
| | 2 | 26.775 | 26,500 | 18,171 | 201,000 | 11.062 |
| | 3 | 24.495 | 34,500 | 20,895 | 201,000 | 9.620 |
| | 4 | 22.305 | 42,000 | 22,469 | 201,000 | 8.946 |
| | 5 | 19.995 | 51,500 | 18,775 | 201,000 | 10.706 |
| 38 | 1 | 40.920 | 8,200 | 14,112 | 201,000 | 14.243 |
| | 2 | 26.775 | 68,000 | 46,628 | 201,000 | 4.311 |
| | 3 | 24.495 | 85,200 | 51,602 | 201,000 | 3.895 |
| | 4 | 22.305 | 103,000 | 55,102 | 201,000 | 3 648 |
| | 5 | 19.995 | 123,800 | 45,134 | 201,000 | 4.453 |
| 41 | 1 | 40.920 | 4,500 | 7,744 | 201,000 | 25.956 |
| | 2 | 26.775 | 33,000 | 22,628 | 201,000 | 8.883 |
| | 3 | 24.495 | 42,500 | 25,741 | 201,000 | 7.809 |
| | 4 | 22.305 | 52,000 | 27,818 | 201,000 | 7.226 |
| | 5 | 19.995 | 64,100 | 23,369 | 201,000 | 8.601 |
| 42 | 1 | 40.920 | 12,000 | 20,651 | 201,000 | 9.733 |
| | 2 | 26.775 | 84,000 | 57,600 | 201,000 | 3.490 |
| | 3 | 24.495 | 106,200 | 64,321 | 201,000 | 3.125 |
| | 4 | 22.305 | 129,000 | 69,011 | 201,000 | 2.913 |
| | 5 | 19.995 | 155,300 | 56,618 | 201,000 | 3.550 |

### 9.1.4 Detailed Stress Analysis — 1/12-Scale Model

Solid Wing

The results of the stress analysis and section properties for the 1/12 scale model are shown on page 113.

TYPICAL CROSS SECTION

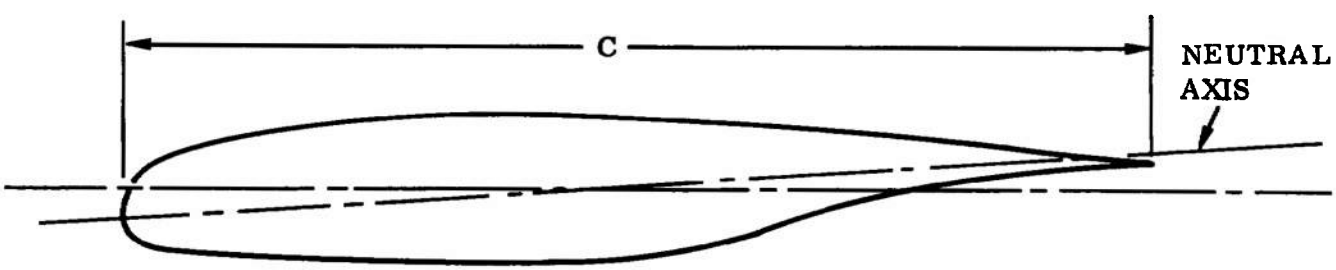

SECTION PROPERTIES (1/12 Scale ATT Wing)

| Section (Ref. Fig. 57) | Wing station (in.) | C (in.) | $y_T$ (in.) | $y_L$ (in.) | $I_{min}$ (in.$^4$) |
|---|---|---|---|---|---|
| 1 | 54.56 | 9.56 | 0.64 | 0.74 | 1.0192 |
| 2 | 35.70 | 12.84 | 0.38 | 0.96 | 3.3184 |
| 3 | 32.66 | 13.38 | 0.92 | 1.00 | 3.9136 |
| 4 | 29.74 | 16.40 | 0.96 | 1.04 | 4.6080 |
| 5 | 26.66 | 19.56 | 1.02 | 1.10 | 7.1520 |

BENDING ANALYSIS (1/12 Scale ATT Wing)

| Condition | Section | Wing station (in.) | $M_{E.A.}$ (in-lb) | $f_b$ (psi) | $F_b$ (psi) | S. F. |
|---|---|---|---|---|---|---|
| 39 | 1 | 54.56 | 7,000 | 5,082 | 201,000 | 39.551 |
| | 2 | 35.70 | 50,100 | 14,494 | 201,000 | 13.868 |
| | 3 | 32.66 | 65,200 | 16,660 | 201,000 | 12.065 |
| | 4 | 29.74 | 80,000 | 18,056 | 201,000 | 11.132 |
| | 5 | 26.66 | 96,700 | 14,873 | 201,000 | 13.514 |
| 40 | 1 | 54.56 | 18,000 | 13,069 | 201,000 | 15.380 |
| | 2 | 35.70 | 128,000 | 37,030 | 201,000 | 5.428 |
| | 3 | 32.66 | 159,900 | 40,857 | 201,000 | 4.920 |
| | 4 | 29.74 | 193,000 | 43,560 | 201,000 | 4.614 |
| | 5 | 26.66 | 231,000 | 35,528 | 201,000 | 5.658 |
| 43 | 1 | 54.56 | 8,000 | 5,808 | 201,000 | 34.607 |
| | 2 | 35.70 | 65,000 | 18,804 | 201,000 | 10.689 |
| | 3 | 32.66 | 81,900 | 20,927 | 201,000 | 9.605 |
| | 4 | 29.74 | 101,000 | 22,795 | 201,000 | 8.818 |
| | 5 | 26.66 | 122,300 | 18,810 | 201,000 | 10.686 |
| 44 | 1 | 54.56 | 23,000 | 16,699 | 201,000 | 12.037 |
| | 2 | 35.70 | 161,000 | 46,577 | 201,000 | 4.315 |
| | 3 | 32.66 | 202,400 | 51,717 | 201,000 | 3.887 |
| | 4 | 29.74 | 245,000 | 55,295 | 201,000 | 3.635 |
| | 5 | 26.66 | 293,900 | 45,203 | 201,000 | 4.447 |

## 9.2 F-111 AIRCRAFT

### 9.2.1 1/12-Scale Model

The 50-deg sweep version of the F-111 is the most highly stressed configuration. Critical wing section stresses vary from 29,300 psi (26 deg sweep) to 70,266 psi (50 deg sweep).

Wing stress vs wing sweep for the solid wings are shown in Figure 62. The structural effects of the different types of wings are illustrated in Figure 63.

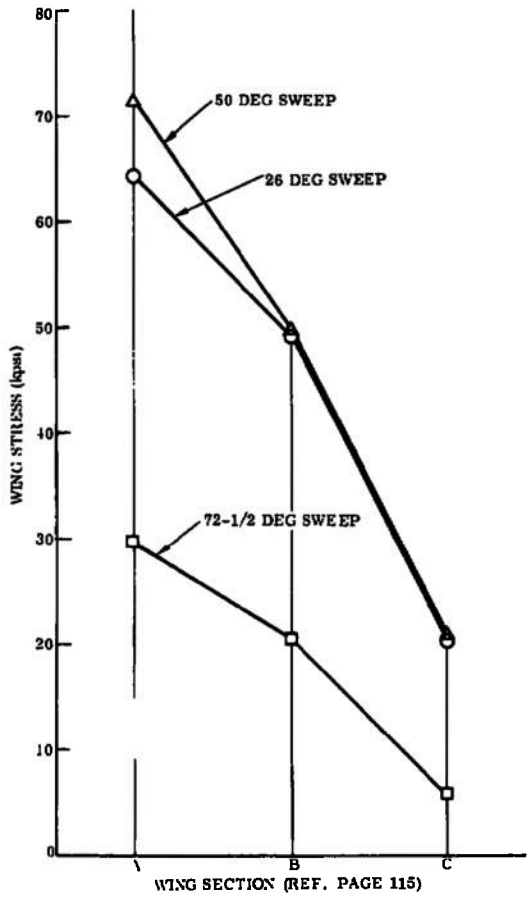


Figure 62. F-111 – Wing Stresses vs Wing Sweeps (Solid Wing)

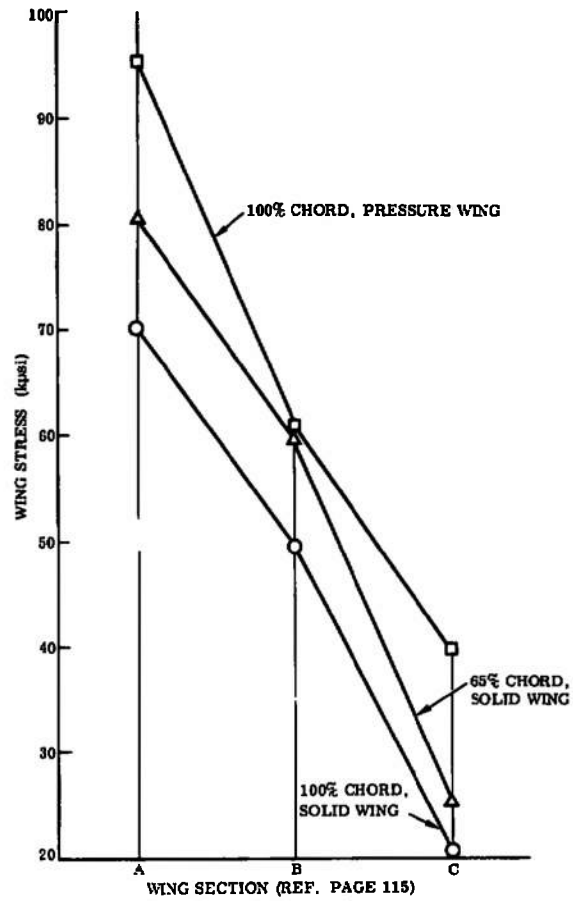


Figure 63. F-111 – Wing Types vs Stress at 50-Degree Sweep

Wing to fuselage attachment is dependent only on the bolt pattern and size. The method shown results in a SF = 4.07.

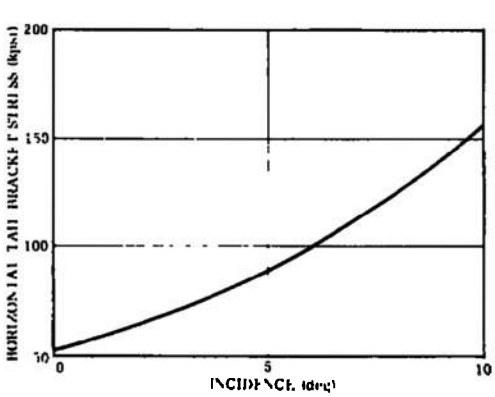


Figure 64. F-111 – Horizontal Tail Bracket Stress vs Incidence

Vertical tail stresses and attachment are no problem. The horizontal tail becomes critical when variable tail incidences are required. Due to the geometry of the tail-to-fuselage area, the horizontal tail begins to unport quickly and leaves little common material between the tail and fuselage at incidence angles of ten degrees or higher. Tail incidence requirements should be weighed carefully. The rise in stress levels vs incidence is shown in Figure 64.

High loads plus a relatively long fuselage contribute to sting stress, model clearance, and aft fuselage modification problems. The sting diameters shown in Figure 8 result in a working stress of 168,400 psi.

The use of 18 Ni-350 grade maraging steel will yield a safety factor of 2+ without the use of any form factor. Larger diameter stings would result in a very poor aft model modification.

### 9.2.2 Detailed Stress Analysis

#### Wing

This analysis is based upon the wing being machined from PH 13-8 Mo stainless steel, condition H1000. The accompanying plan view shows the locations of the sections checked.

PLAN VIEW

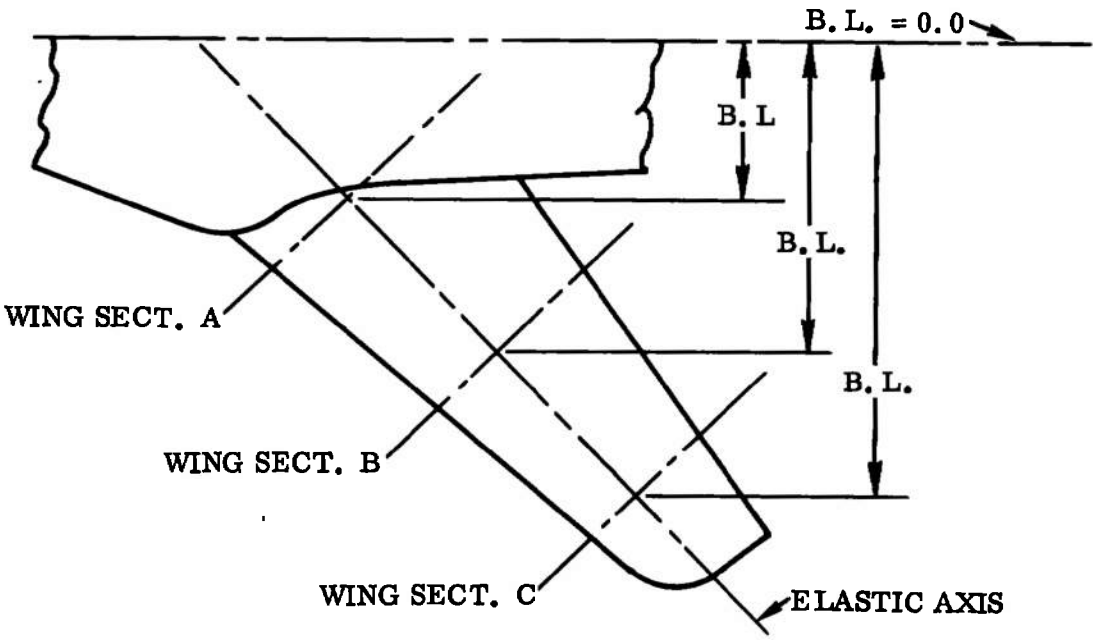


50-DEG WING SWEEP POSITION SHOWN

#### 100% Chord Solid Wing (Ref. Figure 8)

Maximum normal stresses have been calculated for the 26, 50, and 72-1/2 degree wing sweeps. Loads for the critical conditions are shown in Figures 36, 37, 38, and 39.

TYPICAL CROSS SECTION

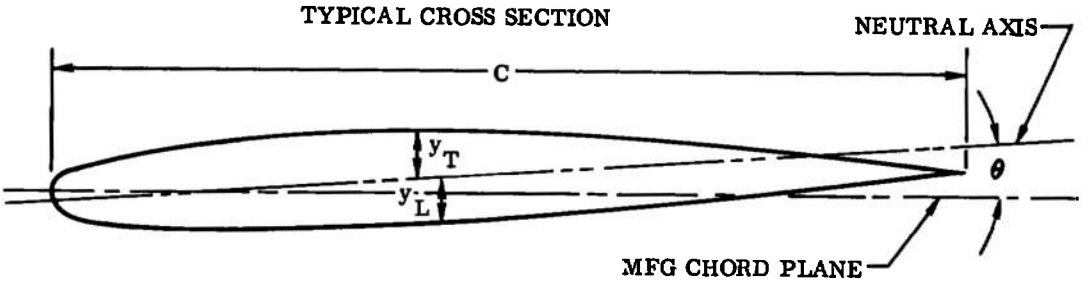

SECTION PROPERTIES (100% Chord Wing)

| Wing section | Area (in.$^2$) | C (in.) | $y_T$ (in.) | $y_L$ (in.) | $\theta$ (deg) | $I_{min}$ (in.$^4$) | $I_{max}$ (in.$^4$) |
|---|---|---|---|---|---|---|---|
| A | 8.117 | 10.30 | 0.584 | 0.576 | 0.261 | 0.652 | 45.495 |
| B | 4.690 | 7.95 | 0.445 | 0.435 | 1.031 | 0.212 | 15.519 |
| C | 2.484 | 5.85 | 0.318 | 0.332 | 2.145 | 0.056 | 4.774 |

BENDING AND TORSION ANALYSIS

| Wing section | B. L. (in.) | Moment (in-lb) | Torsion (in-lb) | $f_{n_{max}}$ (psi) | $F_n$ (psi) | S. F. |
|---|---|---|---|---|---|---|
| | | | 26-DEG SWEEP | | | |
| A | 7.61 | 71,500 | 8,600 | 64,321 | 201,000 | 3.125 |
| B | 16.08 | 22,600 | 3,550 | 47,695 | 201,000 | 4.214 |
| C | 23.62 | 3,500 | 940 | 21,020 | 201,000 | 9.562 |
| | | | 50-DEG SWEEP | | | |
| A | 6.46 | 76,000 | 25,300 | 70,266 | 201,000 | 2.861 |
| B | 12.96 | 23,500 | 4,400 | 49,741 | 201,000 | 4.041 |
| C | 18.76 | 3,500 | 1,300 | 21,347 | 201,000 | 9,416 |
| | | | 72-1/2-DEG SWEEP | | | |
| A | 5.28 | 32,500 | 5,800 | 29,385 | 201,000 | 6.840 |
| B | 8.88 | 9,550 | 3,070 | 20,599 | 201,000 | 9.758 |
| C | 12.08 | 500 | 900 | 4,526 | 201,000 | 44.410 |

65% Chord Solid Wing (Ref. Figure 8)

The aft 35% of the wing is removable and is considered ineffective in bending and torsion. The same loads are applied as for the 100% chord wing.

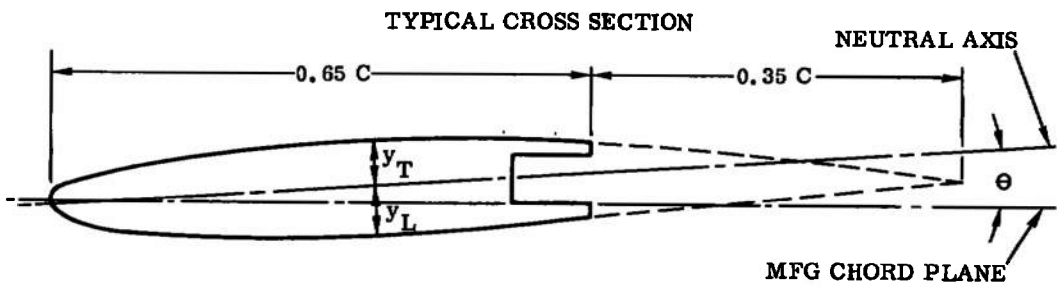

SECTION PROPERTIES (65% Chord Wing)

| Wing section | Area (in.$^2$) | C (in.) | $y_T$ (in.) | $y_L$ (in.) | $\theta$ (deg) | $I_{min}$ (in.$^4$) | $I_{max}$ (in.$^4$) |
|---|---|---|---|---|---|---|---|
| A | 6.005 | 10.30 | 0.583 | 0.577 | 1.119 | 0.564 | 15.458 |
| B | 3.487 | 7.95 | 0.457 | 0.423 | 1.715 | 0.184 | 5.432 |
| C | 1.847 | 5.85 | 0.341 | 0.309 | 2.629 | 0.049 | 1.631 |

BENDING AND TORSION ANALYSIS – 50-DEG SWEEP

| Wing section | B. L. (in.) | Moment (in-lb) | Torsion (in-lb) | $f_{n_{max}}$ (psi) | $F_n$ (psi) | S. F. |
|---|---|---|---|---|---|---|
| A | 6.46 | 76,000 | 25,300 | 81,002 | 201,000 | 2.481 |
| B | 12.96 | 23,500 | 4,400 | 58,919 | 201,000 | 3.411 |
| C | 18.76 | 3,500 | 1,300 | 25,034 | 201,000 | 8.029 |

100% Chord Pressure Wing (Ref. Figure 13)

This wing is subjected to the same loads as the 100% chord solid wing.

TYPICAL CROSS SECTION

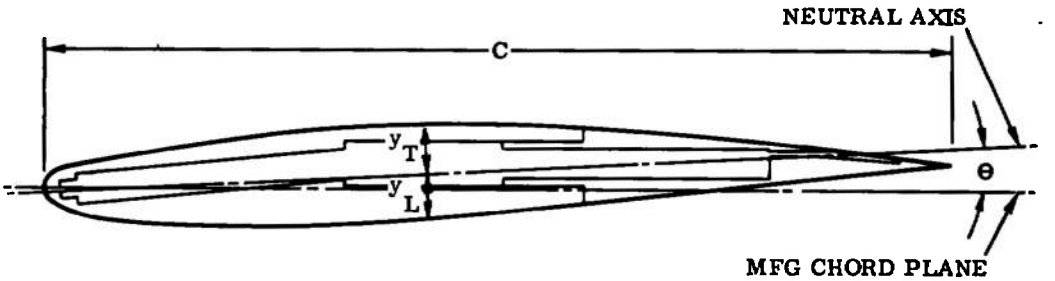


SECTION PROPERTIES

| Wing section | Area (in.$^2$) | C (in.) | $y_T$ (in.) | $y_L$ (in.) | $\theta$ (deg) | $I_{min}$ (in.$^4$) | $I_{max}$ (in.$^4$) |
|---|---|---|---|---|---|---|---|
| A | 5.566 | 10.30 | 0.574 | 0.586 | 0.239 | 0.629 | 28.066 |
| B | 2.892 | 7.95 | 0.442 | 0.438 | 0.926 | 0.200 | 8.818 |
| C | 1.325 | 5.85 | 0.342 | 0.308 | 2.303 | 0.048 | 2.432 |

BENDING AND TORSION ANALYSIS – 50-DEG SWEEP

| Wing section | B. L. (in.) | Moment (in-lb) | Torsion (in-lb) | $f_{n_{max}}$ (psi) | $F_n$ (psi) | S. F. |
|---|---|---|---|---|---|---|
| A | 6.46 | 76,000 | 25,300 | 95,203 | 201,000 | 2.111 |
| B | 12.96 | 23,500 | 4,400 | 60,880 | 201,000 | 3.302 |
| C | 18.76 | 3,500 | 1,300 | 39,221 | 201,000 | 5.125 |

## 65% Chord Pressure Wing (Ref. Figure 13)

The aft 35% of the wing is removable and discontinuous at the fuselage. As such it is considered ineffective in bending and torsion. The same loads are used as for the 100% chord wing.

TYPICAL CROSS SECTION

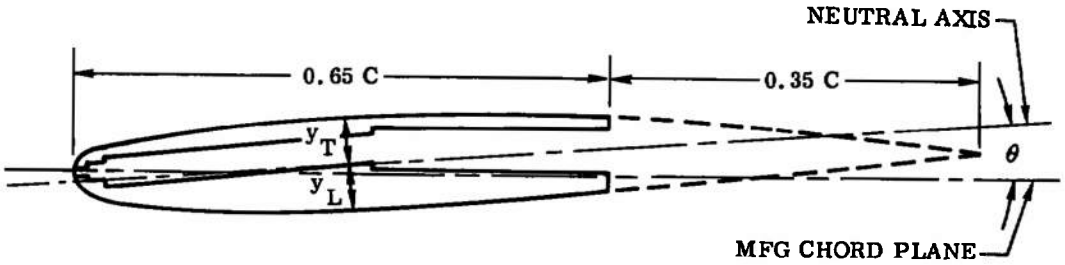


SECTION PROPERTIES

| Wing section | Area (in.$^2$) | C (in.) | $y_T$ (in.) | $y_L$ (in.) | $\theta$ (deg) | $I_{min}$ (in.$^4$) | $I_{max}$ (in.$^4$) |
|---|---|---|---|---|---|---|---|
| A | 4.276 | 10.30 | 0.574 | 0.586 | 0.994 | 0.548 | 9.990 |
| B | 2.212 | 7.95 | 0.451 | 0.429 | 1.645 | 0.174 | 2.995 |
| C | 0.991 | 5.85 | 0.371 | 0.279 | 2.103 | 0.042 | 0.767 |

BENDING AND TORSION ANALYSIS – 50-DEG SWEEP

| Wing section | B. L. (in.) | Moment (in-lb) | Torsion (in-lb) | $f_{n_{max}}$ (psi) | $F_n$ (psi) | S. F. |
|---|---|---|---|---|---|---|
| A | 6.46 | 76,000 | 25,300 | 104,969 | 201,000 | 1.915 |
| B | 12.96 | 23,500 | 4,400 | 69,566 | 201,000 | 2.889 |
| C | 18.76 | 3,500 | 1,300 | 46,213 | 201,000 | 4.349 |

## Check of Wing Splice at 65% Chord

The load on the aft 35% of the chord is assumed to be 10% of the total chord load.

Wing shear at 40% semispan = 6,100 lb (Ref. Figure 36)
Wing shear at 60% semispan - 3,700 lb (Ref. Figure 36)
$\Delta$shear = 6,100 - 3,700 = 2,400 lb
Semispan = 23.5 in.
20% semispan = 4.7 in.
Average span loading between 40% and 60% semispan = 2400/4.7 = 511 lb/in.

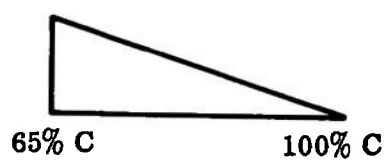


The loading on the aft 35% of the chord = 0.1 × 511 = 51 lb/in. of the span. The loading is triangular from 65% chord to the trailing edge.

Chord at wing section B = 7.95 in.
35% of chord = 2.7825 in.
Moment arm at 65% chord = 2.7825/3 = 0.9275 in.
Unit moment at 65% chord = 0.9275 x 51 = 47.4 in-lb/in. of span.

Couple arm at splice ≈ 0.5 in.

Couple per in. of span = 47.4/0.5 = 94.8 lb

3/16-in. steel screws at 2-in. spacing would be adequate.

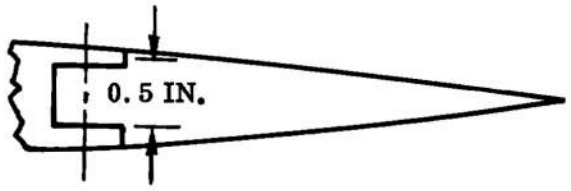


Bolts – Wing-to-Fuselage Attachment

The bolts are 1/2-20 internal wrenching heat treated to 180 ksi. The pattern is shown in Figure 8. Wing loads with respect to the wing elastic axis at model station 29.264 and B. L. 0 are as follows.

$$\left.\begin{aligned} M &= 187{,}322 \text{ in-lb} \\ T &= 28{,}092 \text{ in-lb} \\ S &= 8{,}932 \text{ lb} \end{aligned}\right\} \text{ Ref. Figure 36}$$

Resolving these loads parallel and normal to the fore and aft axis of the model gives the following data.

$$M_{parallel} = M \cos 62.11009° + T \sin 62.11009° = M_{\parallel}$$

$$= 187.322 \times 0.46777 + 28{,}092 \times 0.88385 = 112{,}453 \text{ in-lb}$$

$$M_{normal} = M \sin 62.11009° - T \cos 62.11009° = M_{\perp}$$

$$= 187{,}322 \times 0.88385 - 28{,}092 \times 0.46777 = 152{,}423 \text{ in-lb}$$

The forward bolts are at station 37.657 and the inboard bolts are at B. L. 0.5. Assume bearing along these lines.

$M_{\parallel}$ at B. L. 0 = 112,453 - 0.5 x 8932 = 107,987 in-lb

$M_{\perp}$ at station 37.657 = 152,423 - 8.393 x 8,932 = 77,457 in-lb

$\Sigma x^2 = 2(3.315^2 + 6.632^2 + 9.945^2 + 13.26^2) + 16.6^2 = 934.966 \text{ in.}^2$

$\Sigma y^2 = 6 \times 4.0^2 = 96 \text{ in.}^2$

The aft outboard bolt is critical.

$$\text{Bolt load due to M} = \frac{M_{\perp} x}{\Sigma x^2} = \frac{77,457 \times 16.6}{934.966} = 1,375.2 \text{ lb}$$

$$\text{Bolt load due to } M_{\parallel} = \frac{M_{\parallel} y}{\Sigma y^2} = \frac{107,987 \times 4.0}{96} = 4,499.5 \text{ lb}$$

$$\text{Bolt load due to S} = \frac{S}{\parallel} = \frac{8,932}{\parallel} = 812.0 \text{ lb}$$

Total critical bolt load = 1,375.2 + 4,499.5 + 812.0 = 6,686.7 lb

Allowable bolt load = 27,210 lb (Reference 16)

$$\text{S. F.} = \frac{27,210}{6,686.7} = 4.069$$

Vertical Tail (Ref. Figure 8)

This analysis is based on the vertical tail being machined from PH 13-8 Mo stainless steel, Condition H1000.

The accompanying views show the location of the sections checked.

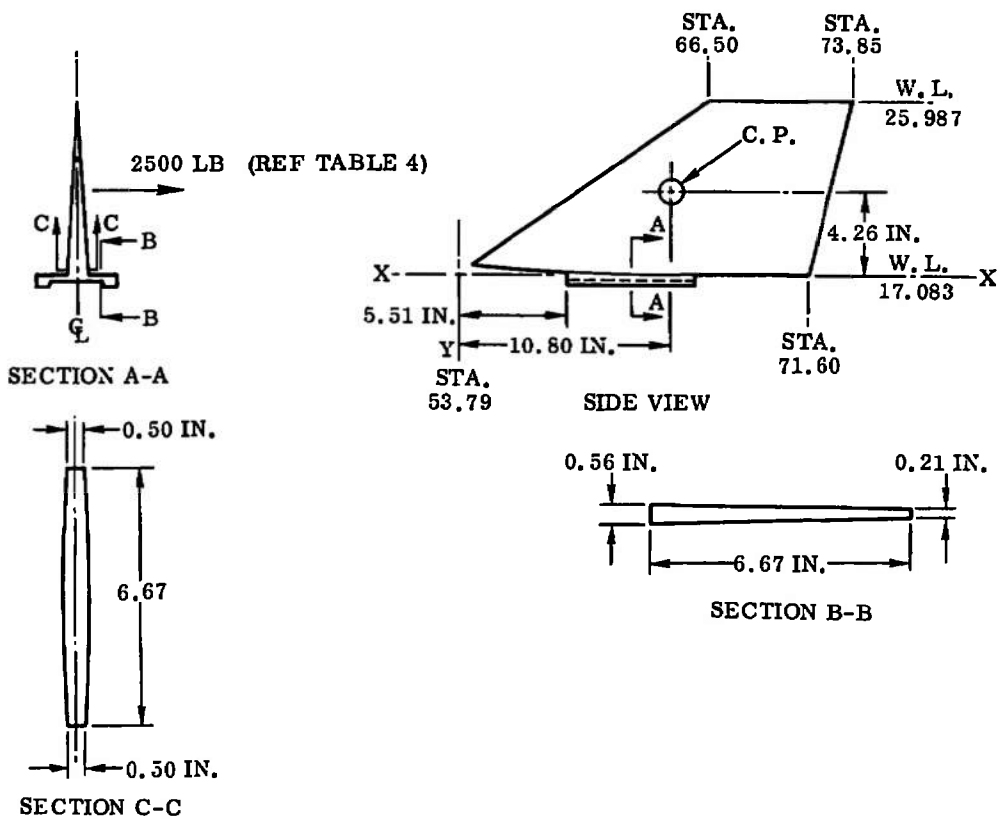

SECTION PROPERTIES

| Tail section | Area (in.$^2$) | y (in.) | x (in.) | $I_{min}$ (in.$^4$) | $I_{max}$ (in.$^4$) |
|---|---|---|---|---|---|
| B-B | 2.537 | 0.28 | 2.83 | 0.0372 | 8.7041 |
| C-C | 3.333 | 0.25 | 3.33 | 0.0695 | 12.3642 |

BENDING AND/OR TORSION ANALYSIS

| Tail section | $Moment_x$ (in-lb) | $Moment_y$ (in-lb) | $f_{n_{max}}$ (psi) | $F_n$ (psi) | S. F. |
|---|---|---|---|---|---|
| B-B | 5,488 | 3,075 | 41,815 | 213,000 | 5.094 |
| C-C | 10,650 | 4,900 | 40,417 | 213,000 | 5.270 |

Horizontal Tail (Ref. Figure 8)

The critical portion of the horizontal tail is the bracket that attaches the tail to the fuselage and the critical section is at the side of the fuselage. This analysis is based on the bracket being machined from PH 13-8 Mo stainless steel, Condition H1000.

The following sketches show the sections checked for incidence angles of 0, 5, and 10 degrees.

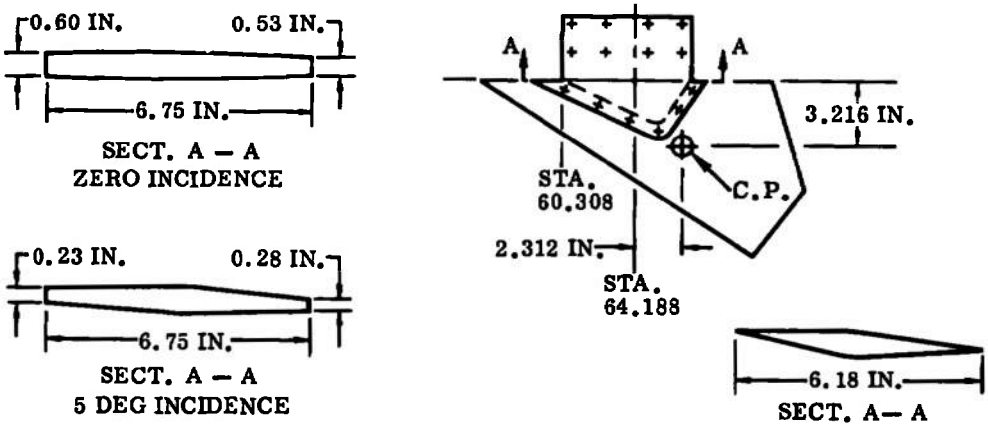


LOAD PER SIDE = 4,500 LB (REF. TABLE 3)

SECTION PROPERTIES – SECTION A-A

| Incidence angle (deg) | Area (in.$^2$) | $y_T$ (in.) | $y_L$ (in.) | $I_{min}$ (in.$^4$) | $I_{max}$ (in.$^4$) |
|---|---|---|---|---|---|
| 0 | 3.712 | 0.300 | 0.300 | 0.0936 | 14.0959 |
| 5 | 2.908 | 0.283 | 0.327 | 0.0526 | 9.0426 |
| 10 | 1.960 | 0.297 | 0.313 | 0.0312 | 3.4635 |

BENDING AND TORSION ANALYSIS

| Incidence angle (deg) | Moment (in-lb) | Torsion (in-lb) | $f_{n_{max}}$ (psi) | $F_n$ (psi) | S. F. |
|---|---|---|---|---|---|
| 0 | 14,472 | 12,677 | 50,173 | 201,000 | 4.006 |
| 5 | 14,472 | 12,002 | 88,038 | 201,000 | 2.283 |
| 10 | 14,472 | 10,512 | 155,298 | 201,000 | 1.294 |

Support System (Ref. Figure 8)

Two different stings were analyzed for relative deflection between the sting support and the aft end of the model: one with a constant cross section; the other with a tapered cross section.

Constant Section Sting Analysis

MAXIMUM VERTICAL FORCE = 30,370 LB (REF. TABLE 3)

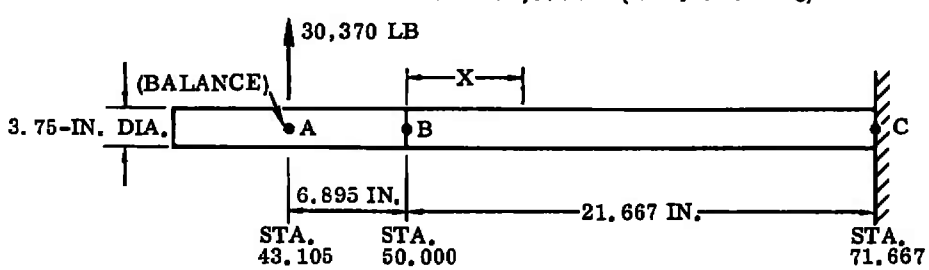


The aft end of the model is at Station 71.667. The model contacts support at point B and forward.

$$M_x = 30,370\,(6.895 + x)$$

Let

$$\alpha = \text{Rotation of Point B} = \int_B^C \frac{M\,ds}{EI}$$

$$= \int_0^{21.667} 30,370\,\frac{(6.895 + x)}{EI}\,dx = \frac{30,370}{EI}\left[6.895\,x + \frac{x^2}{2} + C\right]_0^{21.667}$$

$$= \frac{11,665,828}{EI}$$

$$I = \frac{\pi}{4}\,(R^4 - r^4) = \frac{\pi}{4}\,(1.875^4 - 0.5^4) = 9.658 \text{ in.}^4$$

$$E = 27.0 \times 10^6 \text{ for 18 NI - 300}$$

$$EI = 27.0 \times 10^6 \times 9.658 = 260.8 \times 10^6$$

$$\therefore \alpha = \frac{11,665,828}{260.8 \times 10^6} = 0.04474 \text{ radian}$$

The relative deflection due to rotation at B = $R\alpha$ = 21.667 × 0.04474 = 0.9693 in.

Let

$\delta$ = Translation Deflection of Point B

$$= \int_B^C \frac{Mm\,ds}{EI} = \int_0^{21.667} \frac{30,370(6.895 - x)x\,dx}{EI}$$

$$= \frac{30,370}{EI}\left[\frac{6.895x^2}{2} + \frac{x^3}{3} + C\right]_0^{21.667}$$

$$= \frac{152.125 \times 10^6}{EI} = \frac{152.125 \times 10^6}{260.8 \times 10^6} = 0.5833 \text{ in.}$$

Relative deflection = $R\alpha - \delta$ = 0.9693 - 0.5833 = 0.3860 in.

Assume balance rotation of 0.75° or 0.013089 radian

$R\theta$ = 21.667 × 0.013089 = 0.2836 in.

Total relative deflection = 0.3860 + 0.2836 = <u>0.6696 in.</u>

Check of Sting Bending Stress at Point C

M = 30,370 (6.895 + 21.667) = 867,428 in-lb

$$F_b = \frac{M_y}{I} = \frac{867,428 \times 1.875}{9.658} = 168,402 \text{ psi}$$

Using k = 1.5 and the modulus of rupture curve in the Convair structures manual for extra hard AISI 301 stainless, $F_B/F_{TU}$ = 273/200 = 1.365 (Form Factor).

$F_b$ = 1.365 × 300 ksi = 409.5 ksi

$$\text{S. F.} = \frac{409.5}{168.402} = \underline{\underline{2.432}}$$

Tapered Section Sting Analysis

The aft end of the model is at Station 71.667. The model contacts the support at point B. The forward sting is 4.25-in. O.D. at B and tapers to 3.75-in. O.D. at C. The I.D. is 1.00 in.

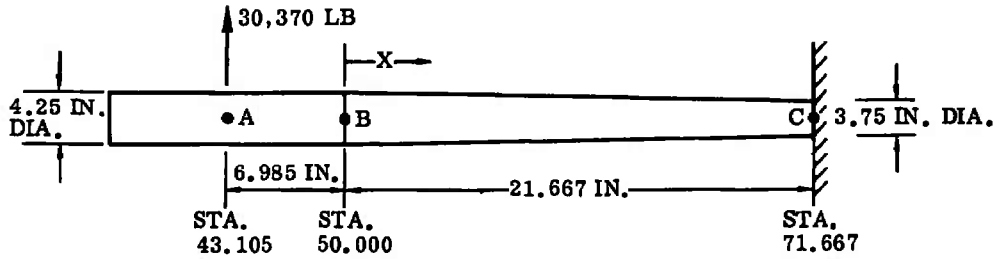


$M_x = 30,370\ (6.895 + x)$

Let $\alpha$ = Rotation of point B = $\displaystyle\int_B^C \frac{M\,ds}{EI}$

$$= \int_B^C \frac{30,370\ (6.895 + x)\,dx}{EI} = \frac{30,370}{EI}\left[6.895\,x + \frac{x^2}{2} + C\right]_B^C$$

Since I is not constant, the integration is made in five steps. The resulting rotation angle, $\alpha$, is 0.03656 radian.

Relative deflection due to rotation at B = $R\alpha$ = 21.667 × 0.03656 = 0.7921 in.

Let $\delta$ = Translation deflection of Point B = $\displaystyle\int_B^C \frac{Mmds}{EI}$

$$\delta = \int_B^C \frac{30,370\,(6.895 + x)\,x\,dx}{EI} = \frac{30,370}{EI}\left[\frac{6.895\,x^2}{2} + \frac{x^3}{3} + C\right]_B^C$$

Integrating in five steps, to account for the variable I, results in a translation of 0.5054 in.

Relative deflection = $R\alpha - \delta$ = 0.7921 - 0.5054 = 0.2867 in.

$R\theta$ = 21.667 × 0.013089 = 0.2836 in. (due to 0.75° balance rotation)

Total relative deflection = 0.2867 + 0.2836 = <u>0.570 in.</u>

<u>Sting Bending Stress at Point C (Dia. = 3.75 in.)</u>

The stress and safety factor are the same as for the constant section.

## 9.3 DELTA CANARD FIGHTER

### 9.3.1 1/9.6-Scale Model

The low aspect ratio delta wing is inherently strong and stiff, therefore the Delta Canard model can be tested throughout its complete operating range under ambient (300°K) tunnel temperature conditions. The maximum wing stress is only 21,800 psi for the pressure-instrumented wing.

Wing-to-fuselage and vertical tail-to-fuselage attachments are more highly loaded than any other components. These attachments can be optimized by proper sizing and spacing of attachments.

A movable canard assembly is included with no large structural problems.

The model support system can be fabricated from PH 13-8 Mo steel with a safety factor of 2.88.

### 9.3.2 Detailed Stress Analysis

Solid Wing (Ref. Figure 9)

The wing is machined from PH 13-8 Mo H1000 stainless steel. The accompanying plan view shows the locations of the sections used for the wing bending analysis.

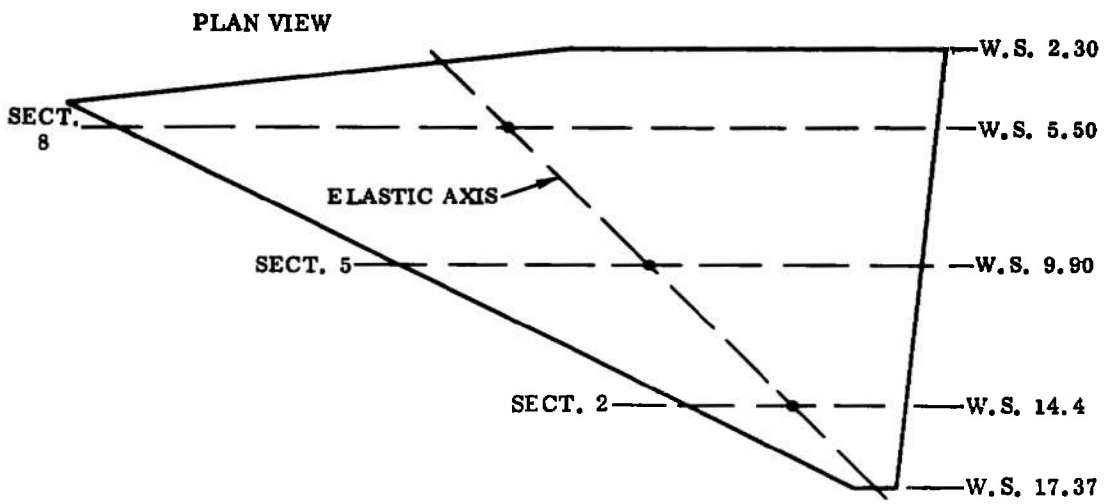


The analysis is performed on three different wing configurations for the critical loads due to the ambient (300°K) temperature condition.

a. 100% chord solid wing.

b. 70% chord solid wing.

c. 70% chord pressure wing.

## Wing Bending Sections

Primary bending and torsional stresses have been calculated for the critical condition, condition 23 (300°K) (Table 2). The following table shows the resulting stresses for the three wing configurations.

BENDING ANALYSIS

| Section | $I^*$ (in.$^4$) | $J^*$ (in.$^4$) | $c_U{}^*$ (in.) | $M^\dagger$ (in-lb) | $T^\dagger$ (in-lb) | $f_{st}{}^\ddagger$ (psi) | $f_b{}^\ddagger$ (psi) |
|---|---|---|---|---|---|---|---|
| | | | 100% SOLID WING | | | | |
| 2 | 0.0050 | 0.010 | 0.14 | 682 | 190 | 2,660 | 19,100 |
| 5 | 0.112 | 0.402 | 0.282 | 5,141 | 1,827 | 1,280 | 12,900 |
| 8 | 0.650 | 2.55 | 0.448 | 14,627 | 5,160 | 906 | 10,100 |
| | | | 70% SOLID WING (T.E. INEFFECTIVE) | | | | |
| 2 | 0.00437 | ≃0.0087 | 0.14 | 682 | 190 | 3,060 | 21,800 |
| 5 | 0.098 | ≃0.350 | 0.282 | 5,141 | 1,827 | 1,470 | 14,720 |
| 8 | 0.636 | ≃2.22 | 0.448 | 14,627 | 5,160 | 1,040 | 10,300 |
| | | | 70% PRESSURE WING | | | | |
| 2 | - | | (Not Applicable) | | | | - |
| 5 | 0.082 | ≃0.350 | 0.282 | 5,141 | 1,827 | 1,470 | 17,200 |
| 8 | 0.620 | ≃2.22 | 0.448 | 14,627 | 5,160 | 1,040 | 10,580 |

* Ref. Figure 65.

† M and T, aerodynamic loads without inertia relief (conservative)

‡ $f_b = \frac{Mc_U}{I}$, $f_{st} = \frac{Tc_U}{J}$

From the table above, the most critical section is section 2 for the 70% solid wing version.

$$f_s = \frac{f_b}{2} + f_{st} = \frac{21,800}{2} + 3,060 = 11,320 \text{ psi}$$

$$f_n = \frac{f_b}{2} + f_s = 10,900 + 11,320 = 22,220 \text{ psi}$$

Material: PH 13-8 Mo H1000

$$F_{tu} = 201,000 \text{ psi}$$

$$\text{S. F.} = \frac{201,000}{22,220} = \underline{\underline{9.05}}$$

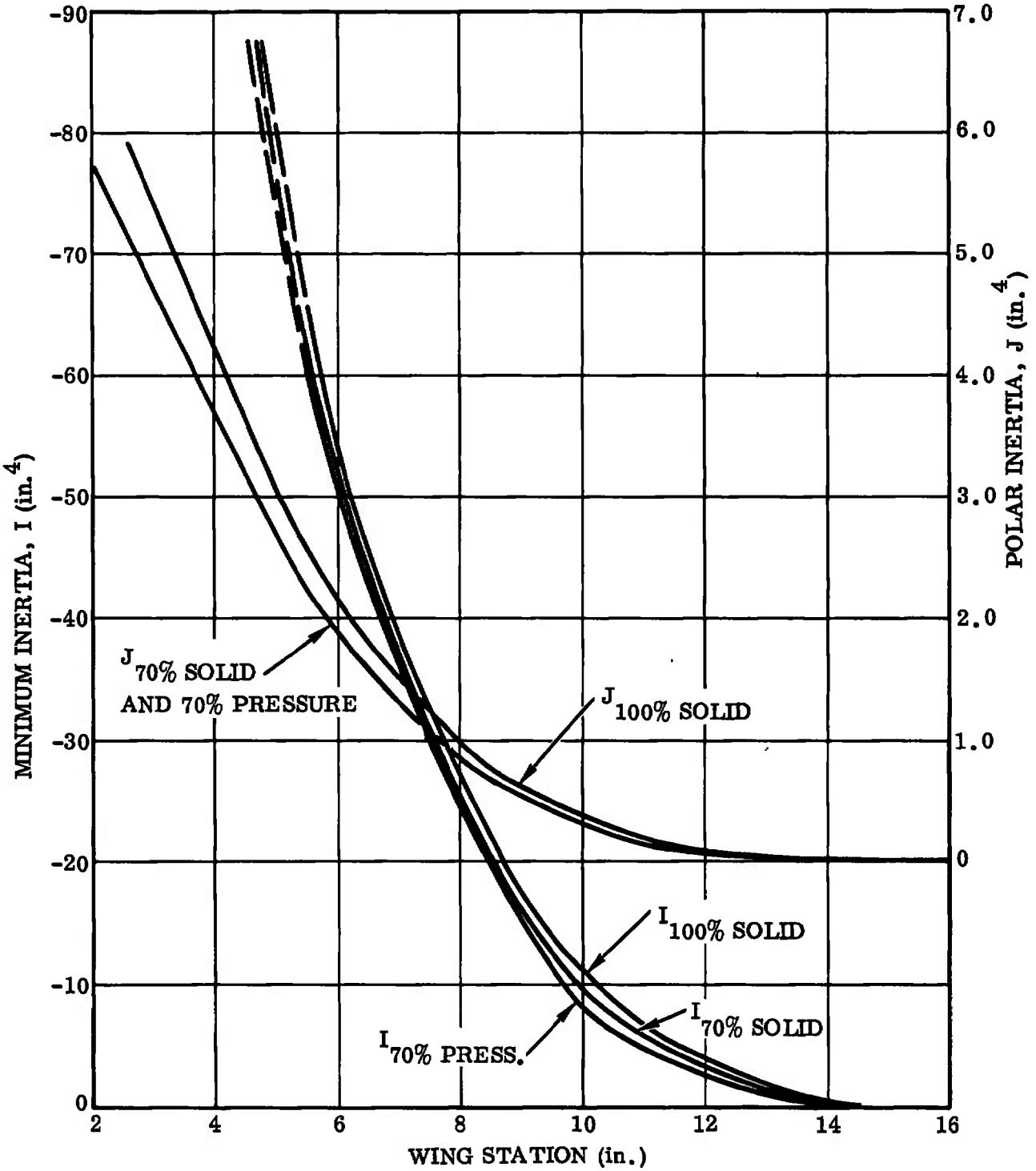


Figure 65. Delta Canard – Wing Section Properties

Wing-to-Fuselage Attachments

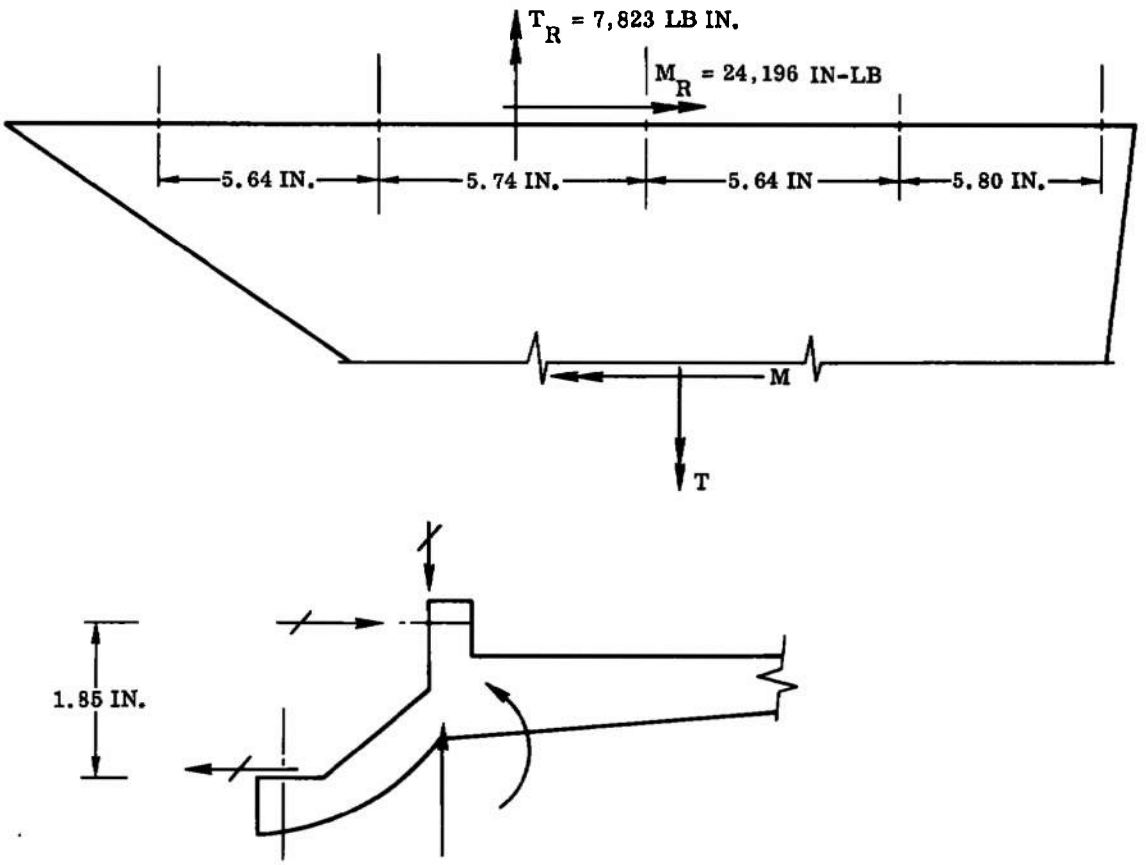


Lower Row of 3/8-in. Screws

Disregarding the aft set of attachments, the maximum shear on the lower set of screws is

$$\text{Couple due to M} = \frac{24,196}{1.85} = 13,100 \text{ lb}$$

$$\text{Couple due to T} = \frac{7,823}{1.85} = 4,220 \text{ lb}$$

$$\frac{\text{Shear}}{\text{3/8-in. screw}} = \frac{13,100}{4} + \frac{4,220}{4} = 3,450 \text{ lb}$$

$$\text{Allow } P_S = \frac{95}{160} \times 13,180 \text{ lb} = 7,800 \text{ lb}$$

$$\text{S. F.} = \frac{7,800}{3,450} = \underline{\underline{2.26}}$$

The upper row of four screws is not critical.

Vertical Tail (PH 13-8 Mo H1000 Steel)

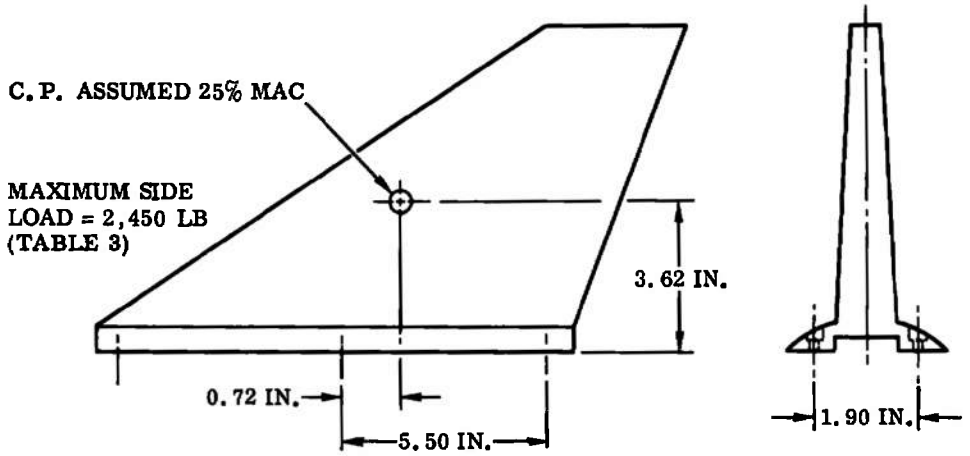


Moment at base = 3.62 × 2450 = 8,850 in-lb

Consider the aft two pairs of screws reacting side moment:

$$\text{Max screw tension} = \frac{4.78}{5.50}(8,850) \div 1.90 \text{ in.} = 4,050 \text{ lb}$$

5/16-in, 160,000 psi screws, $P_{allow}$ = 8,590 lb

$$\text{S. F.} = \frac{8,590}{4,050} = \underline{\underline{2.12}}$$

Critical Bending at Base, Section A-A

Section A-A, 1.40-in. effective width assumed.

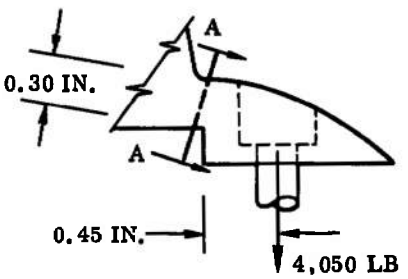


$$f_b = \frac{6M}{bt^2} = \frac{6(4,050 \times 0.45)}{1.4(0.30)^2}$$

$$= 86,600 \text{ psi}$$

PH 13-8 Mo H1000, $F_{tu}$ = 201,000 psi

$$\text{Conservative S. F. (without form factor)} = \frac{201,000}{86,600} = \underline{\underline{2.32}}$$

## Canard

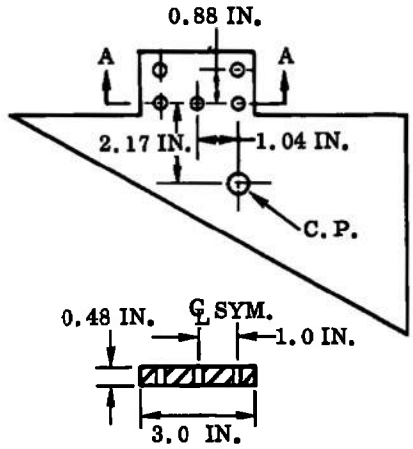

SECTION A—A

The following is a check of section A-A loads.

Assume:

Lift = 1,000 lb at C. P.

$M = 2.17 \times 1{,}000 = 2170$ in-lb

$T = 1.04 \times 1{,}000 = 1{,}040$ in-lb

## Section Properties

To allow for counter sink assume holes are 0.3-in. diameter all the way through.

$$A = 2.1 \times 0.48 = 1.008 \text{ in.}^2$$

$$I = \frac{2.1 \times \overline{0.48}^3}{12} = 0.01935 \text{ in.}^4$$

## Analysis

$$f_b = \frac{M_y}{I} = \frac{2{,}170 \times 0.24}{0.01935} = 26{,}915 \text{ psi}$$

$$f_s = \frac{T(3a + 1.8b)}{8a^2 b^2} = \frac{1{,}040(3 \times 1.05 + 1.8 \times 0.24)}{8 \times 1.05^2 \times 0.24^2} = 7{,}333 \text{ psi}$$

$$f_{s_{max}} = \sqrt{f_s^2 + (f_b/2)^2} = \sqrt{(7{,}333)^2 + (13{,}458)^2} = 15{,}326 \text{ psi}$$

$$f_{n_{max}} = f_{s_{max}} + \frac{f_b}{2} = 15{,}326 + 13{,}458 = 28{,}784 \text{ psi}$$

The material is PH 13-8 Mo H1000.

$$F_{tu} = 201{,}000 \text{ psi}$$

$$\text{S. F.} = \frac{201{,}000}{28{,}784} = \underline{\underline{6.983}}$$

Check of Screws

Taking moments about the inboard row:

$$R_s \times 0.88 - 1,000\ (2.17 + 0.88) = 0$$

$$R_s = \frac{1,000\ (2.17 + 0.88)}{0.88} = 3,466 \text{ lb}$$

The load per screw due to moment = 3,466/3 = 1,155 lb

Taking moments about the forward row and neglecting the screw on ℄,

$$R_s \times 2 - 1,000 \times 2.04 = 0$$

$$R_s = \frac{1,000 \times 2.04}{2} = 1,020 \text{ lb}$$

The load per screw due to torque = 1,020/2 = 510 lb

The maximum screw load = 1,155 + 510 = 1,665 lb

Use 1/4-28 internal wrenching screws heat treated to 180 ksi

$P_T$ = 6,010 lb (Ref. MIL-HDBK-5A page 8.1.2(b))

$$\text{S. F.} = \frac{6,010}{1,665} = \underline{\underline{3.610}}$$

Relative deflection of sting support with respect to aft end of model

Relative deflection at C between sting and fuselage:

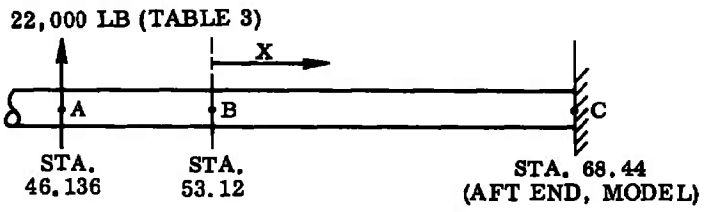


$$\delta_{net} = \alpha_A\ (68.44 - 46.136) + \alpha_B\ (68.44 - 53.12) - \delta_B$$

where

$\alpha_A$ = rotation of balance at A (radians) relative to B

$\alpha_B$ = rotation of B with respect to C (radians)

$\delta_B$ = vertical displacement of B with respect to C

$$\alpha_B = \int \frac{M\,ds}{EI} = \int_0^{15.32} \frac{22,000\,(6.984 + x)\,dx}{EI}$$

where

$$I = \frac{\pi}{4}\,(R^4 - r^4) = \frac{\pi}{4}\,(1.875^4 - 0.5^4)$$

$$I = 9.658 \text{ in.}^4$$

PH 13-8 Mo H1000 steel, $E = 28.3 \times 10^6$ psi

$$\therefore \alpha_B = 153,648x + \frac{22,000x^2}{2}\Bigg]_0^{15.32} \frac{1}{EI} = 0.01805 \text{ radian}$$

Relative deflection of sting support with respect to aft end of model:

$\alpha_A$, balance rotation: assume = 0.75° = 0.013089 radian

$\delta_B$, translation of B with respect to C $= \int \frac{Mm\,dx}{EI}$

$$\delta_B = \int_0^{15.32} \frac{22,000\,(6.984 + x)\,x\,dx}{EI}$$

$$\delta_B = \frac{153,648x^2}{2} + \frac{22,000x^3}{3}\Bigg]_0^{15.32} \frac{1}{EI} = 0.1625 \text{ in.}$$

$$\therefore \delta_{net} = \alpha_A\,(22.30) + \alpha_B\,(15.32) - \delta_B$$

$$= 22.30\,(0.013089) + 15.32\,(0.01805) - 0.1625$$

$$= \underline{\underline{0.406 \text{ in.}}}$$

<u>Bending Check at Point C (Station 68.44)</u>

$$f_b = \frac{22,000\,(22.30) \times 1.875}{9.658} = 95,245 \text{ psi}$$

$F_{tu}$ = 201,000 psi, using the same factor as for maraging steel - Ref. page 123

$$F_b = \frac{409,500}{300,000}\ 201,000 = 274,365 \text{ psi}$$

$$\text{S. F.} = \frac{274,365}{95,245} = \underline{\underline{2.88}}$$

## 9.4 SPACE SHUTTLE BOOSTER

### 9.4.1 1/46.5-Scale Model

The space shuttle booster model is the least critical structurally of all model configurations. The complete model test plan can be covered using ambient temperature tunnel conditions (300°K).

Maximum wing stress at the wing-to-fuselage intersection results in 6,228 psi for a solid wing and 8,000 psi for a pressure wing.

Vertical tail stresses are also low (35,700 psi), and the vertical tail can be assembled to the fuselage with screws with no particular problem.

The model balance is positioned farther aft in the model than the airplane configurations, which results in a shorter sting requiring less clearance at the model aft end. Sting stresses run about 41,000 psi.

### 9.4.2 Detailed Stress Analysis

Solid Wing (Ref. Figure 10)

Check of section at B. L. 4.15 (side of fuselage):

The section will be conservatively checked for the air loads without inertia relief.

$$\left.\begin{aligned} M &= 59{,}296 \text{ in-lb} \\ T &= -20{,}057 \text{ in-lb} \\ S &= 8{,}763 \text{ lb} \end{aligned}\right\} \text{Ref. Figure 42}$$

Section Properties

$I_{min} = 10.762 \text{ in.}^4$

$y = 1.1 \text{ in.}$

$A = 37.071 \text{ in.}^2$

Chord = 22.251 in.

$$\text{Average depth of section} = \frac{37.071}{22.253} = 1.666 \text{ in.}$$

Analysis

$$f_b = \frac{M_y}{I} = \frac{59,296 \times 1.1}{10.762} = 6,061 \text{ psi}$$

$$f_s = \frac{T(3a + 1.8b)}{8a^2b^2} = \frac{20,057(3 \times 11.125 + 1.8 \times 0.833)}{8 \times 11.125^2 \times 0.833^2} = 1,018 \text{ psi}$$

$$f_{s_{max}} = [f_s^2 + (f_b/2)^2]^{1/2} = [(1,018)^2 + (3,031)^2]^{1/2} = 3,197 \text{ psi}$$

$$f_{n_{max}} = f_{s_{max}} + f_b/2 = 3,197 + 3,031 = 6,228 \text{ psi}$$

Using PH 13-8 Mo Condition H1000 stainless steel, $F_{tu} = 201$ ksi

$$\text{S. F.} = \frac{201,000}{6,228} = \underline{\underline{32.274}}$$

Wing-to-Fuselage Attachment

Not critical by inspection.

Pressure Wing (Ref. Figure 15)

The wing will be checked for the same loads and at the same B. L. as the solid wing.

Loads

$M = 59,296$ in-lb

$T = 20,057$ in-lb

$S = 8,763$ lb

Section Properties

$I_{min} = 9.733$ in.$^4$

$y = 1.1$ in.

$A = 20.702$ in.$^2$

Chord = 22.251 in.

$$\text{Average depth} = \frac{20.702}{22.251} = 0.930 \text{ in.}$$

Analysis

$$f_b = \frac{M_y}{I} = \frac{59,296 \times 1.1}{9.733} = 6,701 \text{ psi}$$

$$f_s = \frac{T(3a + 1.8b)}{8a^2b^2} = \frac{20,057\ (3 \times 11.125 + 1.8 \times 0.465)}{8 \times (11.125)^2 \times (0.465)^2} = 3,205 \text{ psi}$$

$$f_{s_{max}} = [f_s^2 + f_b/2)^2]^{1/2} = [(3,205)^2 + (3,351)^2]^{1/2} = 4,637 \text{ psi}$$

$$f_{n_{max}} = f_{s_{max}} + f_b/2 = 4,637 + 3,351 = 7,988 \text{ psi}$$

Using PH 13-8 Mo Condition H1000 stainless steel, $F_{tu} = 201$ ksi

$$\text{S. F.} = \frac{201,000}{7,988} = \underline{\underline{25.163}}$$

Tail (Ref. Figure 10)

The tail is critical at Section A-A.

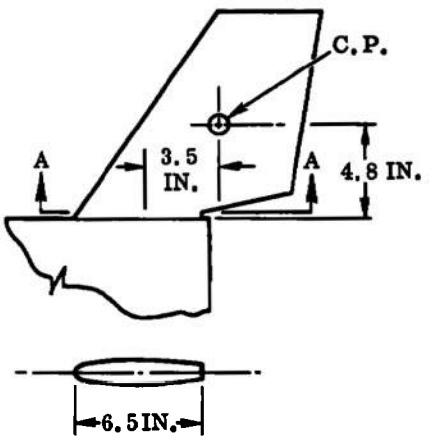

SECT. A—A

Section Properties

$A = 7.16$ in.$^2$

$y_{max} = 0.64$ in.

$I_{min} = 0.80945$ in.$^4$

$$\text{Average depth} = \frac{7.16}{6.5} = 1.102 \text{ in.}$$

Loads

Side load at C. P. = 8,320 lb (Table 3)

$M = 4.8 \times 8,320 = 39,936$ in-lb

$T = 3.5 \times 8,320 = 29,120$ in-lb

Analysis

$$f_b = \frac{M_y}{I} = 39,936 \times \frac{0.64}{0.80945} = 31,576 \text{ psi}$$

$$f_s = \frac{T(3a + 1.8b)}{8a^2b^2} = \frac{29,120\ (3 \times 3.25 + 1.8 \times 0.551)}{8 \times (3.25)^2 \times (0.551)^2} = 12,193 \text{ psi}$$

$$f_{s_{max}} = [f_s^2 + (f_b/2)^2]^{1/2} = [(12,193)^2 + (15,788)^2]^{1/2} = 19,948 \text{ psi}$$

$$f_{n_{max}} = f_{s_{max}} + \frac{f_b}{2} = 19,948 + 15,788 = 35,736 \text{ psi}$$

Using PH 13-8 Mo Condition H1000 stainless steel with $F_{TU}$ = 201 ksi gives

$$\text{S. F.} = \frac{201,000}{35.736} = \underline{\underline{5.625}}$$

Tail-to-Fuselage Attachments (Ref. Figure 10)

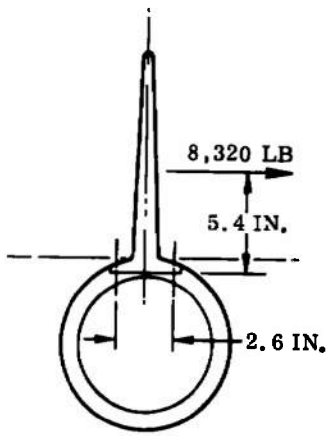


The tail is fastened to the fuselage each side of the ℄ with seven 5/16-24 steel bolts heat treated to 180 ksi.

$$\text{Couple load on bolts} = \frac{8,320 \times 5.4}{2.6} = 17,280 \text{ lb}$$

$$\text{Tension load per bolt} = \frac{17,280}{7} = 2,469 \text{ lb}$$

Allowable tension load = 9,660 lb per bolt

$$\text{S. F.} = \frac{9,660}{2,469} = \underline{\underline{3.913}}$$

Model Sting Support (Ref. Figure 10)

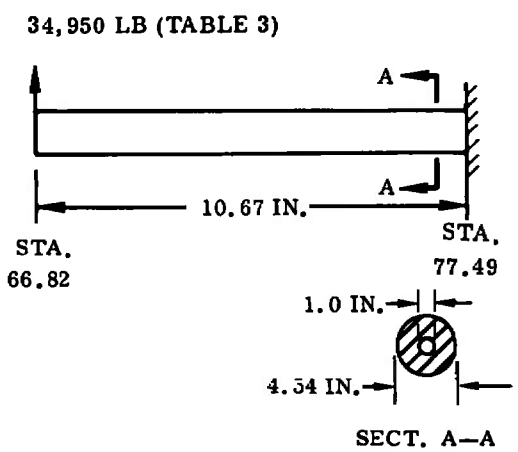


$$M = 10.67 \times 34,950 = 372,917 \text{ in-lb}$$

$$I = \frac{\pi}{4}(R^4 - r^4) = \frac{\pi}{4}(2.27^4 - 0.5^4)$$

$$= 20.805 \text{ in.}^4$$

$$f_b = \frac{M_y}{I} = \frac{372,917 \times 2.27}{20.805} = 40,688 \text{ psi}$$

Using PH 13-8 Mo Condition H1000 with $F_{tu}$ = 201 ksi gives

$$\text{S. F.} = \frac{201,000}{40,688} = \underline{\underline{4.940}}$$

# SECTION X

# MATERIALS ANALYSIS

## 10.1 CURRENT MODEL MATERIALS

The materials commonly used for fabrication of wind tunnel test models are the high-strength steels, such as 17-4PH or AISI 4340, since strength and stiffness have been the overriding factors in the selection of model materials. The 17-4PH stainless steel is most frequently selected because it is readily available in many wrought forms and possesses an excellent combination of strength, ductility, fracture toughness, corrosion resistance, machinability, and weldability.

Another important factor is that 17-4PH can be machined in the solution-annealed condition and then hardened by a low-temperature aging treatment without distortion. In addition, 17-4PH can be heat treated to develop a wide range of properties to meet specific model requirements. The heat-treat condition most commonly used is H900, which provides a minimum ultimate tensile strength of 190 ksi.

AISI 4340 is a conventional quenched and tempered steel, which is generally used at ultimate tensile strength levels up to 200 ksi. This steel also can be used at strength levels of 260 ksi or higher, but the intermediate range between 200 and 260 ksi is not used due to embrittling encountered during tempering in the range 500 to 700°F. Since it is difficult to avoid distortion during heat treatment of quenched and tempered steels, at least the final machining operations must be performed in the fully hardened condition. AISI 4340 is not a corrosion resistant alloy and must be given a protective coating.

## 10.2 HIRT MODEL REQUIREMENTS

Studies of requirements for HIRT test models indicate the need for a material with a suitable combination of properties that include high strength, high modulus, good ductility, and good fracture toughness at temperatures from ambient to -30°F. In addition, the material must be machinable, weldable, dimensionally stable, available in large billet size and low cost. Most design concepts will require bar, plate or forging billets for model construction. Stress analyses of proposed HIRT models indicate that materials with ultimate tensile strength in the order of 200 ksi are needed based on a minimum safety factor of 2. The high stress level and short test duration impose requirements for good fracture toughness and impact strength for service temperatures from ambient to -30°F. A notch toughness (Charpy V-notch) of 15 ft-lb

at -30°F has been considered as a lower limit in preliminary studies of HIRT model materials (Reference 14).

The most frequently used material for contemporary wind tunnel models, 17-4PH H900, does not meet these requirements. The 17-4PH steel in the H900 condition has poor fracture toughness at -30°F and is not considered suitable for structural use at this temperature. The AISI 4340 steel has adequate fracture toughness at -30°F when tempered to strength levels up to 200 ksi but not at higher strength levels. However, several undesirable characteristics of AISI 4340 are motivating the search for a better material for HIRT models. The principal disadvantages of AISI 4340 for this application are:

a. Distortion caused by quenching and tempering.

b. Machining must be performed in fully hardened condition.

c. Marginal dimensional stability.

d. Need for a protective finish to prevent corrosion.

## 10.3 MATERIALS SEARCH

A search was conducted of properties and characteristics of various materials to investigate their suitability for HIRT model construction. Candidate materials were identified and grouped into material classes for comparison.

Twelve classes of materials were considered for the HIRT model application as listed in Table 10.

## 10.4 GENERAL DISCUSSION OF MATERIAL CLASSES

To provide the most realistic basis for evaluation, one representative alloy or material from each class was selected for the properties comparison. Where available, properties data for product form and heat treatment believed most applicable to HIRT models were used.

Three classes of materials that show the greatest promise for meeting the HIRT model requirements are

a. Precipitation hardenable stainless steels.

b. 18% Ni maraging steels.

c. Quenched and tempered steels.

## Table 10. Comparative Properties of General Classes of Materials (Ambient Temperature)

| Material class | Representative alloy & condition | $K_{tu}$ (ksi) | Elong. (%) | E ($10^6$ psi) | $K_{su}$ (ksi) | G ($10^6$ psi) | $\omega$ (lb/in.$^3$) | Fracture toughness and impact strength: Charpy V-notch (ft-lb) | Fracture toughness and impact strength: $K_{ic}$ (ksi $\sqrt{in.}$) | Q & T machinability | Weldability | Availability (bar, plate or billets) | Cost ($/lb) |
|---|---|---|---|---|---|---|---|---|---|---|---|---|---|
| Quenched & tempered steels | D6AC Q & T[a] 1,050F | 230 | 10 | 29 | 132 | 11 | 0.283 | 18 | 90 | Normalized-good Q & T[a] -poor | Good | Good | 0.60 |
| Maraging steels | 18 Ni-250 grade | 250 | 10 | 26.5 | 143 | 10.3 | 0.289 | 40 | 90 | Good | Good | Good | 2.00 |
| Precipitation hardenable stainless steels | PH 13-8Mo H1000 | 215 | 13 | 28.3 | 124 | 11.0 | 0.279 | 30 | 95 | Good | Good | Good | 2.00 |
| Martensitic hardenable stainless steels | AISI 410 Q & T[a] 600F | 190 | 25 | 29 | --- | 12.5 | 0.28 | 35 | --- | Annealed-good Q & T[a] - fair | Fair | Fair | 0.70 |
| Nickel-base superalloys | Inconel 718 STA[c] | 208 | 21 | 29.6 | --- | 11.4 | 0.297 | 21 | 130 | Fair | Good | Good | 3.00 |
| Titanium alloys | Ti-6Al-4V STA[c] | 170 | 8 | 16 | 98 | 6.2 | 0.160 | --- | 60 | Fair | Good | Good | 4.00 |
| Molybdenum alloys | TZM SR[b] | 125 | 15 | 46 | --- | --- | 0.370 | --- | --- | Good | Not recommended | Fair | 17.00 |
| Beryllium-nickel alloys | Be-Ni 440 STA[c] | 215 | 12 | 28 | 15 | --- | 0.302 | --- | --- | Annealed-good aged - fair | Good | Not available | 8.00 |
| Aluminum alloys | 7075-T6 | 83 | 11 | 10.4 | 43 | 3.8 | 0.101 | --- | 30 | Good | Not recommended | Good | 0.60 |
| Boron/aluminum composites | B/6061 unidirectional | 210 | < 1 | 30 | 16 | 6 | 0.096 | --- | --- | Not applicable | Not weldable | Special fabrication | 500.00 |
| Boron/epoxy composites | B/SP-272 unidirectional | 220 | < 1 | 31 | 13 | 1.8 | 0.071 | --- | --- | Not applicable | Not weldable | Special fabrication | 250.00 |
| Graphite/epoxy composites | HT-S/X-904 unidirectional | 180 | < 1 | 20 | 13 | 0.7 | 0.055 | --- | --- | Not applicable | Not weldable | Special fabrication | 125.00 |

(a) Q & T = Quenched and tempered
(b) SR = Stress relieved
(c) STA - Solution treated and aged

The rationale for eliminating the other material classes from further consideration is discussed below.

The advanced composite materials, boron/aluminum, boron/epoxy and graphite/epoxy possess excellent strength and stiffness in unidirectional layups. However, insufficient design and fabrication experience exists to effectively use these properties for general model construction. In addition, the cost of the advanced composites is extremely high compared to the more conventional materials used for wind-tunnel models. Extensive experience is presently being developed with the advanced composite materials for aircraft, spacecraft and missile systems where the superior strength/density properties offer promise of major weight savings. As the experience progresses in working with advanced composites, these materials may become attractive candidates in the future for wind tunnel models.

The aluminum alloys do not possess sufficient strength or stiffness to merit their use in highly loaded HIRT models. Molybdenum alloys exhibit the highest modulus of the material classes evaluated, but low strength, poor fracture toughness at -30° F, and high cost would make their use unattractive for this application. Titanium alloys possess sufficient strength to merit consideration, but lower modulus, more difficult machining, and higher cost make their use less attractive than steels. Superalloys exhibit much similarity in properties to the precipitation hardenable stainless steels including strength, modulus, fracture toughness, and dimensional stability. However, lower cost and better machinability favor the selection of precipitation hardenable stainless steels. From the limited data available, beryllium-nickel 440 appears to have an attractive combination of mechanical properties, but high cost and nonavailability of large billet stock precludes the selection of this alloy. Some of the martensitic stainless steels can be quenched and tempered to develop strength levels up to 280 ksi. However, the alloys of this class that can be hardened to strength levels of 200 ksi or higher have low ductility and toughness at -30° F, which make them unsuitable for HIRT models.

## 10.5 PROMISING MATERIAL CANDIDATES

This discussion concerns the three classes of steels that show the greatest potential for the HIRT model application. Representative high-strength steels of each of the three classes are

a. Precipitation Hardenable Stainless Steels: PH13-8Mo, 17-4PH, 15-5PH.

b. Maraging Steels: 18Ni-200 grade, 18Ni-250 grade, 18Ni-300 grade, 18Ni-350 grade.

c. Quenched and Tempered Steels: D6AC, 300M, 9Ni-4Co, 4330-V Mod, 4340, H-11.

### 10.5.1 Precipitation Hardenable Stainless Steels

The precipitation hardenable stainless steels provide an excellent combination of high strength, notch toughness, corrosion resistance, and dimensional stability. These steels require only a simple one-step heat treatment that avoids distortion or heat scaling. In addition, these alloys have good machinability and weldability and are available in large sections. The excellent corrosion resistance would eliminate any need for protective coating of test models. One disadvantage compared to maraging or quenched and tempered steels is that heat treating to strength levels above 220 ksi results in poor notch toughness.

The PH13-8Mo alloy has the best combination of properties for HIRT test models of the various precipitation hardenable stainless steels available. This alloy was developed primarily for large sections where notch toughness, high strength, and stress-corrosion resistance are important (Reference 15). PH13-8Mo can be used at ultimate tensile strength levels up to 220 ksi with good fracture toughness at both ambient temperature and -30° F. As previously discussed, 17-4PH is not suitable for this application because of poor fracture toughness at -30° F when heat treated to stress levels above 160 ksi. 15-5PH is a modification of 17-4PH and has similar limitations.

### 10.5.2 Maraging Steels

The maraging steels have an excellent combination of strength, notch toughness and resistance to fatigue and stress corrosion cracking. Other favorable factors include good machinability and weldability, availability from multiple sources, and low cost (References 16 through 19). In general, the maraging steels are applicable over the same strength ranges as the quench and tempered steels. The major advantage of maraging steels for HIRT model construction is freedom from distortion during heat treatment. The components can be completely machined and then hardened with a single, low-temperature heat treatment. A slight uniform shrinkage takes place during the aging treatment. Nominal values for dimensional changes in the maraging steels resulting from the precipitation hardening treatment are as follows:

| | |
|---|---|
| 18 Ni - 200 grade | -0.04% |
| 18 Ni - 250 grade | -0.06% |
| 18 Ni - 300 grade | -0.08% |

This dimensional change can be compensated during machining in the case of large parts or very close tolerances. Weldments of maraging steels require only the aging treatment to achieve properties and stress relief. The maraging steels have only slightly better corrosion resistance than quenched and tempered steels and must be protected from corrosion by an appropriate coating system.

### 10.5.3 Quenched and Tempered Steels

The quenched and tempered steels are the most widely used high-strength steels for structural applications. These steels have an excellent combination of strength, notch toughness, and resistance to fatigue and stress corrosion cracking, both in parent metal and welds. Other factors favoring these steels are good machinability, availability from multiple sources, and low cost. These steels are weldable, but welds have lower toughness, particularly when heat treated to high stress levels. Although used extensively for highly stressed aircraft components, 4340 has lower ductility and fracture toughness than some of the more recently developed steels. D6AC, 4330V-modified, and 300M steels are essentially modifications of AISI 4340, providing improved fracture toughness and higher strength. The strength and fracture toughness relationships of these steels at room temperature and -65°F are shown in Figures 66 and 67. The 9Ni-4Co alloys also have good strength and fracture toughness. However, higher alloy content make them more costly than other steels in this class, and alloy segregation can be a problem. The H-11 steels have much lower fracture toughness compared to the modified 4340 steels (Figures 66 and 67). Warpage of complex-shaped parts during heat treatment is a major problem with the quenched and tempered steels. Machining to close dimensional tolerances must be performed in the fully hardened condition. In addition, these steels must be protected from corrosion by an appropriate coating system.

## 10.6 ALLOY SELECTION

The alloys recommended for construction of HIRT test models are listed below for three ranges of ultimate tensile strength. The alloys for the 200-250 ksi and 250-300 ksi ranges are listed in order of preference, with the first alloy having the best combination of properties. The alternate alloys should be used where special considerations such as availabiltiy and cost outweigh the difference in properties.

20-250 ksi

PH13-8Mo H1000*
18Ni-250 grade*
D6AC

250-300 ksi

18Ni-300 grade*
300M
D6AC

>300 ksi

18Ni-350 grade

*NOTE: If tunnel operating temperatures are reduced to -120°F, PH 13-8 Mo steel must be heat treated to condition H1100 or H1050 to maintain an acceptable Charpy V-notch of 15 or greater. 18Ni-250 grade and 18Ni-300 grade are usable at -120°F.

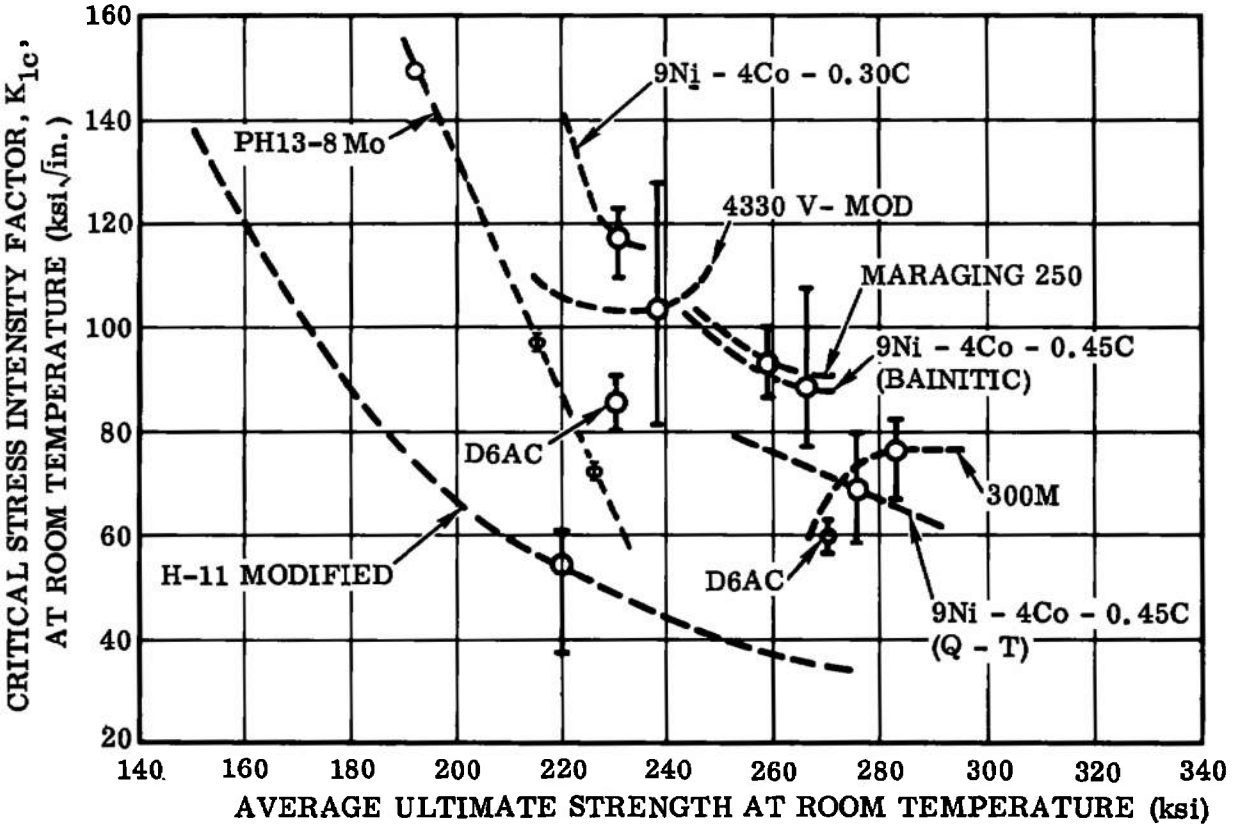


Figure 66. Strength and Room Temperature Fracture Toughness Relationships

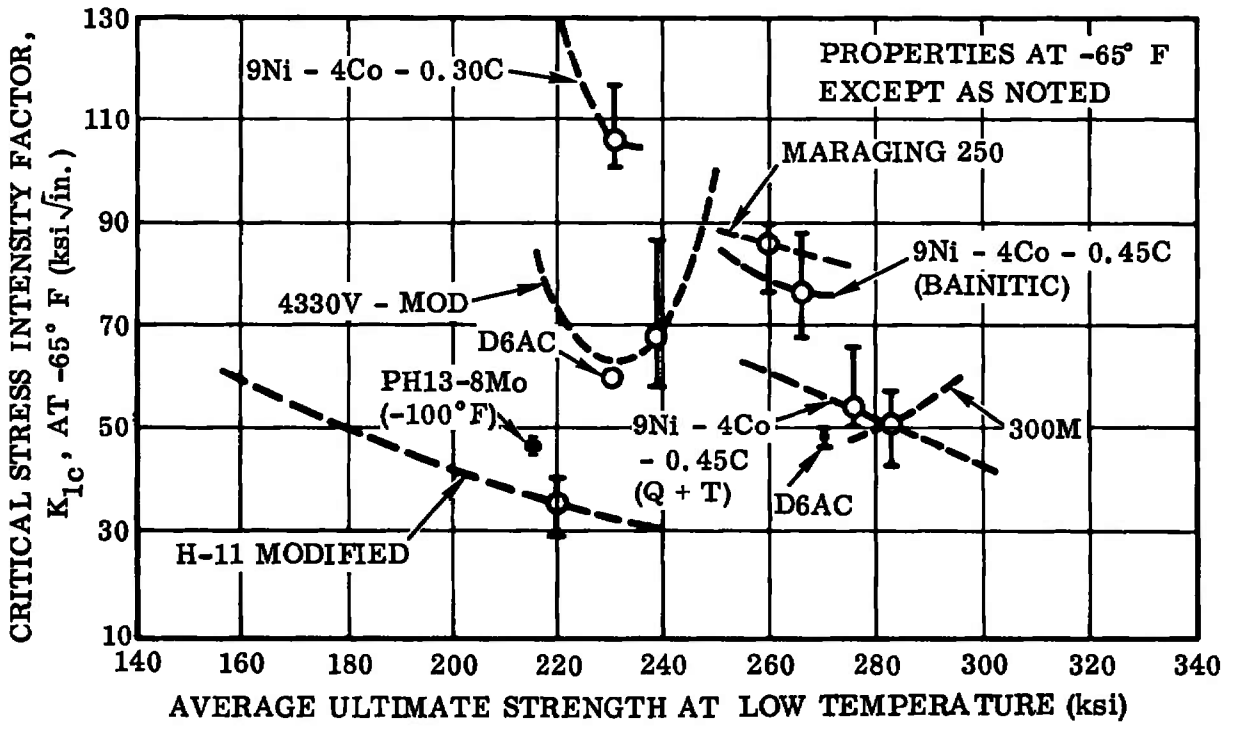


Figure 67. Strength and Low Temperature Fracture Toughness Relationships

Comparison and selection of alloys was based on use of bar, plate or forging billets for model construction. Although many of the selected alloys are available as castings, this product form is not recommended for HIRT models because of lower design allowables introduced by the casting factor and the need for optimum material quality to meet the material finish requirements as discussed in a later section.

## 10.7 PROCUREMENT SPECIFICATIONS

The procurement specifications, product forms, and condition for the recommended alloys are given in Table 11. Only vacuum-melted alloys are specified. Although some alloys are available in air-melted grades, these are not recommended because of the high stress level, low safety factor, and critical surface finish requirements.

Table 11. Material Specifications for Recommended Alloys

| Alloy | Procurement specification | Material form | Condition |
|---|---|---|---|
| PH 13-8 Mo | AMS 5629A | Bar, forgings | Solution annealed |
| 18Ni-250 grade | MIL-S-46850A Type III grade 250 | Bar, plate, forgings | Solution annealed (A) |
| 18Ni-300 grade | MIL-S-46850A Type III grade 300 | Bar, plate, forgings | Solution annealed (A) |
| 18Ni-350 grade | * | Bar, plate, forgings | Solution annealed (A) |
| D6AC | MIL-S-8949 | Bar, plate, forgings | Normalized or normalized and tempered |
| 300M | MIL-S-8844C | Bar, forgings | Normalized or normalized and tempered |

*No procurement specification currently available. Material can be procured by producer specification VASCOMAX 350.

## 10.8 DESIGN ALLOWABLES

The design mechanical and physical properties for the recommended alloys are listed in Table 12. All mechanical properties are for product forms suitable for HIRT models; i.e., bar, plate, and forgings. The design allowables for D6AC and 300M were obtained from MIL-HDBK-5B, 1 September 1971 (Reference 20). The mechanical properties allowables are based on specified minimum values of the appropriate specification ("S"-basis).

Design allowables for PH 13-8Mo are contained in MIL-HDBK-5B but are incomplete. The tentative allowables for PH13-8Mo listed in Table 12 are proposed design mechanical

Table 12. Design Mechanical and Physical Properties of Materials Recommended for HIRT Test Models

| Specification | AMS 5629A | MIL-S-46850A Type III Grade 250 | MIL-S-46850A Type III Grade 300 | None | MIL-S-8949 | | MIL-S-8844C Class 3 - 300 M |
|---|---|---|---|---|---|---|---|
| Alloy | PH13-8Mo | 18Ni-250 grade | 18Ni-300 grade | 18Ni-350 grade | D6AC | | 300M |
| Form | Bar, Forgings | Bar, Forgings | Bar, Forgings | Bar, Forgings | Bar, Billets | | Bar, Forgings |
| Condition | H1000 | STA(a) | STA(a) | STA(a) | Q & T (b) | | Q & T (b) |
| Basis | Tentative A | Tentative S | Tentative S | Tentative S | S | | S |
| Mechanical properties | | | | | | | |
| $F_{tu}$ (ksi) | 201 | 250 | 300 | 350 | 220 | 260 | 280 |
| $F_{ty}$ (ksi) | 190 | 240 | 280 | 330 | 190 | 215 | 230 |
| $F_{cy}$ (ksi) | 200 | 245 | 280 | --- | 213 | 240 | 247 |
| $F_{su}$ (ksi) | 119 | 150 | 170 | --- | 130 | 156 | 168 |
| $F_{bru}$ (ksi): | | | | | | | |
| (e/D = 1.5) | 302 | --- | --- | --- | 297 | 347 | --- |
| (e/D = 2.0) | 402 | --- | --- | --- | 385 | 440 | --- |
| $F_{bry}$ (ksi): | | | | | | | |
| (e/D = 1.5) | 263 | --- | --- | --- | 274 | 309 | --- |
| (e/D = 2.0) | 338 | --- | --- | --- | 302 | 343 | --- |
| e (percent) | 10 | 6 | 5 | 2 | 10L 7T | 10L 3T | 5 |
| E ($10^6$ psi) | 28.3 | 25.7 | 27.0 | 27.0 | 29.0 | | |
| $E_c$ ($10^6$psi) | 29.4 | --- | --- | --- | 29.0 | | |
| G ($10^6$ psi) | 11.0 | --- | --- | --- | 11.0 | | |
| Poisson's ratio | 0.278 | 0.30 | --- | --- | 0.32 | | |
| Physical properties | | | | | | | |
| $\omega$ (lb/in.$^3$) | 0.279 | 0.289 | 0.29 | 0.292 | 0.283 | | |
| C (Btu/ (lb) (F) | 0.11 (32-212F) | 0.107 (at 300F) | 0.11 (at 300F) | --- | 0.114 (at 32F) | | |
| K (Btu/(hr) (ft$^2$) (F)/ft | 8.0 (at 200F) | 14.6 (at 75F) | 12 (at 75F) | --- | 22.0 (at 32F) | | |
| $\alpha$ ($10^{-6}$in. /in. /F) | 5.7 (at 200F) | 5.6 (75-800F) | 5.6 (75-900F) | 6.3 (70-900F) | 6.3 (0 to 200F) | | |

(a) STA = Solution treated and aged
(b) Q & T = Quenched and tempered

and physical properties from the 44th meeting of the MIL-HDBK-5 committee (References 16 and 17). The mechanical properties for PH13-8Mo were established on an "A" basis.

No design allowables for the 18Ni maraging steels have been incorporated in MIL-HDBK-5B. The values presented in Table 8 are tentative values compiled from the appropriate specifications, vendor data sheets, (References 16, 17, and 18) and the Aerospace Structural Metals Handbook (Reference 23). The design mechanical properties are established as the specification minimums where available for 18Ni-250 grade and

18Ni-300 grade. No present specification exists for 18Ni-350 grade, and properties data are very limited. The tentative design properties for 18Ni-350 grade listed in Table 8 are based on vendor data for VASCOMAX 350 (Reference 16).

## 10.9 SURFACE FINISH

Contemporary test models are frequently polished in critical flow areas to a finish of 32 to 16 microinch, but better surface finishes are generally not required. (The surface finish nomenclature microinch is the arithmetical average of deviation from mean centerline, as established by American Standards Association (B46.1-1962) (Reference 24). HIRT models will require a surface finish of 16 microinch or better. Surface finishes of 8 microinch or 4 microinch may be necessary in critical flow areas. However, obtaining these surface finishes on large test models will be costly. It is possible that cost considerations may result in establishing finish requirements that are less stringent than the optimum from an aerodynamic standpoint.

The requirement for superfine finishes makes it important to use the highest quality materials available, such as wrought forms of vacuum-melted alloys. Although castings are sometimes used for current test models, they are not recommended for the HIRT application. It is difficult to produce castings that are completely free from defects such as micro-porosity, inclusions, and coarse grain structure, which have an adverse effect on surface finish.

Procedures must be developed to achieve surface finishes on test models in the range of 4 to 16 microinch. Many types and sequences of polishing and buffing operations have been used to produce mirror-like finishes on metals. From this experience it would appear that the desired results could be achieved with the following sequence of operations: grinding, polishing, hard buffing, and color buffing.

Electropolishing has been found to be very effective as the final polishing operation for steels (a surface finish of 8 microinch can be obtained by removing approximately 1 mil of metal from an existing 16 microinch finish). Substitution of electropolishing for buffing and at least part of the mechanical polishing would reduce the cost of the final finishing operations by more than one-half. An electropolishing process that has achieved excellent results with the candidate steels is the proprietary Molectrics Summa process (Molectrics, Inc., Inglewood, California). (Reference 25.)

Most model fabrication shops use stoning and fine-grit papers for polishing models and have little or no experience with electropolishing. Experience with aircraft parts has shown that multi-piece components must be disassembled and cleaned after electropolishing to avoid potential stress corrosion from entrapped chemicals. Welded, brazed, and soldered parts of either similar or dissimilar metals can be satisfactorily electropolished. In addition to improving the surface finish, electropolishing provides a clean and passivated surface, which improves the corrosion resistance and toughness of the material.

## 10.10 PROTECTIVE COATINGS

Models constructed of maraging steels and quenched and tempered steels will require some form of corrosion protection. Although tunnel testing does not involve a corrosive environment, protection during handling and storage is necessary. In current practice, test models are frequently protected by electroplating or a chemical treatment to produce a black oxide coating. Application of either protective finish could degrade the superfine finish required for HIRT models. The black oxide finishes such as MIL-C-13924B, Class 1, provide only limited corrosion protection, and an oil film is required during storage.

The protective system recommended for HIRT models is a flash plating of chromium or nickel (0.0002-inch maximum thickness), which will provide both corrosion resistance and protection of the surface finish. The proprietary Electrolizing process (Electrolizing, Inc., Los Angeles, Calif.) produces a thin, hard, dense chromium coating of uniform thickness that would be suitable for this application. If nickel plating is used it should be applied by the electroless nickel process to ensure a thin uniform coating on complex shapes. The use of flash plating on test models will generally require final buffing after the plating operation to restore the required surface finish.

Welded, brazed, and soldered parts of either similar or dissimilar metals present no problems with these plating processes. Mechanically fastened components should be dissassembled prior to plating to avoid potential stress corrosion from entrapped chemicals. Masking can be used in any area where the plating would be undesirable.

CAUTION

Steels heat treated to high strength levels are subject to embrittlement from hydrogen absorbed during pickling and plating operations. As a precaution, all high strength steel parts should be baked for 24 hours at 375° F after plating.

# SECTION XI

## MODEL COSTS

The estimated cost of fabricating models for the HIRT facility will be different from present high-speed force or pressures wind tunnel models. Most models for HIRT testing will have less than a 6-foot wing span and will be fabricated mostly from high-strength steel alloys. Models with a large number of variables are not considered in this report.

Cost estimates for fabricating a variety of models are presented in Table 13.

Table 13. Model Fabrication Cost Comparisons

| Type of model | Material | Surface finish | | | Model scales | |
|---|---|---|---|---|---|---|
| | | A | B | C | 32 to 16 $\mu$-in. finish | |
| | PH 13-8 Mo | 32 to 16 $\mu$-in. | 8 $\mu$-in. to 16 $\mu$-in. | 4 $\mu$-in. to 16 $\mu$-in. | 1.5 HIRT | 2 HIRT |
| 1. Solid wing | 1.0 | 1.0 | 1.1 | 1.25 | 1.5 | 2.0 |
| 2. Reduced chord for deflected surfaces | 1.25 | 1.25 | 1.35 | 1.40 | 1.85 | 2.5 |
| 3. Pressure model (400 orifices) | 1.4 | 1.4 | 1.5 | 1.65 | 1.90 | 2.40 |

Three basic types of models are considered:

a. Basic solid wing model with few variables.

b. Basic model with a reduced wing chord to allow for deflected surfaces.

c. Pressure models containing approximately 400 pressure orifices.

Fabrication costs for each of these models are divided into five categories:

a. Complete model finished to a surface finish of 32 to 16 microinches.

b. Minimum of 30% of the airfoils and fuselage finished to 8 microinches with the remainder of the model finished to 16 microinches.

c. Minimum of 30% of the airfoils and fuselage finished to 4 microinches with the remainder of model finished to 16 microinches.

d. Scale equal to 1.5 × HIRT scale.

e. Scale equal to 2.0 × HIRT scale.

It should be noted that although category headings have been limited to five, items such as extra care in handling, adherence to material and fabrication specifications, inspection procedures, etc., have been considered in estimating model costs.

A baseline model is defined as a HIRT scale (approximately 5-foot span), solid-wing model fabricated from PH 13-8 Mo steel, with an overall surface finish of 16 to 32 microinches. The baseline cost factor (1.0) is assumed to be a 6,000 manhour fabrication task. (A comparable model for the Ames 11-foot Wind Tunnel is estimated to cost approximately 5,000 manhours---assuming the use of an aluminum fuselage.)

For example: Reference Table 13.

The estimated cost of a HIRT model with a reduced wing chord requiring a surface finish of 4 to 16 microinches is:

Surface finish factor of 1.40 — 6,000 × 1.40 = 8,400 manhours.

A similar model for a scale of 2 × HIRT (Surface finish of 16 to 32 microinches):

Scale cost factor of 2.50 — 6,000 × 2.50 = 15,000 manhours.

It should be noted that while the engineering task related to the HIRT models is not a part of this study, it is apparent that engineering costs will increase. Typical areas requiring additional effort are:

a. Model loads definition.

b. More detailed stress analysis.

c. Test plans.

d. Material procurement.

e. Model inspection and quality control.

f. Model distortion analysis.

It is estimated that the ratio of engineering manhour effort to the fabrication effort for a basic HIRT model will be approximately 38%.

# SECTION XII

# CONCLUSIONS

The results of this study clearly indicate that wind-tunnel models of the four aircraft considered can be designed and fabricated for testing throughout the entire flight envelope in the proposed HIRT facility. Conventional state-of-the-art materials and fabrication techniques can be used for these models.

Although the models can be designed to be structurally adequate for full-scale Reynolds number testing throughout their operating envelopes, some problems are associated with these models. The high loads and the requirement for better model surface finishes for high Reynolds number testing tend to dictate that HIRT models will have considerably fewer variables than present-day multipiece designs. Careful consideration must be given to minimizing streamwise joints, coverplates, fasteners, etc.

The models covered in this study were not stress limited in most cases. The high model loads produce model deformations that are larger than normal for most existing wind tunnels. Comparisons between the model deformation and the full-scale vehicle deformation (reference Figure 44) for the ATT configuration indicates that the increased flexibility of the wing may allow a closer simulation of the model to full-scale distortion over a broader range of conditions than presently attainable in existing wind tunnels.

It is estimated that a ratio of engineering effort to fabrication effort for a HIRT model will be higher than for a present-day model. Whereas it has been shown that the fabrication costs for the basic HIRT model will be 20% higher, the combined task of engineering and fabrication is estimated as 33% higher than present-day models.

The selection and quality control of materials used for HIRT models must be accomplished with special care. Since operating the HIRT tunnel at -30°F results in a large reduction in the dynamic pressure required to produce a given Reynolds number per foot, the selection of materials for that operating condition is important. The precipitation hardenable stainless steels are recommended as the first choice for general model fabrication. These steels provide an excellent combination of high strength, notch toughness, corrosion resistance and dimensional stability. These steels are simple to heat treat and require no special protective coatings for models. PH 13-8 Mo Alloy is recommended as the best choice of materials for models requiring an ultimate tensile strength of 220 ksi or less. For ultimate tensile strengths of 250 to 300 ksi, 18 Ni-300 grade maraging steel is recommended. 18 Ni-350 grade maraging steel is recommended for requirements of ultimate tensile strengths greater than 300 ksi.

Admissible roughness estimates computed for the models in this study indicate that acceptable surface finishes in critical areas run from 11 to 70 microinches (Reference Table 1). Finishes of that quality are within the present-day state of the art in the fabrication of wind tunnel models.

# SECTION XIII

# RECOMMENDATIONS

## 13.1 RECOMMENDATIONS FOR FURTHER ANALYSES

Due to the scope of the subject of wind tunnel models for the HIRT facility, it was necessary to limit the depth of study in many areas. It is recommended that additional work be performed in various areas where a more specific detailed analysis of a particular problem could yield useful information regarding the design and fabrication of models for testing in the HIRT facility.

## 13.2 ADDITIONAL STUDY AREAS

The following recommendations concern areas that were not covered in the original study program.

a. Conduct a study to determine the possibility of designing a model wing for testing in the HIRT facility with a predetermined jig twist, which would enable the model wing to distort under a given load to match the full-scale airplane distortion. Techniques of varying test conditions should be analyzed to determine a range of test conditions that would allow the model wing to match the full-scale wing twist and/or vertical deflection within a specified tolerance.

b. Determine the model limitations of a present-day multipiece model design and upgrade the design, where necessary, to achieve a test range capable of encompassing the airplane operating envelope. The model should include:

   1. Inlets with provisions for air flow through the fuselage.

   2. Sting support.

   3. Deflected control surfaces.

c. Model loads in the HIRT facility will be very large for the size of model when compared to the normal transonic models of today. A new family of six-component strain gage balances must be designed, built, and calibrated. A study should be conducted to verify the predicted load capability versus diameter of these balances. External balance dimensions should be accumulated for a variety of load capacities that will be in the HIRT range. Balance deflections should also be studied since balance deflection contributes a large increment to the clearance requirement at the model/sting exit.

d. This study was limited to the use of conventional sting-mounted models. Various model support systems and their effect on the design and structural limitations of models for the HIRT facility is of great importance. A study should be conducted to investigate alternate model support systems and their effects on HIRT models.

e. A reflection plane model would offer several advantages in HIRT testing. Model scale could be increased considerably, which would decrease model stress levels and distortions. Model variable surfaces would be fabricated and rigged for less cost (due to the singlehanded parts). Wall or floor mounting would eliminate the need for aft fuselage distortion for sting clearances. A study should be conducted to determine the model limitations of a reflection plane model for the HIRT facility.

f. The high loads imposed on the models in the HIRT tunnel can produce considerable aeroelastic deformation to the primary aerodynamic surfaces. Wing twist and deflection will be produced, and since the models cannot be fabricated to be structurally similar to the flight vehicle, the aeroelastic behavior as a function of dynamic pressure will be different. An undesired wing twist would cause a disturbed span loading, which alters the configuration-induced drag characteristics. Lift and moment characteristics are also affected and lead to errors in trim characteristics caused by a lower lift curve slope and a more unstable configuration. Changes to the wing twist also imply a disturbed chordwise pressure distribution, and at supercritical Mach numbers the upper surface shock wave location and strength can be affected. The latter could bear directly on the drag divergence-buffet characteristics. Experience with supercritical wings has shown considerable angle-of-attack sensitivity. Currently the ability to predetermine the magnitude of these effects outside the tunnel is limited to empirical analysis for supercritical conditions. For subcritical conditions, linear theories may prove to be adequate for data corrections in the linear lift range but will be inadequate for assessing the effects on flow separation characteristics. A study should be directed toward analyzing the aerodynamic corrections dictated by the elastic differences between the model and the full-scale vehicle.

# SECTION XIV

## REFERENCES


1. J. D. Whitfield, C. J. Schueler, and R. F. Starr, ARO, Inc., "High Reynolds Number Transonic Wind Tunnels – Blowdown or Ludwieg Tube," AGARD – CP-83-71, Page 29, April 26, 1971.

2. R. G. Roepke, "The High Reynolds Number Transonic Wind Tunnel HIRT Proposal as Part of the National Aeronautical Facilities Program," AIAA Paper No. 72-1035, September 13-15, 1972.

3. "Report of the AGARD Ad Hoc Committee on Engine – Airplane Interface & Wall Corrections in Transonic Wind Tunnel Tests," AGARD-AR-36-71.

4. "Hypersonic Research Facilities Study," McDonnell Aircraft Company, NASA CR 114323, Volume II, Part I, Pages 6-52, October 2, 1970.

*5 R. F. Starr, ARO, Inc., " Aerodynamic and Systems Considerations for Short-Duration Transonic Testing."

6. H. Schlichting, Boundary Layer Theory, p. 559, McGraw-Hill.

7. "Application of Lifting Line Theory to Aircraft Aeroelastic Loads Analysis," General Dynamics Convair Report No. GDC-ERR-AN-1128, February 1968.

8. W. L. Gray and K. M. Schenk, Boeing Aircraft Co., "A Method for Calculating the Subsonic Steady-State Loading on an Airplane with a Wing of Arbitrary Plan Form and Stiffness," NACA 3030, December 1953.

9. L. H. Schindel, "An Evaluation of Procedures for Calculating Aerodynamic Loads," AFFDL-TR-65-18, May 1965.

10. C. J. Borland, "Methods of Calculating Aerodynamic Loads on Aircraft Structures," AFFDL-TR-66-37, August 1966.

11. J. A. Blackwell, Jr., "A Finite Stop Method for Calculation of Theoretical Load Distribution for Arbitrary Lifting-Surface Arrangements at Subsonic Speeds," NASA TN D-5335, 1969.

12. USAF Stability and Control DATCOM, AFFDL Wright-Patterson Air Force Base, Ohio.

*13. Curves of Flow Properties for HIRT Operation, USAF, June 28, 1972.

*14. R. Underwood, "Possible Materials Suitable for HIRT Models," preliminary draft dated June 15, 1972, USAF-AEDC.


* References supplied by the Government for this contract.

15. Product Data S-33c, "Armco PH 13-8 Mo Precipitation-Hardening Stainless Steel, Bar, Wire, Plate and Forging Billets," Armco Steel Corporation, Advanced Materials Division, Baltimore, Maryland.

16. 18% Nickel Ultra High Strength Maraging Steels, VASCOMAX 200-250-300-350, Vanadium-Pacific Steel Co., Montibello, Calif.

17. Data Sheets, "Specialty Alloys" Latrobe Steel Company, Latrobe, Pennsylvania.

18. Data Bulletin, "18% Nickel Maraging Steels," International Nickel Company, June 1969.

19. A. M. Hall and C. J. Slunder, "The Metallurgy, Behavior, and Application of the 18-Percent Nickel Maraging Steels," NASA SP-5051, 1968.

20. MIL-HDBK-5B, Military Standardization Handbook, "Metallic Materials and Elements for Aerospace Vehicle Structures," Vols. 1 and 2, 1 September 1972.

21. Agenda 44th Meeting MIL-HDBK-5 Committee, Item 70-16, "Additional Data for PH13-8Mo."

22. Private Communication H. Garvin, Armco to R. Tryon, General Dynamics Convair Aerospace Division, November 3, 1972, on Proposed Properties of PH13-8Mo for MIL-HDBK-5.

23. Aerospace Structural Metals Handbook, AFML-TR-68-115, 1972 publication.

24. American Standard ASA B46. 1-1962, "Surface Texture – Surface Roughness, Waviness and Lay," American Society of Mechanical Engineers.

25. "Molectrics Summa Processing," Manufacturing Process Specification GJ-6-289-A, Molectrics, Inc., Inglewood, California.

# APPENDIX I

## TYPICAL COMPUTER RUN PROGRAM 4278

Model loads and deformations for this report were computed using a method and digital program identified as Program 4278. A description of Program 4278 can be found in Section 8. All computer data generated for this report is on file in Department 666-0 at the Convair Aerospace Division of General Dynamics Corporation, San Diego operation, San Diego, California. A typical run (in this case Condition 7, Table 2) is included as an illustration of the type of information available for each test condition shown in Table 2.

1. EXPLANATION OF SYMBOLS AND ABBREVIATIONS (See Page 158)

2. SAMPLE COMPUTER PRINTOUT (See Page 169)

## 1. EXPLANATION OF SYMBOLS AND ABBREVIATIONS

```
P427R      FORTRAN LOADS AEROELASTIC PROGRAM  (IN FORTRAN IV)

           R L HOLT  EXT.2194LF


NOTE- (1) ALL ANGULAR INPUT AND OUTPUT DATA ARE IN DEGREES.
          ANGULAR QUANTITIES INVOLVED IN INTERNAL PROGRAM
          COMPUTATIONS ARE IN RADIANS WITH THE EXCEPTION OF
          ALPHAR WHICH IS IN DEGREES

      (2) ONLY ONE LENGTH UNIT MUST BE USED IN THE PROGRAM

SET  INGM=0  IF WING GEOMETRY IS TO BE COMPUTED FROM PLANFORM
             DATA

SET  INWNO=1  IF WIND TUNNEL DATA IS TO BE USED

SET  INBAL= NUMBER OF SETS OF BALANCE DATA

SET  IFLGS = 0 IF SYMMETRIC LOADS ARE WANTED

SET  IFLGA = 0 IF ASYMMETRIC LOADS ARE WANTED

SET  LTAIL= NSECT+1 FOR CONVENTIONAL TAIL LOAD CONFIGURATIONS

SET  RIGID=1. FOR RIGID CASE

SET  NFUS= NUMBER OF WING STRIPS OF THE HALF WING THAT LIE
           INBOARD OF THE WING-FUSELAGE JUNCTION

SET  NEXTW  = NUMBER OF WEIGHTS THAT LIE ON A WING SEMISPAN.


     LIST OF PROGRAM PARAMETERS ,THEIR UNITS AND DEFINITIONS
*****-*****-*****-*****-*****-*****-*****-*****-*****-*****-


 OTHER FORCE AND LENGTH UNITS  DIFFERENT FROM THOSE SPECIFIED
 IN THE FOLLOWING LIST CAN BE USED

PARAMETER
 NAME        UNITS                  DEFINITIONS
 *****-*****-*****-*****-*****-*****-*****-*****-*****-*****-

 ACLC         IN.       ASYMMETRIC PORTION OF LEFT-WING LOCAL LIFT
                        COEFFICIENT MULTIPLIED BY LOCAL CHORD

 ADG          DEG       INCREMENTAL ANGLE OF ATTACK OF WING SECTION DUE TO
                        AEROELASTIC EFFECTS FROM LOADINGS WHICH ARE NOT
                        EXPLICIT FUNCTIONS OF ANGLE OF ATTACK.

 ADFL         -         FLAP    EFFECTIVENESS

 ADSL         -         SLAT    EFFECTIVENESS

 ADSP         -         SPOILER EFFECTIVENESS
```

| | | | |
|---|---|---|---|
| * | AFAD | DEG | LOCAL WING ELASTIC AXIS SWEEPBACK ANGLE |
| | AFXT | PER LB | EXTERNAL STORES MATRIX ALPHAF DEPENDANT COMPONENT |
| | AINCB | DEG | INCIDENCE OF BODY WITH RESPECT TO SECTION CHORD LINE |
| | AINCF | DEG | INCIDENCE OF FUSELAGE WITH RESPECT TO ROOT CHORD LINE (MINUS. WING INCIDENCE ANGLE) |
| | AINCT | DEG | HORIZONTAL TAIL INCIDENCE ANGLE WITH RESPECT TO FUSELAGE REFERENCE LINE |
| | ALAM | -- | WING TAPER RATIO |
| * | ALFND | DEG | TOTAL ANGLE OF ATTACK OF WING SECTION INCLUDING ALL AEROELASTIC EFFECTS |
| | ALGIB | DEG | INTERFERENCE TWIST DUE TO AERODYNAMIC INTERFERENCE EFFECTS OF NEIGHBORING BODIES (FUSELAGES.NACELLES.EXTERNAL STORES.ETC.) UPON THE WING. DATA IS REDUCED FROM WIND TUNNEL TEST RESULTS |
| | ALPH1 | DEG | KNOWN LOCAL Z.L.L. ANGLE OF ATTACK FOR FIRST MODEL ANGLE OF ATTACK |
| | ALPH2 | DEG | KNOWN LOCAL Z.L.L. ANGLE OF ATTACK FOR SECOND MODEL ANGLE OF ATTACK |
| * | ALED | DEG | LOCAL WING LEADING EDGE SWEEPBACK ANGLE |
| | ALFWT | DEG | ANGLE OF ATTACK AT WING CENTERLINE OF MODEL IN WIND TUNNEL |
| | ALPHAF | DEG | WING SECTION ZERO-LIFT-LINE ANGLE OF ATTACK (SAME AS ALFNO) |
| * | ALREFD | DEG | WING ROOT-CHORD ZERO-LIFT-LINE ANGLE OF ATTACK |
| | AOLSE | DEG | CLEAN WING SECTION ZERO LIFT LINE ANGLE RELATIVE TO ITS CHORDLINE |
| | AOLRT | DEG | ROOT WING SECTION ZERO LIFT LINE ANGLE RELATIVE TO ITS CHORDLINE.(-) FOR LIFT LINE ABOVE CHORDLINE |
| | AR | - | WING GEOMETRIC ASPECT RATIO |
| | ASELD | DEG | INCREMENTAL ANGLE OF ATTACK OF WING SECTION DUE TO AEROELASTIC EFFECTS FROM STORE LOADS WHICH ARE EXPLICIT FUNCTIONS OF ANGLE OF ATTACK |
| | ATAU | DEG | WING JIG TWIST RELATIVE TO ROOT CHORD |
| * | ATED | DEG | LOCAL WING TRAILING EDGE SWEEPBACK ANGLE |

**NOTE: * DENOTES ITEMS OF PARTICULAR INTEREST**

| | | | |
|---|---|---|---|
| * | ATELD | DEG | TWIST DUE TO THE ELASTICITY OF THE WING |
| | ATPAR | - | RATE OF CHANGE OF HORIZONTAL TAIL ANGLE OF ATTACK (AT) WITH ANGLE OF ATTACK OF WING ROOT-SECTION ZERO-LIFT-LINE (ALREFO). (ONE MINUS DERIVATIVE OF DOWNWASH ANGLE WITH RESPECT TO ALREFO) (1-D EPSILON/D ALPHA) |
| | ATPDDE | - | RATE OF CHANGE OF HORIZONTAL TAIL ANGLE OF ATTACK WITH ELEVATOR DEFLECTION (DDF) |
| | AWELD | DEG | INCREMENTAL ANGLE OF ATTACK OF WING SECTION DUE TO AERDELASTIC EFFECTS FROM CLEAN WING LOADS WHICH ARE EXPLICIT FUNCTIONS OF ANGLE OF ATTACK. |
| * | BARL | - | FOR SYMMETRIC LOADINGS-----<br>SOLUTION TO THE SET OF SIMULTANEOUS EQUATIONS COMPRISED OF WING SYMMETRIC DOWNWASH EQUATIONS. VERTICAL FORCE EQUATION. AND PITCHING MOMENT EQUATION. IT IS COMPOSED OF THE WING SYMMETRIC LIFT DISTRIBUTION (CLC). WING ROOT ZERO-LIFT LINE ANGLE OF ATTACK (ALREFO). AND THE BALANCING TAIL LOAD (PT).<br>***OR***<br>FOR ASYMMETRIC LOADINGS-----<br>SOLUTION TO THE SET OF SIMULTANEOUS EQUATIONS COMPRISED OF WING ASYMMETRIC DOWNWASH EQUATIONS. SIDEFORCE EQUATION. ROLLING MOMENT EQUATION. AND YAWING MOMENT EQUATION. IT IS COMPOSED OF THE LEFT-WING ASYMMETRIC LIFT DISTRIBUTION (ACLC). AIRPLANE SIDESLIP ANGLE (BETA). RUDDER DEFLECTION(DELTR). AND EITHER AIRPLANE ROLLING VELOCITY (PHID) OR AIRPLANE ROLL ACCELERATION (PHIDD) DEPENDING ON WHICH VARIABLE HAS BEEN SELECTED (SEE ROLL). |
| | BEXT | PER LB | EXTERNAL STORES MATRIX ALPHAF=0. COMPONENT |
| | BLAMD | DEG | WING QUARTER CHORD LINE SWEEPBACK ANGLE. DEFINED POSITIVE AFT OF LATERAL AXIS |
| * | BMWNG | IN.LB. | AERODYNAMIC WING BENDING MOMENT (ABOUT AXIS PARALLEL TO X-AXIS) |
| | BP | - | WIND TUNNEL MODEL SCALE |
| | C | IN. | LOCAL CHORD PARALLEL TO PLANE OF SYMMETRY |
| * | CBAR | IN. | WING MEAN AERODYNAMIC CHORD |
| | CDEA | PER DEG | EXT. STORE DRAG COEFF. VAR. WITH ALPHAF |
| | CDEZ | - | EXT. STORE DRAG COEFF. AT ALPHAF=0. |
| | CLC | IN. | SYMMETRIC PORTION OF WING LOCAL LIFT COEFFICIENT MULTIPLIED BY LOCAL CHORD |
| | CFS | NON DIMEN. | LOCATION OF FRONT SPAR FROM L.E.(PER CENT CHORD/100) |

| | | |
|---|---|---|
| CLFA | PER DEG | SLOPE OF FUSELAGE LIFT CURVE COEFF |
| CLFO | - | LIFT COEFF OF FUSELAGE AT ALREFO=AOLRT |
| CLEA | PER DEG | EXT. STORE LIFT COEFF. VAR. WITH ALPHAF |
| CLEZ | - | EXT. STORE LIFT COEFF. AT ALPHAF=0. |
| CLWS | - | WING LIFT COEFFICIENT FOR TOTAL WING PLUS STORE AERODYNAMIC LOAD |
| CMEA | PER DEG | EXT. STORE PITCH MOMENT COEFF. VAR. WITH ALPHAF |
| CMEZ | - | EXT. STORE PITCH MOMENT COEFF. AT ALPHAF=0. |
| CMFA | PER DEG | SLOPE OF FUSELAGE MOMENT COEFF AT QUARTER CHORD OF MAC |
| CMFO | - | MOMENT COEFF OF FUSELAGE AT ALREFO=AOLRT AND QUARTER CHORD OF MAC |
| CMOTO | - | TOTAL SECTION MOMENT COEFF. AT SECTION QUARTER CHORD |

ABOVE AERO COEFFS. RELATED TO FUSELAGE AND EXTERNAL STORE EFFECTS ARE BASED ON WINGA AND CBAR.

| | | |
|---|---|---|
| CNAFR | PER RADIAN | SLOPE OF CURVE OF CNA VS ALPHA FOR AIRPLANE WITH FLEXIBLE WING. THIS IS AN EXCEPTION TO THE USUAL PER DEG. INPUT. |
| CONONO | - | CONDITION NUMBER (10-ALPHANUMERIC CHAR.) |
| CONSJ | NON DIMEN. | CONSTANT WHICH IS USED IN THE CALCULATION OF TORSIONAL MOMENT OF INERTIA. USUAL RANGE IS .172 TO .186 |
| * CR | IN | WING CHORD AT AIRCRAFT CENTERLINE |
| CPS | NON DIMEN. | LOCATION OF REAR SPAR FROM L.E.(PER CENT CHORD/100) |
| * CT | IN | WING CHORD AT TIP |
| DCDF | - | INCREMENT DRAG COEFFICIENT OF FUSELAGE |
| DCOT | - | INCREMENT DRAG COEFFICIENT OF TAIL |
| * DOE | DEG | ELEVATOR DEFLECTION |
| DELFL | DEG | FLAP DEFLECTION |
| DELSL | DEG | SLAT DEFLECTION |
| DELSP | DEG | SPOILER DEFLECTION |
| DEWT | DEG | ELEVATOR DEFLECTION IN WIND TUNNEL |

| | | | |
|---|---|---|---|
| | DNZ | - | POSITIVE INCREMENT OF NORMAL LOAD FACTOR TO BE USED IN THE ITERATIVE PROCESS OF OBTAINING THE DESIRED VALUE OF ALREFO WHEN USPLR.NE.0 |
| * | EA | - | LOCAL WING ELASTIC AXIS POSITION. IN FRACTION OF LOCAL CHORD |
| | EAL | - | ELASTIC AXIS POSITION FROM LOCAL WING LEADING EDGE .IN FRACTION OF LOCAL CHORD. |
| | ECLTA | PER DEG. | EFFECTIVE LIFT CURVE SLOPE OF THE HORIZONTAL TAIL BASED ON WING AREA (WINGA) AND FREE-STREAM DYNAMIC PRESSURE (QDYN). TAIL EFFICIENCY FACTOR INCLUDED. |
| * | EI | LBS.IN.SQD. | EFFECTIVE VALUE OF PRODUCT OF MODULUS OF ELASTICTICITY AND WING SECTION BEAM BENDING MOMENT OF INERTIA |
| | ELFT1 | LBS. PER IN. | WIND TUNNEL MODEL TEST LOCAL SPANWISE LOADING FOR FIRST MODEL ANGLE OF ATTACK |
| | ELFT2 | LBS. PER IN. | WIND TUNNEL MODEL TEST LOCAL SPANWISE LOADING FOR SECOND MODEL ANGLE OF ATTACK |
| | [illegible] | - | SET.NE.ZERO TO ENTER AEROX FROM SYBAL (INSERT SET OF AEROX INPUT CARDS AFTER INPUT CARDS FOR SYBAL) |
| | ENST | - | [illegible] .NE.ZERO TO ENTER STORE FROM SYBAL (INSER[illegible]T OF STORE INPUT CARDS AFTER ANY AEROX INPUT [illegible]S FOLLOWING INPUT CARDS [illegible] FOR SYBAL) |
| * | ETA | - | POSITION OF WING STRIP ALONG Y-A[illegible] IN FRACTION OF HALFSPAN |
| | ETABAR | - | POSITION OF TOTAL WING PLUS STORE AERODYNAMIC LOAD ALONG Y-AXIS IN FRACTION OF SEMISPAN |
| * | GJ | LBS.IN.SQD. | EFFECTIVE VALUE OF SHEAR MODULUS OF ELASTICITY AND WING SECTION POLAR MOMENT OF INERTIA |
| | GUSTF | I | SET.NE.ZERO IF GUST CONDITION IS DESIRED |
| | H | IN. | LOCAL WING STRIP HALFWIDTH |
| | IAEROX | - | BODY IMAGE/OVERVELOCITY EFFECT FLAG.... SET.EQ.ZERO FOR BOTH IMAGE/OVERVELOCITY EFFECTS SET.EQ.1 FOR ONLY IMAGE EFFECTS SET.EQ.2 FOR ONLY OVERVELOCITY EFFECTS SET.EQ.3 FOR NO BODY EFFECTS |
| | IFUS | - | FUSELAGE IMAGE/ OVERVELOCITY EFFECT FLAG... SET.EQ.ZERO FOR BOTH IMAGE/OVERVELOCITY EFFECTS SET.EQ.1 FOR ONLY IMAGE EFFECTS SET.EQ.2 FOR ONLY OVERVELOCITY EFFECTS SET.EQ.3 FOR NO BODY EFFECTS |

| | | | |
|---|---|---|---|
| | ITIME | - | SET = 1 EACH TIME OVERLAYD.0 IS ENTERED (USED IN SYBALA TO SAVE DISK2 FOR THE NTH CASE) |
| | LTAIL | - | TAIL BOOM ENTRY STATION NUMBER ( SET EQUAL TO NSTRP+1 FOR CONVENTIONAL TAIL CONFIG.) |
| * | MACHN | NON DIMEN. | MACH NUMBER. (READ INTO BOTH WINDT AND GUST) |
| * | MEAPIL | IN.LB. | WING BENDING MOMENT (AIR PLUS INERTIA) ABOUT ELASTIC AXIS |
| | MD | PER DEG | TWO-DIMENSIONAL LIFT-CURVE SLOPE PER DEG. INCLUDING COMPRESSIBILTY EFFECTS .FOR SECTIONS PARALLEL TO THE PLANE OF SYMMETRY |
| | NB | - | NUMBER OF BODIES PER SEMISPAN FOR WHICH IMAGE/OVERVELOCITY EFFECTS DESIRED (IN ADDITION FOT THE FUSELAGE) |
| | NBSEC | - | SECTION NUMBER WHERE BODY CENTERED |
| | NEXTR | - | NUMBER OF EXTERNAL STORES ATTACHED TO WING |
| | NFUS | - | NUMBER OF WING STRIPS/SECTIONS WITHIN FUSELAGE |
| | NG | NON DIMEN. | STATION NUMBER WHERE WEIGHT IS LOCATED |
| | NJ | - | EXT. STORE LOCATION STATION NUMBER |
| | NSTRP | - | NUMBER OF STRIPS ON WING HALFSPAN. STRIPS ARE ASSIGNED STATION NUMBERS.ONE TO NSTRP.FROM LEFT WING TIP TO WING ROOT |
| | PHID | DEG | WING QUARTER CHORD LINE DIHEDRAL ANGLE DEFINED POSTIVE ABOVE LATERAL AXIS NOTE. ALSO USED IN ASBAL. |
| | PT | LBS | BALANCING HORIZONTAL TAIL LOAD = PTAT + PTDDE |
| | PTAT | LBS. | PORTION OF HORIZONTAL TAIL LOAD DUE TO ANGLE OF ATTACK |
| | PTDDE | LBS. | PORTION OF HORIZONTAL TAIL LOAD DUE TO ELEVATOR DEFLECTION |
| | PTWT | LB | SUM OF ALPHA AND DELTA LOADS ON HORIZONTAL TAIL IN THE WIND TUNNEL |
| | PTZER | PER LB | TAIL LOAD STRUCTURAL MATRIX INFLUENCE ON WING |
| * | QDYN | LBS./SQ.IN. | FREE STREAM DYNAMIC PRESSURE |
| | QM | LBS./SQ.IN. | WIND TUNNEL MODEL TEST DYNAMIC PRESSURE |
| | RAERO | - | SET.NE.ZERO TO REUSE SYMMETRIC SECTION DATA |
| | RB | IN. | RADIUS OF BODY FOR WHICH EFFECTS DESIRED |
| | RF | IN. | EFFECTIVE RADIUS OF FUSELAGE(INFL. CALC.) |

| | | | |
|---|---|---|---|
| * | RHOAL | INLBSEC2/FT4 | DENSITY OF AIR AT ALTITUDE. |
| | RWTS | - | SET.NE.ZERO TO REUSE WTS DATA |
| | S1A | PER IN | WING ASYMMETRIC DOWNWASH MATRIX |
| | S1S | PER IN | WING SYMMETRIC DOWNWASH MATRIX |
| | S2P | PER IN | WING ELASTICITY MATRIX |
| | SAIA | PER IN | ASYMMETRIC IMAGE-VORTEX EFFECT MATRIX. (CORRECTION TO SIA EXPOSED WING COMPONENTS) |
| | SAIS | PER IN | SYMMETRIC IMAGE-VORTEX EFFECT MATRIX. (CORRECTION TO SIS EXPOSED WING COMPONENTS) |
| * | SCLCQ | LB/IN | AERODYNAMIC WING LOADING (CONSTANT ACROSS EACH STRIP) |
| * | SHAPIL | LB | WING SHEAR DUE TO AIR PLUS INERTIA |
| * | SHWNG | LB | AERODYNAMIC WING SHEAR |
| * | SPAN | IN. | WING SPAN |
| | SZERO | - | OVERVELOCITY EFFECT MATRIX. (EFFECT OF K-TH BODY STORED IN THE NBSEC(K)-TH COLUMN. EFFECT OF FUSELAGE STORED IN THE NSTRP-TH COLUMN) |
| * | TEAPIL | IN.LB. | WING PITCHING MOMENT (AIR PLUS INERTIA) ABOUT ELASTIC AXIS |
| | THTDD | DEG/SEC.SOD. | PITCH ACCELERATION OF VEHICLE |
| | TSECT | NON DIMEN | MAXIMUM THICKNESS/CHORD RATIO OF A WING SECTION. |
| * | TQBR4 | IN.LB. | TORQUE ABOUT CBAR DUE TO WING AERODYNAMIC FORCES |
| * | TQCHK | IN.LB. | TORQUE ABOUT CBAR DUE TO AIR PLUS INERTIA LOADS |
| * | TQFUA | IN.LB. | TORQUE ABOUT CBAR DUE TO FUSELAGE AT ANGLE OF ATTACK |
| * | TQFUO | IN.LB. | TORQUE ABOUT CBAR DUE TO FUSELAGE AT ZERO ANGLE OF ATTACK |
| * | TQINR | IN.LB. | TORQUE ABOUT CBAR DUE TO INERTIA OF TOTAL AIRCRAFT |
| * | TOTAL | IN.LB. | TORQUE ABOUT CBAR DUE TO HORIZONTAL TAIL LOAD |
| * | TOWNG | IN.LB. | AERODYNAMIC WING PITCHING MOMENT (ABOUT AXIS PERPENDICULAR TO X-AXIS) |
| | UDEGF | FT/SEC. | GUST VELOCITY (EAS) |

| | | | |
|---|---|---|---|
| | USPLR | DEG | SYMMETRIC PORTION OF UNSYMMETRIC SPOILER DEFLECTION. USE ONE-HALF ACTUAL DEFLECTION--OTHER HALF OBTAINED WITH DLASP. |
| | VEL | FT/SEC. | THE SPEED AT WHICH THE AIRPLANE MOVES THROUGH THE AIR SURROUNDING IT. THIS IS TAS DO NOT CONFUSE WITH CAS, EAS, OR IAS. |
| * | VFCHK | LB | VERTICAL FORCE AT CBAR DUE TO AIR PLUS INERTIA LOADS |
| | VFFUA | LB | VERTICAL FORCE ON FUSELAGE DUE TO ANGLE OF ATTACK |
| | VFFUO | LB | VERTICAL FORCE ON FUSELAGE AT ZERO ANGLE OF ATTACK |
| | VFINR | LB | VERTICAL FORCE DUE TO INERTIA OF TOTAL AIRCRAFT |
| * | VFTAL | LB | VERTICAL FORCE ON HORIZONTAL TAIL |
| * | VNZ | - | VERTICAL LOAD FACTOR ALONG Z-AXIS |
| * | W | LBS. | GROSS WEIGHT OF VEHICLE<br>ALSO WEIGHT DISTRIBUTION ON WING SEMI-SPAN I USED IN SYBAL AND WTS) |
| * | WINGA | SQ.IN. | WING AREA |
| * | WTSH | LB | WING SHEAR DUE TO INERTIA |
| * | WTMEA | IN.LB. | WING BENDING MOMENT DUE TO INERTIA ABOUT ELASTIC AXIS |
| * | WTTEA | IN.LB. | WING PITCHING MOMENT DUE TO INERTIA ABOUT ELASTIC AXIS |
| * | XBAR4 | IN. | FUS. STA. OF CBAR/4 ALONG X-AXIS |
| * | XC4 | IN. | LOCAL QUARTER CHORD POSITION ALONG X-AXIS |
| * | XCG | IN. | FUS. STA. OF VEHICLE C.G. ALONG X-AXIS |
| | XDDE | IN. | DIFFERENCE BETWEEN ANGLE OF ATTACK TYPE AND ELEVATOR TYPE HORIZONTAL TAIL LOAD CENTER POSITIONS ALONG THE X-AXIS.--NEGATIVE IF ELEVATOR TYPE LOAD CENTER AFT OF ANGLE OF ATTACK TYPE LOAD CENTER. |
| | XE | IN. | EXT. STORE POS'N. ALONG X-AXIS |
| | XEA | IN. | FUS. STA. OF ELASTIC AXIS ALONG X-AXIS |
| | XEAIE | IN. | LOCATION ALONG X-AXIS OF INBOARD EDGE OF WING SECTION. |
| * | XFUS | IN. | FUS. STA. OF C.P. OF FUSELAGE LIFT |

| | | | |
|---|---|---|---|
| * | XLE | IN. | POSITION OF WING ROOT LEADING EDGE ALONG THE X AXIS. |
| | XTAIL | IN. | POSITION OF ANGLE OF ATTACK TYPE HORIZONTAL TAIL LOAD CENTER ALONG X-AXIS |
| | XW | IN. | FUSELAGE STATION OF DISTRIBUTED WEIGHT. |
| | YC4 | IN. | LOCAL QUARTER CHORD POSITION ALONG Y-AXIS |
| | YE | IN. | EXT. STORE POS'N. ALONG Y-AXIS |
| | YIY | IN.LBS.SEC.SQD. | MOMENT OF INERTIA OF VEHICLE ABOUT PITCH AXIS THROUGH C.G. |
| | YTAIL | IN. | POSITION OF HALF TAIL LOAD ENTRY ALONG Y-AXIS |
| | YW | IN. | DISTANCE FROM FUSELAGE CENTERLINE TO DISTRIBUTED WEIGHT ALONG THE Y AXIS. |
| | ZBAR4 | IN. | WATERLINE OF CBAR/4 ALONG Z-AXIS |
| | ZC4 | IN. | LOCAL QUARTER CHORD POSITION ALONG Z-AXIS |
| | ZCDF | IN. | WATERLINE POSITION OF FUSELAGE DRAG |
| | ZCDT | IN. | WATERLINE POSITION OF TOTAL TAIL DRAG |
| | ZCG | IN. | WATERLINE OF VEHICLE C.G. ALONG Z-AXIS |
| | ZE | IN. | EXT. STORE POS'N. ALONG Z-AXIS |
| | ZEA | IN. | WATERLINE OF ELASTIC AXIS ALONG Z-AXIS |
| | ZFUS | IN. | FUSELAGE CENTER LINE POSITION ALONG Z-AXIS |
| | ZLE | IN. | POSITION OF WING ROOT LEADING EDGE ALONG Z-AXIS |
| * | ZOEDGE | IN. | DISPLACEMENT ALONG Z-AXIS OF ELASTIC AXIS AT OUTBOARD EDGE OF WING SECTION. |
| | ZW | IN. | WATER LINE OF DISTRIBUTED WEIGHT. |

*****-*****-*****-*****-*****-*****-*****-*****-*****-*****-

THE FOLLOWING VARIABLES OCCUR IN THE ASYMMETRIC SECTION

*****-*****-*****-*****-*****-*****-*****-*****-*****-*****-

| | | |
|---|---|---|
| ABAL | - | FLAG WHICH IS SET EQUAL TO 1.0 FOR THE LAST ASYMMETRIC CASE PRIOR TO RESETTING INBAL. AND IS SET GREATER THAN ONE FOR ALL PRE-CEEDING ASYMMETRIC CASES |

| | | |
|---|---|---|
| AIX | IN LB SECSQDMDMENT DF INERTIA VEHICLE ABOUT THE LONGITUDINAL ROLL AXIS. | |
| APDA | NDN DIMEN. | WING SECTION ANGLE OF ATTACK PEP DLAIL |
| APDSP | NDN DIMEN. | WING SECTION ANGLE DF ATTACK PER DLASP |
| AWD | DEG. | ASYMMETRIC WING TWIST. + WHEN RIGHT WING HAS INCREASED ANGLE DF ATTACK AND VICE VERSA FDR LEFT WING. |
| BETA | DEG. | SIDESLIP ANGLE OF AIRPLANE. + WHEN RELATIVE WIND VECTOR STRIKES DN THE RIGHT SIDE OF THE AIRPLANE CENTERLINE. |
| CNBT | PER DEG. | TDTAL AIRPLANE YAWING MDMENT CDEFF.CAUSEO BY BETA. (+FDR +BETA) NDTE.WING COMPONENT IS ABDUT 3X VERTICAL TAIL CDMPDNENT |
| CNPD | SEC.SQD./DEG | TDTAL AIRPLANE YAWING MDMENT CDEFF. CAUSED BY ROLLING VELDCITY PHID. THE WING CDMPONENT IS DPPDSITE IN SIGN TD THE TAIL CDMPDNENT AND ABDUT 4X AS LARGE. (-FDR+PHID) |
| CNRU | PER DEG. | TDTAL AIRPLANE YAWING MDMENT CDEFF. CAUSED BY RUDDER DEFLECTIDN. (-FDR+DELTR) |
| CRLBT | PER DEG. | TDTAL AIRPLANE RDLLING MDMENT CDEFFICIENT CAUSED BY BETA. (-FDR +BETA ) |
| CRLPD | SEC.SOD./DEG | VERTICAL AND HDRIZDNTAL TAIL RDLLING MOMENT CDEFF. CAUSEO BY RDLLING VELDCITY, PHID. (WING CDNTRIBUTION IS CALCULATED INTERNALLY) (-FOR+PHID) |
| CRLRU | PER DEG. | TDTAL AIRPLANE RDLLING MDMENT COEFFICIENT CAUSED BY RUDDER DEFLECTIDN. (+FOR+DELTR) |
| CYBT | PER DEG. | TDTAL AIRPLANE SLOPE DF SIDE FDRCE CDEFF. VS BETA. (-FOR+BETA) |
| CYPD | SEC.SQD./OEG | VERTICAL AND HDRIZONTAL TAIL SLOPE DF SIDE FORCE COEFF. VS ROLLING VELDCITY.(-FOR+PHID) |
| CYRU | PER DEG. | TDTAL AIRPLANE SLOPE DF SIDE FDRCE CDEFF. VS RUDDER DEFLECTIDN. (+FDR+DELTR) |
| DELTR | DEG. | RUDDER DEFLECTION. A + DELTR YAWS THE NDSE TD THE LEFT. |
| DLAIL | DEG. | AILERDN DEFLECTIDN. + DLAIL ROLLS AIRPLANE WITH LEFT WING DESCENDING FIRST. |
| DLASP | OEG | ASYMMETRIC PART OF UNSYMMETRIC SPOILER DE-FLECTIDN. +DLASP RDLLS AIRPLANE WITH RIGHT WING DESCENDING FIRST. USE ONE-HALF ACTUAL DEFLECTION--OTHER HALF OBTAINED WITH USPLR. |
| PHID | DEG./SEC. | AIRPLANE RDLLING VELDCITY. + WHEN RIGHT WING IS DESCENDING. |

| | | |
|---|---|---|
| PHIDD | DEG./SEC.SQD | AIRPLANE ROLLING ACCELERATION. +PHIDD WHEN RIGHT WING INITIALLY MOVES DOWN. |
| PSIDD | DEG./SEC.SQD | AIRPLANE YAWING ACCELERATION. + WHEN RIGHT WING MOVES BACK. |
| RASYA | - | SET.NE.ZERO TO REUSE ASYMMETRIC SECTION DATA |
| POLL | NON-DIMEN | SET = 1. IF PHIDD IS KNOWN AND PHID IS THE VARIABLE. OTHERWISE PHID IS KNOWN AND PHIDD IS THE VARIABLE. |
| VIZ | IN LB SEC SQD | MOMENT OF INERTIA OF VEHICLE ABOUT THE VERTICAL YAW AXIS. |
| VNY | NON.DIMEN. | LATERAL LOAD FACTOR ALONG Y AXIS. A + YNY TRANSLATES VEHICLE TOWARD RIGHT WING TIP. |

## 2. SAMPLE COMPUTER PRINTOUT

```
P$MAIN2
C            P _ HOLT      HIPT ADVANCED TECHNOLOGY TRANSPORT UNBALANCED
 INGM=0,INWND=0,INBAL=10,IFLGS=0,          IFPRT=0,NOPLT=0,IGEOM=0,
 INBAL = 1,
 SYM4020 = 3HYES,                                                          PROGRAM FLAGS
 SYM4020 = 2HNO,
 ABAL = 0.,
 ASY4020 = 2HNO,          ITIMF=1,
 $END OF DATA

P$INPT14                  GEOMETRIC DESCRIPTION
 CR=28.313,
 PHID(1)=11*0.0,
 SPANBP(1)=.9135, .8279, .7406, .6541, .5577, .4812, .3945, .2961,
 SPANPP(9)=.2073, .1116, 0.,
 NSTPP=11,
 LTAIL=12,
 NFUS =1,
 SPAN =67.550,
 XLE  =25.14,
 ZLE  =8.05,
 XTAIL=96.00,
 YTAIL=0.0,
 EAL  =.405,
 ALED(1)=7*43.5, 45.0, 33.5, 59.0, 47.5,
 ATED(1)=7*36.0, 4*5.0,
C          SOLID WING WITH AFT 75 PERCENT OF CHORD REMOVED      10/13/72
 EI(1)=1.1E+06, 1.4E+06, 2.3E+06, 2.9E+06, 4.6E+06, 5.7E+06,  7.7E+06,
 EI(8)=18.8E+05, 68.4E+06, 242.3E+06, 427.5E+06,


 GJ(1)= 1.6E+05, 2.5E+05, 3.5E+05, 4.9E+05, 7.4E+06, 10.4E+06, 14.3E+06,
 GJ(8)= 33.4E+06, 91.8E+06, 408.4E+06, 638.4E+06,                          WING 6
C          ATT SOLID WING   10/13/72                                       STRUCTURAL BENDING AND
 EI(1)=1.43E+05, 1.98E+05, 2.34E+06, 3.59E+06, 5.30E+06, 7.41E+06, 10.3E+06,  TORSIONAL PROPERTIES
 EI(8)=20.2E+05, 71.8E+06, 251.4E+06, 427.5E+06,
 GJ(1)= 1.79E+05, 2.78E+06, 3.86E+06, 5.54E+06, 7.95E+06, 11.3E+06, 15.4E+06,
 GJ(8)= 37.7E+06, 99.7E+06, 526.4E+06, 639.4E+06,
 $END
                          FUSELAGE DESCRIPTION
P$INPT12
  RF= 3.77,  ZFUS=10.0,
  $END OF DATA
CBAR CALCULATED= 15.955025 AT( 46.823935, 11.594778,  9.050100)
```

**CALCULATED GEOMETRY** (SEE FIGURE 23 FOR USE OF THIS INFORMATION)

| ETA | C | 2H | XC4 | YC4 | ZC4 | EA | ALED | AFAD | ATED | EI | GJ |
|---|---|---|---|---|---|---|---|---|---|---|---|
| ND | IN | IN | IN | IN | IN | ND | DEG | DEG | DEG | LBIN2 | LBIN2 |
| .95 | 5.03 | 2.92 | 64.63 | 32.31 | 8.05 | .40 | 43.50 | 40.66 | 36.00 | 1.43E+06 | 1.79E+06 |
| .87 | 5.68 | 2.92 | 62.02 | 29.39 | 8.05 | .40 | 43.50 | 40.66 | 36.00 | 1.88E+06 | 2.78E+06 |
| .79 | 6.33 | 2.92 | 59.42 | 26.47 | 8.05 | .40 | 43.50 | 40.66 | 36.00 | 2.34E+06 | 3.86E+06 |
| .70 | 6.98 | 2.92 | 56.81 | 23.55 | 8.05 | .40 | 43.50 | 40.66 | 36.00 | 3.59E+06 | 5.54E+06 |
| .61 | 7.63 | 2.92 | 54.20 | 20.63 | 8.05 | .40 | 43.50 | 40.66 | 36.00 | 5.70E+06 | 7.95E+06 |
| .52 | 8.28 | 2.92 | 51.59 | 17.71 | 8.05 | .40 | 43.50 | 40.66 | 36.00 | 7.41E+06 | 1.13E+07 |
| .44 | 8.93 | 2.92 | 48.98 | 14.79 | 8.05 | .40 | 43.50 | 40.66 | 36.00 | 1.05E+07 | 1.56E+07 |
| .35 | 10.78 | 3.33 | 46.39 | 11.67 | 8.05 | .40 | 45.00 | 32.23 | 5.00 | 2.02E+07 | 3.77E+07 |
| .25 | 14.61 | 3.00 | 43.24 | 8.56 | 8.05 | .40 | 58.50 | 45.18 | 5.00 | 7.18E+07 | 9.97E+07 |
| .16 | 21.00 | 3.23 | 38.18 | 5.39 | 8.05 | .40 | 60.00 | 57.76 | 5.00 | 2.51E+08 | 3.25E+08 |
| .05 | 28.59 | 3.77 | 37.60 | 1.88 | 8.05 | .40 | 43.50 | 33.97 | 5.00 | 4.27E+08 | 5.38E+08 |

CR= 28.31 CT= 4.71 SPAN= 67.55 WING A= 791.84 AR= 5.84

CALCULATED CRAR= 15.855 AT(X= 40.82 Y= 11.39 Z= 8.05 )

```
P$MATPS1
  RIGTD =0.0,
 $END OF DATA

P$AEROX1
 IFUS=0,NB=0,NBSEC(1)=0,IAEPOX(1)=0,RR(1)=0,ZD(1)=0,AINCB(1)=0,
 $END OF DATA

P$STOPE1
 NEXTR=0,CBAR=15.AF, XE(1)=0,YE(1)=0,ZE(1)=0,CLEZ(1)=0,CLFA(1)=0,CMEZ(1)=0,
 CMFA(1)=0,CDEZ(1)=0,CDEA(1)=0,NJ(1)=0,
 $END OF DATA

P$SYBAL1
C        ALT= 30000, SF= 24.0,    TEMP= 240 DEG K      MANEUVER
 XFUS=23.17, AINCF=-3.0, DCDF=.0072, ZCDF=10.0, DCDT=.0022, ZCDT=20.0,
 CLFA=.0030, CLFO=0.,   CMFA=.0141, CMFO=0.,   DELFL=0.,  DELSP=0.,
 DELSL=0.,  DDYN=52.78, THTDD=0.,  WG=11250.,  XCG=44.79,  XBAR4=44.79,
C        IF AINCF AND AO.PT BOTH = 0, DIVISION BY 0 WILL OCCUR AT 580 IN SYBALC
 YIY=200.0, ZBAR4=7.25, ZCG=7.25, AOLPT=-.008,CONSJ=.174, UDEOF=0.,
 CNAFR=.111, RADAL=.02145,  VEL=334.84,GUSTF=0., MACHN=1.0, USPLP=0.00,
 ECLTA=.0073, ATPAP=.794, AINCT=0.,   ATPODE=1.00, XDDE=-1.0, PWTS=0.,
 RAERO=0., ENAX=0., ENST=0., IFPPT=0., CONDNO=9H 7 ATT   ,
 DNZ= 0.00001,
 VNZ=2.5,
 ALFWT=7.95 ,DEWT=0., HPT4020 = 3HYES,
 HPT4020 = 2HNO,
 $END OF DATA
```

SINGULAR INPUT VARIABLES

CONDITION NUMBER 7 ATT

```
P&SYBAL7
 AOLSC(1)=10*-2.7, 0.,
 ADFL(1)=11*0.,
 ADSP( 1)=11*0.,
 ADSL(1)=11*0.,
      ATAU(1)= -5.0, -4.4, -3.8, -3.2, -2.6, -2.0, -1.4, -.8, -.4, -.2, 0.,      JIG TWIST
 CMOTO(1)=10*-.13, 0.,          SECTION PITCHING MOMENT
 TSECT(1)=11*.11,
 CRS(1)= 11*.61,
 CFS(1)= 11*.15,
 MO(1)= 9*.157, .106, .001,     SECTION LIFT CURVE SLOPE
 $END OF DATA

P&WTS1
 NEXTW=10,
 NG(1)= 1, 2, 3, 4, 5, 6, 7, 8, 9, 10,
 W(1)= .89, .92, .99, 1.00, 1.02, 1.05, 1.11, 1.32, 1.27, 1.55,
 XW(1)= 65.3, 62.7, 60.2, 57.7, 55.2, 52.7, 50.2, 47.9, 45.3, 41.2,
 YW(1)= 32.3, 29.4, 26.5, 23.6, 20.6, 17.7, 14.8, 11.7, 8.5, 5.4,
 ZW(1)= 10*8.35,
 $END OF DATA
```

WING INERTIA

INTEGRATED WING INERTIA

| | SHNZ | EMONZ | ETONZ | SHTH | EMOTH | ETOTH | SHPH | EMOPH | ETOPH |
|---|---|---|---|---|---|---|---|---|---|
| NSECT= 1 | 8.90000E-01 | 1.63779E+00 | 6.90397E-02 | -1.44453E-04 | -2.85798E-04 | 1.32140E-05 | -2.17284E-04 | -3.99[illegible]E-[illegible] | -1.68553E-05 |
| NSECT= 2 | 1.81000E+00 | 6.71898E+00 | 2.16655E-01 | -2.93776E-04 | -1.13319E-03 | 1.44977E-05 | -4.41892E-04 | -1.64136E-[illegible] | -5.28939E-05 |
| NSECT= 3 | 2.80000E+00 | 1.54788E+01 | 3.82450E-01 | -4.34460E-04 | -2.57870E-03 | 1.47515E-05 | -6.83589E-04 | -3.77[illegible]E-03 | -9.33709E-05 |
| NSECT= 4 | 3.80000E+00 | 2.80998E+01 | 5.56936E-01 | -6.16767E-04 | -4.65035E-03 | 1.38675E-05 | -9.27728E-04 | -6.66[illegible]E-[illegible] | -1.35970E-04 |
| NSECT= 5 | 4.82000E+00 | 4.45328E+01 | 6.75615E-01 | -7.82321E-04 | -7.34158E-03 | 2.25930E-05 | -1.17675E-03 | -1.[illegible]722E-02 | -1.64944E-04 |
| NSECT= 6 | 5.87000E+00 | 6.49877E+01 | 8.05153E-01 | -9.52743E-04 | -1.06863E-02 | 3.03778E-05 | -1.43310E-03 | -1.58[illegible]E-02 | -1.96569E-04 |
| NSECT= 7 | 6.98000E+00 | 8.95883E+01 | 9.49882E-01 | -1.13290E-03 | -1.47053E-02 | 3.73431E-05 | -1.73439E-03 | -2.18720E-02 | -2.31903E-04 |
| NSECT= 8 | 8.30000E+00 | 1.18789E+02 | -1.13902E+01 | -1.34715E-03 | -1.94404E-02 | 2.20004E-03 | -2.02635E-03 | -2.90[illegible]E-02 | 2.92727E-03 |
| NSECT= 9 | 9.57000E+00 | 1.56290E+02 | 1.51223E+01 | -1.55329E-03 | -2.56125E-02 | -2.21037E-03 | -2.33641E-03 | -3.81564E-02 | -3.69208E-03 |
| NSECT=10 | 1.11200E+01 | 2.11634E+02 | 4.93014E+01 | -1.80496E-03 | -3.45809E-02 | -7.77871E-03 | -2.71483E-03 | -5.16681E-02 | -1.19631E-02 |
| NSECT=11 | 1.11200E+01 | 2.59884E+02 | -5.16547E+01 | -1.80486E-03 | -4.27879E-02 | 8.72891E-03 | -2.71483E-03 | -6.34477E-02 | 1.26109E-02 |
| CMOTO= | -.1300 | -.1300 | -.1300 | -.1300 | -.1300 | -.1300 | -.1300 | -.1300 | 0.0000 |

MATRIX BARL

| | |
|---|---|
| NSECT= 1 | 1.92246E+00 |
| NSECT= 2 | 2.74001E+00 |
| NSECT= 3 | 3.41456E+00 |
| NSECT= 4 | 4.17053E+00 |
| NSECT= 5 | 5.02998E+00 |
| NSECT= 6 | 5.99255E+00 |
| NSECT= 7 | 7.09651E+00 |
| NSECT= 8 | 8.69329E+00 |
| NSECT= 9 | 9.70193E+00 |
| NSECT= 10 | 9.60128E+00 |
| NSECT= 11 | 6.05400E+00 |

**SOLUTION OF SIMULTANEOUS EQUATIONS** ($C_\ell c\ q$)

NOGO= 1

PTAT= 1.90151E+03 PTDDE= 0. DDE= 0.

| DELSP | USPLR | VNZ | DNZ | ALPEFD |
|---|---|---|---|---|
| 0. | 0. | 2.50000E+00 | 1.00000E-05 | 7.95000E+00 |

| VFFUA | VFTAL | VFINP | VFFUO | VFCHK | CLWS | STABAR |
|---|---|---|---|---|---|---|
| 1.01968E+03 | 1.90151E+03 | -2.81250E+04 | 0. | -4.02884E+03 | 5.13137E-01 | 5.95934E-01 |

| TDBR4 | TOFUA | TOTAL | TOINP | TOFUO | TOCHK |
|---|---|---|---|---|---|
| -4.63972E+04 | 1.08781E+05 | -8.59675E+04 | -0. | -3.91841E+04 | -1.09165E+05 |

**FORCES AND MOMENTS ON TOTAL VEHICLE AND COMPONENTS**

VERTICAL AERODYNAMIC FORCE ON THE WIND TUNNEL MODEL AT THE QUARTER MAC = 24096.16 LBS
AND THE AERODYNAMIC MOMENT ON THE WIND TUNNEL MODEL AT THE QUARTER MAC = -109165.40 IN LB

**STING REACTION**

SHWNG THROUGH TOTEA ARE AERODYNAMIC LOADS AND MOMENTS. WTSH, WTMEA, AND WTTEA ARE INERTIA LOADS AND MOMENTS.

SHAPI, MEAPI, AND TEAPI ARE AIR + INERTIA LOADS AND MOMENTS.

ALL SHEAR/MOMENT VALUES ABOUT ELASTIC AXIS AT INBOARD EDGE OF SECTION

+SIGN CONVENTION * NOSE UP, RIGHT WING DOWN AND BACK

| | XFATE | SHWNG | BMWNG | TOWNG | SHSTO | BMSTO | TOSTO |
|---|---|---|---|---|---|---|---|
| NSECT= 1 | 5.41599E+01 | 2.96441E+02 | 4.33032E+02 | -5.48471E+02 | 0. | 0. | 0. |
| NSECT= 2 | 6.16505E+01 | 7.18947E+02 | 1.91624E+03 | -2.19763E+03 | 0. | 0. | 0. |
| NSECT= 3 | 5.91443E+01 | 1.24486E+03 | 4.78163E+03 | -4.94532E+03 | 0. | 0. | 0. |
| NSECT= 4 | 5.60350E+01 | 1.88797E+03 | 9.35796E+03 | -9.17703E+03 | 0. | 0. | 0. |
| NSECT= 5 | 5.41287E+01 | 2.66268E+03 | 1.59377E+04 | -1.51095E+04 | 0. | 0. | 0. |
| NSECT= 6 | 5.16134E+01 | 3.58674E+03 | 2.51267E+04 | -2.31386E+04 | 0. | 0. | 0. |
| NSECT= 7 | 4.91131E+01 | 4.67975E+03 | 3.71582E+04 | -3.35818E+04 | 0. | 0. | 0. |
| NSECT= 8 | 4.70115E+01 | 6.20901E+03 | 6.53580E+04 | -4.51252E+04 | 0. | 0. | 0. |
| NSECT= 9 | 4.39931E+01 | 7.74511E+03 | 7.62642E+04 | -6.71004E+04 | 0. | 0. | 0. |
| NSECT= 10 | 3.88686E+01 | 9.38308E+03 | 1.03946E+05 | -1.15435E+05 | 0. | 0. | 0. |
| NSECT= 11 | 3.66059E+01 | 1.05875E+04 | 1.41583E+05 | -1.33037E+05 | 0. | 0. | 0. |

AIR LOADS AND MOMENTS PERPENDICULAR TO FREE STREAM

| | CWMEA | CWTEA | STMEA | STTEA | SHTEA | BMTEA | TOTEA |
|---|---|---|---|---|---|---|---|
| NSECT= 1 | 7.51012E+02 | -2.09792E+02 | 0. | 0. | 2.96441E+02 | 7.51012E+02 | -2.09792E+02 |
| NSECT= 2 | 2.38557E+03 | -4.18586E+02 | 0. | 0. | 7.18947E+02 | 2.38557E+03 | -4.18586E+02 |
| NSECT= 3 | 6.84950E+03 | -6.36077E+02 | 0. | 0. | 1.24486E+03 | 6.84950E+03 | -6.36077E+02 |
| NSECT= 4 | 1.30653E+04 | -8.49394E+02 | 0. | 0. | 1.88797E+03 | 1.30653E+04 | -8.49394E+02 |
| NSECT= 5 | 2.19835E+04 | -1.03879E+03 | 0. | 0. | 2.66268E+03 | 2.19835E+04 | -1.03879E+03 |
| NSECT= 6 | 3.41372E+04 | -1.18180E+03 | 0. | 0. | 3.58674E+03 | 3.41372E+04 | -1.18180E+03 |
| NSECT= 7 | 5.00914E+04 | -1.24540E+03 | 0. | 0. | 4.67975E+03 | 5.00914E+04 | -1.24540E+03 |
| NSECT= 8 | 7.08771E+04 | -8.66104E+03 | 0. | 0. | 6.20931E+03 | 7.08771E+04 | -8.66104E+03 |
| NSECT= 9 | 1.01353E+05 | 6.80189E+03 | 0. | 0. | 7.74511E+03 | 1.01353E+05 | 6.80189E+03 |
| NSECT= 10 | 1.53033E+05 | 2.63355E+04 | 0. | 0. | 9.38308E+03 | 1.53033E+05 | 2.63355E+04 |
| NSECT= 11 | 1.89855E+05 | -4.12256E+04 | 0. | 0. | 1.05875E+04 | 1.89855E+05 | -4.12256E+04 |

AIR LOADS AND MOMENTS PERPENDICULAR TO ELASTIC AXIS

+SIGN CONVENTION * NOSE UP, RIGHT WING DOWN AND BACK

| | INERTIA SHEARS AND MOMENTS | | | AIR + INERTIA SHEARS AND MOMENTS | | | WING LOADING (AIR ONLY) |
|---|---|---|---|---|---|---|---|
| | WTSM | WTMEA | WTTEA | SHAPIL | MEAPIL | TEAPIL | SCLCO |
| NSECT= 1 | -2.22500E+00 | -4.09447E+00 | -1.72599E-01 | 2.94216E+02 | 7.46917E+02 | -2.09954E+02 | 1.51467E+02 |
| NSECT= 2 | -4.32500E+00 | -1.67974E+01 | -5.41638E-01 | 7.14422E+02 | 2.86377E+03 | -4.19127E+02 | 1.44618E+02 |

| | | | | | | | |
|---|---|---|---|---|---|---|---|
| NSECT= 3 | -7.00000E+00 | -3.86959E+01 | -9.56125E-01 | 1.23786E+03 | 6.81[illegible]E+03 | -6.3[illegible]E+02 | 1.[illegible]E+02 |
| NSECT= 4 | -9.50000E+00 | -7.02495E+01 | -1.39234E+00 | 1.87847E+03 | 1.29[illegible]E+04 | -[illegible]E+02 | 2.2[illegible]E+02 |
| NSECT= 5 | -1.20500E+01 | -1.11372E+02 | -1.68904E+00 | 2.6[illegible]E+03 | 2.18[illegible]E+04 | -1.[illegible]E+03 | 2.[illegible]E+02 |
| NSECT= 6 | -1.46750E+01 | -1.62469E+02 | -2.01293E+00 | 3.5[illegible]E+03 | 3.59748E+04 | -1.1[illegible]E+03 | [illegible]E+02 |
| NSECT= 7 | -1.74500E+01 | -2.23971E+02 | -2.37471E+00 | 4.66230E+03 | 4.98674E+04 | -1.2[illegible]E+03 | 3.74[illegible]E+02 |
| NSECT= 8 | -2.07500E+01 | -2.96972E+02 | 2.99754E+01 | 6.1[illegible]56E+03 | 7.[illegible]E+04 | -8.6[illegible]E+03 | 4.[illegible]E+02 |
| NSECT= 9 | -2.39250E+01 | -3.90724E+02 | -3.78072E+01 | 7.72119E+03 | 1.00962E+05 | 6.7[illegible]E+03 | 5.12[illegible]E+02 |
| NSECT= 10 | -2.78000E+01 | -5.29045E+02 | -1.22603E+02 | 9.35528E+03 | 1.52560E+05 | 2.62[illegible]E+04 | 5.06[illegible]E+02 |
| NSECT= 11 | -2.78000E+01 | -6.49709E+02 | 1.29137E+02 | 1.0[illegible]597E+04 | 1.39206E+05 | -4.1[illegible]E+04 | 3.1[illegible]E+02 |

| | CALC EI | CALC GJ | ZOEDGE VERTICAL DEFLECTION |
|---|---|---|---|
| NSECT= 1 | 1.75179E+05 | 2.24239E+05 | 1.721 |
| NSECT= 2 | 4.09235E+05 | 4.39147E+05 | 1.401 |
| NSECT= 3 | 8.48439E+05 | 8.27353E+05 | 1.092 |
| NSECT= 4 | 1.57937E+06 | 1.46034E+06 | .819 |
| NSECT= 5 | 2.70623E+06 | 2.42456E+06 | .562 |
| NSECT= 6 | 4.35919E+06 | 3.82576E+06 | .359 |
| NSECT= 7 | 6.68814E+06 | 5.78570E+06 | .205 |
| NSECT= 8 | 1.14523E+07 | 9.93158E+06 | .103 |
| NSECT= 9 | 2.30202E+07 | 2.02659E+07 | .042 |
| NSECT= 10 | 5.27492E+07 | 4.75871E+07 | .016 |
| NSECT= 11 | 8.79794E+07 | 9.13951E+07 | .004 |

| | ALFND ELASTIC EQUILIBRIUM ANGLE OF ATTACK | ATELD ELASTIC WING TWIST | AWELD ELASTIC TWIST DUE TO $C_\ell^c$ | ASELD ELASTIC TWIST DUE TO STORES | QSBEXTD | ACMOED ELASTIC TWIST DUE TO $C_{M_0}$ | ACMOGD |
|---|---|---|---|---|---|---|---|
| NSECT= 1 | 2.30457E+00 | -3.40387E+00 | -2.62226E+00 | 0. | 0. | -4.05565E-01 | -3.76044E-01 |
| NSECT= 2 | 3.01752E+00 | -3.30462E+00 | -2.57916E+00 | 0. | 0. | -3.77[illegible]E-01 | -3.48[illegible]E-01 |
| NSECT= 3 | 3.87306E+00 | -3.06755E+00 | -2.43664E+00 | 0. | 0. | -3.27374E-01 | -3.03541E-01 |
| NSECT= 4 | 4.86914E+00 | -2.69690E+00 | -2.18001E+00 | 0. | 0. | -2.6[illegible]E-01 | -2.49906E-01 |
| NSECT= 5 | 5.96534E+00 | -2.23729E+00 | -1.83653E+00 | 0. | 0. | -2.0[illegible]E-01 | -1.93998E-01 |
| NSECT= 6 | 7.15154E+00 | -1.70625E+00 | -1.41866E+00 | 0. | 0. | -1.4[illegible]E-01 | -1.38959E-01 |

| | | | | | | | |
|---|---|---|---|---|---|---|---|
| NSECT= 7 | 8.42553E+00 | -1.12120E+00 | -9.41528E-01 | 0. | 0. | -9.29990E-02 | -9.65733E-02 |
| NSECT= 8 | 9.70169E+00 | -6.14976E-01 | -5.18363E-01 | 0. | 0. | -5.35953E-02 | -4.50021E-02 |
| NSECT= 9 | 1.07624E+01 | -3.10930E-01 | -2.61436E-01 | 0. | 0. | -7.1[illegible]E-03 | -1.77133E-02 |
| NSECT= 10 | 1.19476E+01 | -1.39145E-01 | -1.17793E-01 | 0. | 0. | -1.24122E-02 | -4.73915E-03 |
| NSECT= 11 | 7.99773E+00 | -3.42651E-02 | -2.90113E-02 | 0. | 0. | -1.78[illegible]E-03 | -3.48424E-03 |

```
P$PLOTDAT
 PLTTITL(1)=10HATT M=1.0 , 10HH=30000 T=, 10H24CK A=7.9, 10H5 SOLTD X-,
 PLTTTTL(5)=10HC UNBAL   ,  10H          ,
 SYU(1) = 14000., 300000., 1000.,  60.,      5., 0.1,
 SYL(1) =    1.0, -100000.,   1.0,.04, 0.,  -7.,
 PLOT=3HYES,
 PLOT=2HNO,
 $END OF DATA
```

SC4020
PLOTTING
INFORMATION

# APPENDIX II

## SAFETY FACTOR BASED ON FRACTURE MECHANICS

Design procedures using fracture mechanics have not been rigidly established, because the entire field is still under development. However. it is important in selection of high-strength materials and design of structures operating at high stress levels that consideration be given to fracture resistance to ensure reasonable safety from catastrophic failure. This is particularly true for high-strength steels, where toughness generally decreases with increasing yield strength and decreasing temperature.

The most commonly used measure of crack propagation resistance of high-strength alloys for use in heavy sections* is plane strain fracture toughness, $K_{1c}$. Variations in $K_{1c}$ can be expected for any given alloy and strength level due to metallurgical aspects and nonstandardization of testing procedures. For example. variations in $K_{1c}$ have been observed for melting practice, processing history, size and shape of product form, and grain orientation. This variability makes the selection of a "design allowable" for $K_{1c}$ extremely difficult.

Flaws are inherent in all materials, and these defects can propagate under an applied stress, depending on a number of factors including size, shape, location and orientation. Therefore, the minimum flaw size that can be detected by available nondestructive testing (NDT) inspection processes is important in application of fracture mechanics. The detection capability of most NDT techniques varies with different types of materials. Fabrication of highly stressed models from high-strength steels will generally require ultrasonic inspection of the raw stock and magnetic particle inspection of the finish machined components. Both inspection requirements must be specified on the drawings, since present material specifications do not define these inspection requirements.

The minimum flaw size that can be detected in high-strength steels by these NDT inspection techniques has not been established. In application of fracture mechanics to design, some investigators have assumed minimum initial crack dimensions of 0.15 inch deep by 0.75 inch long as "standard minimum-detectable values" (Reference 2). These are considered conservative values, but are useful for safety factor calculations.

---

*ASTM E399-72 (Reference 1) defines that for plane strain conditions, material thickness must exceed $2.5\ (K_{1c}/\sigma_{ys})^2$.

The tensile strength and fracture toughness properties at room and subzero temperatures for three high strength steels are shown below (References 3, 4, and 5).

| Alloy & Condition | Temperature (°F) | $F_{tu}$ (ksi) | $F_{ty}$ (ksi) | Fracture Toughness, $K_{1c}$ (ksi $\sqrt{in.}$) |
|---|---|---|---|---|
| PH13-8 Mo | RT | 201(1) | 190(1) | 90 |
| H1000 | -110 | 230 | 220 | 18 |
| 18 Ni Maraging | RT | 250(1) | 240(1) | 90 |
| 250 Grade | -65 | 260 | 245 | 85 |
| | -110 | 270 | 260 | 71 |
| 18 Ni Maraging 300 Grade | RT | 300(1) | 285(1) | 52 |

All values are typical except as noted.

(1) MIL-HDBK-5 or material specification minimums.

Using the above data, calculations were made of the critical flaw size for an operating stress of one-half the yield strength, critical stress for "minimum detectable flaw size", and safety factor for PH13-8Mo H1000 and 18Ni maraging 250 grade steel at room temperature. The calculations assumed a "standard minimum detectable flaw size" of 0.15 inch deep by 0.75 inch long. The safety factor is defined as the ratio of the operating stress to the critical stress for the "standard minimum detectable flaw size."

| | PH13-8 Mo H1000 | 18 Ni Maraging 250 Grade |
|---|---|---|
| Operating Stress $\sigma = 0.5\,\sigma_{ys}$ (ksi) | 95 | 120 |
| Critical Flaw Size for $0.5\,\sigma_{ys}$ (in.) (a = flaw depth) | 0.29 | 0.18 |
| Minimum Detectable Flaw Size (in.) (a = flaw depth) | 0.15 | 0.15 |
| Critical $\sigma$ for Minimum Detectable Flaw Size (ksi) | 130 | 130 |
| Safety Factor ($\sigma_{\text{Minimum Detectable Flaw Size}}/0.5\,\sigma_{ys}$) | 1.36 | 1.08 |

The resulting safety factors of 1.36 and 1.08 appear reasonable in view of the conservative value used for the minimum detectable flaw size.

The calculations were made using the following equations (Reference 6):

$$\left(\frac{a}{Q}\right)_c = \frac{1}{1.21\pi}\left(\frac{K_{1c}}{\sigma}\right)^2 \tag{1}$$

where

$\left(\frac{a}{Q}\right)_c$ = critical normalized flaw size

$K_{1c}$ = plane strain fracture toughness

$\sigma$ = applied stress

a = flaw depth

Q = flaw shape parameter

The equations for determining Q are:

$$Q = \phi^2 - 0.212\left(\frac{\sigma}{\sigma_{ys}}\right)^2$$

where

$$\phi^2 = \int_0^{\pi/2} \sqrt{1 - \frac{c^2 - a^2}{c^2}\sin^2\theta}\, d\theta$$

For the "standard minimum detectable flaw size" (a = 0.15 and c = 0.75 inch), the eliptical integer $\phi$ = 1.3 (from table of eliptical integers), and Q = 1.2 (by calculation). The fracture toughness data are shown in Figure I-1.

The observations from these preliminary studies are that PH13-8Mo H1000 and maraging 250 grade steels have good fracture toughness at room temperature. However, the limited data available for PH13-8Mo H1000 show a drastic decrease in fracture toughness at subzero temperatures, which should be more fully explored for low-temperature service. Changes in heat treatment or alloy may be necessary; for example, the use of maraging 200 grade, which has a $K_{1c}$ value of 160 ksi$\sqrt{\text{in.}}$ at -100°F compared to PH13-8Mo H1000, which has a $K_{1c}$ of 18 ksi$\sqrt{\text{in.}}$ at -110°F (Reference 7).

The lower fracture toughness of maraging 300 grade steel at room temperature and lack of data at subzero temperatures indicate a vital need for further investigation of this alloy.

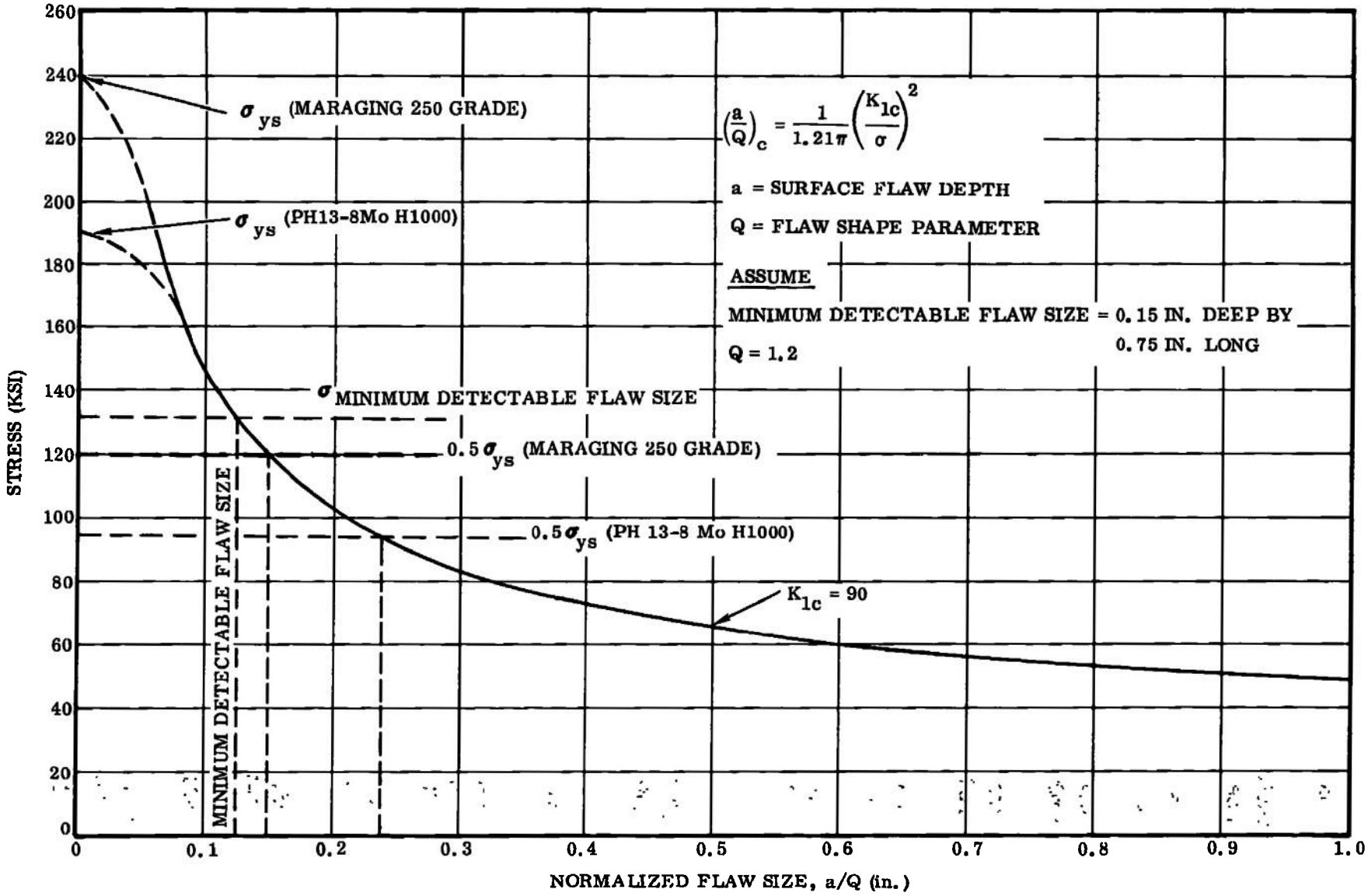


Figure I-1. Relationship Between Critical Flaw Size $(a/Q)_c$, Applied Stress $(\sigma)$, and Plane Strain Fracture Toughness $(K_{1c})$

The following studies are recommended:

a. Comprehensive compilation of available fracture toughness data on selected high-strength steels for the full range of potential service temperatures.

b. Determine safety factors and critical flaw sizes using the above fracture toughness data for the full range of potential service temperatures.

c. Establish statistically significant "minimum detectable flaw sizes" for selected high-strength steels, based on currently available NDT techniques.

d. Establish fracture toughness "design allowables" for the recommended high-strength steels, based on the wind tunnel operating temperature and environment.

e. Analyze the effect of cyclic loading and sustained-stress loading on subcritical flaw growth.

f. Evaluate the feasibility of proof testing highly stressed wind tunnel models to ensure an adequate safety factor from catastrophic failure.

REFERENCES

1. ASTM E399-72 "Standard Method of Test for Plane Strain Fracture Toughness of Metallic Materials."

2. C. C. Osgood, "What is Fracture Mechanics," Machine Design, July 22, 1971, August 5, 1971, August 19, 1971, September 2, 1971, September 16, 1971.

3. R. T. Bubsey, and W. F. Brown, Jr., "Crack Toughness Characteristics of Several Alloys for Use in Heavy Sections of High Speed Aircraft," NASA TN D-4998, January 1969.

4. W. F. Brown, Jr. and J. E. Srawley, "Plane Strain Crack Toughness Testing of High Strength Metallic Materials," ASTM STP 410, 1966.

5. H. A. Wood, "Fracture Control Procedures for Aircraft Structural Integrity," AFFDL-TR-71-89, July 1971.

6. NASA SP-8040 , "Fracture Control of Metallic Pressure Vessels," May 1970.

7. C. Vishnevsky and E. A. Steigerwald, "Plane Strain Fracture Toughness of Some Cryogenic Materials at Room and Subzero Temperatures," ASTM STP 496, Fracture Toughness Testing at Cryogenic Temperatures, August 1971.

UNCLASSIFIED
Security Classification

## DOCUMENT CONTROL DATA - R & D

*(Security classification of title, body of abstract and indexing annotation must be entered when the overall report is classified)*

| | |
|---|---|
| 1. ORIGINATING ACTIVITY *(Corporate author)*<br>General Dynamics Corporation<br>Convair Aerospace Division<br>San Diego, California | 2a. REPORT SECURITY CLASSIFICATION<br>UNCLASSIFIED<br>2b. GROUP<br>N/A |

3. REPORT TITLE
WIND TUNNEL MODEL PARAMETRIC STUDY FOR USE IN THE PROPOSED 8 FT X 10 FT HIGH REYNOLDS NUMBER TRANSONIC WIND TUNNEL (HIRT) AT ARNOLD ENGINEERING DEVELOPMENT CENTER

4. DESCRIPTIVE NOTES *(Type of report and inclusive dates)*
Final Report - June through December 1972

5. AUTHOR(S) *(First name, middle initial, last name)*
Walter K. Alexander, Stanley A. Griffin, Robert L. Holt, et al.

| | | |
|---|---|---|
| 6. REPORT DATE<br>March 1973 | 7a. TOTAL NO. OF PAGES<br>175 | 7b. NO. OF REFS<br>25 |

| | |
|---|---|
| 8a. CONTRACT OR GRANT NO<br>F40600-72-C-0015<br>b. PROJECT NO.<br>c.<br>d. | 9a. ORIGINATOR'S REPORT NUMBER(S)<br>AEDC-TR-73-47<br>9b. OTHER REPORT NO(S) *(Any other numbers that may be assigned this report)*<br>GDCA-DHJ72-001 |

10. DISTRIBUTION STATEMENT
Approved for public release; distribution unlimited.

| | |
|---|---|
| 11. SUPPLEMENTARY NOTES<br>Available in DDC | 12. SPONSORING MILITARY ACTIVITY<br>Arnold Engineering Development Center, Air Force Systems Command, Arnold AF Station, Tenn. 37389 |

13. ABSTRACT The need for a High Reynolds Number Transonic Wind Tunnel (HIRT) has been recognized throughout the industry for some years. The proposed HIRT facility at Arnold Engineering Development Center will provide a much needed tool for the study of phenomena sensitive to Reynolds number. The usefulness of the HIRT facility will be largely influenced by the ability of industry to design and build wind-tunnel models for an acceptable cost capable of operating within the severe environment of the tunnel. The object of this study is to determine the feasibility of designing and building models capable of withstanding the loads and environmental conditions of the facility. The aircraft configurations chosen for study cover a wide spectrum of flight conditions. A test plan is developed for each configuration which encompasses its complete flight envelope. Model loads and deformations, stress analyses of each configuration, a summary of materials suitable for use in the HIRT facility, and cost comparisons are presented. The study concluded that models capable of running in the HIRT facility can be built at a reasonable cost with present-day techniques and materials.

DD FORM 1 NOV 65 1473

UNCLASSIFIED
Security Classification

| 14. KEY WORDS | LINK A ROLE | LINK A WT | LINK B ROLE | LINK B WT | LINK C ROLE | LINK C WT |
|---|---|---|---|---|---|---|
| wind tunnel models | | | | | | |
| configurations | | | | | | |
| design | | | | | | |
| fabrication | | | | | | |
| high Reynolds number testing | | | | | | |
| materials | | | | | | |
| model distortion | | | | | | |
| aerodynamic loads | | | | | | |

AFSC
Arnold AFS Tenn